BREAKING WAVES.

BY

MATTHEW W.P. GRIFFITHS.

DOCTOR OF PHILOSOPHY.

UNIVERSITY OF EDINBURGH.

1989

To Friends.

DECLARATION

I declare that all the work contained in this Thesis is entirely my own

ACKNOWLEDGEMENTS.

Not all students praise their supervisors privately. I wish to take this opportunity to say publicly what I have said on many occasions privately, that is, that Dr. Clive Greated and Dr. Bill Easson have been supporting, encouraging, critical and resourceful in good measure. They neither left me in the cold nor made me a technician or programmer for their own ends, they gave me both freedom and direction.

I acknowledge the funding received from the SERC for the first three years of this work. And thank BP for contributing to this by way of the CASE award scheme. I should also like to thank the DSS, formerly the DHSS, for their support of basic scientific research. I thank Frank Morris for his technical support and for being a breath of human air in the department.

I am most grateful to all people who have helped to hold my head together while I have been writing this thesis. My largest debt is to my friends. Thanks go to my immediate family, my supervisors and their families, Richard and the Colversons all of whom have given me background. More immediatly, Olivia and her flat, all my flat mates past and present, in particular the Howe St. boys. To Rob and Jenny, Tom and Dave in the office, and Ian in illness. You have all given me strength. I am also grateful to the galleries of Edinburgh and to the Scottish hills. To the west coast, in particular to Eillean Fladday, the little island of flat island and to all who have helped me to enjoy them.

Abstract

This work studies the breaking of monochromatic waves on straight beds, and achieves two specific goals :

(A) ; the systematic description of breaking waves. The complete range of breaking from a gentle spiller to a severe plunger is described by accurate and detailed measurements of the wave surface. It is demonstrated that monochromatic wave breaking is a function of two independent parameters, and that any single shoaling parameter is only an approximation. The present description provides a useful base line for work on more general and complex wave breaking.

(B) ; the measurement of internal kinematics within a range of breaking wave crests. A range of wave types covering breaking waves that are to be expected in the design of offshore structures were studied in more detail. The water particle velocities and accelerations within the wave crests were accurately measured and ~~three~~ four important conclusions drawn.

Conclusion 1. It is incorrect to conclude, as has been done from partial results, that the low order wave theories over predict the internal velocities.

Conclusion 2. The maximum water particle velocity in the crest at breaking is equal to or slightly above the wave celerity.

Conclusion 3. Spilling breaking is well modelled by high order theories.

Conclusion 4. Plunging long period waves have velocities significantly higher than predicted by theory. For the worst case measured here this was a 30% increase. This corresponds to an increase in drag force of 70%.

"Great waves, ... How they come on and break, come on and break, one after another, endlessly, idly, empty and vast! And yet, like all the simple, inevitable things, they sooth, they console, after all. I have learned to love the sea more and more. Once, I think, I cared more for the mountains - because they lay farther off. Now I do not long for them. They would only frighten and abash me. They are too capricious, too manifold, too anomalous - I know I should feel myself vanquished in their presence. What sort of men prefer the monotony of the sea? Those, I think, who have looked so long and deeply into the complexities of the spirit, that they ask of outward things merely that they should possess one quality above all: simplicity. It is true that in the mountains one clambers briskly about, while beside the sea one sits quietly on the shore. This is a difference, but a superficial one. The real difference is in the look with which one pays homage to the one and to the other. It is a strong, challenging gaze, full of enterprise, that can soar from peak to peak; but the eyes that rest on the wide ocean and are soothed by the sight of its waves rolling on forever, mystically, relentlessly, are those that are already wearied by looking too deep into the solemn perplexities of life. - Health and illness, that is the difference. The man whose strength is unexhausted climbs boldly up into the lofty multiplicity of the mountain heights. But it is when one is worn out with turning one's eyes inward upon the bewildering complexity of the human heart, that one finds peace in resting them on the wideness of the sea."

Buddenbrooks, Thomas Mann.

BREAKING WAVES

Chapter 1 Introduction.

1.1 AIMS OF AND JUSTIFICATION FOR PRESENT RESEARCH.

There are two main reasons for the present work : Firstly, a substantial proportion of the worlds oil reserves are situated below the sea bed in areas with very hostile wave environments. Although the technology exists to build offshore structures, the design process has to make very large allowances for the uncertainty in the environmental loading. This area may be one in which significant economic savings may be made. Secondly, and to some extent prompted by the above, the mathematical modelling of wave behaviour is an area of active research. These models are very sensitive in the breaking limit, but in this limit there has been a lack of accurate measured data for comparison. (Longuet-Higgins, 1980)

There are several sources of uncertainty in environmental loading and of these the most significant arises from the wave motion. Present research aims to reduce the size of this uncertainty by increasing our knowledge of fluid mechanics and wave behaviour in particular.

The uncertainty in wave loading lies in two areas, this reflects the current design process. The design method has a bottle-neck where the extreme wave state description is reduced to just three parameters. The sea in storm conditions is a random environment, from which an extreme, "design", wave is predicted. The first uncertainty arises from the choice of this design wave. The second uncertainty occurs in the prediction of the internal kinematics within the specified design wave. The local velocities and accelerations are used directly in the prediction of force. Knowledge of wave behaviour is required at both these stages.

The present research bears on both aspects of this problem, most directly on the latter. There are many mathematical models of waves, which vary in complexity from the linear, sinusoidal approximation, to the time stepping methods which can model overturning waves. The simple models are easy to use and can be run by a non-specialist on a low powered computer. Given the random nature of the real sea, the approximations made in determining a design wave and the limited accuracy of environmental data, the simple models with a large safety factor have found wide favour in design. However, one area where it was thought that errors might exceed the generous safety factors was in the crest of breaking waves. Research showed widely differing predictions for the maximum velocities found at breaking with a range of measured values from 0.5 to 2.8 times the wave celerity. As the drag force produced by the flow is proportional to the square of the water velocity this corresponds to a factor of 30 between the extreme cases. This is significantly larger than the factors of safety.

This work includes measured values for the internal kinematics of waves which break with various severities, ranging from gentle spilling to dramatic plunging. The results for these show that the internal velocities over the range of breaking types tend to maximum values of a little over the wave celerity, and that the region of extreme velocities is quite restricted. This work also includes detailed study of the surface parameters of breaking waves. These show that the design ratios at which breaking is assumed to occur are true only in special cases.

The occurrence of breaking is one of the major factors which determines the extreme wave conditions at any location. The extreme sea state is the result of the energy balance between incoming wind forcing and outgoing dissipation through breaking. At present the extrapolation from measured sea records to a predicted extreme design wave takes no account of the breaking process. Work on these problems is in a sense convergent: as understanding grows, the description of breaking becomes more complex and the findings can be used in both the calculation of force and in the statistical prediction of the design wave.

The ability to measure accurately the parameters that describe monochromatic wave shoaling, and to provide evidence to discriminate between different wave models in the breaking limit has been made feasible by the developments of (i) accurate and non-intrusive flow measurement (laser Doppler anemometry, section 3.4 and Durrani and Greated, 1977) and (ii) clean wave generation (the absorbing wave paddle, section 3.2 and Edinburgh Wave Power Project, 1978).

The measurement of flow within waves using laser Doppler anemometry was reported as early as 1970 by Greated & Manning, and several people have measured the water particle velocities within waves since. Earlier work has been inadequate on several counts. There has been a lack of a systematic study of internal kinematics, many workers considered only one or two cases, and the breaking waves have often only been defined qualitatively.

The spread of results was unacceptably large and the bulk of measured kinematics relate to positions away from the crest region, often restricted to elevations below the trough depth. Comparison of velocities at these low levels has led to wrong conclusions about the applicability of various wave theories. Also, work carried out with simply driven paddles operating in shallow water has substantial errors arising from the creation of free harmonics. (Flick and Guza, 1980)

1.2 GENERAL DESCRIPTION OF WAVES AND THEIR ENVIRONMENTS.

The waves that are important in offshore design occur in a very complex and hazardous environment. They are created by the effect of the wind on the sea and are a combination of many periodic motions each sustained by the displacement of water and the restoring force provided by gravity. The scales of these waves are typically in hundreds of meters in length, tens of meters in height and in tens of seconds for wave periods.

The offshore environment consists of three main factors, the wind, the waves and the currents. The condition of these is determined by the topology of the sea bed and the prevailing weather conditions. All three factors interact significantly with each other and any complete description would account for this.

At present the wind is considered the prime mover and is described by its fetch and the time history of its velocity. The wave behavior is treated as a stochastic process where the stationary quantities are governed by the wind history and fetch and the water depth, (Darbyshire and Draper, 1963 and Sobey, 1989). The currents are considered as either slab currents (velocity constant with depth) arising from tides, oceanic streaming or mixing or as storm driven currents with non-slab profiles (Srokosz, 1987 and Vyas et al 1988).

All the factors themselves are complex; for a start, they are all three dimensional. The prevailing wind direction can change over the time scale of a typical storm. This is most noticeable in the case of hurricanes. The wind also has a smaller scale structure, gusting. The three-dimensionality of the waves is very important for offshore structures: Three-dimensional waves can be larger than any that can exist in two-dimensions and could cause more extreme loads, (Kjeldsen, 1983a). For shipping there is the additional danger of polymodal seas. A ship has only one axis of major stability and if the waves arrive from two directions then one set of waves will force the ship about its less stable axis, (Kjeldsen, 1981). Any three-dimensionality in the currents is not so much a problem in itself, but if waves propagate from water moving at one speed to water moving at another, then their energy can be spread or more dangerously localised. This can result in very severe sea conditions, (Department of Energy, 1974 and Kjeldsen and Myrhaug, 1980). The three-dimensionality of the sea bed causes wave refraction and in extreme cases reflection. This can greatly enhance the three-dimensional nature of the waves. One particularly dangerous case of this is the focusing effect of submerged islands, (Kjeldsen, 1983b). They can act as lenses to the waves, producing an area behind the island of very extreme seas.

As the offshore environment can only be deterministic when considered as fully four-dimensional all manageable descriptions and simplifications regard it as a random process. The wave conditions are described in spectral form, the energy given as a function of wave period. The full spectral description includes both energy and phase information and also the direction of travel of each component. This full description is only available after the event. Models based on substantial quantities of real sea data have been developed that predict the two-dimensional spectral form of any sea state as functions of the wind fetch and history. The two most widely used of these are those of : Pierson and Moskowitz (1964), and the JONSWAP (Hasselman et al., 1973).

The hostility of offshore environments is a severe problem in the study of waves. Any description can only be as good as the data on which it is based and measurements of the extreme sea conditions are notoriously difficult and inaccurate. Many well intentioned attempts to measure extreme conditions have literally come unstuck, with measuring equipment not surviving the waves they were intended to measure. A second problem, that of access, arises because the acquisition of real sea data is very expensive and some of that which has been collected by commercial companies operating offshore is not made freely available.

One particular area where data is poor is that of the current profiles in the presence of waves. The distinctions between different current profiles is of limited use at present as there is little measured data where the wave and current motions can be convincingly separated, in the wave crests.

Waves within the laboratory or within computational environments have peculiarities distinct from those at sea:

Laboratory waves have properties that arise from the fact that they are kept within a box. These include tank resonances , reflection , side wall friction , finite length and no net current. There are also effects arising from the paddle generation, in particular the production of free harmonics(Flick and Guza, 1980). Further, there are effects of scale including the boundary layers, the surface tension, the difficulty of including wind above the surface, and objects within the water. Problems associated with laboratory measurements are discussed at greater length in Kjeldsen (1981).

Mathematical wave models that include the non-linear aspects of finite amplitude waves are usually two-dimensional, have periodic boundary conditions and flat beds. These restraints make it impossible to model natural shoaling and breaking has to be forced. This has been done by creating an initial wave which is unstable, and letting it propogate to breaking (New et al., 1985,) or alternatively by applying a non-uniform pressure distribution on the free surface.

Both laboratory and mathematical models have difficulty incorporating objects. The problems are either in terms of scaling of the physical processes or because the modelling of body/fluid interactions is completely separate mathematically.

1.3 PRAGMATIC SIMPLIFICATIONS AND LIMITING CASES.

1.3.1 Universal simplifications.

With the most general description of the sea as the starting point for all modelling, there are three substantial simplifications that are almost universally made. These are (i) the wave behaviour can be studied separately from the wind, the structure (for drag dominated structures.) and the currents, (ii) the water is assumed to be an inviscid, incompressible fluid of uniform density, (iii) waves are assumed to be gravity driven with negligible effects from surface tension.

The wind is assumed to have only a long term effect. That is, extreme wave events are caused by the change in depth, the constructive superposition of wave motions from waves of different periods and directions and the change in current velocity, the local effect of the wind on breaking being taken as negligible. Studies have been made on the short term interaction of the wind on extreme wave motion. Banner and Phillips (1974) and Phillips and Banner (1974) demonstrate how a thin high vorticity layer at the free surface can substantially reduce the maximum attainable wave height. Douglass and Weggel (1988) describe laboratory observations in the near shore region where an offshore wind retards breaking and causes the waves to break in shallower water by plunging; conversly onshore winds encourage earlier, deeper water spilling breaking. However, a separation between the statistically defined sea condition and the wind itself remains an almost universal simplification in environmental models.

In most cases the structure is assumed to have no effect on the properties of the wave in which it finds itself. This is true in drag dominated design. However a separate design route and set of models are used where inertial forces are significant. Where the structure is large the effects of reflection and diffraction also have to be considered in design (Sarpkaya and Isaacson, 1981).

The currents are normally assumed to be separable from the wave motion to the extent that the kinematics can be described in isolation and subsequently superimposed. This is true of slab currents where the entire effect is that of a shift in reference frame and a subsequent Doppler shift in the wave period. Such currents are idealised, but they are appropriate for describing some tidal or oceanic currents. However they are not appropriate for describing the storm driven currents which are likely to be very different from those of a slab current. The profiles of storm driven currents are still a matter for conjecture, (Eastwood , Townend and Watson, 1987).

1.3.2 Further simplifications.

The reduction of the general case to a practical level takes two forms.

(a) Many models are based on a linear or small amplitude approximation. The simplicity of the wave description allows a correspondingly more complex environment to be modelled. These can describe reflection, refraction and diffraction effects, and they can model three-dimensional problems (Bryden and Greated, 1984) with complex bed topology (Svendsen and Jonsson, 1980). Some have been extended to include weakly non-linear behaviour and some higher order effects, (Kuo and Wang, 1986).

The Fourier approach which analyses the sea state in terms of the sinusoidal components present in time histories of the surface usually assumes a linear model. This is an assumption made in much measurement of sea spectra. Energy at any frequency is taken to represent a free wave of that frequency. However, much of the higher frequency energy is actually associated with the bound harmonics of lower frequency fundamental waves (Laing, 1986).

(b) The alternative high order or fully non-linear models are restricted in applicability. They are two-dimensional and can only model flat or quasi-flat beds. Only a few can describe time dependent behaviour. However, for waves of moderate height or above, non-linear effects become very important. Some properties such as the celerity are well approximated by weakly non-linear models. However the description of the behaviour of the high crest, including the internal kinematics given by the simpler models, is entirely inadequate. See section 5.4.

1.3.3 Limiting cases.

The understanding of waves can be greatly aided by considering their behaviour in limiting cases. Those most commonly used are described below:

"Shallow water", is taken to be where the water depth is small compared to the wavelength, that is when their ratio is less than 1/20 . Strange as it may at first appear, shallow water conditions are most commonly associated with large water depths. This is because the lengths of the waves are larger still. Examples of shallow water waves are ; tsunami, "tidal" waves caused by sub sea earthquakes; seiching of lochs and seas; and the tides. The cnoidal theory was designed for describing shallow water waves.

"Deep water", is taken to be where the depth to wavelength ratio exceeds 1/2 or even 1/3 . In this limit the sea bed can be ignored so slope and depth become irrelevant and the waves are completely defined by their period, amplitude and direction.

"Flat bed", is the limit where the depth is important, but the bed is either truly flat or the slope is considered negligible. The importance of the slope depends on the depth; in deep water, steep slopes can be neglected but in shallow water even small slopes affect the wave behaviour. The slopes occurring in much of the north sea, are shallower than 1:50 and for the wave breaking they can be considered flat. For longer term behaviour such as refraction, these slopes cannot be so easily be ignored.

In computations of wave kinematics, the slope is taken to be zero because it allows cyclic boundary conditions to be applied. Peregrine and others at Bristol University are trying to model laboratory slopes and have an approximation to a slope based on the abrupt change in depth below a wave. The "slope" is calculated as the change in depth over the distance (celerity x time) that their wave takes to develop to breaking. Theories not aimed at calculating the kinematics explicitly but designed to show diffraction, changes in amplitude and shoaling have been developed. These make the "shoaling assumption", that the wave kinematics at any one time are those of a wave on a flat bed whereas the longer term properties are affected by the slope. These models are addressing essentially different problems to that which is of interest here.

"Monochromatic" waves, are waves of a single period. They are only sinusoidal in the limit of infinitesimal amplitude. Care must be taken when interpreting the Fourier transform of wave surfaces. Finite amplitude waves, which are monochromatic, are of single period, but when artificially reduced to their sinusoidal components will appear as a fundamental period wave with a series of harmonics. These harmonics do not behave as separate waves, but travel at the speed of the fundamental and are termed "bound harmonics" . To avoid confusion, the term monochromatic is used rather than single period (monochronic) likewise the wavelength is not used to define the wave as it is depth dependant.

"Two-dimensional" waves occur naturally as swell but also at the coast or where the bed topology refracts the originally three-dimensional waves to two-dimensional waves parallel to the bed contours. These are also known as "long crested" waves. Extreme two-dimensional waves occur only where depth is the factor causing steepening and breaking. The extreme two dimensional flat bed wave used in design is purely notional and has no natural manifestation.

"Solitary" waves form a useful limit, that where the period tends to infinity and the necessarily two-dimensional wave is fully described by its height to depth ratio and the bed slope (usually zero). This is mainly a mathematical limit though the shoaling of small steepness waves comes into this category.

"Sea" refers to waves generated by a local wind, and is typified by short waves with a large directional spread. Waves in a sea are also known as "short crested".

"Swell" is the residual wave motion from a storm. The random waves caused during the storm, propagate at the phase speeds determined by their individual wave periods. Long waves, travelling faster, will draw-ahead of the shorter waves. At a point some distance from the storm, the waves will arrive as monochromatic waves, the long period waves arriving first. Note that as these have radiated some distance from their source, they are of non-extreme amplitude and are locally two-dimensional.

"Capillary" waves are waves where the restoring force comes from surface tension rather than gravity. These are only of interest here as a source of error in laboratory flumes.

"Infinitesimal amplitude". This is the limit where the linear wave theory is valid. Surprisingly the prediction of wave behaviour from this limit can give results relevent to examples of waves of finite amplitude.

"Breaking". This is the limit explored in this thesis. It is distinct from the other limits described here as it is determined by a change of behaviour rather than by limiting any of the parameters effecting the waves. Breaking can be defined in various ways, these are discussed in section 1.4.

"Stokes limiting wave". This is similar to the breaking limit and sometimes confused with it. It is the mathematical limit to a "Stokes" wave when the highest velocity of the fluid within the wave equals the wave celerity (Stokes, 1880). The wave is characterised by a sharp 120 degree cusp at the crest, and has a limiting Lagrangian acceleration of 0.5g away from the crest. The Eulerian acceleration is infinite in the limit because the gradient of the surface is discontinuous at the cusp.

1.4 DEFINITIONS OF BREAKING.

This section describes two aspects of breaking; the definition of the type of breaking and the definition of the point of breaking.

1.4.1 Types of breaking.

There are many distinguishable types of breaking. The range of two-dimensional breaking types appears as a continuous spectrum, with one type merging into the next, (Galvin, 1968). The three-dimensional breaking adds a further complication, the angular focusing of the component waves. The three-dimensional cases can be regarded as modifications of the two-dimensional in so far as they exhibit the range of breaking from plunging to spilling and bores, (Kjeldsen, 1983b). However, the waves can achieve heights beyond those possible in two-dimensions. The three-dimensionality of waves can be described in terms of their crest length.

The breaking that occurs in two-dimensions reflects the rate at which the wave becomes unstable. At one end of the range, a wave with only a little more energy than it can contain stably will form a spilling region in the crest but will maintain most of its unbroken characteristics. However, where a wave has a rapid increase in energy and cannot dissipate the excess gradually, it will break violently, overturning and throwing out a spout of water (plunging).

Considering the shoaling of waves, the breaking severity increases with both beach slope and decreasing deep water steepness. The gentlest breaking starts with ripples on the front edge of the crest followed by a rolling motion and air entrainment. This spilling motion is self sustaining. As the severity increases the water at the crest appears to move faster forming a region that shoots forwards over the preceding trough. Waves that are more severe still form a spout in the crest which plunges clear of the water below it and strikes the front face of the wave leaving an air gap. As the breaking severity increases, the size of the air gap grows and the point where the spout impinges on the front surface moves away from the crest. The waves studied here are of these first categories, spilling and plunging, but as the severity increases further, breaking more associated with inshore regions occurs. These are in turn the collapsing and surging breakers, (Galvin, 1968). For very steep slopes the wave shoaling is replaced by wave reflection.

1.4.2 Definitions of the point of breaking.

Many definitions of breaking exist. In this work the point of breaking is taken as the first point where the wave is vertically fronted. This definition is favoured by the offshore industry as it produces the worst possible load condition from both Morison type forces and slamming. This definition is also favoured in the laboratory. A second choice for the point of breaking is that where the maximum elevation is reached. This again is easy to implement in the laboratory, but is of no use in detecting breaking in wave elevation records measured at a single fixed point in space. The distance between the breaking points, described above, is very small with the latter preceding the former. Vertically fronted waves appear in wave elevation records as jumps in the wave height and can be used to measure breaking events, Longuet-Higgins and Smith, (1983).

Some definitions of breaking are based on other phenomena. The appearance of white water is often taken as the observable characteristic of breaking at sea. This has been used in the estimation of the occurrence of breaking. However care must be taken to separate true breaking with its air entrainment from the white mist and water droplets blown off the top of waves in storms. Conversly, Banner and Phillips (1974) discusses wave breaking in the absence of both spout formation or air entrainment.

There are several other breaking limits derived from theoretical considerations of the internal kinematics. The source of these is usually the assumption that the maximum horizontal velocity that water can obtain within a non-breaking wave is the wave celerity, and that this occurs at the top of the wave crest. This has been applied to define the Stokes limiting wave; the resulting limiting 120 degree cusp at the surface and the limiting 0.5g Lagrangian acceleration have become synonymous with the breaking limit.

Limiting design ratios or pseudo-breaking limits have found widespread use. These arose from considerations of the maximum particle velocity in two special cases. A deep water wave is believed to break when the ratio of height to wavelength exceeds 1/7 , (Mitchell, 1893). In shallow water the result for a shallow water solitary wave is used, that is, that the limiting height to depth ratio is 0.78 , (Munk, 1949). These are not universally valid or conservative but have been widely taken to be so. They are shown in context in chapter 4.

Longuet-Higgins (1985) discusses a breaking limit based on a maximum downwards Lagrangian acceleration. Several limiting values have been suggested. Phillips (1958) suggested a limit of -g at the free surface, Snyder, Smith and Kennedy (1983) used the value of 0.5g, and Srokosz 1986 proposed a value of 0.4g.

While the rest of this thesis relates to waves at the point where they become vertically fronted, reference should be made to work on waves at other stages of breaking. Basco (1985) reviews work on waves after the breaking point in a qualitative manner. Jansen (1986) discusses the kinematics in the aerated region produced by a plunging wave. Sakai et al. (1986) report on large scale vortex formation, both horizontal and slanting. Kirkgoz (1986) measures the horizontal velocities at a point where the wave first exhibits horizontal assymmetry, his "transformation" point. Energy dissipation and breaker travel are studied by Galvin (1969), Stive (1984), Battjes and Stive (1985) and Sakai et al. (1986). Also the spectral characteristics of breaking waves are studied in, Sawaragi and Iwata (1976), Phillips (1985) and Bruce (1987).

1.5 CAUSES OF BREAKING.

The causes of breaking separate naturally into two categories; depth-related and energy focused. Energy focusing occurs by two means, waves travelling in different directions can come together at a single point or focus. Similarly in time, waves travelling at different speeds can arrive in phase at a single point. Depth induced breaking, or shoaling, exhibits little energy focusing as any initial three-dimensionality is lost as the waves are refracted and the shallow water makes the celerities less period dependent.

Depth related breaking is the area of breaking covered by this thesis and has many advantages as the initial area of wave breaking studies. The vast majority of mathematical models are only available in two-dimensional forms. It was only a moderate tightening of scope to restrict this study to fully two-dimensional monochromatic waves shoaling on flat beds. The shoaling results here form a basis for studies of more complex breaking.

1.5.1 Depth induced breaking or shoaling.

The sea bed can cause breaking in two ways. It may do so indirectly by refracting waves such that breaking occurs as the waves are focused; this is counted as focused breaking. Alternatively the bed may cause breaking directly by allowing the waves to propagate into water of shallower depth where they become unstable.

As the wave travels into progressively shallower water, the wave height grows and the crests steepen. A point is reached where the energy in the wave is larger than can be contained in a stable wave at the reduced depth. Breaking then occurs. This direct effect is what is used throughout this thesis as the source of breaking. The type of breaking depends on the rate at which the energy becomes in excess.

Two separate parameters affect this rate. The obvious choice for one of these is the beach slope, the other must be independent from this and be based on an appropriate combination of the period, depth or other surface parameters. In this work the second parameter was taken; for experimental work as the deep water steepness of the incoming wave; and for analysis and in the design related sections as the non-dimensional breaking depth.

The wave shoaling was kept as simple as possible, with the two parameters, slope and deep water steepness, varied independently. There are several complicating factors in shoaling that have been suppressed in this work:

The interaction of waves with the back rush from the previous waves leads to a cycle in the wave breaking over several periods (surf beat or infragravity waves, Guza and Thornton, 1985). As this is an effect associated with the shoreline rather than with the local wave breaking it was not of interest here. Because the measurements of internal kinematics rely on high repeatability, the beach was terminated some distance before it crossed the mean water level eliminating the surf beating. Similarly, all reflections were kept to a minimum.

Other phenomena associated with fully three-dimensional shoaling were not reproduced in the laboratory. Notably cellular tidal motions (rip tides) are not reproduced as the tank is in this context two-dimensional.

This work only seeks to investigate the shoaling on straight impervious and rigid beds. The shoaling in nature occurs on a variety of beach profiles and materials. The effects of these, the wave run up, and the effects of the waves on the beach geometry, are not investigated here. They are however of interest to nearshore and coastal design. A review of run up is given in Golfoploop en Golfoverslag (1972), reprinted in english for the Technical advisory committee on protection against inundation (1974). Attention is also drawn to Van Dorn (1976) and Longuet-Higgins (1983) for discussion of run up percolation and undertow ; to Powell (1988) for the effect of waves on beach geometry ; and to Svendsen and Lorenz (1989) for three-dimensional current motions caused by wave shoaling. The interactions of beach geometry and wave breaking are currently being investigated by a joint project between Edinburgh University and "Hydraulics Research" (Wallingford, England).

1.5.2 Focussed breaking.

Away from the nearshore region, breaking is predominantly caused by the superposition of waves rather than by a single wave or wave train shoaling. The superposition occurs through energy focusing. This can occur in time, (Kjeldsen et al., 1980). Alternativly waves arriving from different directions can coincide at a point because they are focused in space. This has been studied in a three-dimensional wave basin by crossing wave trains, (Halliwell and Machen, 1981). Or in a more restricted manner by using a narrowing flume to represent one sector of a circular, focused wave front, (Van Dorn and Pazan, 1975 and Ramberg and Griffin, 1987).

The breakers observed in rough seas are of a variety of types, at one extreme a localisation of energy can cause gentle spilling over a short period with an area of white aerated water at the top of an otherwise unbroken wave. At the other extreme, freak waves can reach extreme heights but with correspondingly small probabilities of occurring. Unfortunately these causes of breaking cannot be simply parameterised or deterministically modelled and a statistical approach has to be taken for their description.

The calculation of the probabilities of occurrence for any of these waves requires the modelling of the wave environment as a random process, dependent on the site and the state of development of the sea, (Nath and Ramsey, 1976 and Ochi and Tsai, 1983).

For design it is important to know the relevance of three-dimensionality and a great deal of research has been undertaken on the statistical description of real sea wave environments. However this is usually based on wave elevation records where wave breaking is only included implicitly as a process affecting the measured data. This has led to observations that the statistical behaviour of the data changes as the breaking process becomes more dominant in severe seas, (Tayfun, 1981). However the majority of statistical models used to describe sea states, or to predict extreme events for design, ignore the physical processes of wave breaking, (Houmb and Overvik, 1976 and Department of Energy, 1986).

Even if the design is based on a two-dimensional wave, the extra three-dimensional effects must be estimated and allowed for. It appears that although freak waves can be substantially larger than the limiting monochromatic cases, the parasitic effect of small scale breaking causes the extreme waves in a confused sea to be significantly smaller than the monochromatic breaking limit, (Ochi and Tsai, 1983). The frequent breaking of smaller waves in seas that are fetch rather than breaking limited is relevent to fatigue design, (Weissman et al. 1984).

1.6 BACKGROUND ON RESEARCH AND DESIGN.

The dangers an environment poses for a structure separate into short and long times of action. Over a short time an extreme load case can exert possibly destructive forces, whilst over the lifetime of a structure less extreme forces occurring very many times cause fatigue and hence possible failure. Wave breaking is very important in both cases but the main emphasis of this work is in relation to the design for the extreme load case.

This design process can be described as follows.

(The starting point is the fully complex real storm environment).

(i) Measure environmental data for wind, waves and currents.

(ii) Determine a representative case for the extreme winds, waves and currents.

(iii) Calculate the water motion under the wave.

(iv) Combine the water motion for both wave and current.

(v) Predict the forces due to this water motion.

(vi) Predict the forces due to the wind motion.

(vii) Combine these loads.

(Finally design a structure that can withstand these total loads). Reference: Department of Energy (1974).

(i) Measurement of the environment.

The offshore environment is very hostile and full scale measurement is difficult and expensive. The data that there is comes from several different sources. Many rigs have environment measuring equipment; ships and boats record some storm conditions and projects have been undertaken which were specifically designed to record storm data. For example the Christchurch bay tower project, (Bishop et al., 1980). However the scope, detail, and availability of data is at present limited, (Department of Energy, 1986).

More fundamentally the type of measurement restricts what is known. The wind speed is well recorded and can be well predicted. The topology of the sea bed is also well known. However, there is less data available on wave climates. Most of what there is is in the form of wave elevation records measured through time at a single position, and thus carries no information about the three-dimensional aspects of the waves. Recently arrays of wave staffs have been deployed yielding some three-dimensional wave information.

Very little data is available on the internal kinematics of the waves in storms. It is extremely difficult to measure this at sea. And as yet not enough is known about wave-current motions to convincingly separate the two in storm conditions, (Srokosz, 1987).

(ii) Determination of the design wave.

Only a limited amount of measured data is available for the three factors, wind, wave and current, at any design site. Hence extrapolation is needed to predict possible extreme cases. There is a trade off between the strength of any structure and its cost. Determining the strength of the structure is based on its ability to withstand the worst loading that is likely to occur over a time of fifty or a hundred years. The wind, wave and currents that make up this extreme event are predicted seperately by extrapolating the results from data gathered at or near the proposed site.

The extrapolation takes no account of the fluid mechanics occurring at the site. This is particularly important in the extrapolation of wave height. If the data includes waves that are predominantly non-breaking then the extrapolation will not reflect the effect of wave breaking. Some methods of extrapolation do bias in favour of the more extreme measured waves and so may indirectly reflect the influence of breaking, (Department of Energy, 1986).

Although the design method does recognise the existence of breaking, it makes use of it in an ad hoc manner. Only if the extrapolated wave height exceeds either 0.78 times the water depth or 0.143 times the wave length is the design wave thought to be breaking. The fact that breaking is the natural limit to wave heights in storms and that consequently the extreme waves a structure will meet will almost certainly be breaking has been ignored. It is worthwhile noting that it is precisely because waves in storms do break that they do not have heights in excess of the above limits which cause them to be regarded in design as non-breaking, (Kuo and Kuo, 1974). The breaking of extreme waves is a source of concern to offshore designers.

It may be possible at a future date to define a design wave solely in terms of the breaking limit. This would have to include studies with wave focusing as the factor causing wave breaking.

(iii) Calculations of kinematics within waves.

Having reduced the general wave condition to a three parameter design wave, the motion of the fluid must then be predicted. Before this work there was no systematic laboratory study of internal kinematics within waves. However many mathematical models have been available. The predictions from these vary considerably, particularly in the limit of large or breaking waves, precisely the limit at which danger is greatest.

(iv) Combination of water motion from waves and current.

The water kinematics from the wave and the current are linearly superposed. It is assumed that there is negligible interaction between the two. It is also usual to assume that the worst design load occurs when the wave and current motion is in the same sense. Limiting heights that a wave can obtain increase with period. Thus for a given period as measured at a fixed point, the limiting wave on stationary water is less high than the limiting wave on a forward current.

The combination of wave motion with non-slab currents is an area where laboratory work is necessary. Some mathematical models can incorporate the interaction of waves with slab, linear and bi-linear shear currents. Unfortunately the interaction is most critical in the extreme high crest region where breaking makes the flow behaviour difficult to measure and model. Banner and Phillips (1974) and Phillips and Banner (1974) discuss possible implications of a strong if thin surface shear layer and Eastwood et al. (1987) describes several of the current profiles presently used in design.

(v) Prediction of force from the water motion.

The combined wave and current action is described as a periodic motion of the water. This motion is applied to a model of the rig, and the worst relative position chosen as the design case. This usually corresponds to the rig being at the crest phase of the wave. For this phase the forces at all positions on the structure are estimated. At present Morison type expressions are used. One term in the expression for force is proportional to the square of the fluid velocities and the other linearly proportional to the accelerations, (Morison et al. 1950 and Lighthill, 1986). If the coefficients are judiciously manipulated the Morison approach can give good estimates of the fluid loading.

(vi) Prediction of force from the air motion.

This is kept totally distinct from the water loading. For a full investigation of wind loading on offshore structures see Drabble, 1989.

(vii) Combination of the loads.

The two sets of loads are simply combined; they act on different areas of the structure. The loads are used in two ways; the local loads are used to analyse individual members and joints; and the structure as a whole is tested against the net force and overturning moment.

Design must also account for the dynamic loading on the structure. The excitement of resonances in the whole structure or on individual members should be avoided.

Chapter 2 Mathematical Wave Modelling.

"Counting counting they wer all the time... They had machines et numbers up . They fed numbers and they 'fractioned out the Power of things. They had the Nos. of the rain bow and the Power of the air all workit out with counting which is how they got boats in the air and picters on the wind. " Riddley Walker by Russel Hoban.

2.1 INTRODUCTION.

This chapter should be regarded as background to chapters four and five and, with the exception of that part of section 2.7 which describes the finite difference scheme mounted on the Distributed Array Processor, this chapter reports no new work. This chapter describes the main wave theories in terms of their ability to represent the physical aspects of real waves, and discusses their accuracy and regions of applicability. This is supplemented by the comparisons made in chapter five between measured internal kinematics and those derived from the various theories.

2.1.1 Phenomena modelled.

A complete model should account for all the physical processes described in chapter 1. This would include the interactions between wave and wave, wave and current, wave and wind and wave and body. It would also model refraction, diffraction, change in water depth, and wave breaking. Finally, a full description would also model the time dependent behaviour, particularly relevant at breaking.

There are several properties of the wave behaviour and wave environment which are modelled to a greater or lesser extent by present wave theories. The much used linear theory, only strictly applicable to waves of infinitesimal amplitude, gives reasonably good results for surface properties. Higher order expansions can describe the kinematics of finite if not breaking waves, and boundary integral methods can describe some aspects of plunging breaking.

Before showing how the various wave models differ, the core of common assumptions is described. This can be seen by considering the mathematical definition of the basic problem. This is well described in the literature, (Stoker, 1957 and Lamb, 1945, 1932) and is stated briefly here.

The problem is one of describing the travelling waves in a region occupied by two fluids of different densities, in a uniform gravitational field. The fluids have a free common surface and surface tension is taken to be negligible.

The top fluid (the air) is taken as influencing the lower fluid (the water) only through the pressure it applies at the free surface. The upper fluid is otherwise unbounded. However the lower fluid is bounded by a rigid impermeable bed of fixed geometry and the ends are usually considered to match each other (cyclic boundary conditions). The lower fluid is taken to be inviscid, incompressible and irrotational.

As a direct consequence of the above characteristics of the water, the flow can be represented by the velocity potential. The water particle velocity of the fluid is by definition the vector gradient of the velocity potential.

The velocity potential or the simply related stream function, forms the basis for all wave models. This obeys Laplace's equation and consequently has the extremely useful property that if its value is known over the boundary of an ideal fluid then its value is uniquely defined for all points within the body of the fluid. Thus, for waves if the velocity potential is known at the free surface and on the bed, and the end boundary conditions can be specified, then the potential and more importantly the velocities can be calculated for all points within the wave.

As no fluid passes across the bed the stream function along it is a constant value. It also follows directly from the definition of the problem that Bernoulli's equation is satisfied on the free surface. This can be expressed as :-

$$\Phi_t + \frac{1}{2}(u^2+v^2+\omega^2) + \frac{P}{\rho} + g y = \emptyset$$

where ρ is the water density, g the gravitational acceleration and P the pressure. Thus the velocity potential Φ is simply related to the vector velocity and the elevation y for each point on the surface.

There are several ways of proceeding from this basic problem. However there is one case that is so central to offshore design that its additional assumptions are described here. This is known as the "design wave" because of the requirement in design to reconstruct wave kinematics from three single parameters, the period, depth and height of the wave.

The design wave is derived from the three parameters according to the following additional assumptions:

It is one of an infinite train of waves, all identical, travelling in a constant depth of water. That is, periodic boundary conditions are assumed. The waves propagate without change in form and the pressure along the free surface is constant.

As a corollary to the surface being of constant shape the free surface like the bed is a streamline and hence has a constant value of its stream function along its length. These simplifications mean that computationally the problem is of a finite domain and in terms of the expansion methods, the functions used have to be periodic with a spatial frequency that is an harmonic of the fundamental.

2.2.1 Linear theory.

This theory, first developed by Airy in 1845 uses the assumption that the wave height, H, is very much smaller than both the wavelength and the still water depth d. This allows the non linear free surface boundary conditions to be made linear by discarding all terms above the first order in the wave height. Explicitly, the linear free surface boundary conditions are :-

$$\left.\frac{\partial \phi}{\partial z} - \frac{\partial \eta}{\partial t} = 0 \quad \text{and} \quad \frac{\partial \phi}{\partial t} + g\eta = 0 \right\} \text{ at } z = d$$

If the periodicity is enforced, and the variables separated in the velocity potential, then it transpires that the velocity potential has a periodic component, that is :-

$$C_1 \cos[k(x-ct)] + C_2 \sin[k(x-ct)]$$

Further, if the crest is chosen to be at the x origin then C1=0 and in full the velocity potential is :-

$$\phi = C \frac{\cosh(kz)}{\cosh(kd)} \sin[k(x-ct)]$$

These linear boundary conditions are then applied at the still water level, leading to the following results :-

linear dispersion relation $\quad c^2 = \frac{g}{k} \tanh(kd)$

velocity potential $\quad \phi = \frac{gH}{2\omega} \frac{\cosh(kz)}{\cosh(kd)} \sin[k(x-ct)]$

surface elevation, η, $\quad \eta = \frac{H}{2} \cos\theta$

Where k = wavenumber = $\frac{2\pi}{L}$.

These results are only strictly applicable to infinitesimally small amplitude waves, and there is some ambiguity as to how they should be applied to the practically important finite amplitude waves. However the results are surpisingly good and have found widespread use. In particular, the linear dispersion relation is often used as a measure of the wave celerity. Also, the full set of results is almost universally used for problems such as random seas and complex three dimensional bed conditions where many wave components are present and the rapid accumulation of terms would make the more sophisticated theories too demanding on resources.

2.2.2 Stretching methods.

Because linear theory only applies strictly to infinitesimally small amplitude waves and the purpose of wave theories is to predict finite waves, there is pressure to extend the theory into the crest and if necessary modify the trough .

Several methods have been put forward. Here we present the commonly used extension method and also those proposed by Wheeler (1970) , Chakrabarti (1971) and Mo & Moan (1984)

(i) Extension. The simplest method and the one usually assumed by default is that of taking a sinusoidal profile of the required amplitude and assuming that the expressions derived for the the infinitesimal wave are valid at all positions within the finite wave.

(ii) Wheeler stretching. This method assumes the finite sinusoidal profile. For each phase of the wave all the expressions are stretched in the vertical direction such that the top value defined for z=0 becomes the value at the surface of the wave. All the values within the body of the fluid are similarly shifted.

(iii) Chakrabarti (1971) proposed modifying the expression for pressure such that it exactly satisfied the dynamic boundary condition at the surface of the finite wave.

(iv) Mo & Moan (1984) proposed that the velocity at all points above the still water level should be equal to the value at the still water level.

2.3 CNOIDAL AND SOLITARY WAVES.

First developed by Kortweg & de Vries in 1895, this method is an attempt to move away from the unnatural use of trigonometric functions in the representation of all wave motion. In particular shallow waves with their peaky crests and long shallow troughs have obviously non-sinusoidal surface profiles. The cnoidal method uses and takes its name from the more general and more complex Jacobian elliptical function, cn. This has two important limiting cases that tie it in with other wave representations. For short waves, the cn function reduces to being sinusoidal and in the long wave limit, it describes the solitary wave or soliton. These are the waves with sharply peaked crests and infinite length troughs that are discussed by Russell (1844), Boussinesq (1871), Rayleigh (1876) and again by Rayleigh (1914).

Like the sinusoidal approach, the cnoidal function can be made the basis of an expansion method. It was extended to second order by Laitone (1960) , third order by Chappelear (1962) and later explicitly to fifth, and generally to any desired order by Fenton (1979).

The bulk of the laboratory waves reported here are too short to be directly comparable with cnoidal theory. Where they are compared, the cnoidal theory significantly over-predicts the horizontal velocities in all but the very highest regions of the crest.

Hyperbolic theory is a simplification of the cnoidal theory, introduced by Iwagaki (1968). This replaces the Jacobian elliptic functions by simpler hyperbolic functions. As a consequence of using these functions, the solutions are not strictly periodic. This theory is applicable for Ursell numbers greater than about 58. $(U_r = H k^{-2} d^{-3})$.

2.4 STOKES.

The Stokes method is the classic solution to the Design Wave Problem. The method works by expressing the velocity potential, or the stream function, as a truncated Taylor series expansion in circular functions of the horizontal coordinate.

The boundary conditions are applied by substituting quantities derived from the series expansion of the potential in their analytic expressions. These expressions are subsequently simplified by excluding all terms of higher order than that previously chosen for the expansion parameter in the expression of the potential.

The work involved in the mathematical manipulation for the evaluation of the coefficients is tedious and lengthy, and increasingly so for higher orders. Stokes (1847) develops the general case for second order and the simplified deep water case for third. Using newly available computing resources, Skjelbreia & Hendrikson (1961) developed the theory at fifth order and presented the values for the coefficients in tabular form. This has led to the very widespread use of Stokes fifth in engineering practice. The extension to high order has been presented by Schwartz (1974), but higher order terms are not always convergent as has been pointed out by Koh & Le Mehaute (1966). Accuracy does not always increase with order, as the depth becomes small, so lower order expressions can become preferable to those of higher order.

Besides the expansion above, Stokes also introduced two wave related concepts that have kept his name.

The first of these is the Stokes drift. Stokes (1847) notes that one consequence of going above first order is the prediction of a net motion of the fluid in the direction of the wave travel.

The second is the Stokes limiting wave. Stokes (1880) uses a simple argument to show that the minimum angle the crest of an unbroken travelling wave can obtain is 120 degrees. This occurs where the horizontal particle velocity in the crest equals the wave celerity. Banner and Phillips (1974) show that Stokes waves travelling on a rotational flow produce fluid velocities equalling the phase speed for wave amplitudes below those for the irrotational Stokes waves.

The reference frame in which one chooses to describe wave motion is somewhat arbitrary. The two most fundamental frames are :-

(i) The rest frame of the wave. That is the frame where the wave profile is fixed but where there is a substantial net mass flux.

(ii) The "laboratory" frame, where there is no net flow of water.

The two frames move with respect to each other at a speed which is the wave celerity. However there is more than one definition for zero net flow of water. The two most usual definitions are introduced in Stokes (1847). These are (a) " the mean horizontal velocity at each point of space occupied by the fluid is zero." And (b) " the mean horizontal velocity of the mass of fluid comprised between two very distant planes perpendicular to the axis of x (wave direction) is zero."

2.5 DEAN'S STREAM FUNCTION.

There are two applications of this method, both described explicitly in the original paper, (Dean, 1965). First, the solution to the problem of a wave of steady, defined surface profile, Dean's case A. Second, Dean's case B is a solution to the "design wave" problem.

The solution proceeds in a similar way for both. The stream function is described as an expansion in sinusoidal terms. The coefficients are then derived by reducing the errors between the model predictions and the explicit values for the boundary conditions.

The two cases are different as they have different restrictions on the boundaries. In both cases there is no error associated with the bottom and the end (periodic) boundary conditions. The expansion satisfies these implicitly. There is however a difference associated with the free surface. In case A there are errors derived from the position of the wave profile and also from the dynamic free surface boundary condition. The latter is expressed in terms of the Bernoulli constant. In case B, the surface profile is initially undefined, and the error has no term from the matching of the profiles. However some error can arise from the positioning of the mean water level.

There is choice in the weighting of the errors when they are being minimised. Firstly, the errors are calculated as the sum of contributions from points along the free surface, the position of and the weighting for the various points is somewhat arbitrary. The method given in Dean (1965) gives equal weighting to all points and they are equally spaced in the horizontal direction. Secondly a relative weighting must also be applied between the positional and the Bernoulli type errors.

The second case, Dean's case B, is of particular importance because (i) it has found widespread use in engineering design and (ii) it is directly comparable with the wave models of Airy, Stokes, Korteweg & de Vries and others, being a solution for the design wave.

When considering the Dean's solution and that of Stokes, it should be noted that what are known as the orders of each are somewhat different. In the Stokes method, the order is based on the power of the expansion parameter. Each order is capable of having both sine and cosine terms (the former usually set to zero). However in the Dean's method, the order is derived from the number of coefficients used in the Fourier expansion, starting with a cosine term and then alternating sine and cosine terms. Dean also dismisses the sine terms on grounds of the horizontal symmetry of the boundary conditions. Thus if we consider a wave represented by five cosine terms, it will be called fifth order if it is a Stokes representation, but ninth if Dean's.

The Dean's method has been extended to very high order by Chaplin (1980), section 2.6. It has also been developed to include the case of a wave travelling on a shear current, (Dalrymple 1974).

2.6 HIGH ORDER AND ANALYTIC SOLUTIONS.

The mathematical problem of the periodic wave of permanent form can in one sense be considered resolved as Cokelet (1977) provides an exact analytic solution. However the area is still one of interest as solutions are wanted that are more easily applicable. In design there is room to allow approximation in the description of the design wave because its prediction is imprecise and its appropriateness questionable. In particular no solution to the design wave with a steady profile can describe the effects of breaking.

Very high order approximations have been developed. These are based on the Stokes, Dean's and the Cnoidal approaches, and are reported in Schwartz (1974), Chaplin (1980) and Fenton (1979) respectively.

These solutions to some extent conclude work on solutions for the design wave. However they focus attention on the important related topics such as the validation of the solutions by comparison with laboratory experiments, an objective central to this thesis.

Results for the maximum attainable wave height calculated from Cokelet's method are presented in chapter four for comparison with the measured flat bed results. Also, the internal kinematics calculated by Chaplin using his own extended Dean's model are used for comparison in chapter five. Chaplin (1980) has already demonstrated the close agreement for high waves between his high order solutions and Cokelets results, so the comparison here can be thought of as one between the results of experiment and those of the exact solution of the "design wave" problem.

2.7 OTHER WAVE MODELS.

The theories discussed so far in this chapter are, with the exception of Dean's case A, all solutions of or approximations to the design wave problem. There are many other wave theories, categorised here in three groups. There are also some noteworthy extensions to wave models which are discussed briefly at the end of this section.

2.7.1 Other wave models.

(i) Those which solve the same problem as Dean's case A very much the same problem as the "design wave" except that the surface profile is explicitly defined. It is usually the case that the restriction of a steady solution is kept, allowing the surface to be taken as a stream line, i.e. an equi~~potential~~ stream function. When high quality measurements are available of both the surface and the velocity over it, then a generalisation to a time dependent surface would become very valuable. Solutions to this problem include the finite difference methods, a version of which has been mounted and run on the 64x64 Distributed Array Processor (DAP) at Edinburgh, and results from which were seen to be in good agreement with measured results. Unlike any of the other wave theories studied here the theory over-predicts the velocities in the high crest region (Griffiths, 1985).

These theories have the future advantage of being applicable to quasi-random seas. This can be achieved by enlarging the length scale for periodicity so as to make a wave packet periodic rather than any particular wave within it. They can also be simply extended to three dimensions.

(ii) There is a very important group of theories which, as above, use a region of fluid with completely defined boundary conditions, but unlike the above, are not restricted to a measured profile, but rather, develop their own. The most important of these is the boundary integral technique. This was applied to wave breaking by Longuet-Higgins and Cokelet (1976) and subsequently developed by Peregrine and others at Bristol University. These theories time step a region of fluid, allowing the previous motion to determine the shape and movement of the surface profile, ie predicting the boundary conditions which are imposed on the solutions as in (i).

Appropriate comparisons have been sought between these results and measurements taken here, but at present they have to be somewhat inexact. The experimental facility generates waves in a finite region of water and causes them to break by allowing them to shoal on an inclined beach. The numerical waves however, instantaneously appear as infinite trains of waves on water of a fixed depth. If they are too large to remain stable then their development to breaking can be calculated through time. Whilst working on methods of modelling a wave paddle and non-horizontal beds, Peregrine has provided us with interim results where a flat angled bed is crudely modelled by finding iteratively the steady wave, given by its height and depth, which, when dumped onto a new depth, takes the correct length of time to break. This length of time is correct if it corresponds to the wave crest travelling a distance such that the ratio of change in depth to this distance is the bed slope used in our laboratory. This method although crude, does produce remarkably good results; these are compared with experimental results in chapters four and five. One problem with this method is that it can produce significant reflections, and this is likely to increase as the slope studied increases. This corresponds to the more highly plunging breakers.

(iii) The third group of wave models is a loose collection of those which do not fall into any of the first two groups. There are many of these, mostly based on linear theory and describing three dimensional conditions, wave refraction and other wave/body and wave/current effects. They are used where the wave height rather than the internal kinematics is the required result and are not relevant to the present work.

2.7.2 Extensions to wave models.

One very important area in design is the effect of the combination of a wave and a current. There is a great deal of argument at present as to how a current should be represented, particularly the current velocity profile with depth. This is usually described for the current alone and many almost arbitrary solutions have been proposed for its extension in to the crest of waves. However, this is where the current has its most significant effect on wave behavior.

Several theories are now able to include constant vorticity, linear or bi-linear shear currents. The theories extended are Stokes third, (Tsao, 1959); solitary wave, (Benjamin, 1962) ; stream function, (Dalrymple, 1974) ; boundary integral, (Simmen & Saffman, 1985).

2.8 REGIONS OF APPLICABILITY.

Many different methods have been used to establish the validity of the various wave theories. Ideally their predictions of internal kinematics would be compared with full scale waves over a range of conditions. Unfortunately this is impractical. The present work takes the next best approach and compares the internal kinematics with measurements from laboratory waves.

Prior to this, the validity of the theories was based on several factors. In absolute terms, comparisons had been made of the surface parameters of waves; for example, between measured and predicted phase speeds. Also some comparisons had been made with incomplete measurements of the water particle velocities. Also the relative validities of theories within a family of solutions was establishable. Thus the Dean's and Stokes approximations have been compared to the predictions from Cokelet's complete solution, and Dean (1968) established the relative validities of wave theories based on their ability to fit pre-specified boundary conditions.

In terms of the design use of wave theories, there are a range of waves which need to be described. The three parameters, period, height and depth, determine an environment with two degrees of freedom. The regions of applicability have usually been drawn as areas on a graph with the y axis as non-dimensional height and the x axis as non-dimensional depth.

As the present work is directed at the extreme height limit, the area of applicability reduces to a line. Dean's results, based on his boundary condition criterion commend Cnoidal in the solitary wave limit (d' less than 0.03), Deans Vth (d' over 0.09), Linear theory (intermediate values), if the Dean's theory results are ignored Stokes Vth (d' over 0.09)

where $d' = \frac{d}{gT^2}$

Note that these comparisons do not include the high order or analytic solutions.

Experimental verification is usually performed by comparing the measured and predicted values of the internal velocities at the crest phase of the wave. This phase is where the maximum velocities and heights occur and therefore the phase at which the maximum force and overturning moment on a structure would be generated.

Comparisons between measured and theoretical results have been explicitly made: Le Mehaute, Divoky and Lin (1968) compared the horizontal velocities below the crest for measured results and various theories. Other researchers have reported measured results and used them in comparisons, but the results have been inconclusive, with few measurements above the still water line. This and the limited nature of the offshore data has led to dangerous conclusions being drawn. In particular, the Department of Energy in its background notes to "Offshore Installations : Guidance on Design and Construction (1984)" writes when describing the comparison of measured velocities in extreme waves ; " Information that is available, however , tends to show that non-linear regular wave theories overpredict particle velocities at all levels. ..."

The present work invalidates this statement and shows that it is dangerously misleading.

Chapter 3 Experimental Facilities and Procedures.

3.1 GENERAL DESCRIPTION OF FACILITIES.

3.1.1 Schematic description of the experiment.

All the experiments reported here were performed in the Edinburgh tank (1), the long wave flume. A schematic description of the facilities is given here with a diagram fig. 3.1.1 and this is followed by a brief physical description and a sketch of its development from Sept. 1985 to Sept. 1988. Sections 3.2 , 3.3 and 3.4 describe in more detail the wave generator, the flume and bed and the laser Doppler anemometer.

The high accuracy in this experiment relies on the performance of three separate functions: 1 The generation and propagation to breaking of very pure waves. That is, waves without free, travelling, harmonics; waves free from tank idiosyncracies such as cross waves or seiching and waves with minimal disruption from reflected waves. 2 The accurate and non-disruptive measurement of the flow, in this case using the technique of laser Doppler anemometry (LDA). 3 Where a repeated or accurately positioned measurement is required, there must be a highly accurate timing system linking the generated wave and the measurement system.

The diagram of the system presented in fig 3.1.1 shows the information flow in the experiment which is split into seven different functional areas. These are described below:

1. Accurate clock: The majority of the work reported here used a highly accurate fixed 16 Hz oscillator. The experiments on the flat bed used instead an accurate analogue signal generator.

An accurate clock is important because wave behaviour is highly time dependent. For a given generated wave, an error in time produces an error in the position and also in the stage reached in the breaking process of the wave. Also a change in the period of the generated wave changes the wave celerity and produces an error in timing when the wave breaks exaggerated because of the distance it will have travelled up the tank, (up to four wave lengths.)

The latter effect was used in reverse as a way of observing possible errors associated with the oscillator time source, and as a method of retuning the analogue source used in the flat bed experiments to a previously used frequency.

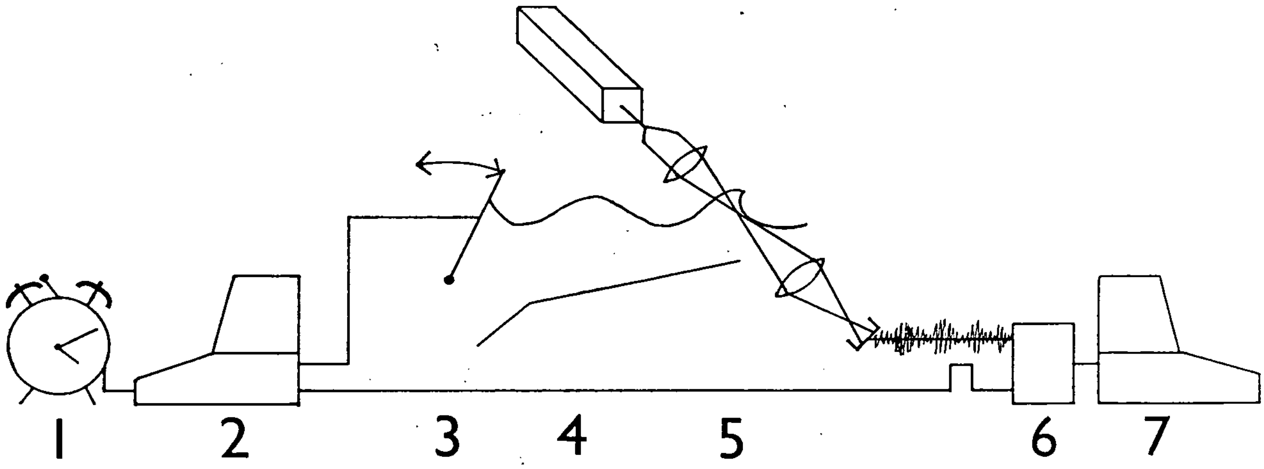

Fig. 3.1.1 Schematic diagram of the experimental facility.

2. The first micro has two main functions; it produces the request signal to the wave generator and also a phase locked trigger pulse. In this work, where monochromatic waves are studied, the demand signal is a simple sinusoid. The micro is programmed to simulate much more complex sea states, but can only accept components, or in our case single frequencies, which are integer multiples of 1/16 Hz. The second function of the micro is to produce a trigger pulse, phase locked to the generated wave. This trigger exactly fixes in time the point for which the laser Doppler anemometer signal is to be recorded. The relative position of the wave and the trigger signal is set by the operator.

A similar phase locked signal can be taken from the micro to be used as the trigger for a camera or a flash gun. Note that the finite response time of the camera and flash introduces a time delay between the photograph and the recorded LDA signal.

3. The wave maker is of the absorbing hinged flap type and is situated in the "deep water" section of the tank, the shallow water conditions being achieved by running the waves up an initial steep slope. This deep water generation method is observed in Flick and Guza (1980), to virtually eradicate the unwanted free second harmonics associated with waves generated in shallow water.

4 . The beach consists of the steep initial section, running from deep to intermediate water depth, and the test section of the required slope. The beach is sealed to the tank walls so as not to allow any recirculation or periodic streaming produced by the changing pressure under the waves. The bed is truncated

at a position well before it would have crossed the still water level, typically at a depth of about 8cm $\sqrt{5}$. The LDA optics run continuously, and the two beams cross at the single position at which a measurement is to be taken. Only one component of the kinematics is measured at any one time; the beams are rotated to measure the second component. For ease of moving the measuring volume, the optics are mounted on a gantry which can move horizontally along the tank. On the gantry the final sections of the transmission and the reception optics are mounted on optical benches and can be simply reset at different vertical positions.

6. The continuous signal from the laser Doppler anemometer arrives at the high speed digital recorder and the timing of the measurement is achieved by sampling the signal when the recorder is triggered to do so by a signal from the first micro. Once the signal is recorded, analysis can proceed outside real time.

7. The second micro receives the data from the digital recorder. This runs a suite of analysis programs which Fourier transform various sections of the record. The vast majority of this work used the velocity and acceleration measuring option. This transforms the first and last quarters of the record separately and calculates their mean and difference. See section 3.4.2 for a fuller description.

3.1.2 Physical description of the experiment.

The tank is a glass walled flume 0.3 m wide with an available water depth of 1.0 m . It is microcomputer controlled and uses an absorbing wave generator and a laser Doppler anemometer.

Development.

The tank was initially designed for deep water random wave studies (Easson and Greated, 1984). Hence, while it had a versatile wave generation program, it was short (only 9 m long) and was of a fixed uniform depth (1 m) . There was also a light beach that had been used for early work on shoaling: This was flimsy, not sealed to the side walls and stood on the tank floor on independently adjustable legs. The electronic signal processing for the laser Doppler anemometer was performed by an autocorrelator (Easson and Greated, 1985), and the wave generating micro.

After analysing some of the theoretical aspects of acceleration measurement using the pulsed correlation technique, see appendix 1 (Easson et al., 1986), the correlator was decomissioned and replaced by the digital transient recorder and the second microcomputer.

The optics were realigned avoiding the previous temperature dependent functioning of the phase shifter. The original bed was replaced by a more sturdy version with close fitting seals to the side walls and floor. The feet were replaced by an easily adjustable top mounted system. A current facility was added.

The tank was extended to 12.9m by adding an extra 2 bays giving an extra 3 m in the working section . This enabled slopes of less than 1:30 to be studied and allowed much longer entrance lengths to be used for current work. The current facility was also up-rated.

Extra tank bracing was added in the high centre of the glass sections. The contraction in the tank width that this caused was used to hold the bed enabling the unwanted surface piercing bed mounts to be removed. See section 3.3.

3.2 THE ABSORBING WAVE GENERATOR.

The wave generator used here is of the absorbing type designed and built at Edinburgh University by the Mechanical Engineering Department. Further details of the generators and their operational characteristics are given in "Edinburgh wave power project, fourth year report 1978".

The generator consists of a 0.64 m flap, hinged at the lower edge. This is air backed and has the static water pressure compensated for by a steady tension in the drive cable. The required outgoing wave is specified by the microcomputer (2) and this is the input "demand" signal to the wave generator. In order to have the generated wave identical to the demanded wave, account must be taken of the pre-existing wave environment at the paddle. This mainly consists of waves caused by the reflection at the beach end of the tank. If the paddle was simply driven, exactly following the demand signal, then it would appear to these returning waves as an almost perfect reflector. However the wave generator has both velocity and force sensors, the signals from which are used to modify the demand signal such that the returning waves are largely absorbed and the outgoing wave best matches the demand signal.

The paddle is driven by a stepping motor and is mounted such that the hinge is at a position 0.55 m below the still water level. The operating range of the paddle is from 0.5 to 2.0 Hz. The wave amplitudes used here are well within the range of the generator and apart from frequencies above 1.6 Hz., the absorption at the paddle is above 80% .

The paddle as shown in fig 3.2.1 is mounted as a separate unit within the tank. which gives some versatility in terms of its positioning, in both depth and position along the tank. Versatile depth positioning had been sought so that the

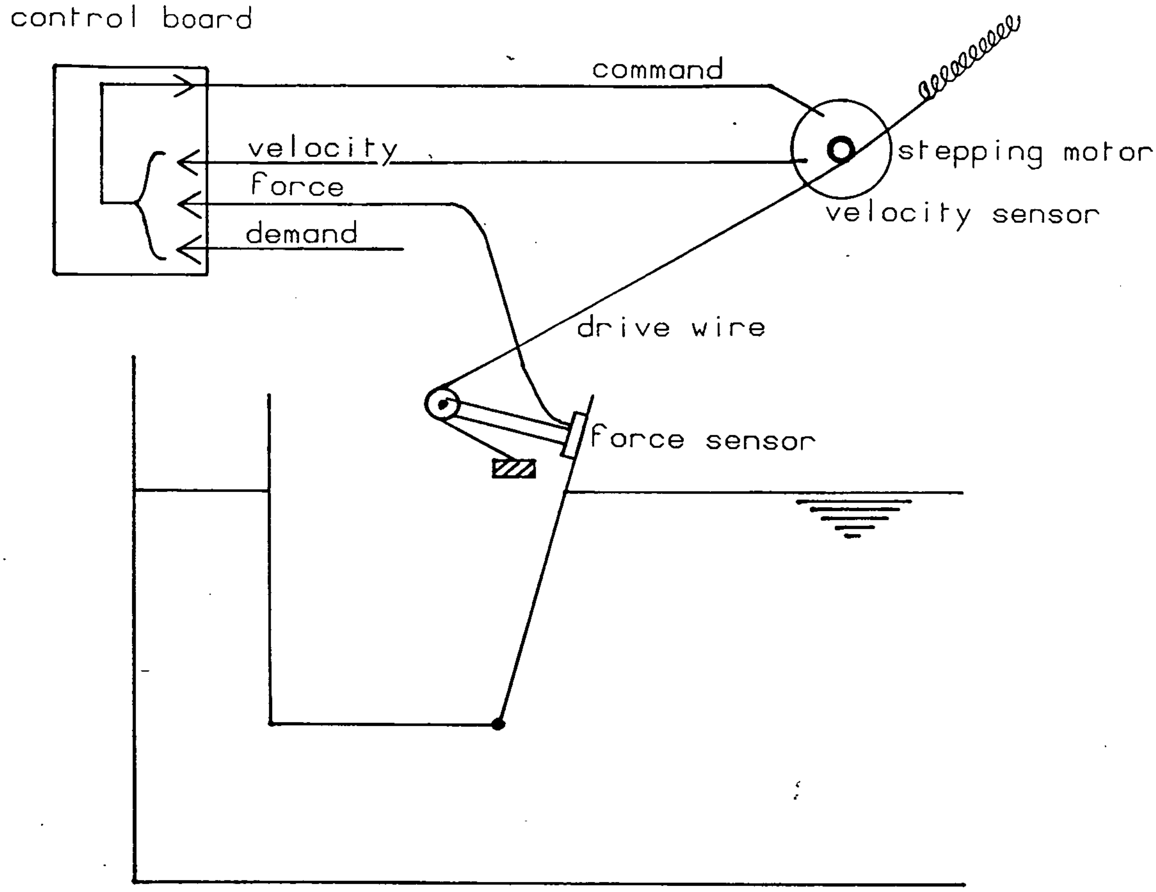

Fig. 3.2.1 The absorbing wave generator. water level and paddle could be changed together giving an effective change in water depth, and also because the optimal depth of the flap pivot was a function of wave frequency. This facility was bought at the cost of having a considerable gap between the edges of the flap and the tank walls.

3.3 THE FLUME, WALLS AND BED.

The wave flume is of uniform cross-section, 1 m deep, 0.3 m wide and varied in length from 9 m initially to 12.9 m after 1987. The tank is constructed in sections, each section consisting of a pair of glass sheets 18 mm thick, 1.85 m long and 1.07 m high. These are held in place by a framework of "Dexian" and the

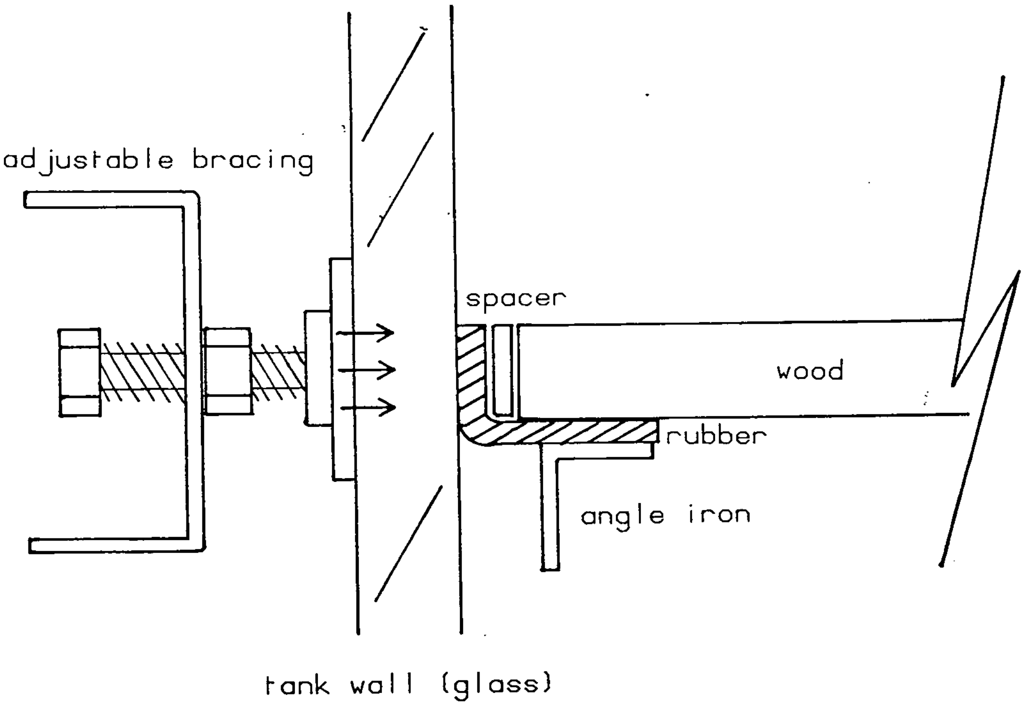

Fig. 3.3.1 Half crossection of the tank showing bed construction and fixing.

bottom of the tank is glass for most of its length. The final, beaching, section is constructed of 18 mm thick marine plywood. This was used instead of glass as the final section does not have to be transparent.

The initial dexian framework was supplemented in 1987 by additional bracing as it had been noticed that the glass walls bowed out under the static water pressure. At the worst point mid-way between the vertical supports, this amounted to a displacement of about 2.5mm .Bracing was applied at these mid points at a vertical position some thirty or forty centimeters below the still water level. This additional support was designed to be applied with the tank full. The net force, and therefore the width of the tank, at the points of bracing could be varied.

The sturdy bed replaced the original flimsy structure and was used throughout the present work. The bed is constructed of 20 mm thick marine plywood, strengthened by angle iron running along the length. A water tight seal was provided between the sides of the bed and the tank walls by stiff rubber running the length of the bed, held between the plywood and the angle iron.

The cross-section of the bed is shown in fig 3.3.1. The seal was included to stop the periodic rushing of water up and down the gap as the waves passed, and also to stop any recirculation occurring below the bed.

The play in the side walls was used to change the manner in which the bed was held in position. The sturdy bed was a close fit in the tank and could only be moved when tank was full of water and the static water pressure sprung the walls slightly apart. Initially it was held in place by thin steel members aligned with the flow and clamped to the tank above the water surface. A further consequence of straightening the bowed side walls was that the walls tended to grip the bed. This was enhanced by adding thin aluminium shims between the bed and the side walls. The gripping effect was then sufficient to remove the need for additional methods of supporting the bed and the vertical supports were removed.

With the extra bracing slackened the bed could be repositioned from above. Then, with the bracing re-tightened, the bed was held firmly in place.

The bed was hinged at five points along its length, allowing the beach geometry to be varied. The experiments reported here were performed on four different slopes; the complete beach geometries are shown in fig 3.3.2.

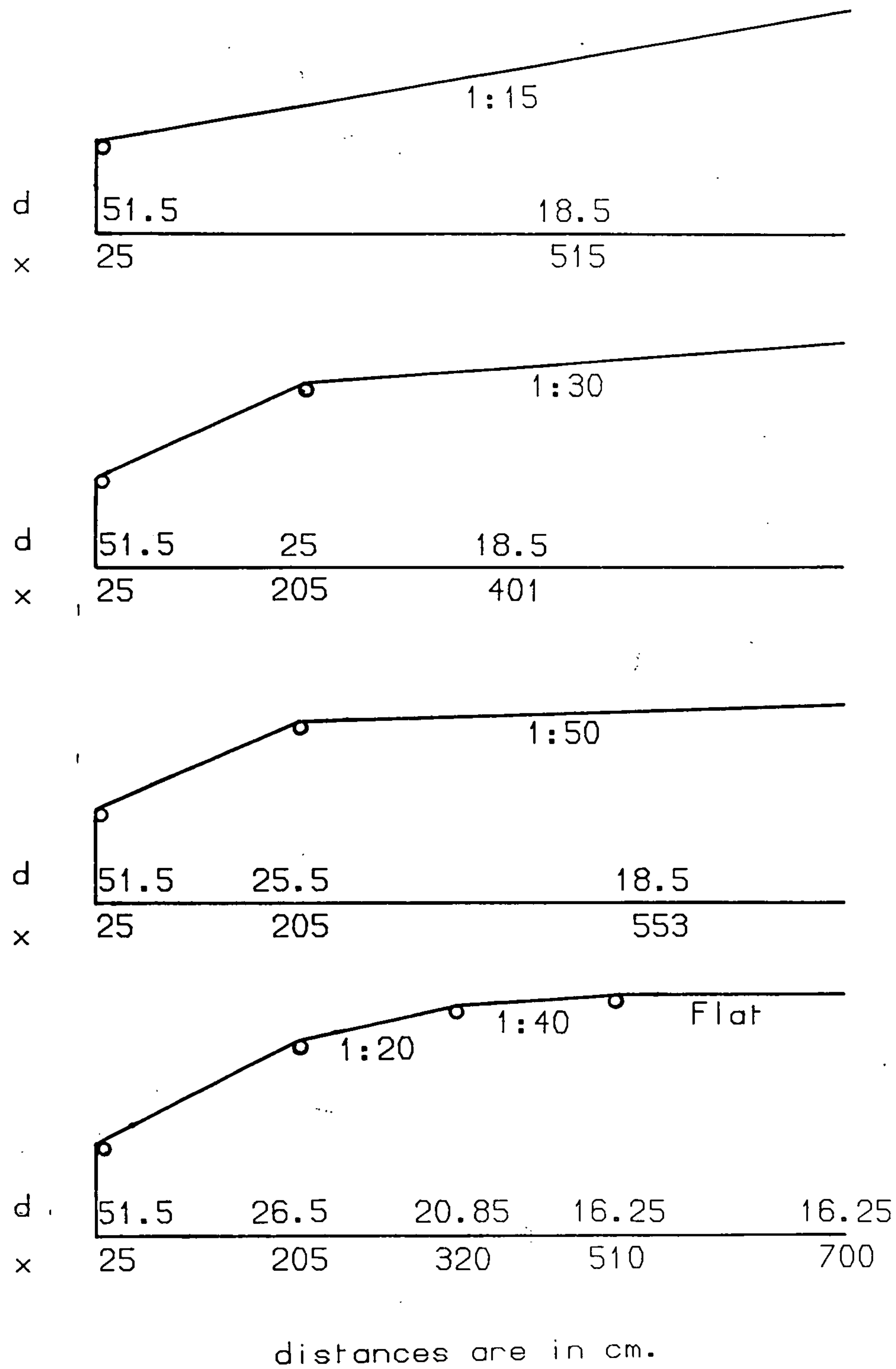

Fig. 3.3.2 Diagram showing bed geometries.

3.4 LASER DOPPLER ANEMOMETER.

3.4.1 Laser Doppler anemometer ; optics.

The laser Doppler anemometer used here is a dual beam forward scatter type with the beams being of equal intensity.

The optical arrangement is a modified version of that described in Easson and Greated (1984). The transmitting optics consist of, in order, a low power He-Ne laser (5 mW.), a beam splitter, a phase shifter, a condensing lens and a system of prisms.

The beam splitter was used to produce a pair of beams of equal intensity. The positioning and the focal length of the condensing lens were chosen to give a narrow angle of intersection and a measuring volume closer to the wall of the tank that the beams enter through. This minimises the loss of signal due to blocking of the beams by the water surface. The receiving optics consists of a pair of beam stops, a collecting lens, a pin hole and a photodiode (fig. 3.4.1).

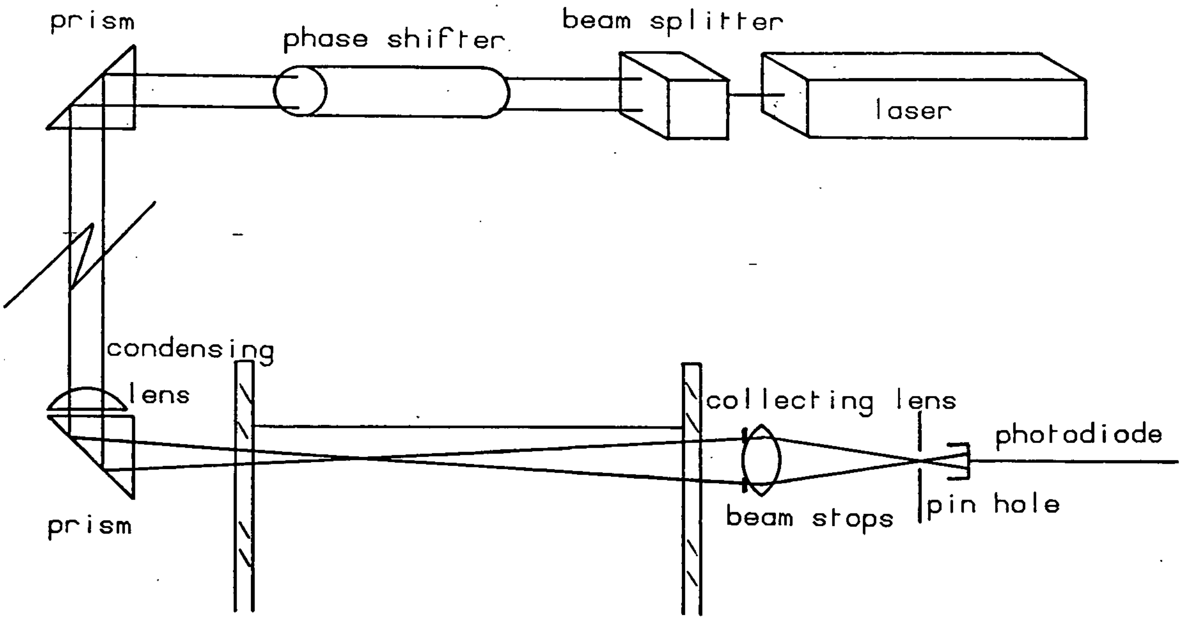

Fig. 3.4.1 Diagram of laser Doppler optics.

All the receiving optics on one side of the tank and the condensing lens and the final prisms on the other are mounted on two separate vertically hung optical benches. The components can be moved to change the vertical position of the measuring volume. The entire optical arrangement is mounted on a gantry that allows horizontal re-positioning.

The LDA system is sensitive in two areas; Firstly, a slight loss of alignment, of the order of 0.3 mm causes a large if not complete loss of signal. Secondly, low Doppler frequencies, below 10 kHz, are ambiguous in terms of flow direction and occur in a frequency range that already has high noise levels.

Problems of alignment increase with the separation of the transmitting and the receiving optics. In the present case the tank is a physical barrier and the optics have to be mechanically joined by a framework going over the flume. This framework, made from "Dexian" was only semi-rigid and frequently lost alignment. However, as the point of measurement was often moved, and because the method of alignment was simple, the inconvenience caused by this problem was accepted. Many LDA systems are difficult to align, but with complete access to the separate components, alignment of this system was easy. It consists of removing the beam stops, relocating the actual intersection of the beams on the pin hole and replacing the beam stops.

The loss of signal in the low frequency noise and the ambiguity in flow direction about zero are remedied by the use of the phase shifter. This introduces a shift of the phase between the two beams in the form of a sawtooth (ref. Durrani and Greated, 1977). If one considers the two beams to be producing a Young's two slit interference pattern at the measuring volume, then the introduction of the phase shifting causes the fringe pattern to move with the effect of shifting the Doppler frequency. The phase shifter in this system could be set to 20, 50 or 100 kHz.

The fundamental relation in laser Doppler anemometry is that between the Doppler frequency, fd, and the measured velocity. It is shown (Durrani and Greated, 1977) that, for the forward scatter anemometer used here :-

u = (laser wavelength / (2 Sin P)) fd

where u is the component of flow velocity being measured and P is the half angle of the beam intersection (1.88 degrees.)

The He Ne lasing frequency is 632.8×10^{-9} m

Hence u (m/s) = (9.64×10^{-6}) fd (Hz)

The half angle was found accurately by measuring the beam separation when they had travelled over 17 m from their point of intersection. (Separation = 1.12 m, distance from intersection = 17.065 m, hence P = 1.88 degrees.)

3.4.2 Laser Doppler anemometer ; signal processing.

The signal from the photodiode contains information on the flow at the measuring volume as a high frequency signal. The frequency is kept between 20 and 90 kHz by judicious use of the phase shifter. The signal is passed through a band pass filter set at 20 to 90 kHz and amplified before being passed to the digitiser. This filtering removes both low and high frequency noise. In exceptional circumstances where the 50 kHz noise is dominating the signal and the signal is of a frequency significantly different from 50 kHz then the band width of the filter can be reduced to remove the 50 kHz noise. Having recorded the signal, further processing need not occur in real time.

Because the filtering removes all frequencies higher than the Nyquist frequency, prior to digitising, there are no aliased signals which would otherwise have arisen due to the discrete nature of the sampling of the signal.

The recorded signal is displayed on an oscilloscope; the operator then has the option of rejecting it on grounds of signal strength. A good record has strong signal in both its first and last quarters. An experienced operator can also detect at this stage such faults as one beam passing the edge of the wave which appears as two short lengths of zero signal with a short length of loud signal between. Other recognizable faults that can be detected at this stage include the leakage of part of one of the main beams around a stop and into the detector, this being characterised by regular patterns showing the interference between a fixed frequency and that of the digitisation.

Good signals are then passed to the second micro which performs separate Fourier transforms on the first and last quarters of the record. The transforms are displayed and the operator has a second chance to reject the signal. Rejection at this point can be for either of two reasons: 1 if the signal exhibits a dominant noise peak, typically at 50 kHz, or 2 if the spread of Doppler frequencies is broad and the micro has selected an extreme and unrepresentative value. Note that the presence of a Doppler signal indicates that some particles are travelling at the related speed, but the strength of the signal indicates loud scattering at this speed, rather than the predominance of this speed within the measuring volume.

Satisfactory Doppler frequencies are then recorded. Many values are taken for each position of the measuring volume. The number taken varies depending on the repeatability that the individual values are showing. Thus for elevations low in the wave where the flow is highly repeatable, as few as four individual values are recorded, but in the high crest region, where the scatter of measured velocities is largest and where most design importance is attached, as many as 16 individual values are recorded.

For several positions near the surface it was not possible to record continuous good signal. In these cases the acceleration measurement was abandoned and the micro directed to transform short regions with high signal quality, giving results for velocity.

Having recorded sufficient results at any one position, the phase shift frequency is recorded on the disc and another position chosen. When required, the second micro reads the records from disc and calculates the velocities and accelerations.

3.5 SURFACE MEASUREMENT TECHNIQUES.

The parameters used to describe the waves were measured in various ways. Those measured were : period , breaking point , depth , crest elevation and trough depth , set down , wavelength , celerity and the surface profile. The different techniques used to measure each of these are described below:

Period: The period is the fundamental characteristic of any wave and was measured or defined by the time keeping of the clock and the period as specified on the wave generating micro. This defined period is to all intents and purposes, completely accurate.

Breaking point: Defined as the point where the wave becomes vertically fronted. This is measured in both space and time by watching the wave as it breaks from a point slightly in front of the crest. This was made easier by holding a straight object vertically on the near wall of the tank. Allowance was made for parallax and the position recorded.

The waves are not perfectly two dimensional. In particular, small cross waves or ripples were generated at the point where the top of the crest meets the side walls. Some waves break at the sides first, the breaking spreading inwards. Other waves, where the ripples from the previous crest meet at the centre of the crest, would break from the centre out. Where immature breaking occurred because of such triggering, allowance was made and the point of breaking taken as somewhat later. Where possible in these circumstances, an undisturbed region of the crest was watched and the point where it broke noted. If however the triggered breaking seemed to have delayed the breaking of the otherwise undisturbed section then some position between these two points was taken as the breaking point. In the worst cases the variation in position was about 15 percent of the wavelength, but these were rare, the majority of the waves breaking uniformly across the tank.

The time of the breaking was found by using the photographic flash controlled from micro (2) and phase locked to the wave. The relative phase of the wave and flash was adjusted and retinal retention used to freeze the wave image at the measured breaking point. The technique of retinal retention could be used at this point to give a better picture of the manner in which the wave broke. This sometimes resulted in a minor correction in the breaking position. Note that the timing in the photographic flash circuit and the LDA measurement circuit were slightly different. The delay between the LDA trigger pulse and the pick up of the flash in the LDA photodiode was measured as 30 ms, and the phase of the LDA trigger accordingly adjusted to locate the LDA measurements at the breaking point.

The breaking depth was calculated from the horizontal position of breaking using the known bed geometry.

Crest height and trough depth: The height measurements were also taken by eye to avoid errors occurring from the three dimensionality of the crest, and because photographs emphasize the side wall boundary layer effects.

The method for measuring height consisted of holding a metre stick horizontal at the height of the crest. As the wave crest is also horizontal and orthogonal to the stick, the two lines define a horizontal plane, and therefore it is not only possible to sight the wave crest on the stick but it is possible to know that one's eye is at the appropriate height. The same is done to measure the trough depth. This method is preferred to the use of a conventional wave gauge or photographic methods because the former only measures at a single position across the tank and the latter records the curved meniscus above the surface and the disturbed breaking caused by the side walls.

Wavelength: The period is so exactly known that the wavelength and the celerity are essentially two measurements of the same quantity. Measurements of the wavelength are supplemented by and, in the results, amalgamated with the measured values of the celerity. The wavelength was measured by setting the timing for the flash trigger to be one half period from the breaking time and measuring the distance between the crest positions immediately before and immediately after breaking. Again retinal retention was used to freeze an image of the wave at the time of the flash. The position of a marker could be clearly seen and moved to the position of the crest between successive flashes.

The measurement of wavelength is crude in comparison to the period, height and depth measurements, particularly as the broken wave crest, travelling like a turbulent bore, had an ill-defined crest.

Celerity: The celerity was measured from video recordings and supplemented on a few occasions by still photographs. To measure the celerity, the video tape was analysed frame by frame and the rate of travel of the zero and plus five centimeter up and down crossings measured. The use of four positions on the profile was included to average out effects due to the change in shape of the wave. For accuracy, measurements were taken averaged over five or six waves.

Surface curvature: Photographs were taken to record the surface of the wave crests. No numerical results were taken from these, but prints of them are included in later chapters.

3.6 SOURCES OF ERRORS AND CORRECTIONS

APPLIED TO MEASURED VALUES.

The present research has been made possible by the use of accurate timing, an absorbing wave maker and the accurate and non-intrusive laser Doppler anemometry. Whilst this has allowed more accurate results than were previously possible, there remain several distinct areas which are sources of error:

(i) Reflection: The reflection of waves at the end opposite the generator was made as low as possible but remained at about 8 % by height (measured at the breaking position). This was calculated from the standing wave pattern along the tank. The experimental arrangement naturally reduces the wave reflection as a substantial amount of the incoming wave energy is lost during the breaking process. To reduce the reflection the final section was packed with aluminium mesh. The mesh was introduced gradually, starting with loosely packed mesh low in the wave, and followed by successively more densely packed mesh throughout the wave zone. Sharp changes in mesh density were avoided.

This reflected wave travels the length of the tank and is incident on the wave generating paddle. The absorbing wave generator successfully removes about 80 % of this incident wave. This reduces the size of the doubly reflected wave to below 3 % of the initial wave. This is considered insignificant. The effect of a partial standing wave is investigated in section 3.7.

(ii) Tank attenuation. Waves travelling along a flume will lose energy and therefore height due to friction with the walls. In addition to the distance travelled by the wave, the attenuation is dependent on both the wave period and the flume width. Those results that are defined in terms of parameters measured at the same point (the breaking point) avoid this error. However, the analysis made in terms of the deep water steepness compares results measured from 3 to 6 metres apart. In this case all the values of deep water steepness were corrected before being plotted.

The correction is based on the attenuation rates quoted in Buhr Hansen and Svendsen (1979). The scale and range of wave periods in their experiment was the same as here. However their values of height reduction per metre were doubled for our correction, our flume being half the width of theirs.

(iii) Set down: This can be regarded as a potential source of error. Care must be taken in using any laboratory or shoaling results for comparison with models or in design that the water depths used are equivalent. The results measured here are quoted with their depths measured from still water level. However, the fluid around the breaking point, and therefore that which is determining the breaking behaviour, has a mean water level below that of the still water. Where wave breaking is occurring at many locations, for example randomly spread over a large area during a storm, the mean water level will remain essentially that of the still water. However, if the mean water level is measured with a time constant sufficiently small to localise the breaking to a single event, then it may be seen that set down occurs at this point.

The set down occurring at breaking was measured, section 3.7, and the resulting values are shown in Fig. 3.7.3 .

(iv) Surface tension: Surface tension effects become significant in two regions. Firstly, small wavelength waves, those shorter than 5 cm, have surface tension providing a significant restoring force. For longer waves, the gravitational restoring force makes the restoring force due to surface tension negligible. Secondly, surface tension becomes relevent where the radius of curvature of any part of the surface becomes small, in particular in the region of the spout.

The waves studied here have wavelengths of the order of metres, and the effect of surface tension on the restoring force is negligible. However, the crosswaves generated at the junction of the wave crest and the side walls were of the order of centimeters. The addition of detergent to the water in the flume reduced the surface tension and resulted in a much smoother surface, with smaller though more defined crosswaves.

The effect of the surface tension on the crest at breaking may indeed be significant (Miller, 1972) and is likely to be the limiting factor in the scale independence of laboratory waves. In this work, as already mentioned, the water contained detergent markedly reducing the effect of surface tension. Also the main area of interest here is the wave up to and at the point at which the surface is vertically fronted. The very small radii of curvature occur after this, in the formation and development of the jet or in the spilling region.

Any influence of surface tension is expected to be related to the scale of the waves studied. The present results, chapter 4, show no scale dependence. Also the scale independence of wave breaking behaviour over the wave height range of 0.1m to 1.5m is supported by the quantitative comparisons presented in Stive (1985).

(v) Back rush. This is a complication that must be noted for direct comparison between different sets of results rather than an error as such. In this work the emphasis is on studying the breaking of waves in the context of the design of offshore rather than coastal structures. As a consequence of this, the experiment sought to avoid back rush from previous waves. This was achieved by truncating the bed some distance short of the crossover with the still water level. This stopped the shoaling process short of the run up and hence before the back rush. This has the secondary effect of making the experiment more repeatable as surf beating does not occur.

(vi) Stokes drift, recirculation: As with any wave of finite amplitude, a net forward motion of water in the crest region occurs. As the flume does not allow a net current to develop, recirculation must occur in the wave region. Thus a net reverse flow is set up lower in the wave. The errors that arise because of the net recirculation and are considered small enough to be neglected.

(vii) Secondary wave generation: One particular error that occurs in the measurement of celerity at breaking is caused by the generation of a new wave in front of the original crest. This is negligible in the case of the spilling breakers but can be a problem in the case of plungers. This is illustrated by the photograph in Fig 3.6.2. Care was taken in the celerity measurements to avoid this error.

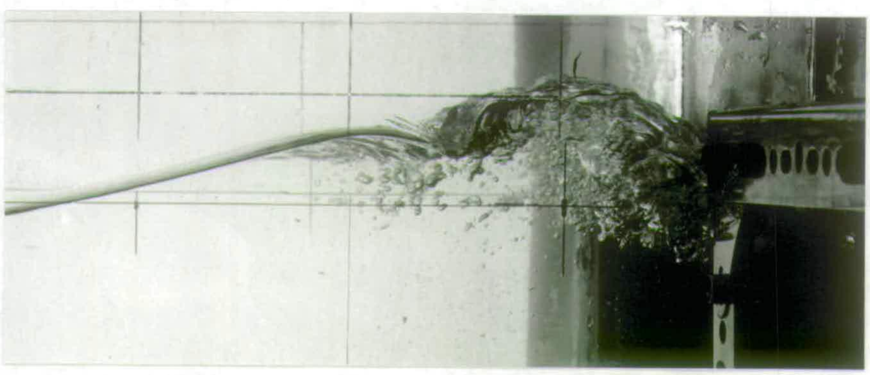

Fig 3.6.2 The generation of a second wave by a plunging breaker.

(viii) Bi-stable breaking: This is included here for completeness as an observed phenomenon. For one and only one combination of period, slope and amplitude, (T=1.6 , slope 1:30 , 0.022), a wave was observed that could break repeatedly at one position in the flume and then for no apparent reason begin to break repeatedly in another position. This did not appear to be an effect of reflection, and the only plausible explanation that is suggested is that the breaking may be related to the retention of vorticity in the water which could cause early breaking.

(ix) Repeatability: This is not a source but a symptom of error. This is studied in two ways; as the repeatability of the surface and as the repeatability of the internal kinematics. The repeatability of the surface at breaking was established to be within 0.2 cm. This was achieved by comparing up to six photographs of profiles taken at the same phase of different crests in a train of waves.

The internal velocity measurements are calculated as the mean of about eight individual measurements, and the analysis routine was programmed to calculate the standard deviation of these results. It was found that the repeatability was best low in the wave and at the front of the crest. The range of standard deviations measured was from 2 % to 7 % of the local velocity, the worst cases only occurring at the top and back face of the high crest region.

3.7 PERIPHERAL STUDIES.

Four studies were conducted that are peripheral to the main thrust of the work reported in chapters 4 and 5. Three of these are described here; they are studies of the reflection, the set down and the effect of the run up section on the flat bed results. The study of the time development of breaking is reported in section 5.1.

(i) Reflection was studied in two ways; Firstly, during all running of the main experiment the effect of reflection was monitored and many measurements of the size of reflection were taken. Secondly, for one sample case the effect of reflection on the internal kinematics was measured.

Whilst care was taken to minimise reflection, some was always present. The size of the reflected component was calculated from measurement of the maximum and minimum excursions of the crest and trough. The levels of the crest and the trough varied with distance along the tank because of the standing wave component caused by the reflected wave. The size of the reflected wave is considered relative to the incoming wave and is quoted here as the ratio of the reflected to incoming wave amplitudes.

The amount of reflection varied with both the period and amplitude of the incoming wave. Waves with a large initial amplitude broke early and lost energy as they travelled along the length of the tank. Consequently, less energy arrived at the end wall and the reflection measured at breaking was very small. The waves with periods at the extremes of the range used here had reflections significantly higher than those for the mid-range. The 0.8 s. and 1.6 s. waves had reflections about 10 percent and periods between these had reflections of about 6 percent. The lowest reflections occurring in the initially largest waves were about 3 percent.

The influence of the reflection on the internal kinematics was studied for the case of a wave with a 1 s. period on a horizontal bed at a depth of 0.1625 m. The wave amplitude was selected so that the wave did not break and three values for reflection were chosen, being 23 % , 12 % and 1.3 %. The last of these is essentially the standard result of zero reflection. The horizontal velocities were measured in the main travelling crest at four equally spaced phases in the cycle of the reflected wave. Phase "0" corresponds to the crest of the reflected wave, "2" to the trough and "1" and "3" to the mid-phases behind and before the crest respectively, see fig. 3.7.1.

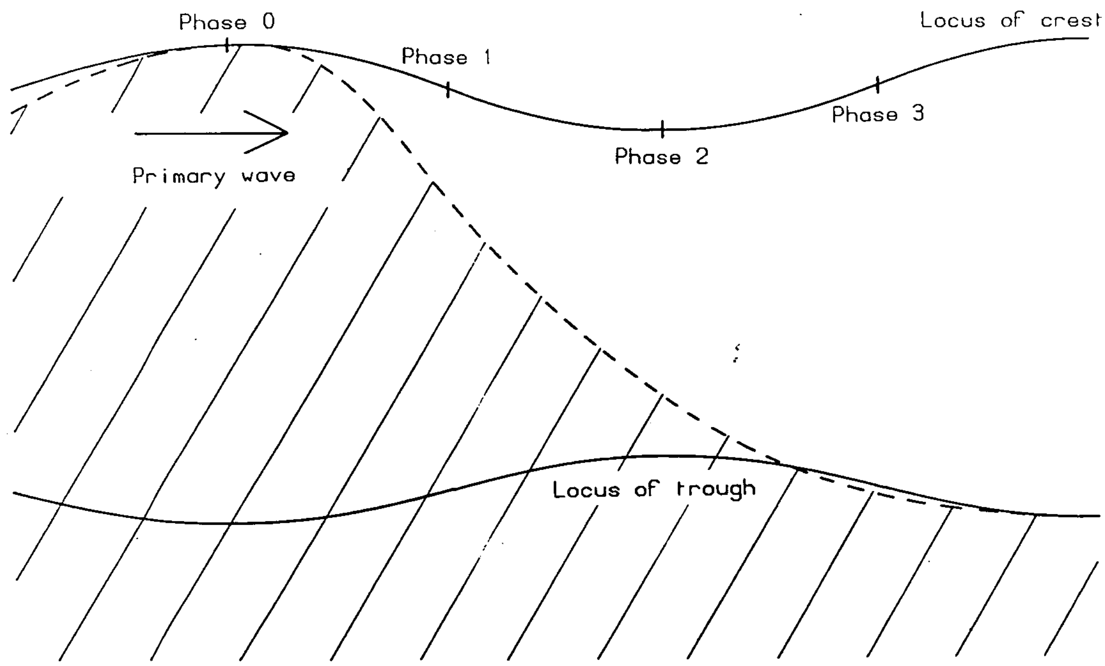

Fig. 3.7.1 Phase positions between a traveling and reflected wave.

Fig. 3.7.2 shows the expected reduction in forward velocities when the crests coincide, and the reinforcement of the velocities when the main crest coincides with the trough of the reflected wave. The second effect is smaller since the velocities in the reflected wave trough are smaller than in its crest. It is interesting to see that there is considerable difference in the behaviour between the 12 and 23 percent reflection cases. Most importantly, the reduction in velocities at phase 0 is three times as large in the latter case where there is only a two-fold increase in reflected wave amplitude.

The 12 percent results are entirely compatible with the superposition of a reflected wave described by linear theory, and the large increase in the reduction at phase 0 with larger reflection is consistent with the reflected wave becoming non-linear with an increase in its crest velocities. However, the reduction in forward velocity at phases 1 and 3 in the 23 % reflection case is stronger than the phase 0, 12 % case.

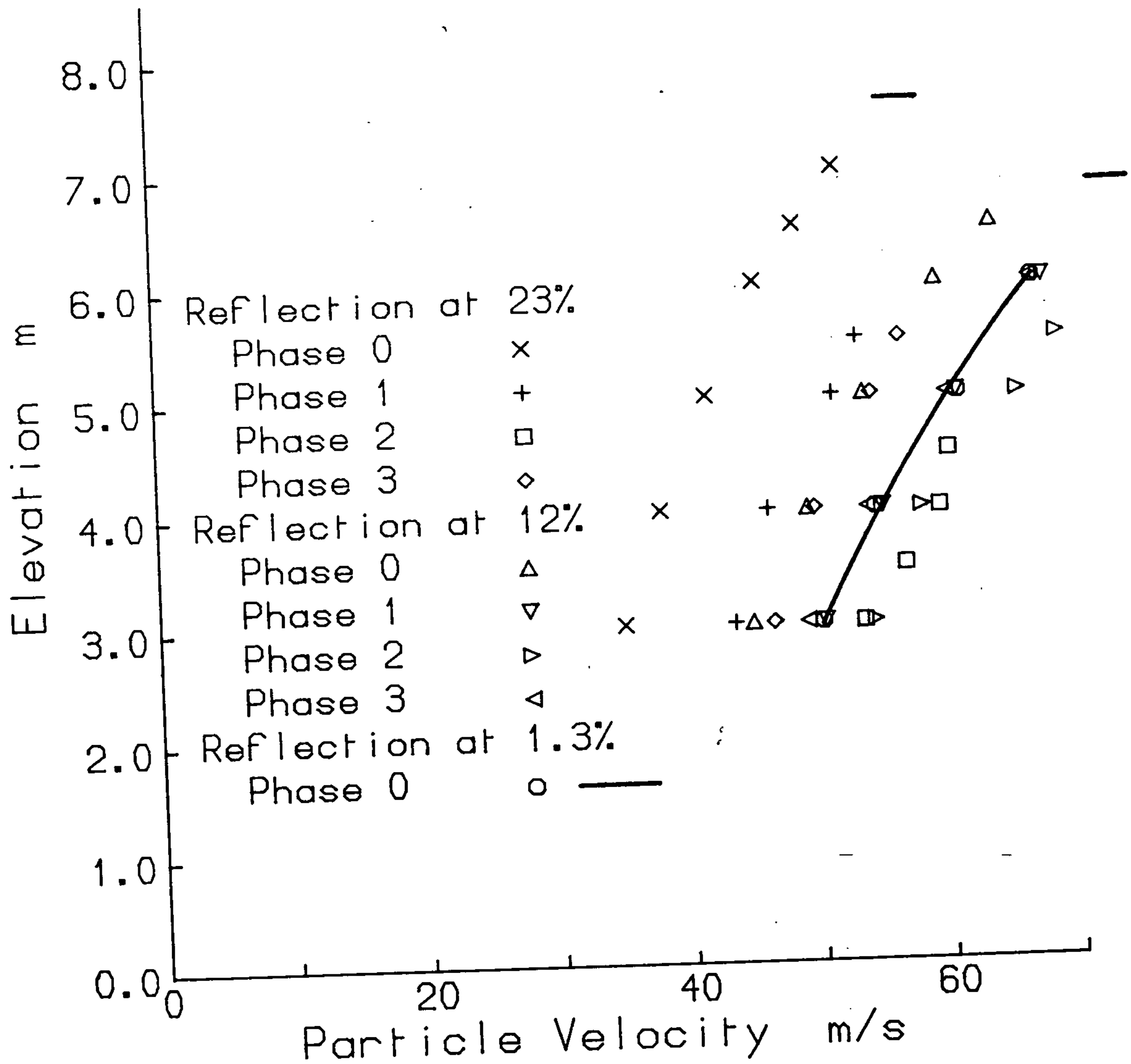

Fig 3.7.2 The influence of reflection on internal kinematics.

For the purposes of this work, it is sufficient to note that the internal kinematics are not unduly sensitive to the reflection for values of reflection below 12 percent. For reflections of 12 percent, the maximum change in velocity, that recorded at phase 0, is itself 12 percent, and is considerably less for other phases.

In the rest of this work, we are considering the waves at breaking, and if it is assumed that the breaking is caused by the particle velocity exceeding the wave celerity, then the phase of the reflection at breaking is unlikely to be around phase 0. In the most likely case, that of phase 2, the change in internal velocities is 8 percent in the case where the reflection measured by amplitude is 12 percent. Thus the errors introduced into the measurement of kinematics is expected to be at most 0.8 times the amplitude reflection. Recalling that amplitude reflection was typically 8 % the corresponding maximum error in the velocities is 6 %. As we expect a spread in the phases, of the reflection at breaking and because cases of high reflection were looked for and avoided, the influence of reflection on internal kinematics could be regarded as an error substantially below 6 %. Unfortunately the effect is systematic and is not apparent in the results for internal kinematics.

(ii) Set down: Measurements were made of the set down at the breaking point of those waves on sloping beds for which the internal kinematics were measured. The measurements were made by comparing the elevation and trough depth measured visually with those measured by the wave gauge. The latter filters out the low frequency and d.c. components and hence measures with respect to the mean water level, while the former measures with respect to the still water level. The difference between the two results is the set down. The results are presented in fig. 3.7.2 .

The results show that set down is generally below 5 percent of the wave water depth, and that there is a strong trend of increasing set down with wave period. The scatter in the results is considerable but they do agree in general with theoretical predictions given in Svendsen and Jonsson (1980) who show that for shallow water , set down b is given by :- $b = -\frac{H^2}{16d} G$

(See also Svendsen and Buhr Hansen, 1976).

Using our measured values for H/d, this gives values for b of 0.015 d for our short period waves and 0.035 d for our long period waves.

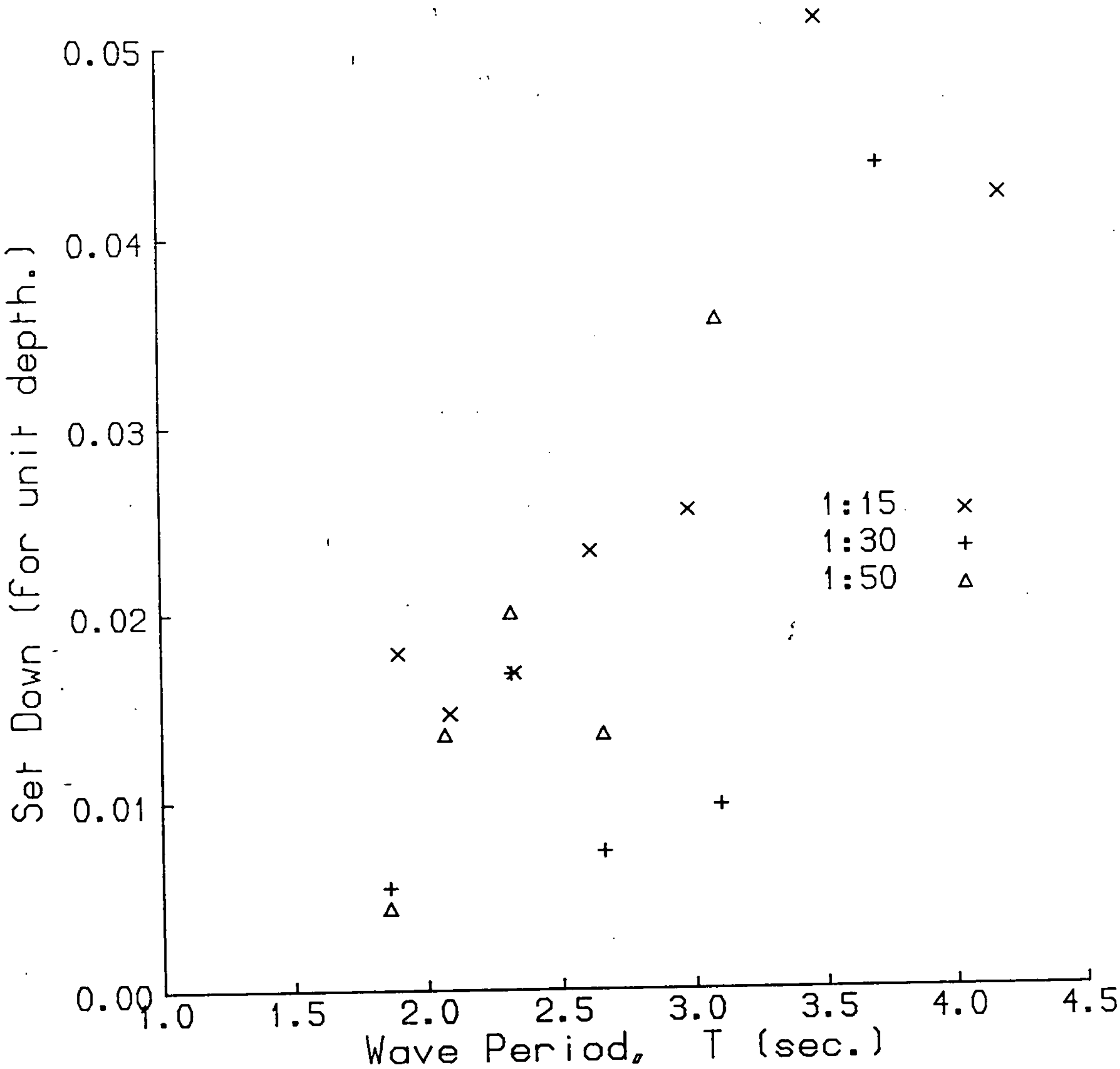

Fig 3.7.3 Set down, measured at the point of breaking.

(iii) Run up slope.

The study of breaking of monochromatic waves breaking on a flat bed has a problem in the initiation of breaking. In this study, all causes of breaking apart from the localisation of energy by the bed slope have been suppressed; this is fine for sloping beds but there is no localisation of energy on the flat bed.

The creation of waves of extreme amplitude on the flat bed was achieved by creating the waves in deep water and allowing them to progress up an initial slope to the shallow region. The waves generated in deep water were far from their limiting steepness and a steep initial slope could be used without disrupting the pure nature of the wave. In the final stages of the run up the wave was of almost limiting amplitude and the water depth was shallow. Therefore the waves were very sensitive to the bed. A slope of 1:40 was used in this final section. It is important to demonstrate that the breaking characteristics are those of the flat bed rather than those of the run up slope so an initial study was conducted to determine the sensitivity of the waves to the slope of the run up.

To this end, one parameter, the breaking wave height, was measured over a range of periods for run up slopes of 1:30 , 1:40 and 1:50. The change in wave height in going from the 1:30 to the 1:40 amounted to a seven percent change, but the change from 1:40 to 1:50 only amounted to just over an one percent change in height. It was therefore concluded that the effect of the 1:40 run up slope was negligible. That the breaking does reflect the flat working section is demonstrated by the results. The flat bed results do indeed fall distinct from those for the other slopes and at a position consistent with the trend towards shallower slopes, see section 4.3.3 fig. 4.3.5.

Chapter 4 Surface Parameters Describing Monochromatic Wave Shoaling.

"I can see them often even on the blank paper on my working table. I look and find them in the bends of waves on the sea between the open-work of the foaming crests ; their apparition may be sudden, it may come and vanish in a second ... in that instantaneous flash I might see the very line for which I have searched in vain for months and months. "

Nuam Gabo July 1944.

4.1 INTRODUCTION.

The waves studied here are two-dimensional, monochromatic, and shoaling on a straight, rigid and impermeable bed. This study is restricted to travelling waves, so reflections occurring at the beach end are minimized. In this way the results are akin to extreme waves at sea and parallel the design waves. Specifically they do not ride on the fast moving undercurrent caused by the back rush of the previous wave that is associated with near shore conditions.

Surface parameters are defined in section 4.2, in section 4.3 results are presented in terms of the laboratory parameters, of slope and deep-water steepness. Section 4.4 also presents these results, but plotted in terms of the design parameters of non-dimensional depth and bed slope.

Comparison is made in section 4.4 with results from other sources for monochromatic shoaling. Comparisons with random and three dimensional wave breaking are discussed in section 6.5.

Many gently spilling breakers were produced in this experiment where it was not possible to observe any spout formation. In these cases the point of breaking was taken as that where surface disturbances and aeration first appeared on the front face of the wave. There may be a distinct mechanism initiating spilling in which case there might be a limiting rate of expansion which would show as a limit to the local slope of the front face of the waves. Because of this, the maximum slopes attainable on the front faces of the spillers were measured, these results are presented and discussed in section 4.6.

4.2.1 Input Parameters.

In the laboratory creation of these waves there are three variable parameters, the bed slope, the wave period and the wave amplitude. In the experiment these formed a hierarchy. It was laborious to move the bed and time consuming setting it to a new slope so the bed slope was fixed first. In the wave generating software the wave frequency is more fundamental than the amplitude and hence frequency was the second parameter to be fixed. The experiments were performed with the three parameters varying independently.

However there is a redundancy in the problem, consider figure 4.2.1, where two waves are in deep water and no object, not even the depth, gives a scale then two waves with the same steepness are indistinguishable. (This is a corrollary to Froude scaling laws). The continuous straight slope, while changing the depth, does not introduce a length scale, it appears identical to both the incoming waves, and until such forces that are scale dependent occur, the waves break identically.

The three input parameters were varied to include a sizeable overlap in deep water steepness between waves of different periods and hence scales. The collapse of these results to a description completely defined by two parameters (deep-water steepness and bed slope) demonstrated the scale independence of the results.

This repetition of measurements also reduced the significance of any random errors that might arise from scale or position dependent effects within the flume.

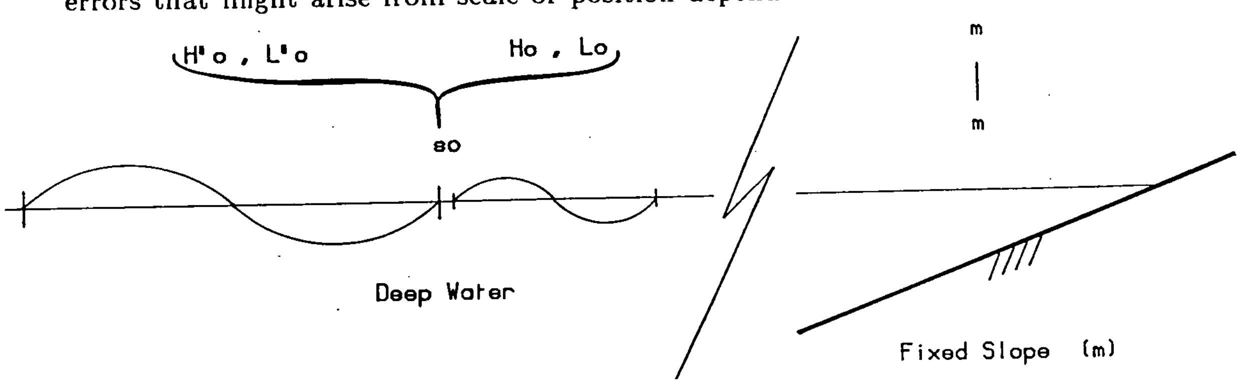

Fig. 4.2.1 Scale independent input parameters.

Four bed slopes were used, flat, 1:50, 1:30 and 1:15. These cover the range of slopes commonly encountered in shallow and intermediate depth waters but ignore the very steep slopes that can be found associated with the actual shoreline. Slopes steeper than 1:15 are not considered for two reasons. Firstly, they are not typical of the design situations prompting this work. Secondly, the breaking behaviour on steep slopes is very much affected by wave reflection , run-up, backrush, surf-beat and other effects arising from the surface piercing nature of the beach. These aspects are deliberately avoided in this work as the present measuring system is very dependent on the repeatability of the waves.

For each slope, some or all of the following frequencies were explored: 0.5 , 0.625 , 0.75 , 0.875 , 1.0 , 1.125 , 1.25 and 1.375 Hz. The range and the particular combinations of slope, frequency and amplitude studied was restricted by the operating range of the wave generator and the behaviour of the tank.

For all chosen slopes and frequencies the amplitude of the incoming wave was varied such that about nine different waves were measured for each frequency, all breaking at different positions along the beach. To avoid any unwanted influence from the the ends of the slopes, no results were taken for waves breaking within about three quarters of a wavelength of either end of the test slopes.

4.2.2 Measured parameters.

For each of the input conditions various parameters were measured, mostly at the point of breaking. These are described below along with other parameters which are simple derivatives of them, the measured parameters written first and the derived parameters following in parentheses. Fig 4.2.2 is a definitive sketch showing the parameters which were measured in these experiments.

H1o , H2o (Ho=H1o + H2o) The deep water wave amplitude Ho, is identically the sum of the crest elevation, H1o, and the trough depth, H2o, measured from the still water level in deep water.

xb (db) The breaking position, xb, was measured as the distance along the tank from the wave paddle to the breaking point. The derived depth at breaking, db, was calculated from the tank geometry.

H1b , H2b (Hb=H1b+H2b) The breaking amplitude, Hb, crest elevation, H1b, and trough depth, H2b are similar to those in deep water, but are measured at breaking. Note that the trough depth is measured at the breaking point rather than at the breaking time.

R: The reflection coefficient, R, of the tank varied with bed geometry and from wave to wave. It is calculated as the ratio of the reflected to the travelling wave amplitude at a position about breaking. Values for R were measured for many of the waves used in this research and are discussed in section 3.7.

Lb , cb: These are related parameters, Lb= cb x T . Both the wavelength, Lb, and the celerity, cb, at breaking were independently measured and subsequently combined, the resultant being quoted as the celerity.

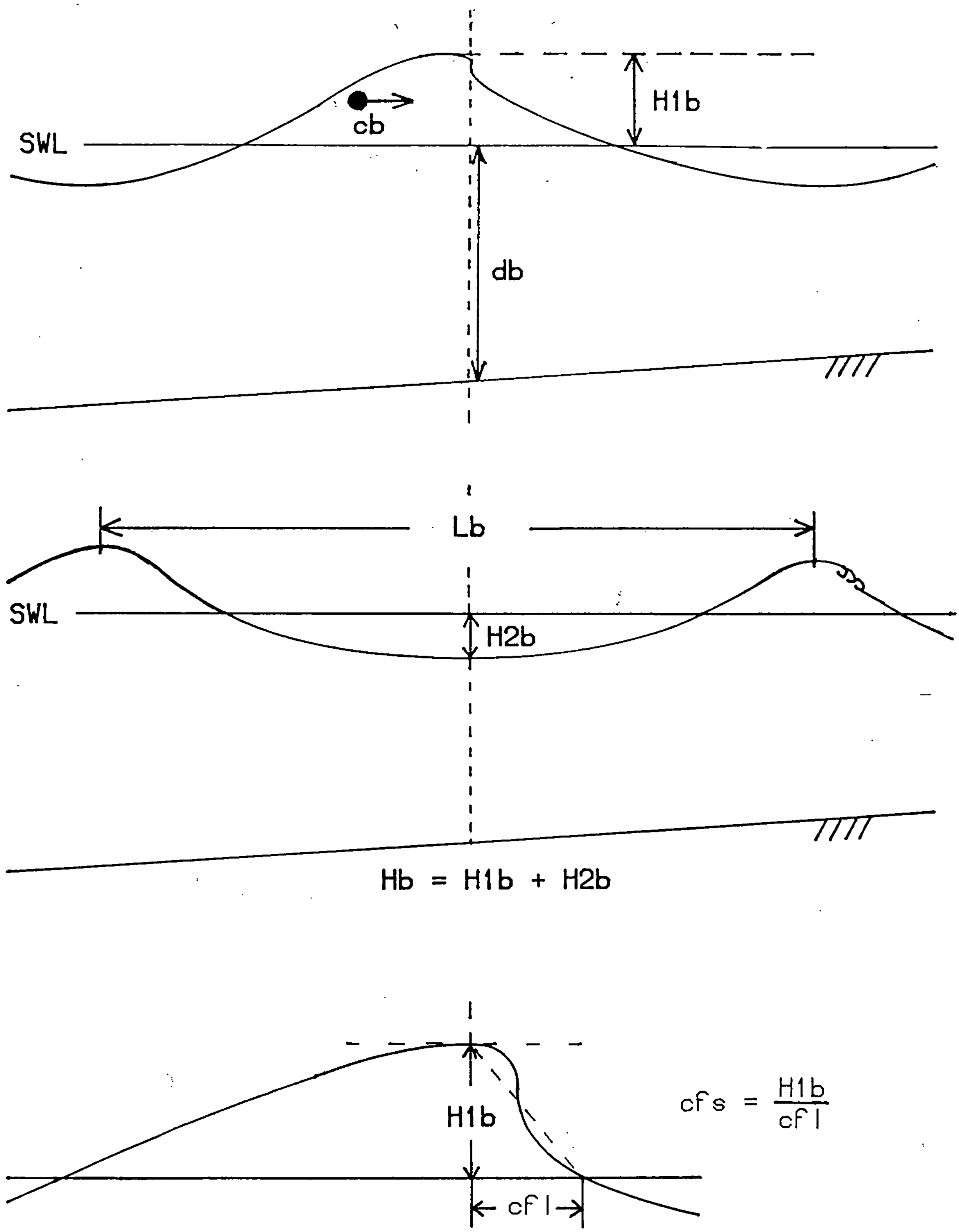

Fig 4.2.2 Definitive sketch for measured parameters.

CFL: The crest front length is measured as the horizontal length at breaking between the highest point in the crest and the cross over of the free surface and the still water level in front of the crest.

4.2.3 Non-dimensionalising.

All non-dimensionalising is achieved here by division by the combination of gravitational acceleration, g, and wave period, T, which has the dimension of the original parameter. The acceleration g is fundamental to these experiments and the wave period, T, is the constant characteristic of each wave. Thus lengths are non-dimensionalised by division by gT^2 and velocities by gT. 4.2.4 Combined parameters.

So: The deep water steepness, So, is the ratio of the measured deep water height, Ho, to the deep water wavelength, Lo, calculated from the wave frequency using the linear theory dispersion relation. This is the fundamental input parameter used in the subsequent analysis.

Hb/Lb: The breaking steepness, Hb/Lb, is the ratio of the breaking amplitude to the measured breaking wavelength . This is much used in design and is often mistakenly taken as 0.142, a result derived for deep water from Stokes theory by Michell (1893).

Hb/db: The breaking height to depth ratio, Hb/db. This is the other ratio used to predict breaking in design and is often incorrectly taken as a constant value, 0.78, (this being the solitary wave limit calculated by Munk (1949)).

CFS: The crest front steepness is defined as the ratio of the crest elevation, at breaking, H1b, to the crest front length, CFL. This is similar to the crest front steepness defined and used by Myrhaug & Kjeldsen (1984). Their definition, having the horizontal length defined in time, can be simply related to the present one by the linear dispersion relation.

Note however that the application of the linear dispersion relation cannot precisely relate the two definitions since the wave shape changes in time, and the rate of change of crest front length can be quite large.

4.3 MEASURED VALUES OF BREAKING PARAMETERS AND DISCUSSION.

The measured values of the surface parameters defined in section 4.2 are presented and analysed in this and the next section. In this section the results are plotted as functions of the deep water steepness and the bed slope. These two parameters, as shown in section 4.2, are sufficient for the complete parameterisation of monochromatic wave breaking. It is an important consequence that in the complete analysis of these results two independent parameters are not only sufficient, but necessary.

In the next section (4.4) the non-dimensional breaking depth is used as the x ordinate and the bed slope is kept as the second independent parameter. It is seen from results in that section that they too completely parameterise the breaking.

The orthogonality of the non-dimensional breaking depth to bed slope is a direct consequence of the fact that the slope dependence does not collapse when non-dimensional breaking depth is plotted against deep water steepness. This can be seen in fig 4.3.1.

This second presentation of the results is performed for three reasons. Firstly, in offshore design the depth is the basic parameter and the period of the extreme waves is the most easily measured of the wave properties. Thus the non-dimensional depth is the natural designers choice for parameterising the waves. Secondly, it is a parameter defined at the breaking position. Thus it avoids all error arising from attenuation between the deep water and breaking positions. Thirdly not all work that is available for comparison includes measurements of the deep water wave amplitude or steepness.

4.3.1 Limiting behaviour in deep water.

The fundamental limit in deep water is the wave height to wavelength ratio. The exact value of this is uncertain, but lies in the range 0.11 to 0.142. Comparison is made in this section between the present results and the experimental deep water limit derived from Van Dorn and Pazan (1975) and Ramberg and Griffin (1987), and also with the theoretical deep water limit from the Stokes 120 degree wave. These results are included in this section, but being at the deep water limit these cannot be plotted on the axes favoured for the main comparisons in section 4.4.

The experimental limit from Van Dorn and Pazan (1975) is taken as Ho/Lo = 0.128 and that from Ramberg and Griffin (1987) as Ho/Lo = 0.132 The former result is read from figure 10 in Van Dorn and Pazan (1975), and corresponds to a low wave growth rate. The latter result is given explicitly in Ramberg and Griffin (1987) and is based on their own results and those of their five sources, (these sources being; Melville (1982), Su et al. (1982), Duncan (1983), Ochi and Tsai (1983) and Bonmarin and Ramamonjiarisoa (1985)).

The second source of deep water limiting behaviour is theoretical. The very widely used limiting value of deep water steepness is that of the Stokes limiting wave in deep water calculated as Ho/Lo=0.142 (Michell, 1893).

The experimental limits are in good agreement with each other, while differing significantly from the theoretical Stokes result. Because of this, the mean of the experimental values, (Ho/Lo = 0.13), and the theoretical Stokes result (So= 0.142) are used. All parameters become independent of the bed slope in deep water and the limiting values are as follows:-

Non-dimensional breaking depth (fig. 4.3.1). If deep water is taken as any depth greater than half the wavelength, then in non-dimensional terms this corresponds to depths over 0.08. This is substantially beyond the largest measured depth and so is left unmarked. However asymptotes are included at the two limiting steepnesses.

The non-dimensional breaking height tends in the deep water to the limit of:

Non-dimensional breaking height = (2π) x deep-water steepness This is shown as a straight line on figure 4.3.3.

For non-dimensional breaking celerity (fig 4.3.4) the limiting value from linear theory, cb' = $1/2\pi$ = 0.159 is shown.

The combined parameter Hb/db tends to zero as db tends to infinity.

4.3.2 Shallow water or solitary wave limit.

All the single breaking parameters, being non-dimensionalised by period rather than by depth, tend to zero in this limit where the period tends to infinity. Any researcher interested in this limit should keep the parameters finite by non-dimensionalising by depth.

The height to depth ratio (fig. 4.3.5) shows the much abused flat bed solitary wave result of McCowan (1891) Hb/db = 0.78.

4.3.3 Results and discussion.

The shallow water limits are depicted as full diamonds and the deep water experimental and theoretical limits as full squares and circles respectively. Where appropriate asymptotes are included. Best fit lines have been drawn through the data and where possible the results for the different slopes have been shown with separate lines.

All results show a low degree of scatter consistent with experimental errors estimated at about five percent.

The theoretical predictions all agree well with the measured results, and special attention is drawn to fig 4.3.5 where the commonly accepted value of Hb/db of 0.78 is seen in context as the limiting case of a solitary wave breaking on a flat bed, while the full behavioural characteristics of the height to depth ratio are seen as a function of both deep water steepness and beach slope.

The graphs demonstrate clearly the reduction of all of the breaking parameters to well behaved functions of just two parameters. This can be read as demonstrating the independence of the breaking behaviour from any scaling within the range used in the experiment. It also shows that the effects causing breaking that we are measuring arise from the slope and are not associated with breaking due to positional effects within the tank.

As a visual demonstration of the scale independence of the breaking within the tank, photographs, figs. 4.3.6 , 4.3.7 and 4.3.8 show for comparison three waves of different scale but identical in terms of deep water steepness and slope. Wave I breaks at an unscaled laboratory depth of 0.186m, wave II at 0.146m, and wave III at 0.113m.

From these it can be seen that the behaviour up to breaking appears very similar in all cases, but that differences appear after breaking due to scale dependent effects.

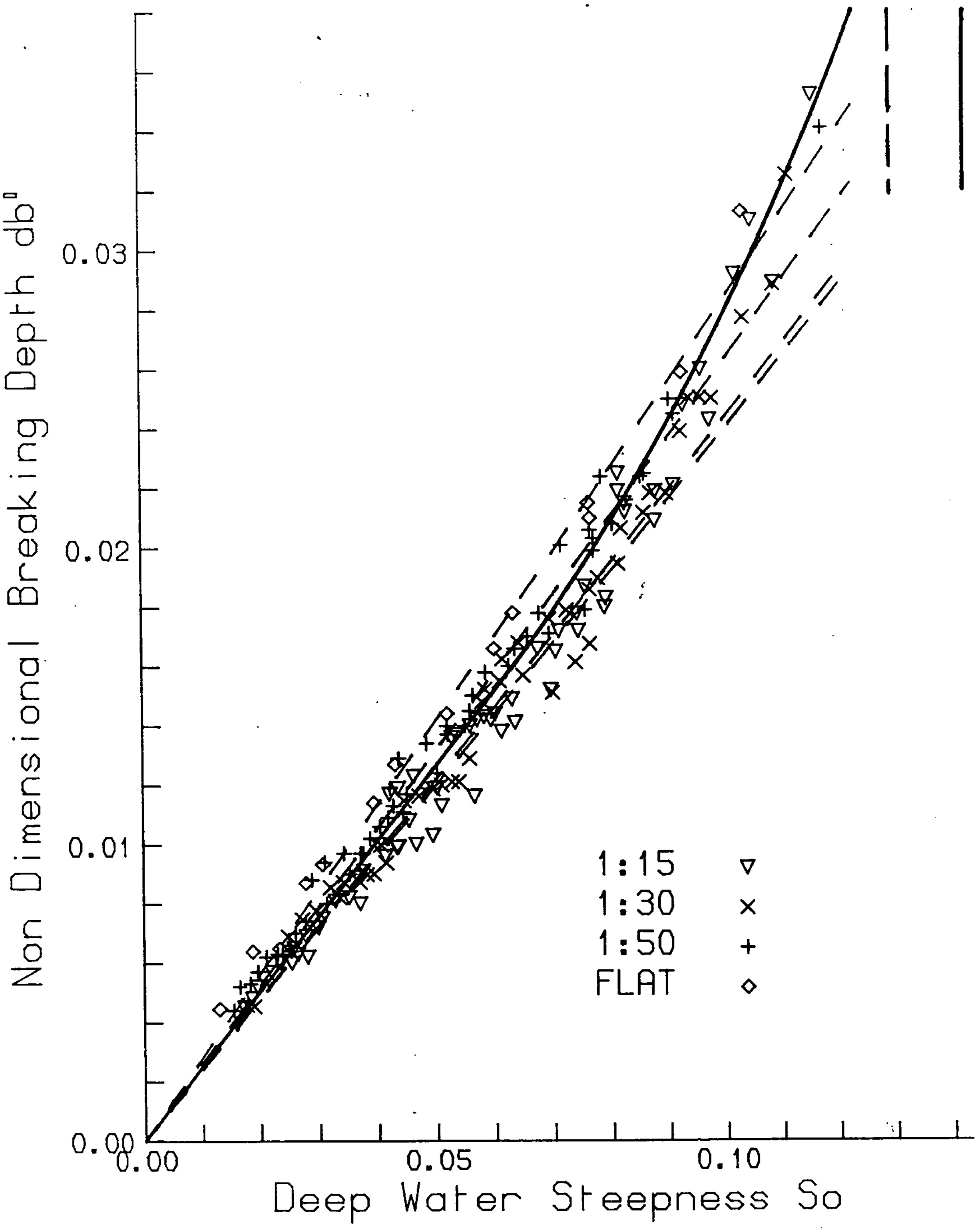

Fig. 4.3.1 Non-dimensional breaking depth.

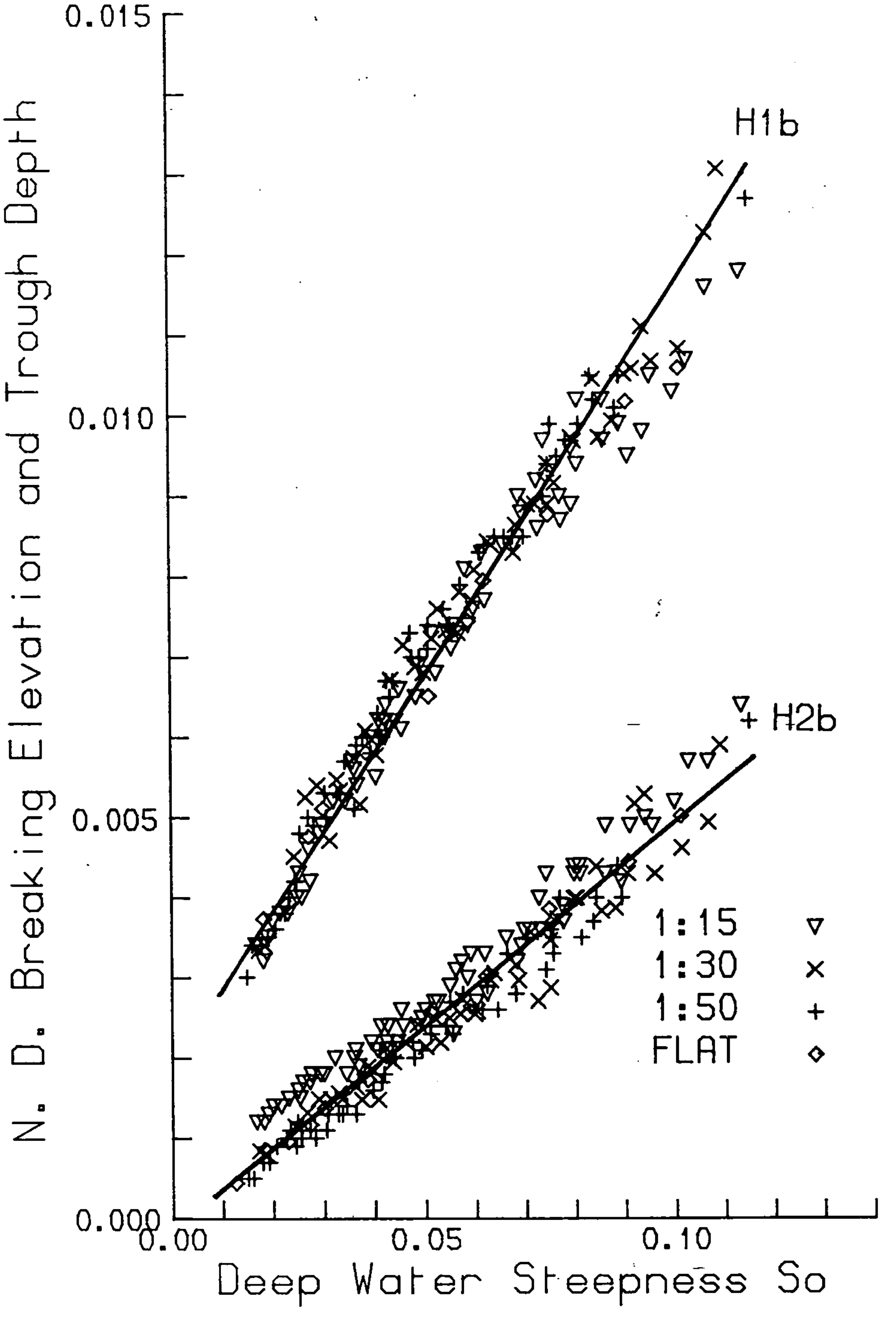

Fig. 4.3.2 N-d breaking elevation and trough depth.

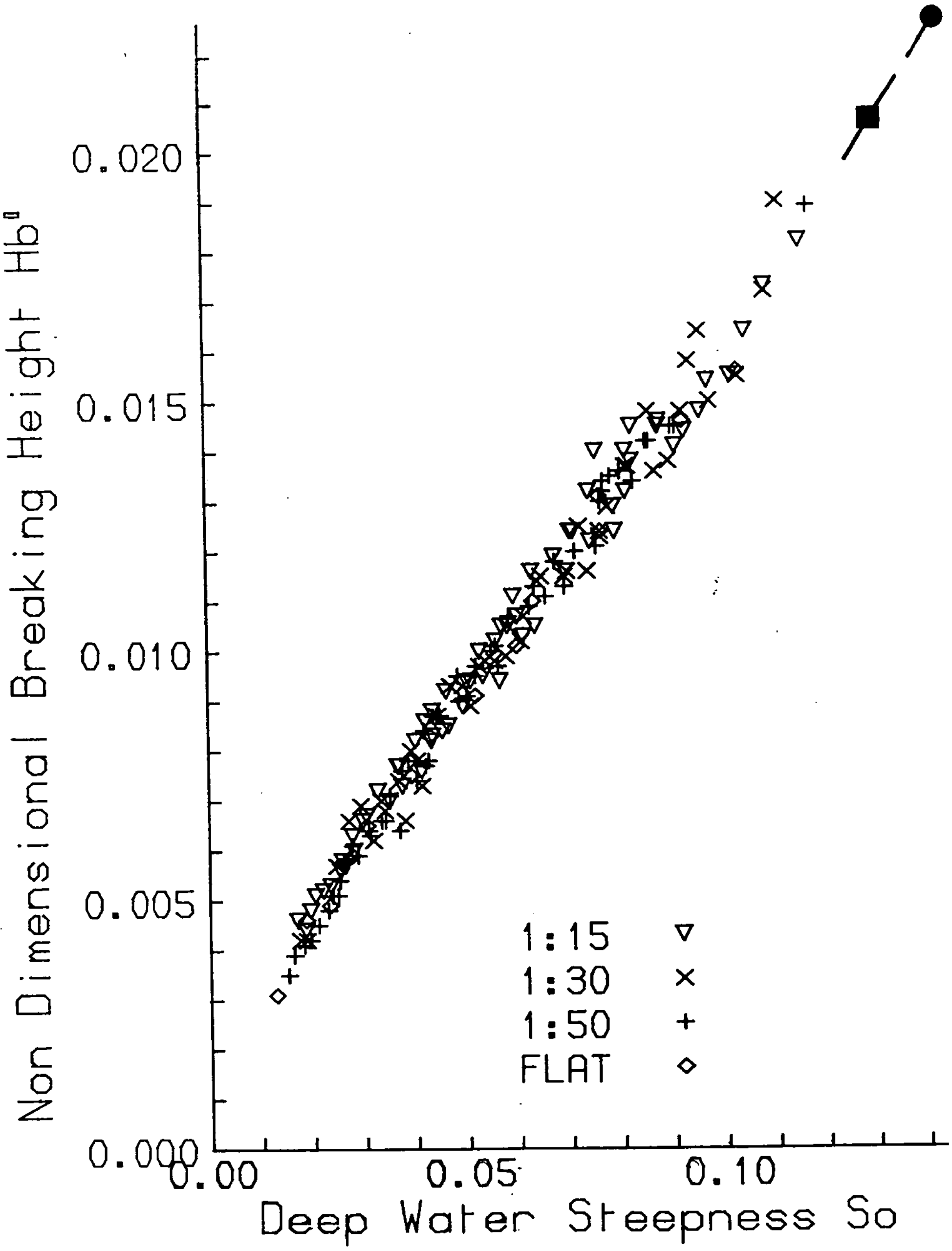

Fig. 4.3.3 Non-dimensional breaking height.

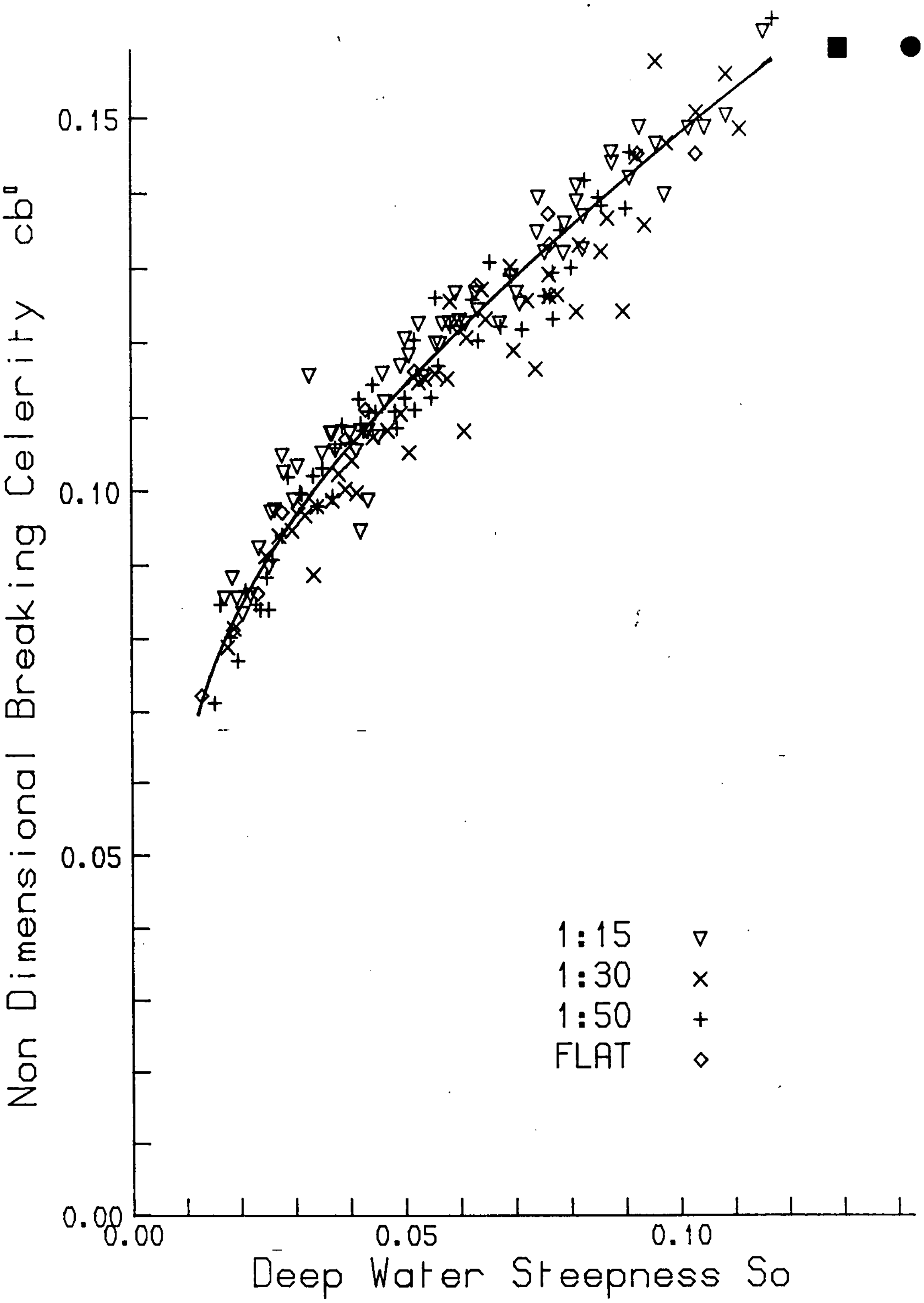

Fig. 4.3.4 Non-dimensional breaking celerity.

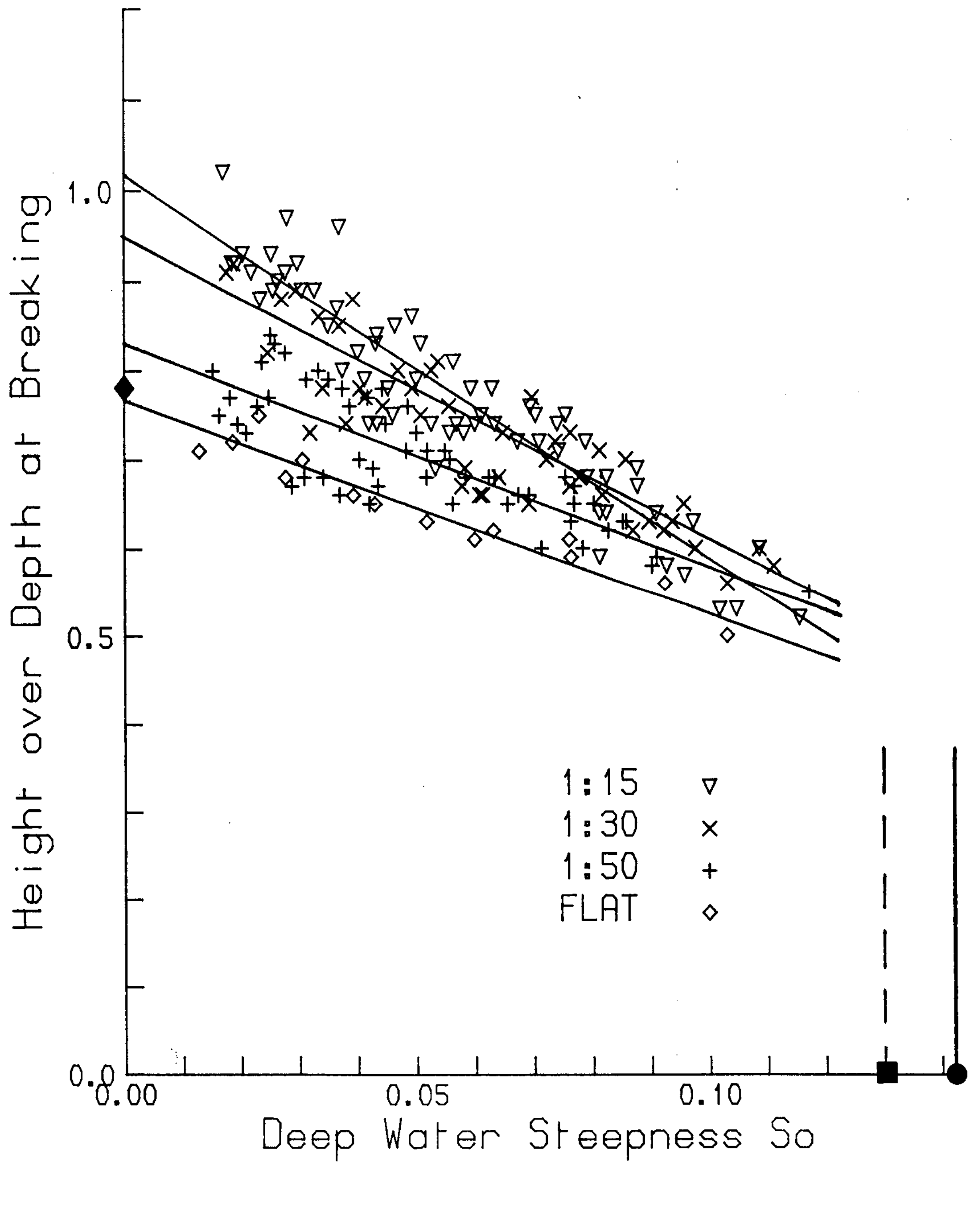

Fig. 4.3.5 Height to Depth ratio.

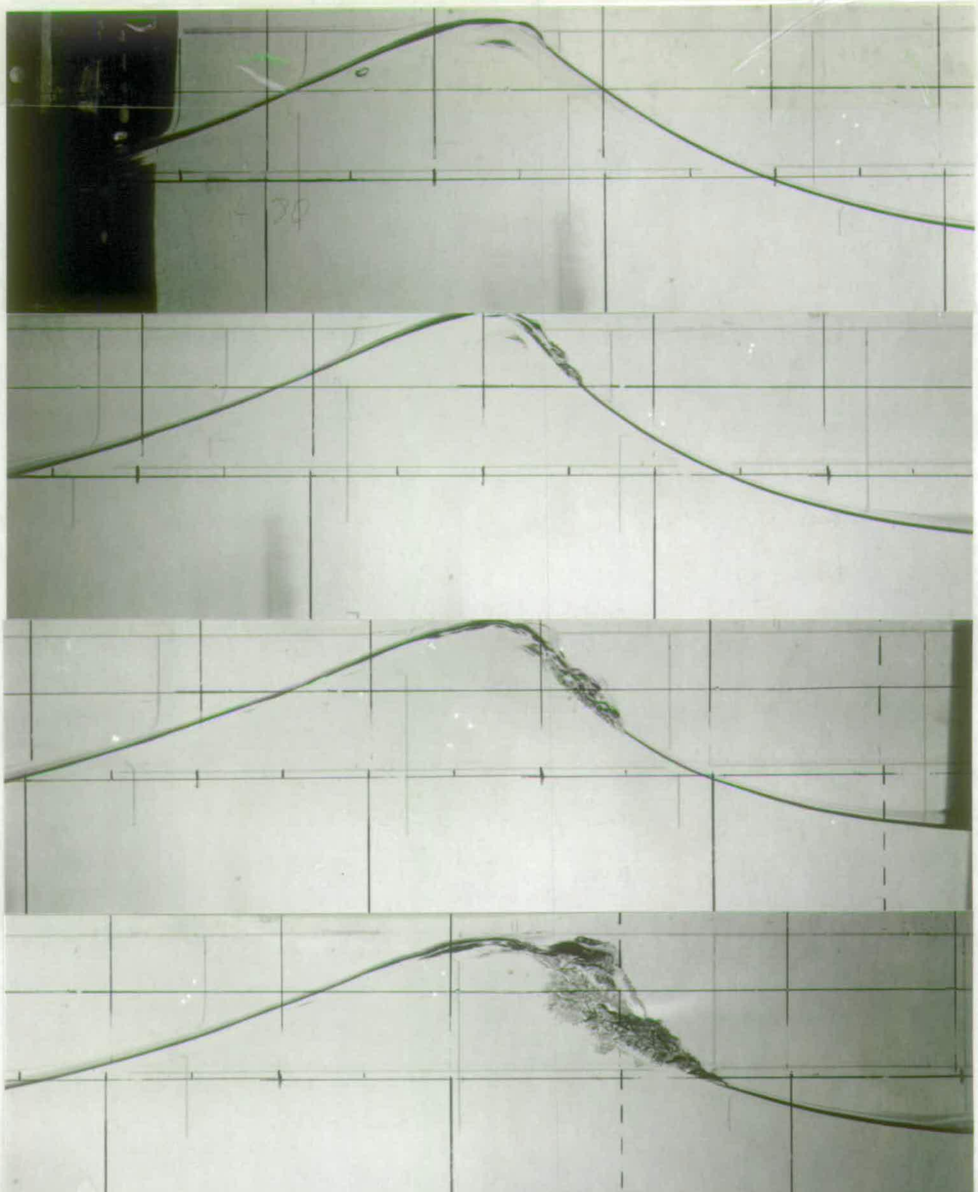

Fig. 4.3.6 Development of breaking , Wave I

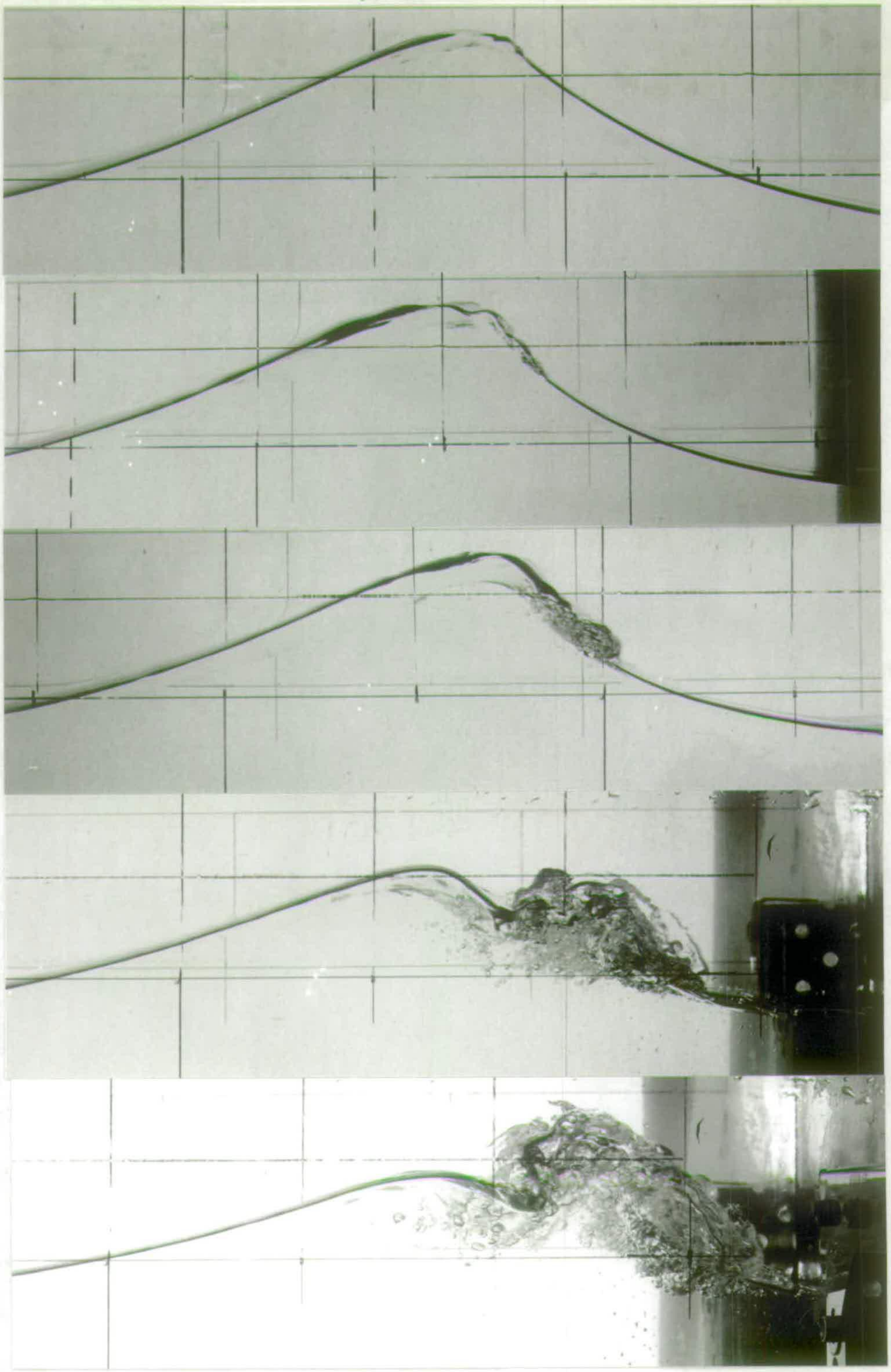

Fig. 4.3.7 Development of breaking , Wave II

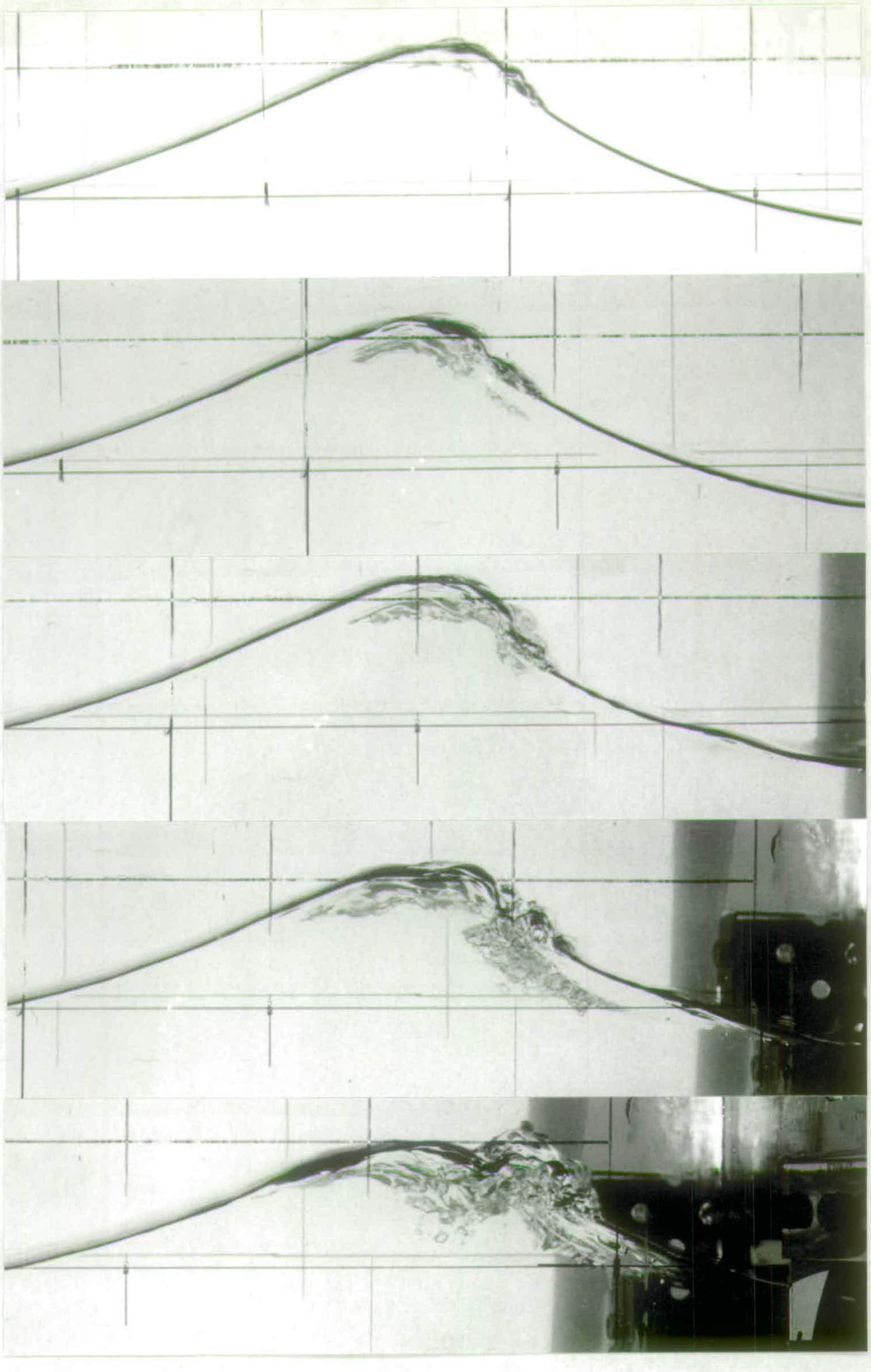

Fig. 4.3.8 Development of breaking , Wave III

4.4 COMPARISON WITH OTHER RESULTS FOR MONOCHROMATIC WAVE BREAKING.

The literature relating to wave behaviour has been surveyed in depth and work containing results for wave breaking has been gathered. In this section comparison is made between present results and those that are exactly comparable, ie, results for monochromatic waves breaking by shoaling on straight impermeable beds of various slopes. Further comparison is made in chapter 6 between the synthesis of all the results in this section and results for breaking in more general environments.

In this section the non-dimensional breaking depth is used as the x ordinate (rather than the deep water steepness,) for reasons outlined in section 4.3. As in the last section, the slopes are distinguished by symbol.

The breaking limit waves as calculated for flat bed conditions according to Cokelet's model are included for comparison with measured parameters. They are taken from Holmes, Chaplin and Tickell (1983) table 1 and drawn as pecked curves on the graphs figs. 4.4.1 ,2 ,4 and 6.

4.4.1 Results.

The following graphs, figures 4.4.1 to 4.4.8, show the basic breaking parameters H1b , H2b ; Hb ; cb ; Hb/db and cfs . With the exception of the first and last graphs, all the graphs are in pairs. The first of each pair show the present results, their best fit lines (full) and the predictions of Cokelet's theory (pecked lines). The second of each pair show the results found in the literature and the best fit line carried over from the previous graph. In this way comparison can be made between results without unnecessarily cluttering the plots. The first graph has no pair because, no results were available from the literature to compare with the breaking elevation and trough depth.

The results used come from four different sources and cover a range of slopes from 1:5 to 1:45. The sources are labelled on the diagrams according to slope and source; the sources are given in the following key.

(1) Buhr Hansen and Svendsen (1979)

(2) Galvin (1969)

(3) Sakai and Iwagaki (1978)

(4) Van Dorn (1978)

The slopes are listed explicitly on the figures.

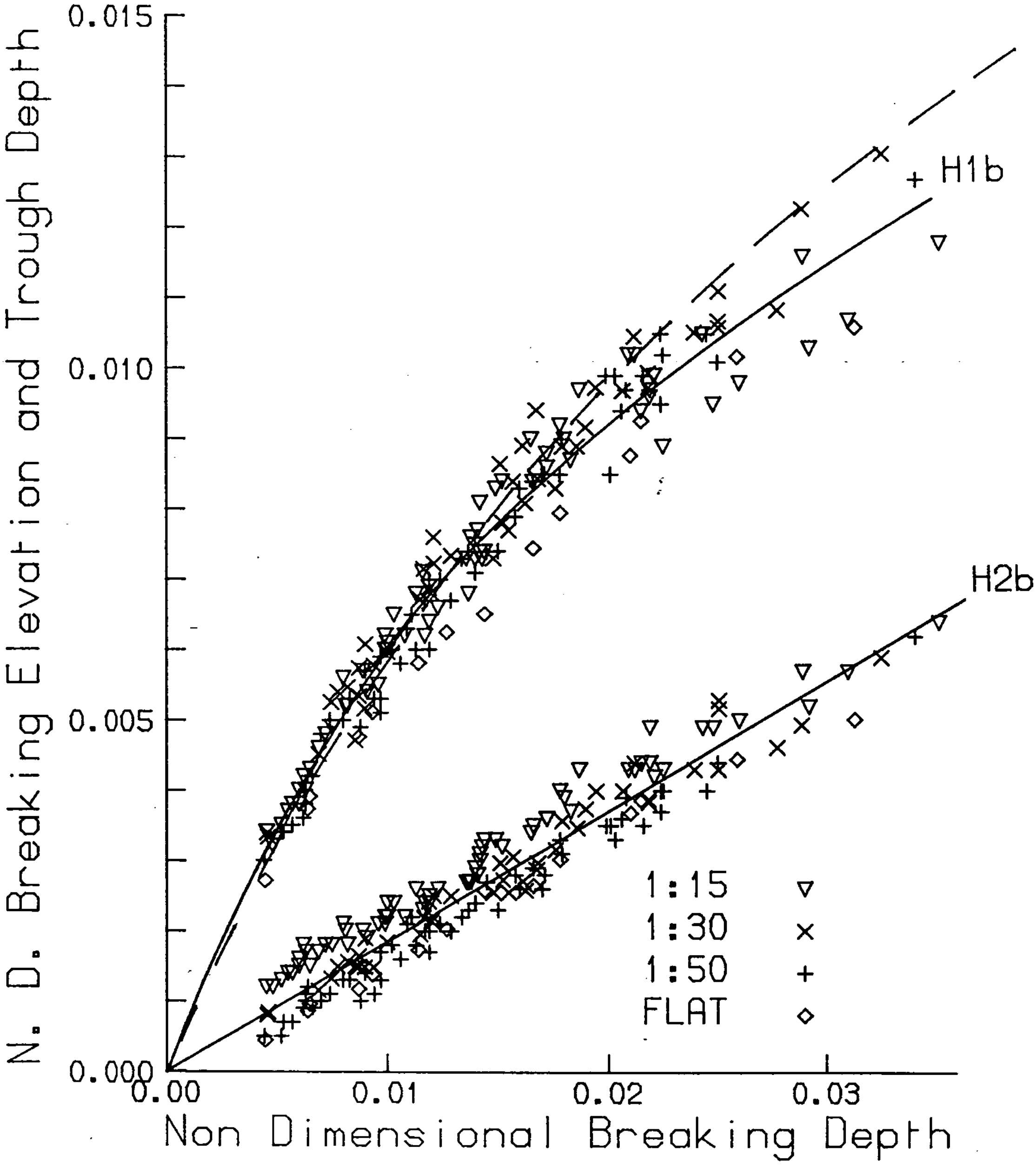

Fig. 4.4.1 N-d breaking elevation and trough depth, own.

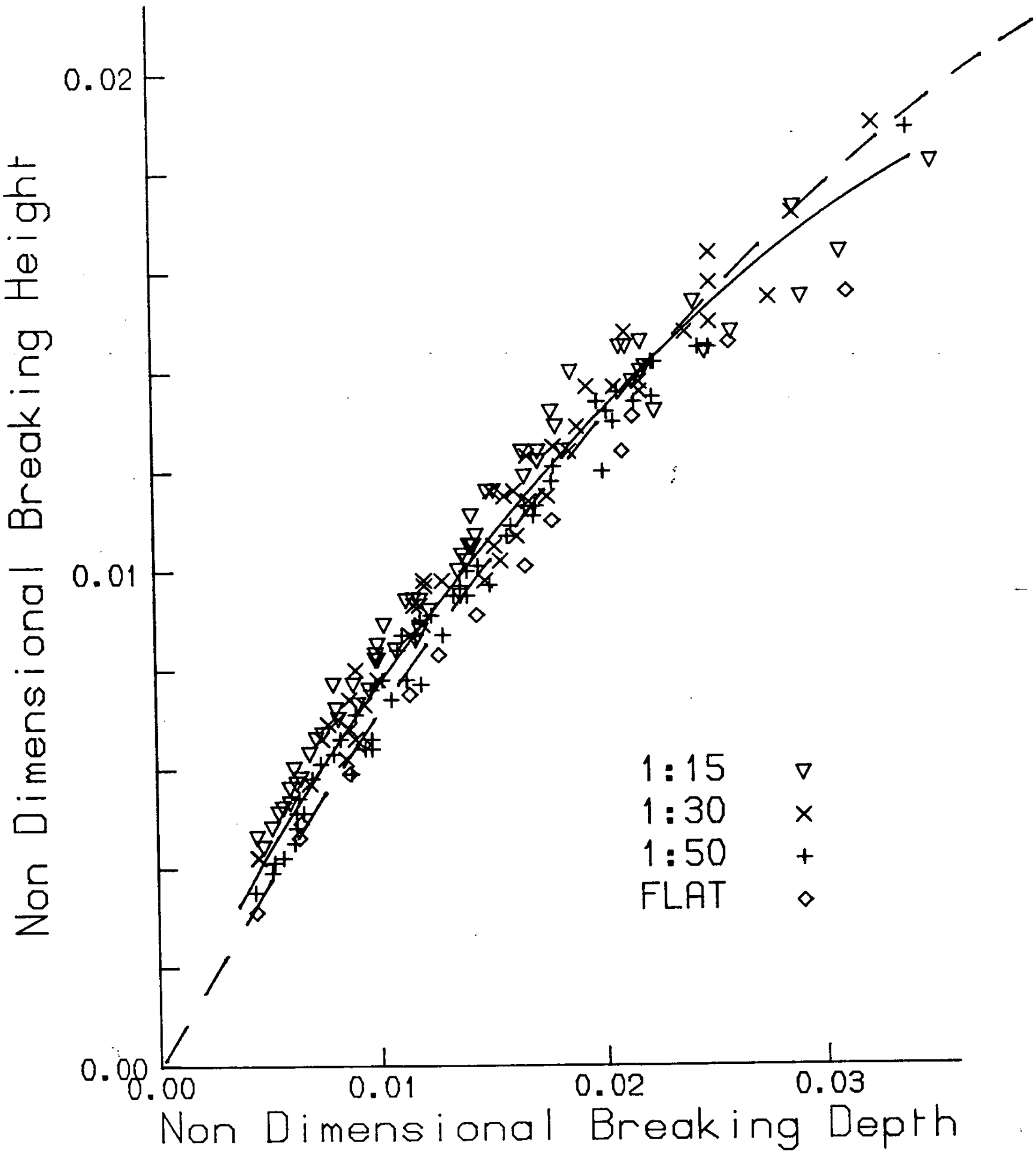

Fig. 4.4.2 Non-dimensional breaking height , own.

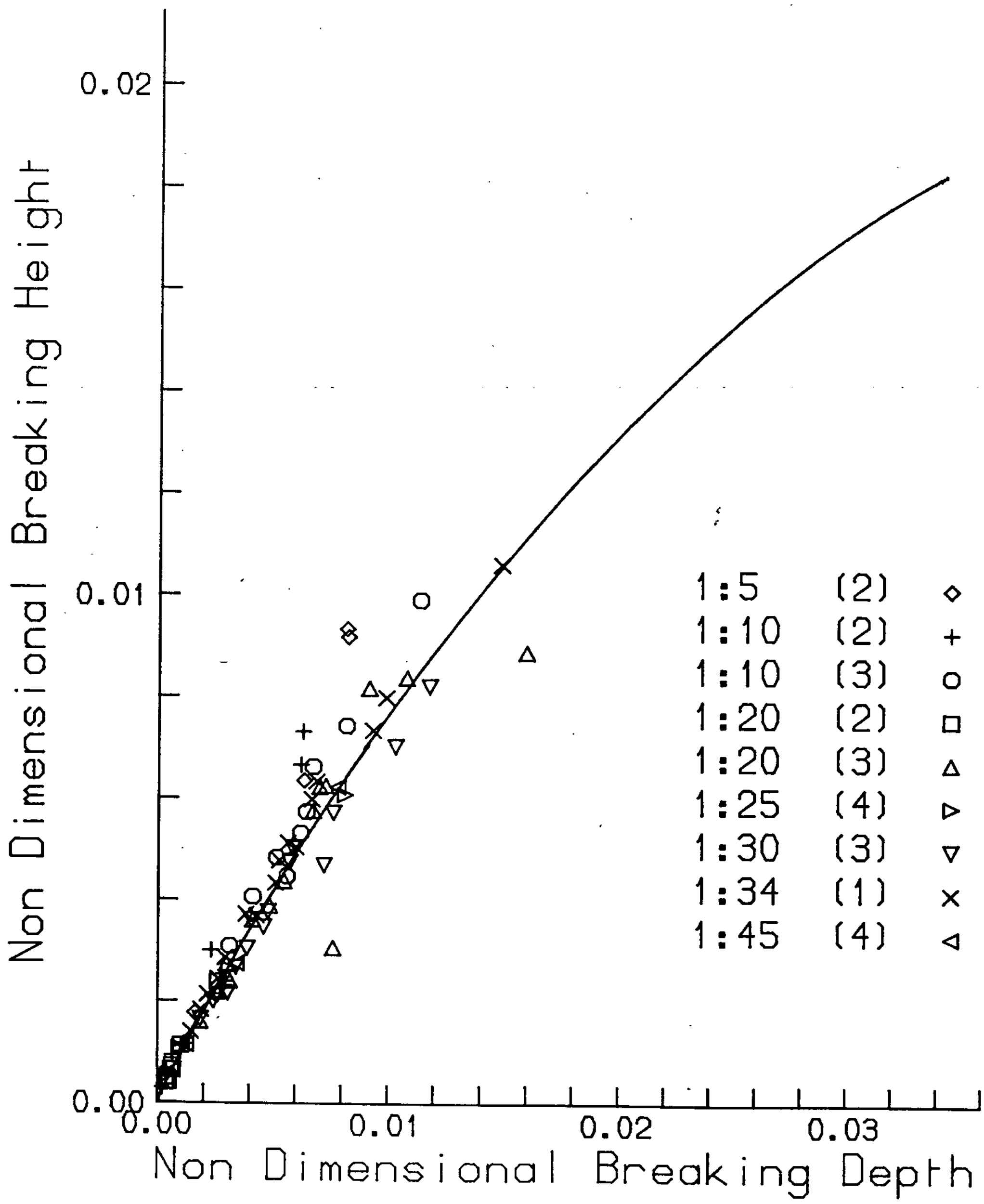

Fig. 4.4.3 Non-dimensional breaking height other.

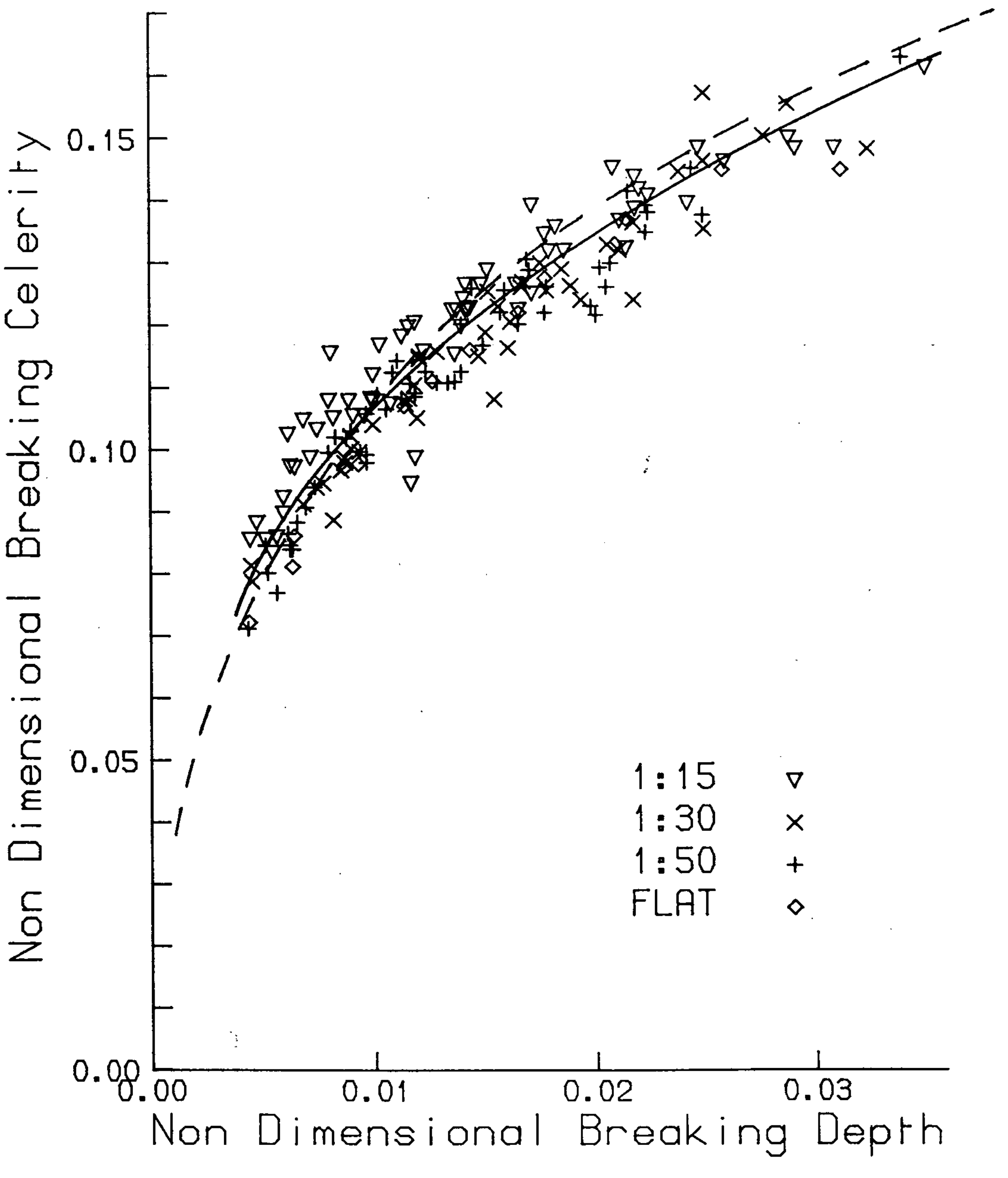

Fig. 4.4.4 Non-dimensional breaking celerity , own.

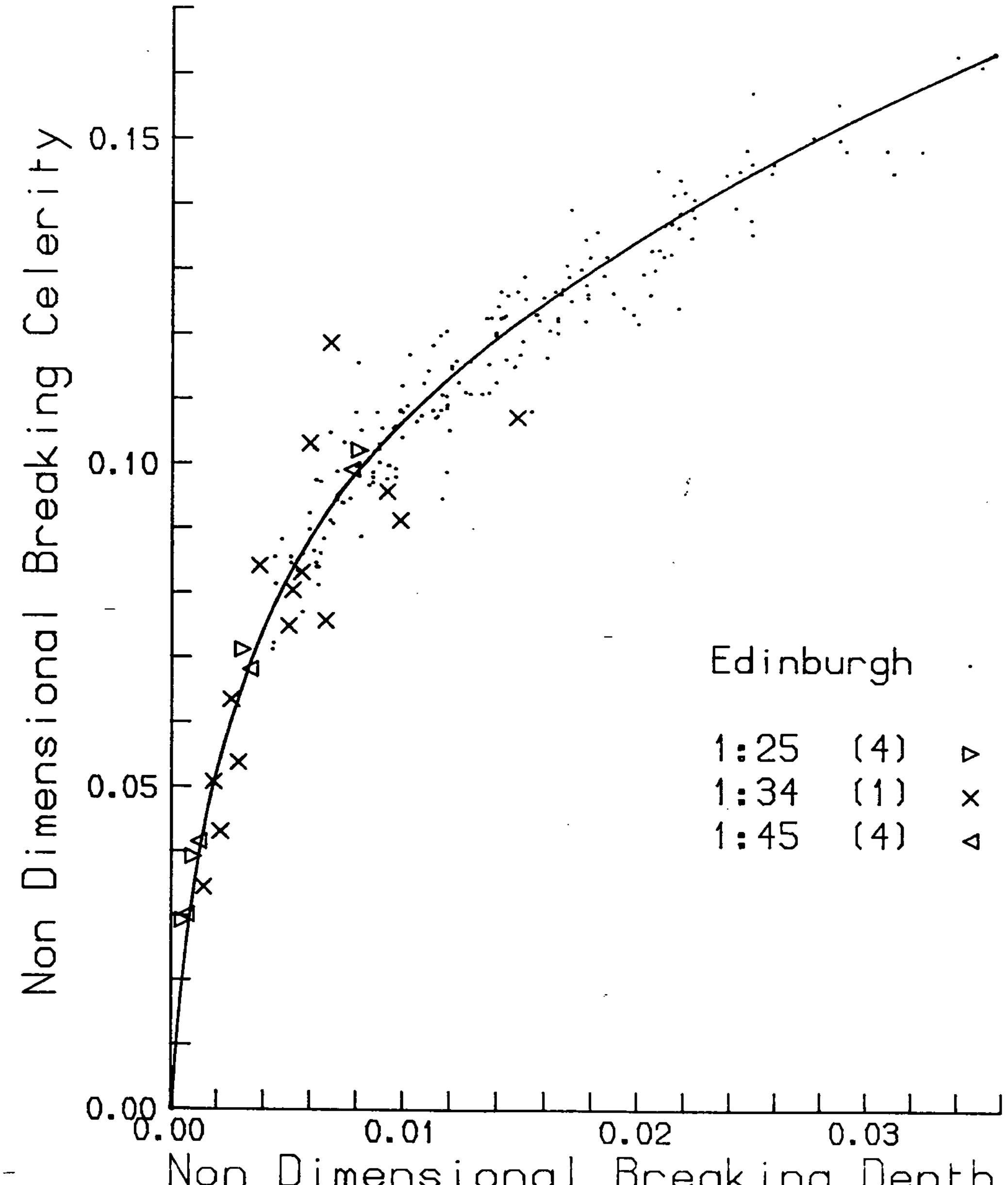

Fig. 4.4.5 Non-dimensional breaking celerity , other.

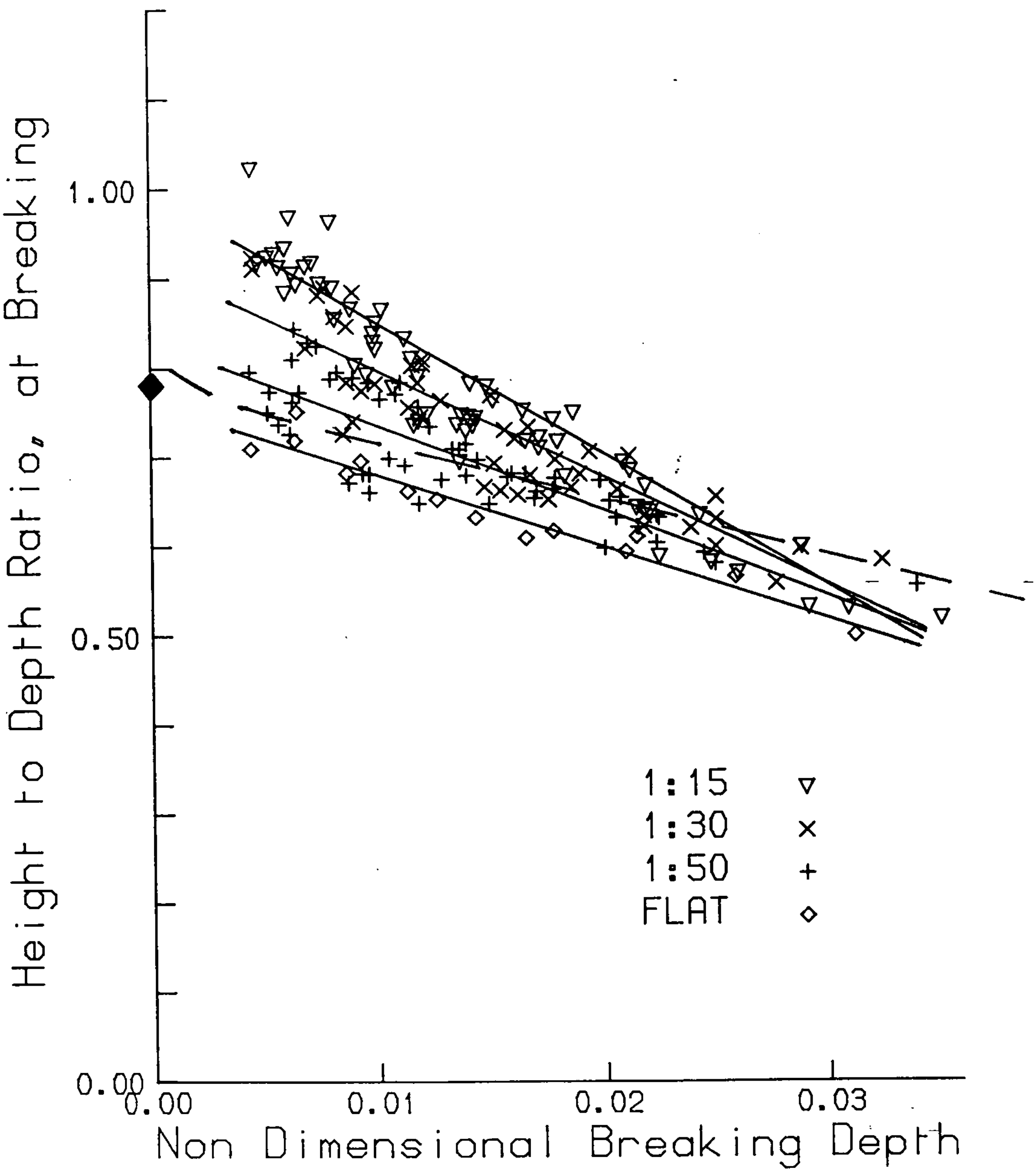

Fig. 4.4.6 Height to depth ratio , ·own.

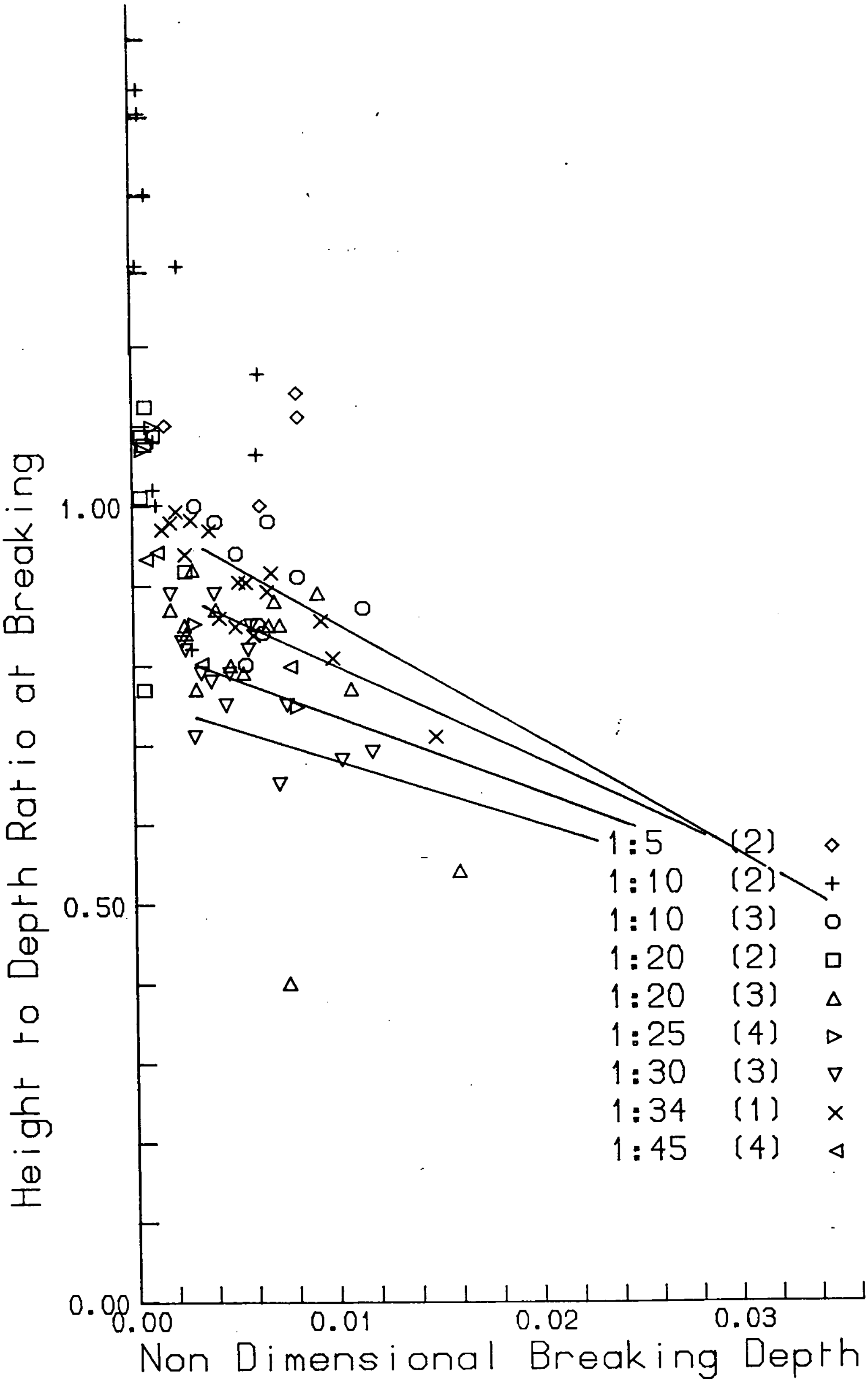

Fig. 4.4.7 Height to depth ratio , other.

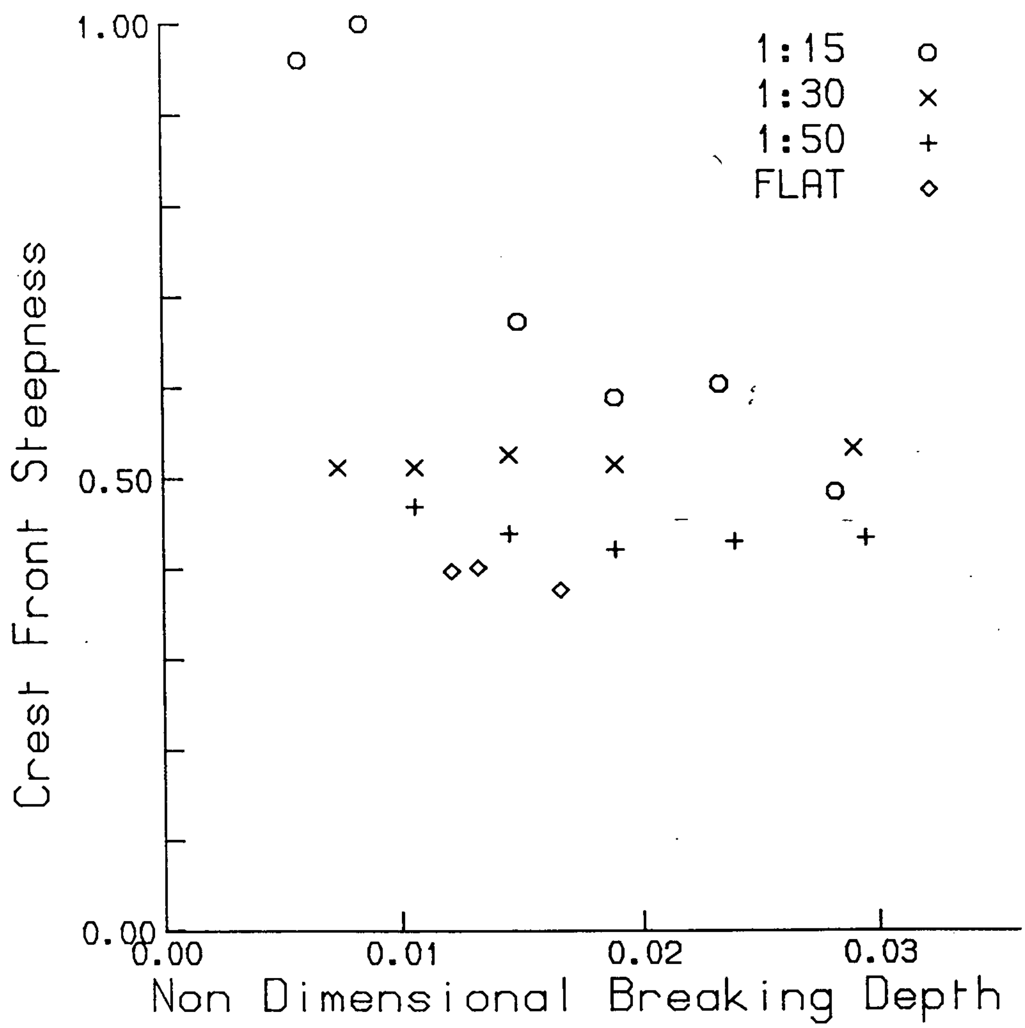

Fig. 4.4.8 Crest front steepness.

4.4.2 Discussion of results.

It can be seen from the comparison that the two sets of results are highly complimentary, the results from the literature being available for non- dimensional depths almost entirely below 0.012 and those from Edinburgh overlapping the higher end of these and extending the results to deep water.

Where the two sets of results do overlap there is very good agreement. The one exception is the height to depth ratio, where the clear slope dependence of the results in the Edinburgh data is not matched in the other results.

The results derived from Cokelet's model are only directly comparable with the flat bed results. They are in remarkably good agreement but systematically over predict flat bed results by five to ten percent. This difference is significantly less than that which is caused by the change of bed slope from flat to 1:15.

The difference in value between crest elevation and trough depth are clearly seen in fig. 4.4.1. There is also some slope dependence. The values of crest elevation are distinctly lower for the flat bed results than for the steeper slopes. Also, the trough depths are larger for the 1:15 results than for the other slopes. These trends are again visible in figures 4.4.2 and 4.4.3 where total wave height increases with bed slope.

The values of celerity, figure 4.4.4, are similar for the less steep slopes, however the results for the 1:15 slope are significantly higher. Note this does not imply that any particular wave will travel faster on a steeper slope ; the comparison is between waves of the same non-dimensional breaking depth.

The height to depth ratio, figure 4.4.6, shows the slope and non-dimensional breaking depth dependence most explicitly. The solitary wave result, $H/d = 0.78$ is seen as the limit to the flat bed results, which drop to 0.5 in deeper water. The deeper water results are, as expected, independent of bed slope. However, the slope dependence in shallower water is very pronounced. Figure 4.4.7 includes the results for very shallow water, where the height to depth ratio grows rapidly. This behaviour is generally restricted to non-dimensional depths of less than 0.003.

The crest front steepness, fig. 4.4.8 , is seen to vary significantly with the wave condition. The waves breaking on slopes of 1:30 or shallower all have steepnesses below 0.55, these correspond to spilling breakers. The 1:15 results by contrast show a rapid change from $\bar{cfs} = 0.5$ in deeper water, where the bed influence is small, to values of cfs of 1.0 in the shallower water where the waves plunge severely.

4.5 SHOALING SIMILARITY PARAMETERS.

It has been understood that two independent parameters, in particular the deep water steepness and the beach slope, are sufficient to fully describe monochromatic shoaling (cf. section 4.2).

Many shoaling similarity parameters have been proposed, the general aim being to find one single parameter, which can be used to describe the complete range of monochromatic wave breaking. That is, all other parameters describing the wave breaking are single valued functions of this parameter.

Irubaren and Nogales (1949) and Galvin (1968) both introduce shoaling similarity parameters. These are:

Irubaren parameter Eo = tan a (So)

Galvin (in shore parameter) $G = Hb/gsT^2$

Useful though a single parameter would be, the results presented here show that this would only provide an incomplete description.

This can be demonstrated by considering the graphs in section 4.3. The breaking height fig 4.3.3 is clearly a single valued function of deep water steepness and is independent of beach slope. Also the breaking height to depth ratio, fig 4.3.5, is dependent on both deep water steepness and beach slope. Any shoaling similarity parameter made of a combination of deep water steepness and beach slope which is constructed to collapse the breaking depth to a single valued function, would necessarily disrupt the single valued nature of the breaking height. Thus to search for a single shoaling parameter is futile.

4.6 OTHER BREAKING CRITERIA.

The most obvious and widely used breaking criterion is that a wave breaks when the velocity of the water in its crest exceeds the wave celerity. There has been some discussion as to whether this is the sole breaking criterion (Skjelbreia, 1987). In particular, attention is drawn to the initiation of spilling. Many spilling breakers begin with the plunging of a small spout at the top of the crest, but such a spout has not been observed in all spillers.

Experimental results are presented here for two measurable quantities that might have limiting values reflecting a second mechanism initiating breaking.

Crest front steepness, introduced by Kjeldsen and Myrhaug (1978), is used in the analysis of storm wave data, Kjeldsen and Myrhaug (1980), and for the prediction of extreme events, Myrhaug and Kjeldsen (1987). Figure 4.4.8 shows the values of crest front steepness measured for some of the waves used in this study. This figure clearly demonstrates the existence of a lower bound associated with spilling breaking. Additionally, the marked rise in cfs with breaking severity may provide a useful parameter in distinguishing severe breaking. Values of cfs below 0.55 being associated with spilling and values above with plunging, the severity of the plunging increasing with crest front steepness.

The second measured parameter is the maximum steepness attained at breaking on any part of the wave surface, Longuet-Higgins and Smith (1983). For plunging breakers, this becomes infinite as they are vertically fronted. The results for spilling breakers are plotted in figure 4.6.1. These results show that (a) the maximum steepnesses for the 1:30 beach are higher than for the less steep slopes and that (b) there is a lower limit to the measured steepness of about 0.65.

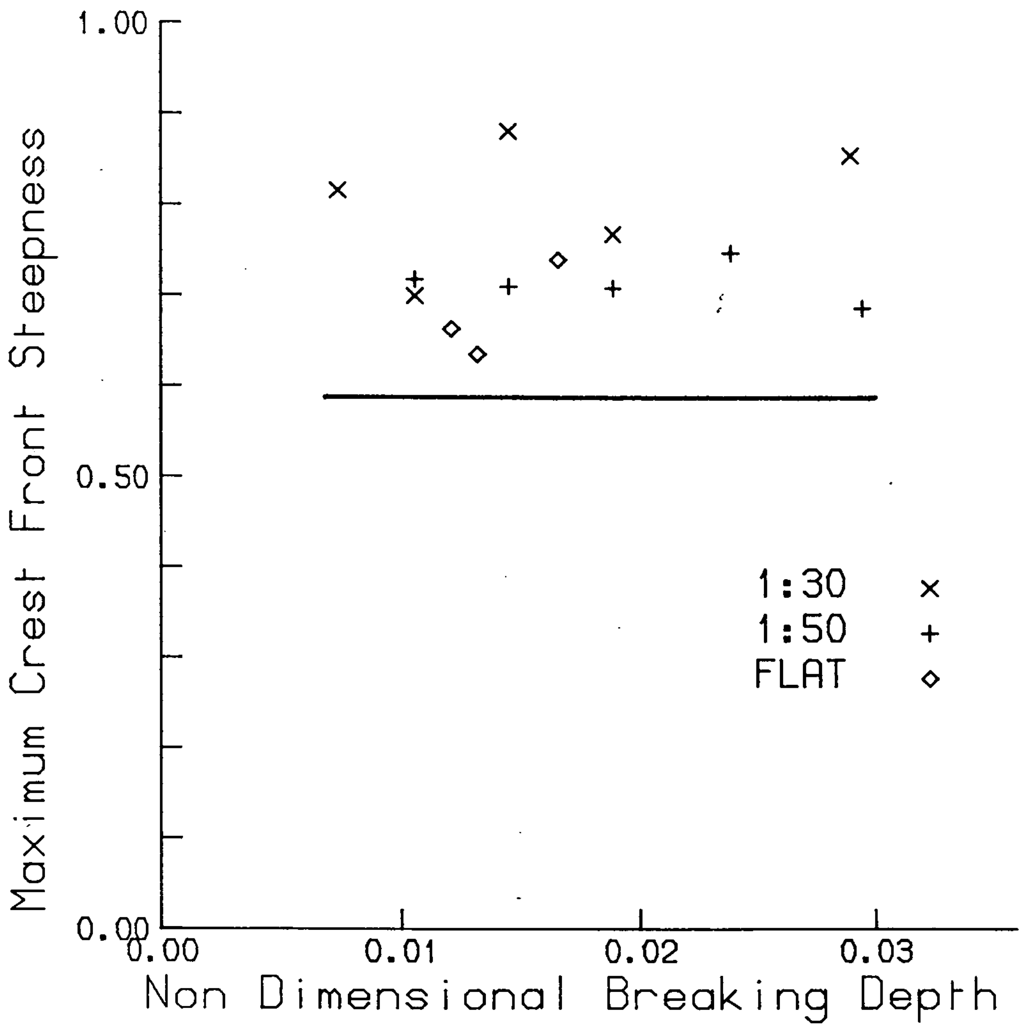

Fig. 4.6.1 Maximum crest front steepness.

The limit of 0.586 derived from numerical calculations by Longuet-higgins and Fox (1977) is shown as a horizontal line.

Chapter 5 Internal Kinematics of Shoaling Monochromatic Waves.

5.1 DEFINITIONS OF WAVES STUDIED.

The results presented in this chapter are from many different waves with breaking type ranging from very gently spilling to highly plunging.

The amount of detail in each of the measurements varies, this is because the operation of the LDA system is time consuming and therefore only the most significant values were measured. The LDA measurement is being supplemented by the particle image velocimetry (PIV) system now well developed at Edinburgh University which will enable rapid measurement of velocity fields. However the PIV in its present state of development is unable to measure accelerations (Gray and Greated, 1988).

The "targeted" measurements fall in three categories.

Firstly, results are used in section 5.2 to establish that the loading a wave imposes on a pile is, or very nearly is, a maximum at the point defined here as the breaking point. This justifies the use of the point of breaking as the single point in its development at which to measure any particular wave. The waves used in section 5.2 are the two extreme waves studied, the gentlest spiller and the strongest plunger. For each one the internal kinematics in the high crest region are shown for positions in the development of the wave before, at and after the breaking point.

Secondly, the velocities and accelerations at points directly below the highest point of the breaking crest are presented for an array of wave types covering most conceivable design situations. That is, a range of non-dimensional breaking depth of 0.057 to 0.842 and slopes of 1:15 to horizontal. (sections 5.3.1 and 5.3.2)

Thirdly, measurements were taken over an array of points showing the full flow field of four waves, very typical of those encountered in design circumstances. These are identical in terms of their depths and periods but show effects due to their differing bed slopes. (section 5.3.3)

Tables are presented which define the waves studied, firstly in laboratory terms in table 5.1.1 and then again in table 5.1.2 re-scaled to a depth of one meter with corresponding periods.

Table 5.1.1 Table showing waves used in the study of internal kinematics. Values quoted at the scale of the laboratory experiments.

	TIME DEVELOPMENT		FULL FIELD		CREST PHASE	
Bed Slope	db (cm)	f (Hz)	db (cm)	f (Hz)	db (cm)	f (Hz)
FLAT	16.25 SPILLER	1.0	18.5	0.915	18.5	0.799, 0.836, 0.915
1:50			18.5	1.0	18.5	0.75, 0.875, 1.0, 1.125, 1.25
1:30			18.5	1.0	18.5	0.625, 0.75, 0.875, 1.0, 1.25
1:15	14.6 PLUNGER	0.625	14.6	1.125	14.6	0.625, 0.75, 0.875, 1.0 1.125, 1.25, 1.375

Note the db=14.6, f=1.125 wave on a 1:15 slope scales to db=18.5 and f=1.0. This is for direct comparison with the f=1.0 Hz results from other slopes.

Table 5.1.2 Scale of db = 1m with waves defined by period.

Bed Slope	TIME DEVELOPMENT T (sec.)	FULL FIELD T (sec.)	CREST PHASE ONLY T (sec.)
FLAT	2.48 SPILLER	2.54	2.91, 2.78, 2.54
1:50		2.32	3.10, 2.66, 2.32, 2.07, 1.86
1:30		2.32	3.72, 3.10, 2.66, 2.32, 1.86
1:15	4.19 PLUNGER	2.33	4.19, 3.49, 2.99, 2.62 2.33, 2.09, 1.90

The graphs in this chapter present results at the scale used in the later table which facilitates comparison with other results. This is also aimed at design where the length scale factor taking these results to full scale would simply be the full scale water depth.

5.2 DEVELOPMENT THROUGH BREAKING OF SPILLING AND PLUNGING WAVES.

Two waves were chosen for this study, bracketing all the waves measured in this chapter. The aim is to establish that design based on a wave as it first becomes vertically fronted is conservative with respect to all other phases of that same wave. All results in this section are presented in laboratory coordinates.

The spilling breaker.

The spilling wave studied here is the shortest period wave of those which are considered in this chapter, breaking on a flat bed. It has a frequency of 1.0 Hz and breaks on a water depth of 16.25 cm and has a breaking height of 9.3 cm and a celerity of 122 cm/s. It has a non-dimensional breaking depth of 0.017.

The photographs in fig. 5.2.1 show the time development of the surface profile and it can be seen from these that the spilling is very gentle.

The breaking point was determined in the laboratory to be 5.45 m from the paddle (x=5.45.) It can be seen from the photographs that the assumption made in most wave models that the wave can be considered to be stationary is good over a length of roughly 30 cm about the breaking point, that is, for a corresponding time of about 0.25 T. Over larger distances the development of the spilling can be clearly seen.

The wave is travelling over a horizontal bed and there is no increase in energy density; in fact the spilling is causing a decrease in energy. The fact that the spilling region grows shows that the spilling is self sustaining.

Internal motion. Fig 5.2.2 shows the flow field in the high crest region of this wave at positions before, at and after the breaking point. With the exception of the pre-breaking wave, all show the velocities increasing with height to values near to that of the celerity in the region immediately below the crest. This satisfies the most fundamental breaking criterion.

Considering the change in the flow structure, two developments can be observed. Firstly, that the velocities immediately below the crest are higher once breaking has been established than they were prior to this. This is true for positions x=580 and 620 where the spilling is highly developed and where the wave is significantly reduced in height and energy. Secondly, the rate of increase in

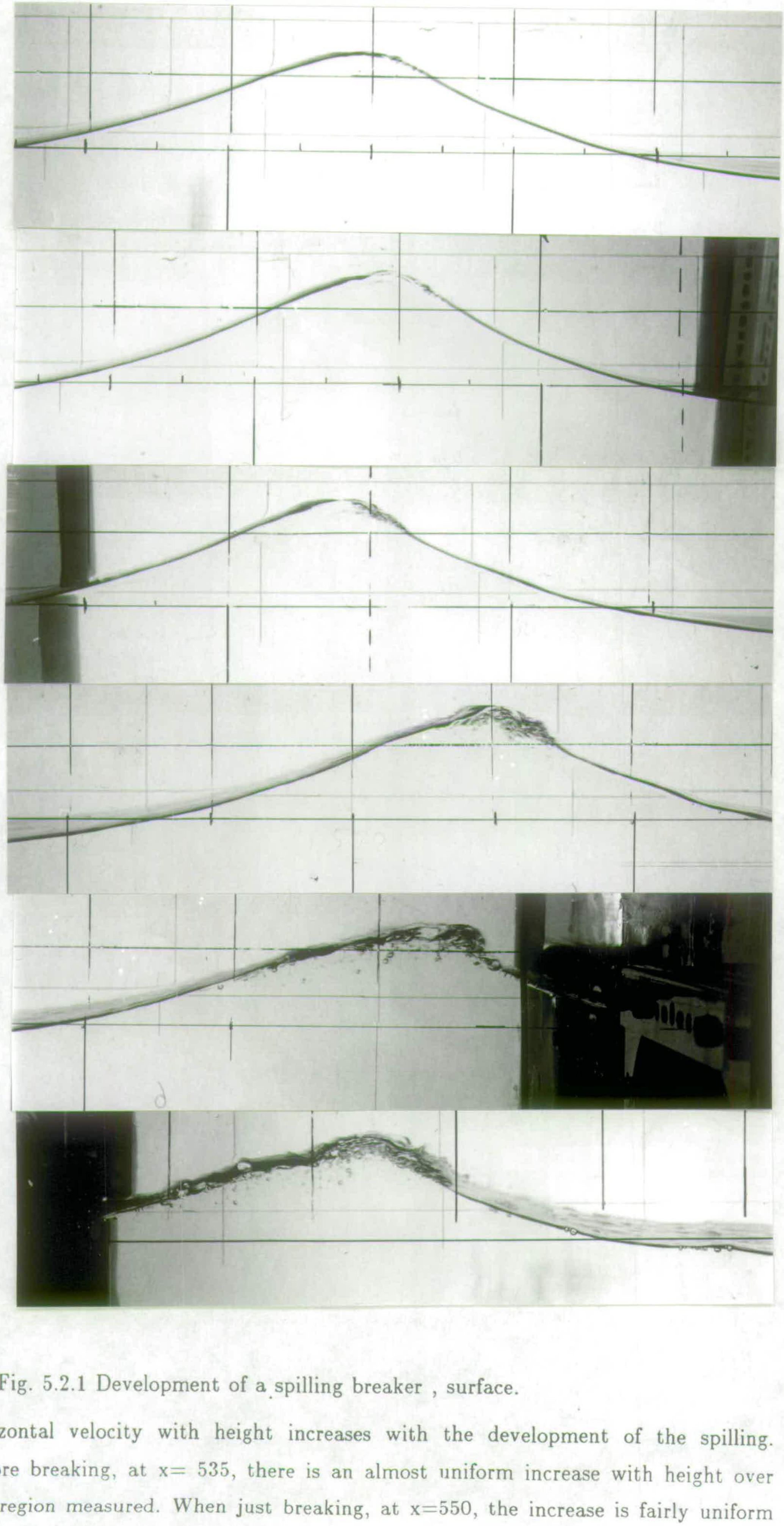

Fig. 5.2.1 Development of a spilling breaker , surface.

horizontal velocity with height increases with the development of the spilling. Before breaking, at x= 535, there is an almost uniform increase with height over the region measured. When just breaking, at x=550, the increase is fairly uniform though with a greater rate of increase with height.

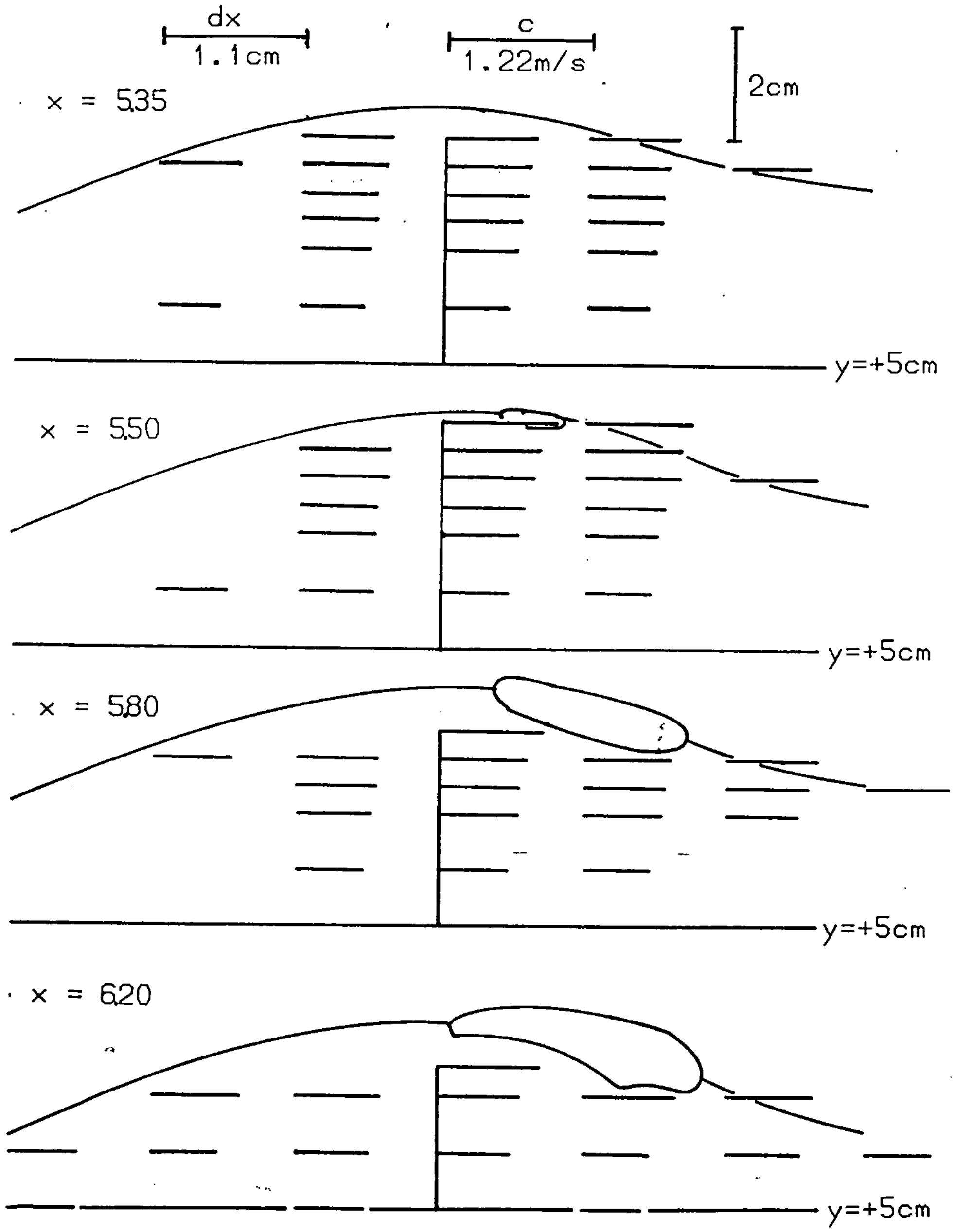

Horizontal velocities below a spilling breaker.

T = 1 sec. db = 16.25cm cb = 1.22m/s xb = 5.45m

Fig. 5.2.2 Development of a spilling breaker , internal velocities.

In the fully developed spillers, at x= 580 and 620, the increase is steeper still but localised to a region close to the surface, (within about 0.15 of the crest elevation). This local vorticity may be central to the sustaining of the breaking.

The plunging breaker.

The plunger studied here is the most extreme of all the breakers measured in this chapter. It has the longest period and breaks on the steepest slope. It is a 0.625 Hz wave and breaks at a water depth of 14.6 cm on a 1:15 slope with a breaking height of 13.15 cm and a celerity of 138 cm/s. This has a non-dimensional breaking depth of 0.0058 .

The photographs in fig 5.2.3 show the development of the surface profile through breaking. They exhibit the rapid growth and decay of the wave height and the steepening of the front of the crest, the formation and overturning of the plunging spout and the touch down and throw up as the spout meets the trough. The new wave thrown up by the impinging of the spout can also be seen.

This wave is very different in character from the spiller shown in fig. 5.2.1 and in particular the strong time dependence of its surface profile casts serious doubt on the assumption that the wave can be treated as stationary for modelling purposes. The distance over which the profile could be considered stationary at breaking is 3 cm, an order of magnitude down on that of the spiller. These measurements are only rough, and the values should be seen as estimates.

Fig. 5.2.4 shows the time development of flow within the plunging breaker before, at and after the breaking point. There is a marked rise in the velocities over the 10 cm prior to breaking, but there is no decrease over the 20 cm immediately following the breaking point. Also the velocity of the water at the front of the wave is consistently and significantly higher than that directly below the highest point. This is consistent with the water forming a spout at the crest travelling slightly over the wave celerity at the point of breaking.

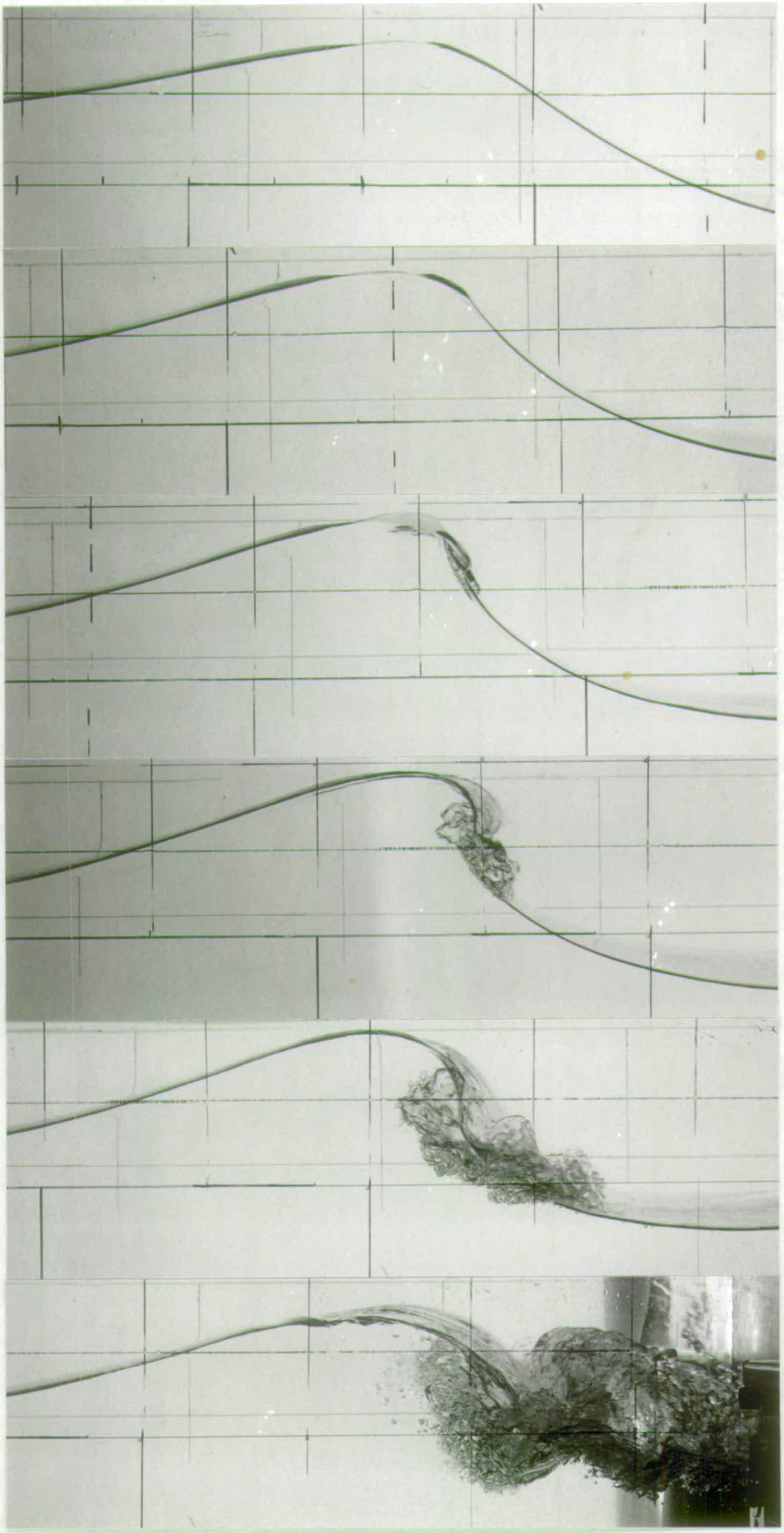

Fig. 5.2.3 Development of a plunging breaker , surface.

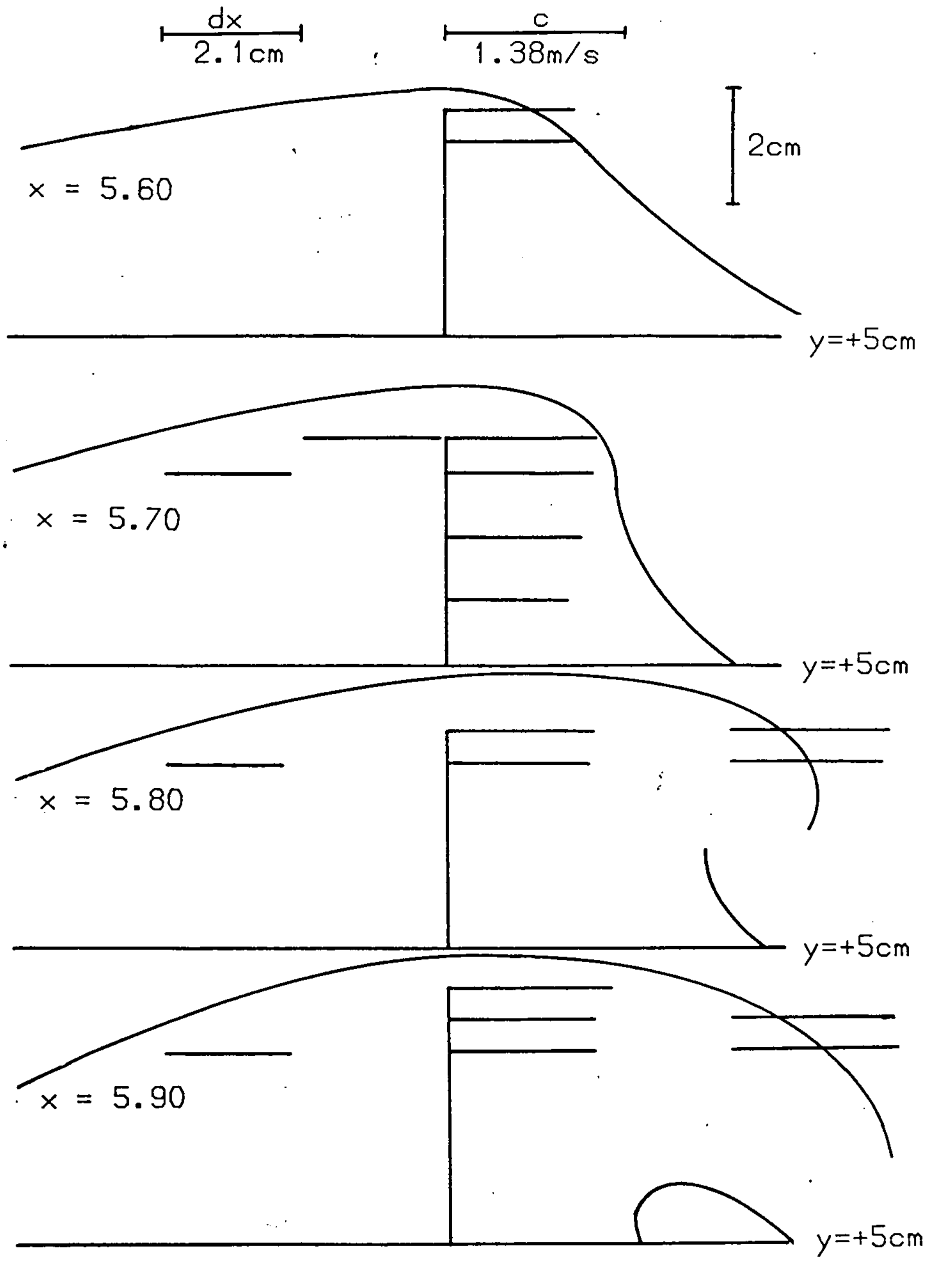

Horizontal velocities below a plunging breaker.

T = 1.6 sec. db = 14.6cm cb = 1.38m/s xb = 5.70m

Fig. 5.2.4 Development of a plunging breaker , internal velocities.

Conclusion.

The main conclusion that is drawn from these two studies is that the breaking position defined as the point where the wave first becomes vertically fronted produces the most extreme estimate of the net force the breaking wave will exert on a slim vertical cylinder.

This is shown to be the case as before this position the velocities within the fluid are smaller, and after this position the velocities are smaller for the case of the spilling breaker and equal but acting over a reduced height in the case of the plunging breaker. The faster moving spout of the plunger will cause larger local force on members in the high splash zone but will not produce larger forces than the breaking point where the full height of the wave acts.

A second argument for choosing this position for design purposes is based on the danger posed by the high peak forces associated with the slamming of the vertical wave face (Easson, 1983).

5.3 MEASURED RESULTS.

This section is divided into three subsections, the first two contain results for measurements of the horizontal velocity and the vertical acceleration taken at points directly below the crest in waves at their breaking point. In the first section they are grouped by bed slope and show the influence of wave period. In the second section they are grouped by wave period and show the influence of bed slope. The third section contains velocities and accelerations measured over a two dimensional grid and shows the flow fields below selected waves. The values for the surface parameters describing the waves studied here are contained in the tables, figs. 5.1.1 and 5.1.2. Note, the value of the celerity is plotted as a final point at the measured crest elevation.

5.3.1 Influence of wave period. 5.3.1 to 5.3.4 show the particle velocities measured below the crest for waves breaking on 1:15 , 1:30 , 1:50 and flat slopes respectively and similarly figs. 5.3.5 to 5.3.8 show the accelerations measured for the same waves.

Note, the value of the celerity is plotted as a final point at the height of the crest elevation.

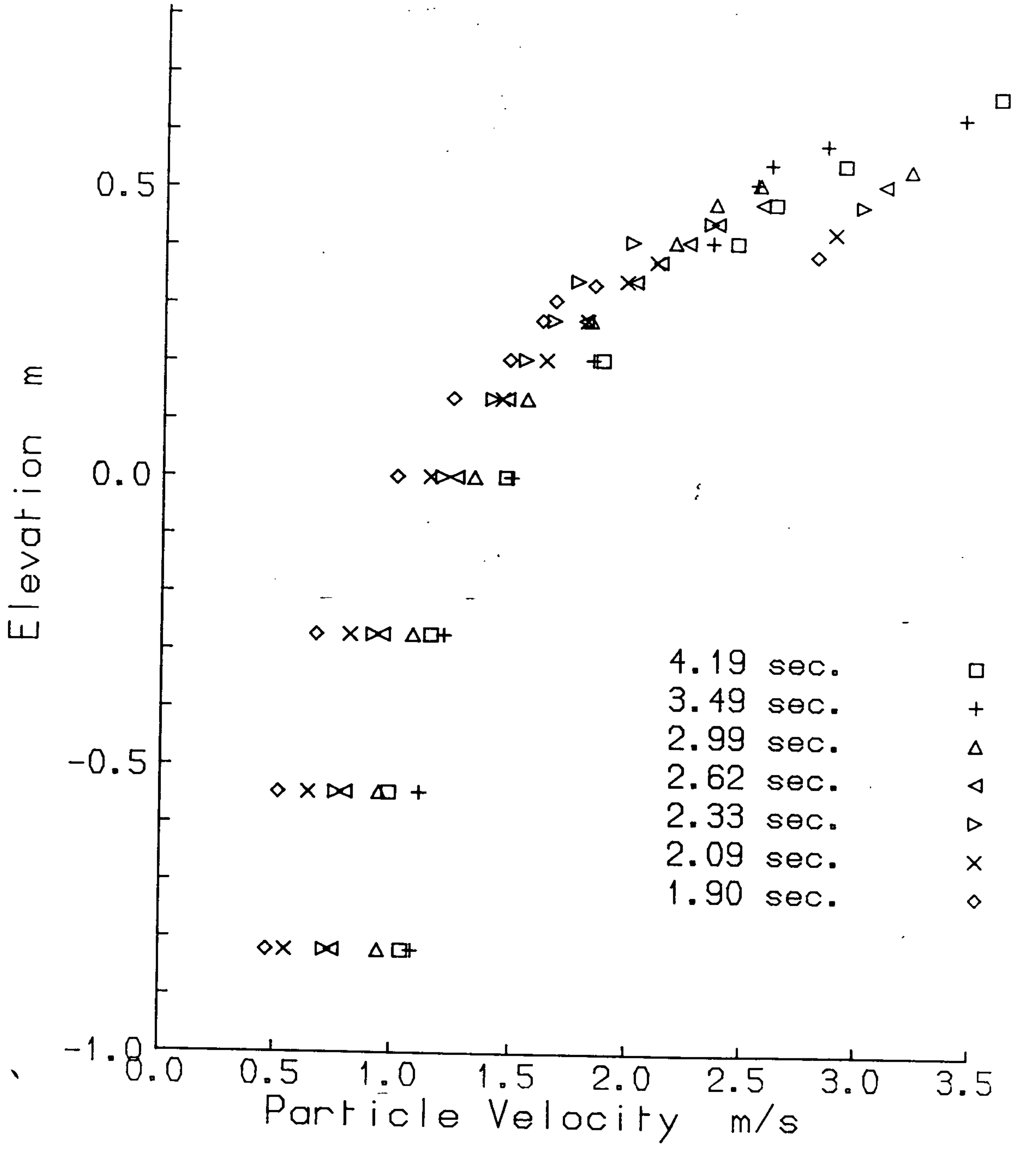

Fig. 5.3.1 Measured horizontal particle velocity, 1:15 slope.

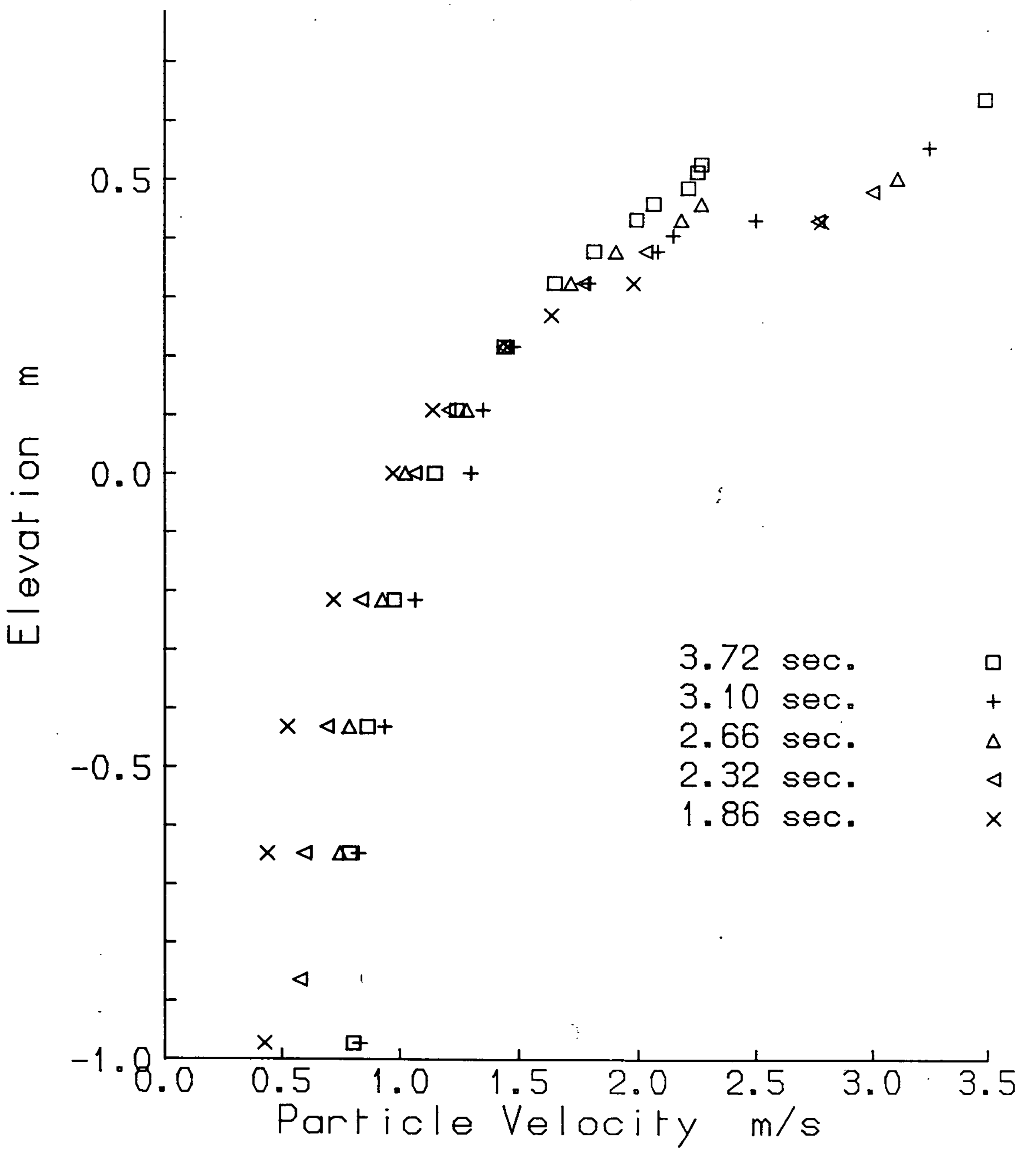

Fig. 5.3.2 Measured horizontal particle velocity, 1:30 slope.

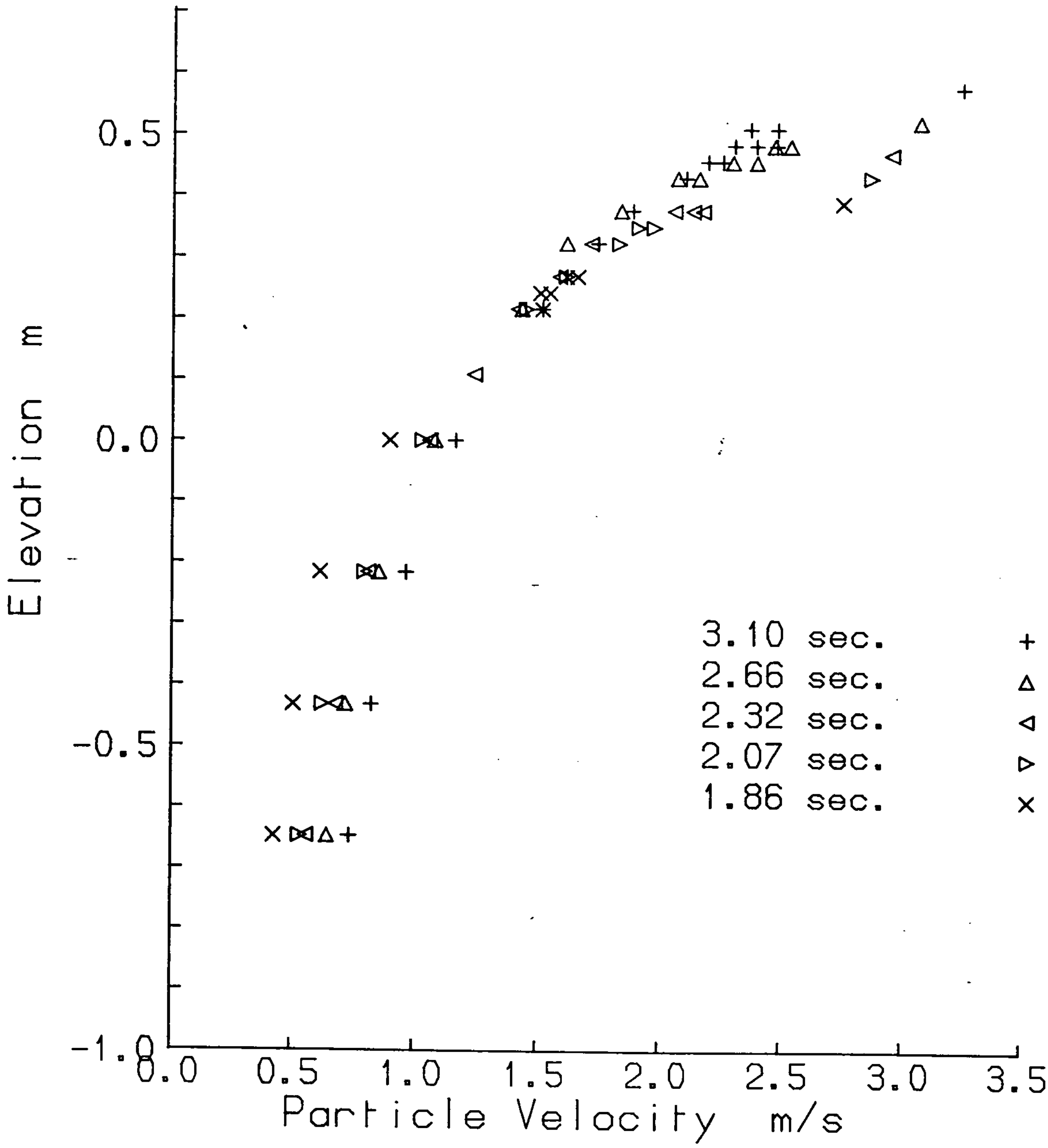

Fig. 5.3.3 Measured horizontal particle velocity, 1:50 slope.

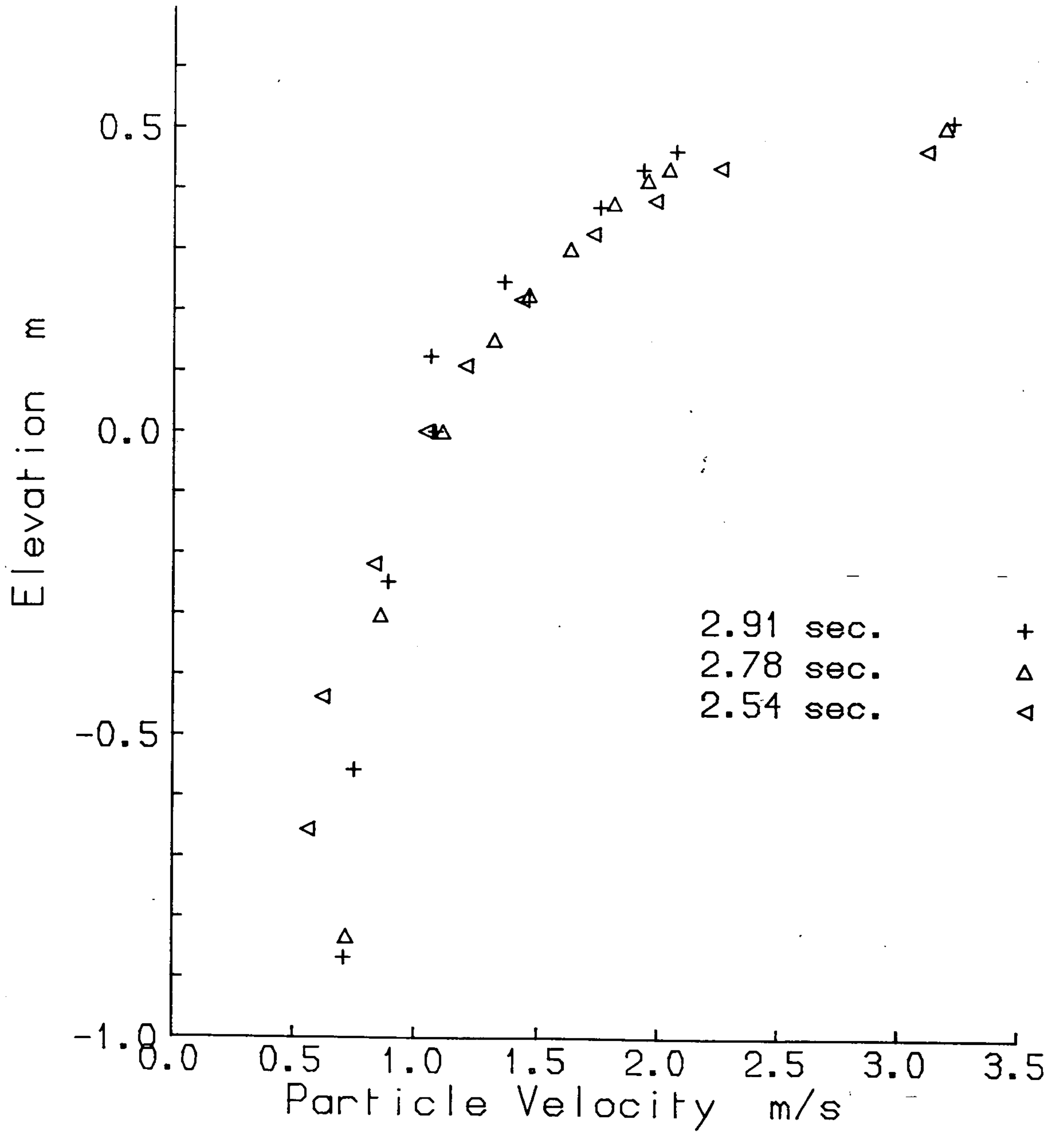

Fig. 5.3.4 Measured horizontal particle velocity, flat slope.

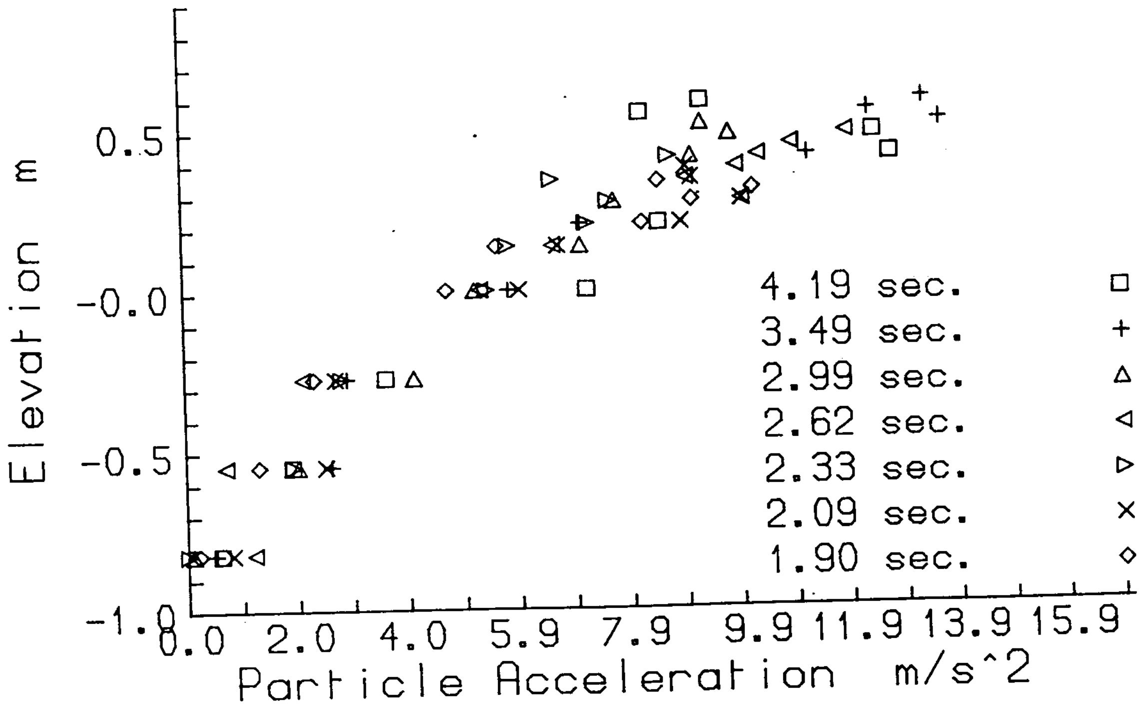

Fig. 5.3.5 Measured vertical particle acceleration, 1:15 slope.

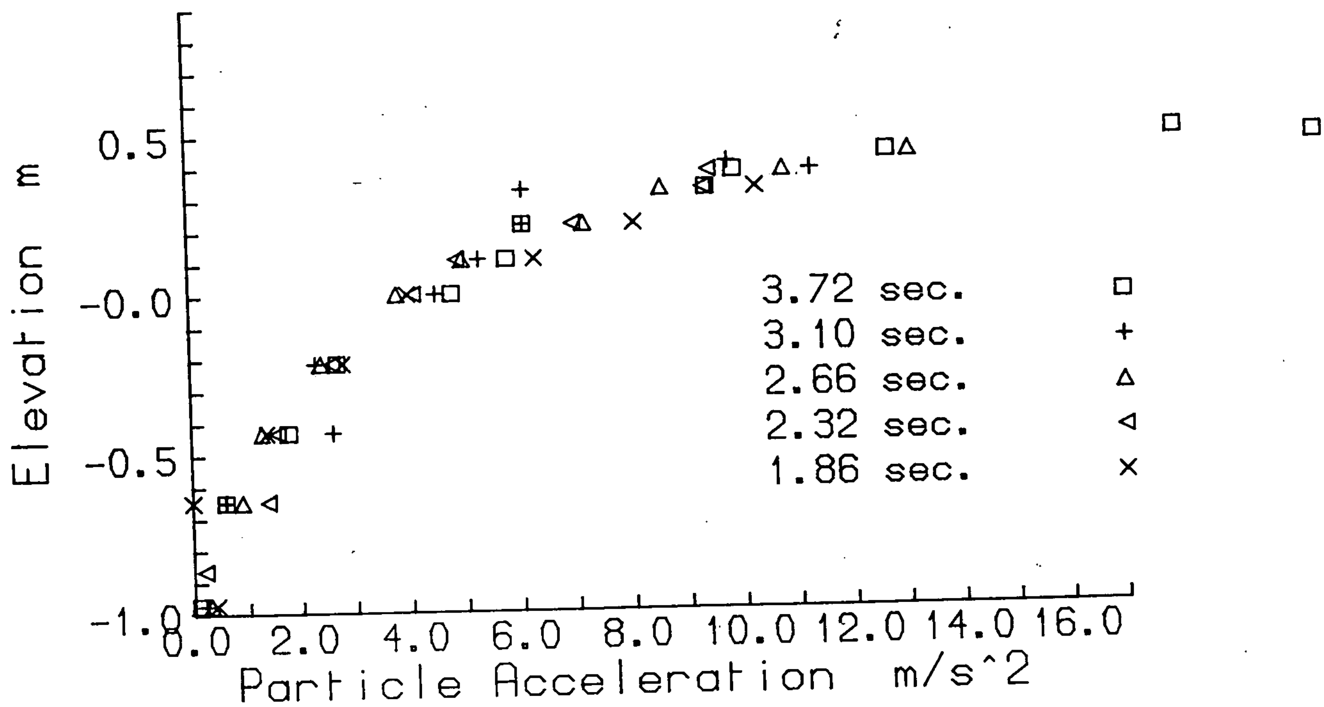

Fig. 5.3.6 Measured vertical particle acceleration, 1:30 slope.

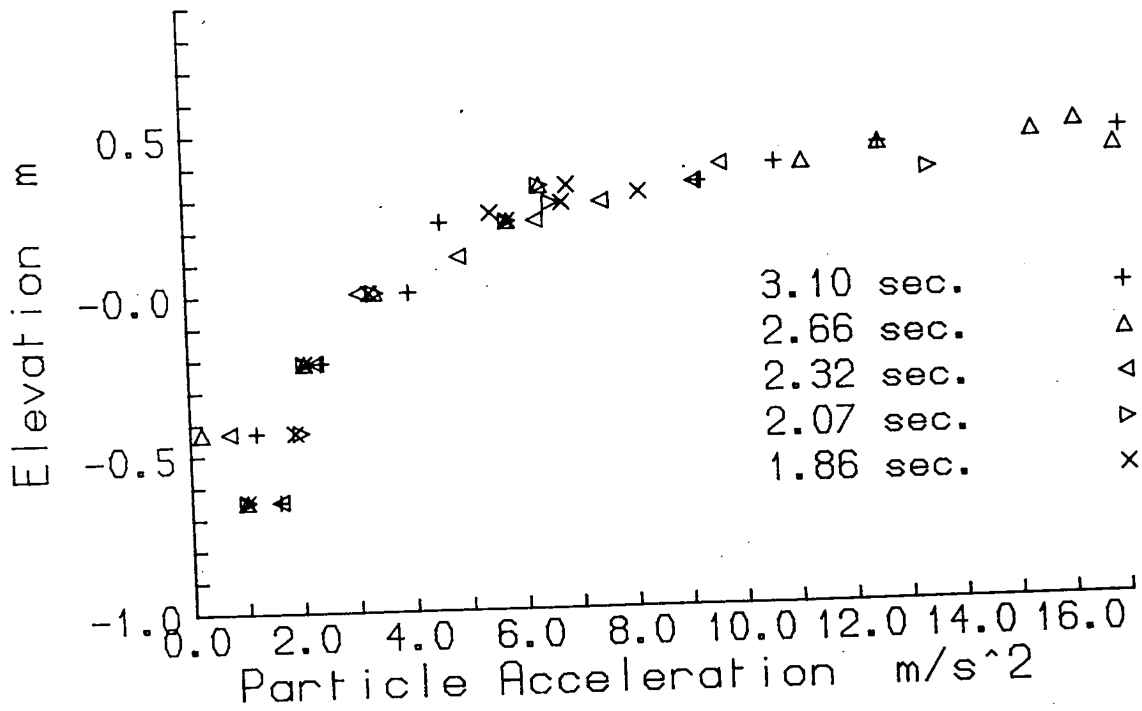

Fig. 5.3.7 Measured vertical particle acceleration, 1:50 slope.

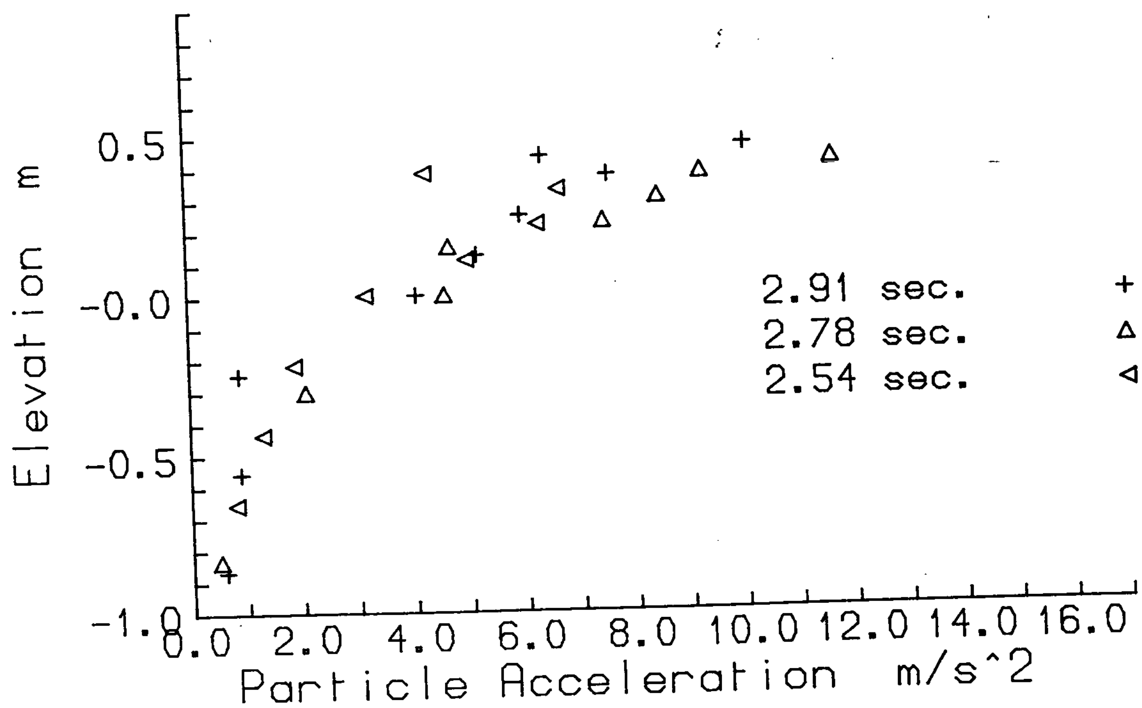

Fig. 5.3.8 Measured vertical particle acceleration, flat slope.

Concerning the velocities, there are several observations to note.

1 All the results show velocity increasing monotonically with height, the increase getting larger with height. The rate of increase remains finite and the value of particle velocity seems to approach the limit of the wave celerity at the crest elevation.

2 Below the still water level the curves are ordered by period, the velocity increasing with period. For all the non-flat bed results this amounts to a factor of two between the velocities of the extreme cases studied here. 2a The extreme plunging breaker T=4.19 on the 1:15 slope has lower velocities below the still water level than the T=3.49 wave. This is an anomaly and may be due to back rush from the previous wave.

3 The velocities at the top of the crests also show strong ordering reflected blatantly in the points marking maximum elevation and celerity. This order is the exact reverse of the order below the still water level and requires the curves for all waves to cross. This crossing is most obvious in the figures showing the 1:30 and 1:50 results where the crossing occurs at the same level for all the waves producing a necking effect in the graphs.

4 Related to the above is the fact that the smaller period waves have a more rapid increase in velocity with height than the larger period waves.

5 For some levels the velocity at the extreme top of a lower shorter period wave is larger than the velocity below the top of a taller larger period wave. This is of importance for the design of individual members, particularly for fatigue.

Concerning the accelerations, there are several observations to note.

1 As with the velocities, all the results show acceleration increasing monotonically with height. But rather than having a finite rate of increase and associated limiting values, the accelerations, most notably on the 1:30 and 1:50 slopes, have a very rapid increase with height and no apparent limiting value. 1a The largest accelerations occur in the waves with the largest periods. This may be a valid observation artising from the celerity dependence of the Eulerian acceleration. However, high accelerations might be present but not measured in the experimentally less stable shorter period waves.

2 Below the still water level the accelerations are generally less than 2g/3 and decay almost linearly to zero at the bed.

3 There is no apparent period dependence in the accelerations.

5.3.2 Influence of bed slope.

The results from the last section are re-plotted here grouped by period to show the slope dependence of the results. The six graphs figs. 5.3.9 to 3.3.14 show particle velocities measured below the crest for waves of periods 1.9, 2.1, 2.3, 2.7, 3.1 and 3.7 sec. respectively, and similarly figs. 5.3.15 to 5.3.19 show the accelerations for the same waves.

The top point in each of the velocity graphs is the celerity marked at the crest elevation. This is shown with a + symbol.

Concerning the velocities there are several observations to make.

1 The results converge in the high crest region. This strongly supports the breaking criterion that the maximum water velocity tends to the wave celerity.

2 Away from the high crest region the results separate with the steeper slopes having larger horizontal velocities.

This effect increases with period and is most observable in fig 5.3.14, the 3.7 second wave, where it amounts to an almost universal 30 % increase in velocity.

The same slope dependence is seen in the accelerations as is seen in the velocities.

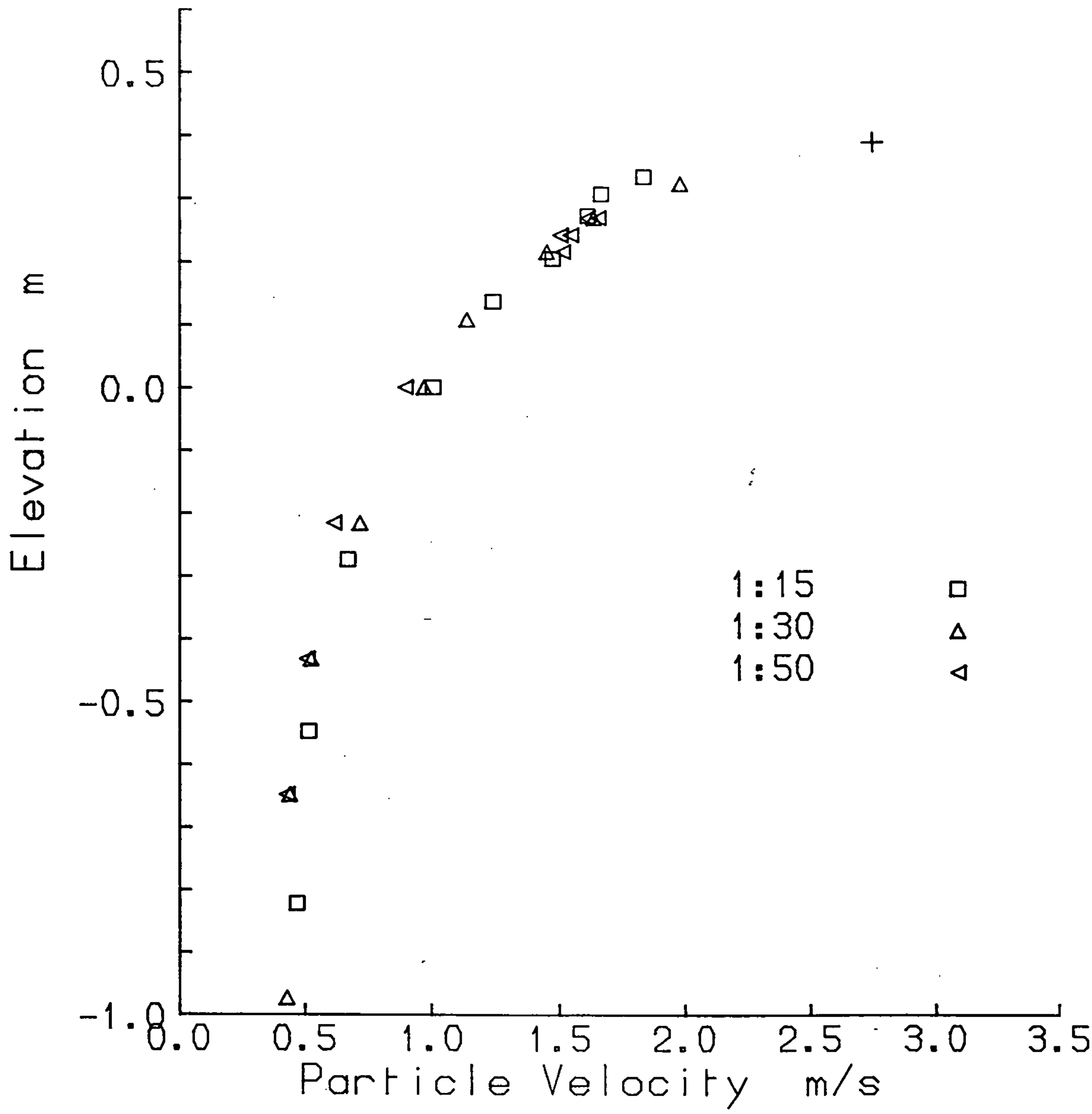

Fig. 5.3.9 Measured horizontal particle velocity, T = 1.9 sec.

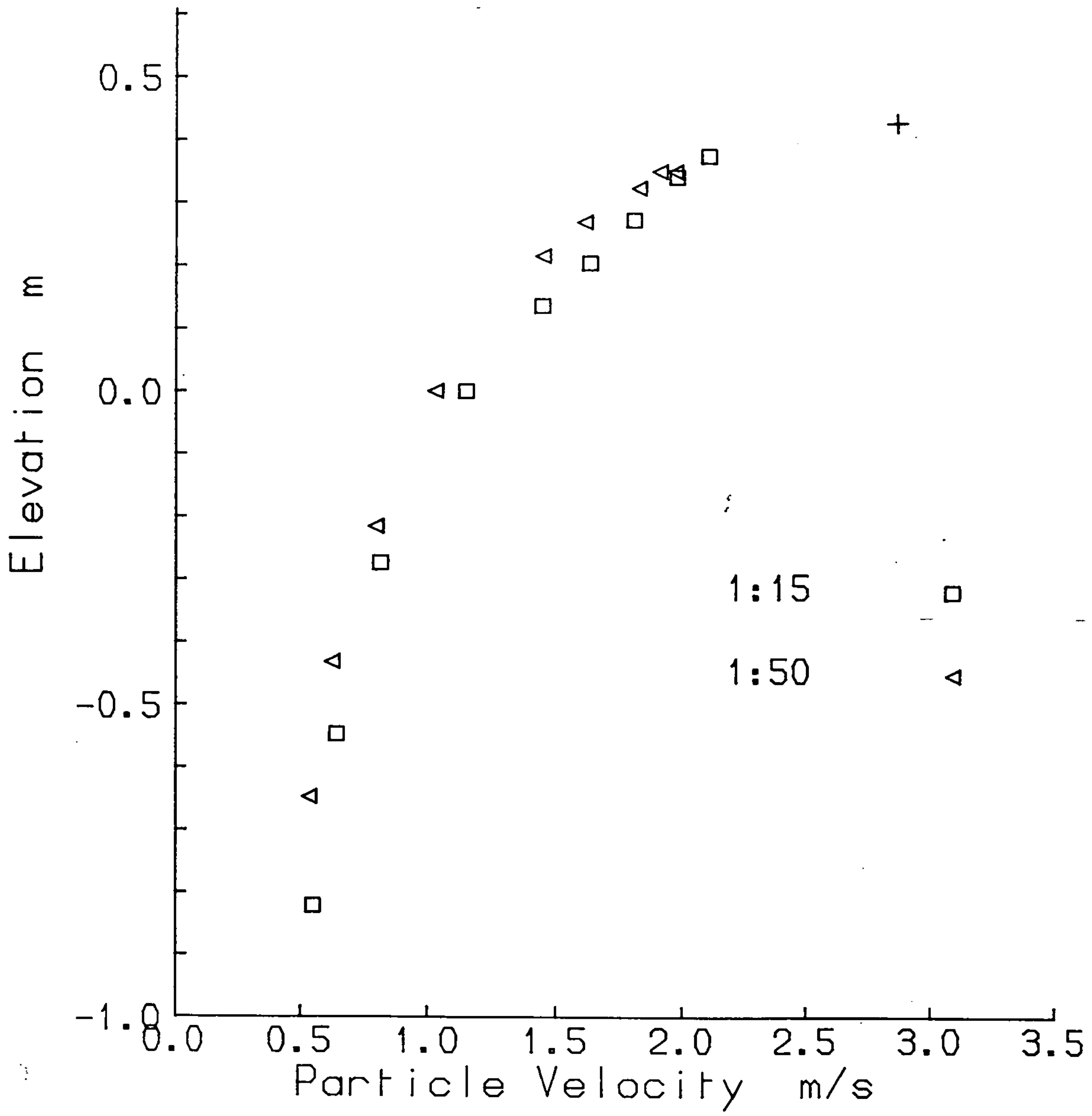

Fig. 5.3.10 Measured horizontal particle velocity, T = 2.1 sec.

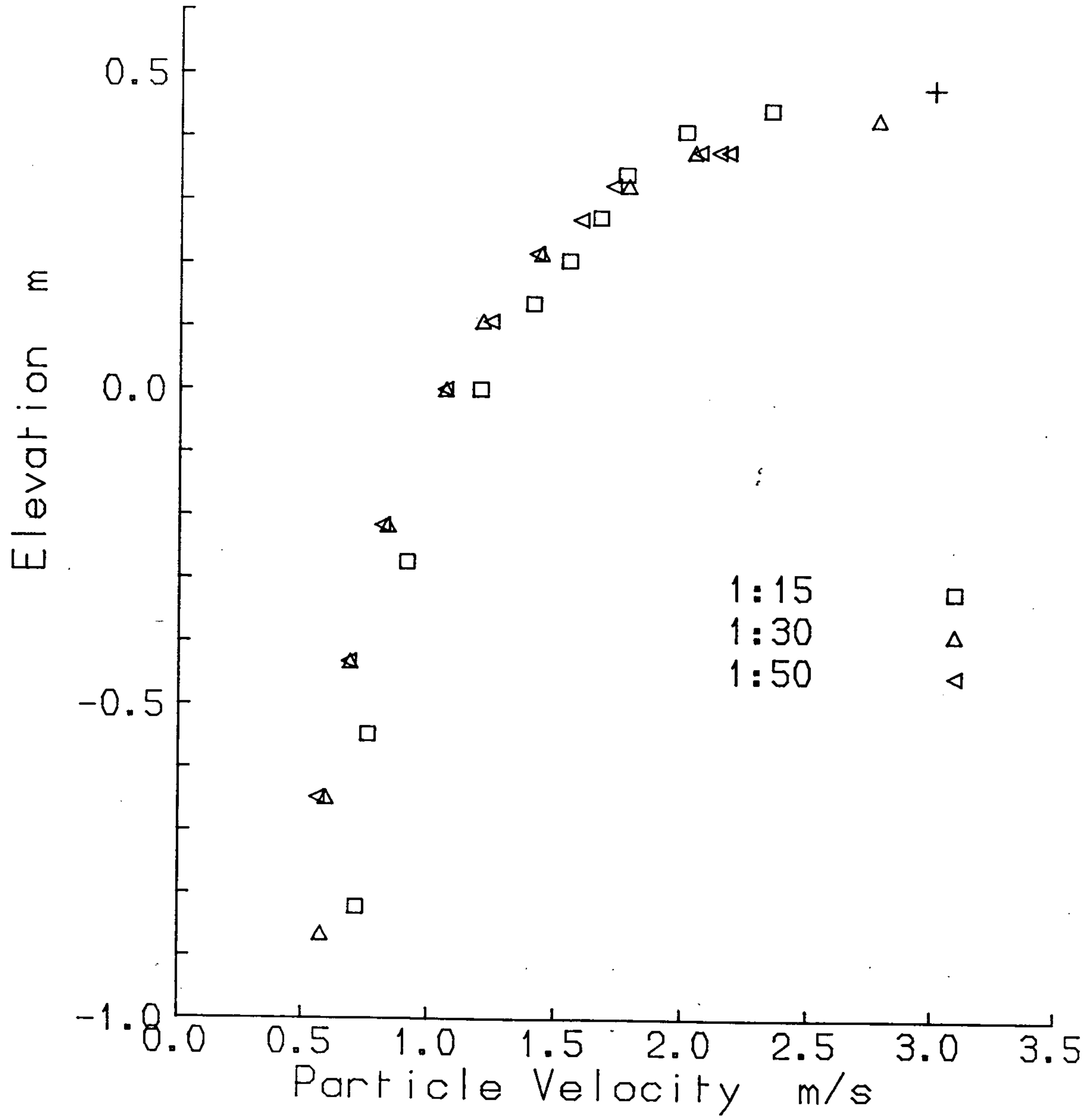

Fig. 5.3.11 Measured horizontal particle velocity, T = 2.3 sec.

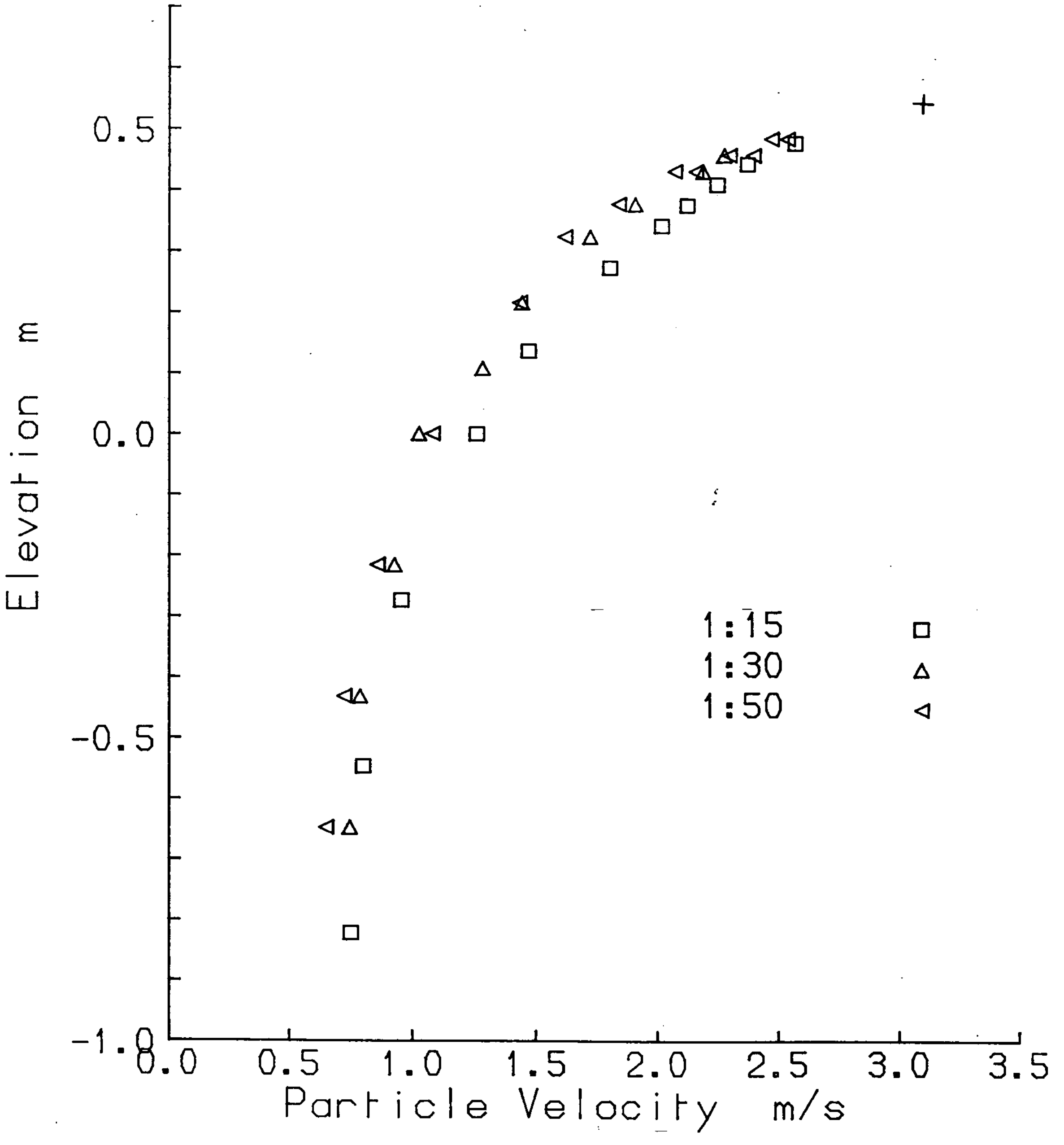

Fig. 5.3.12 Measured horizontal particle velocity, T = 2.7 sec.

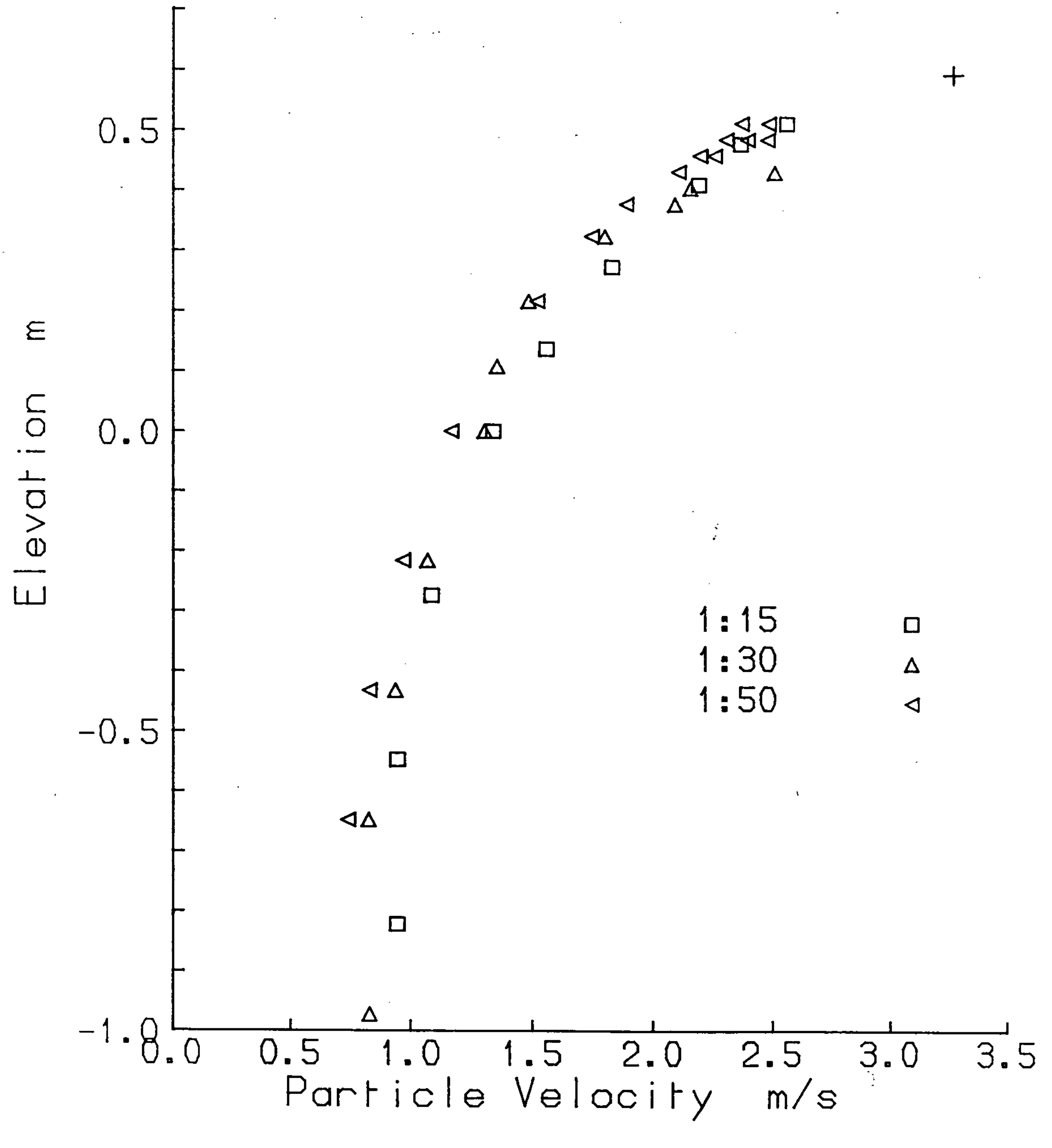

Fig. 5.3.13 Measured horizontal particle velocity, T = 3.1 sec.

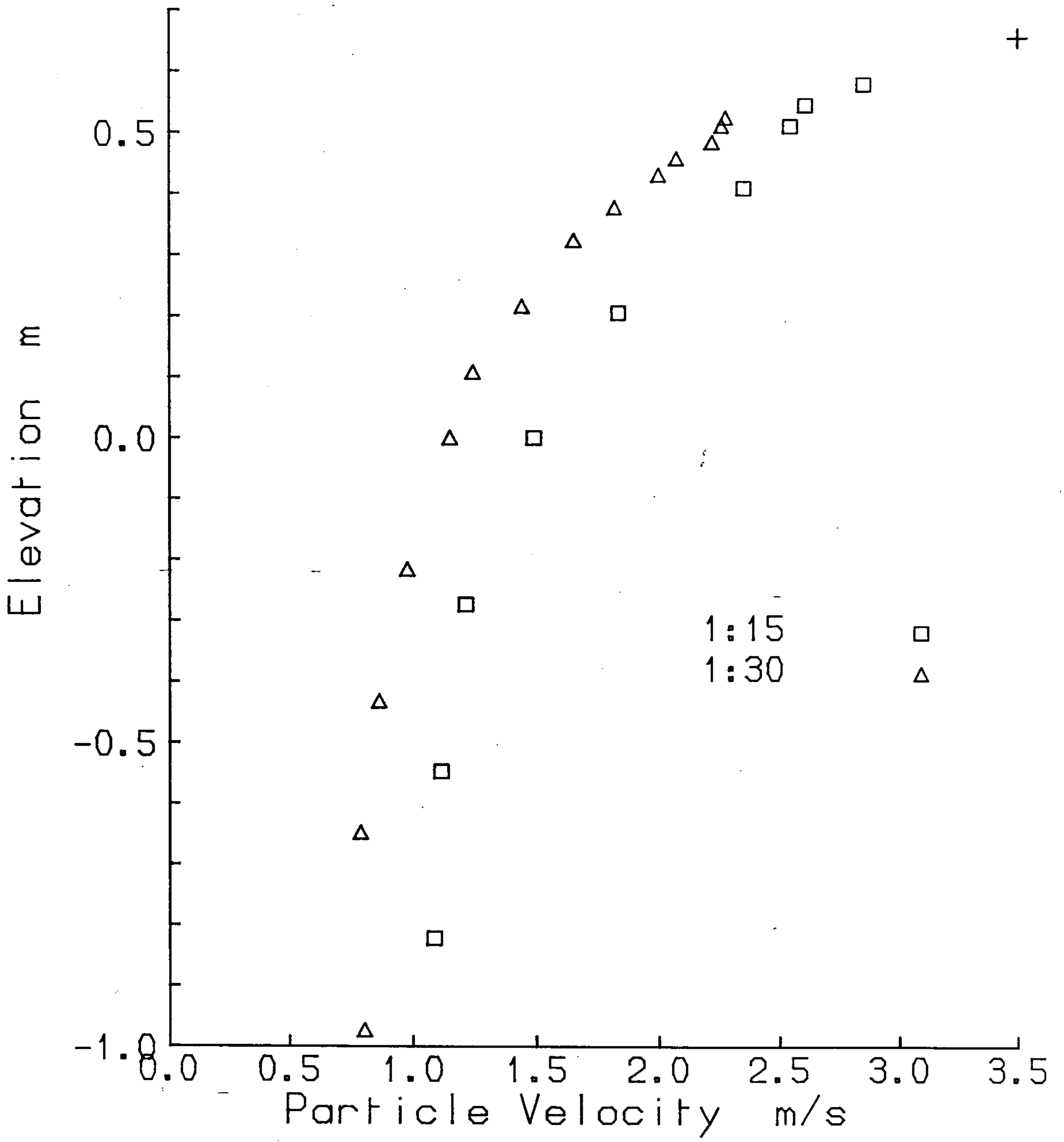

Fig. 5.3.14 Measured horizontal particle velocity, T = 3.7 sec.

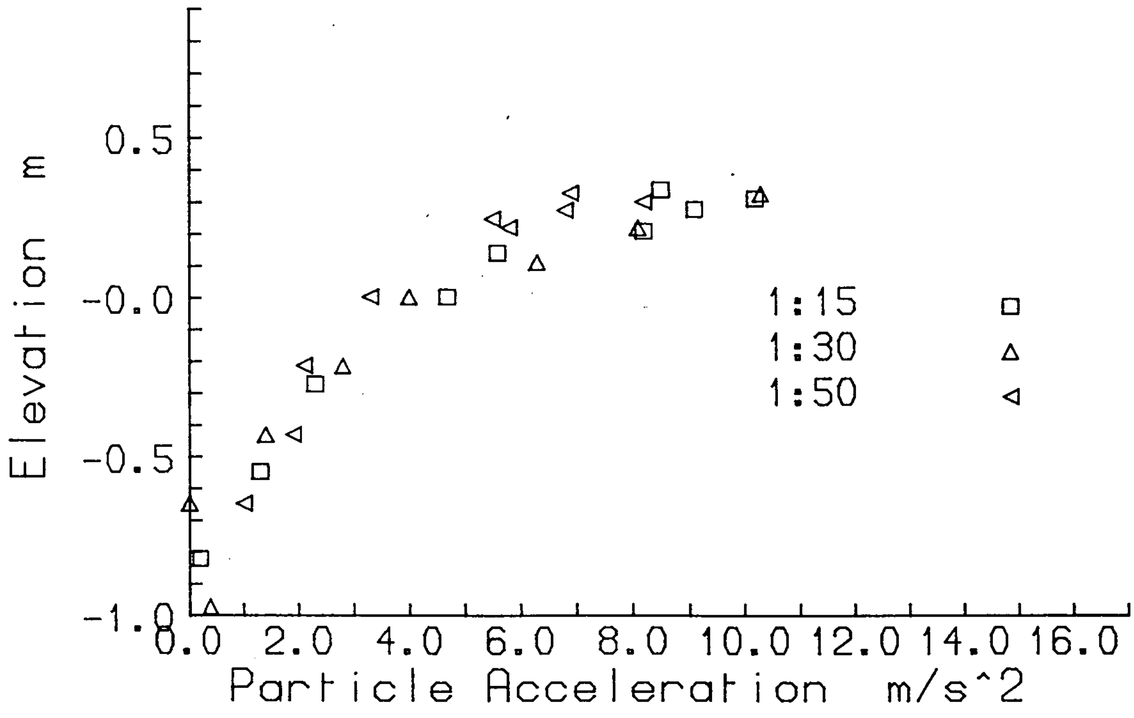

Fig. 5.3.15 Measured vertical particle acceleration, T = 1.9 sec.

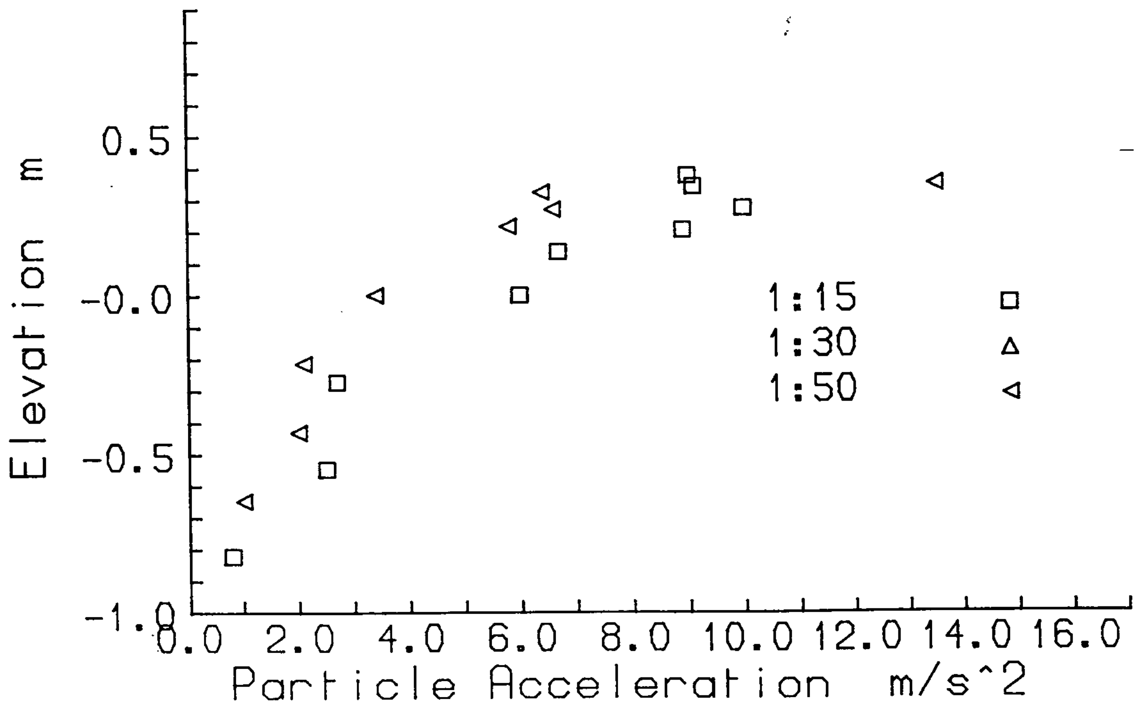

Fig. 5.3.16 Measured vertical particle acceleration, T = 2.1 sec.

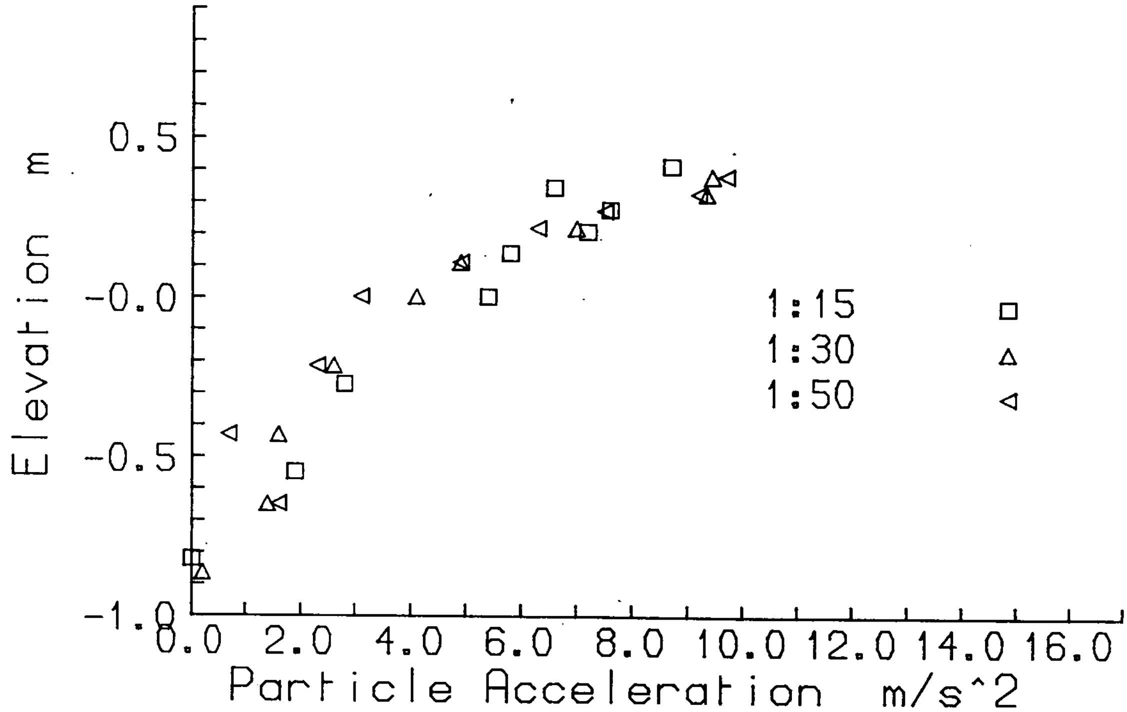

Fig. 5.3.17 Measured vertical particle acceleration, T = 2.3 sec.

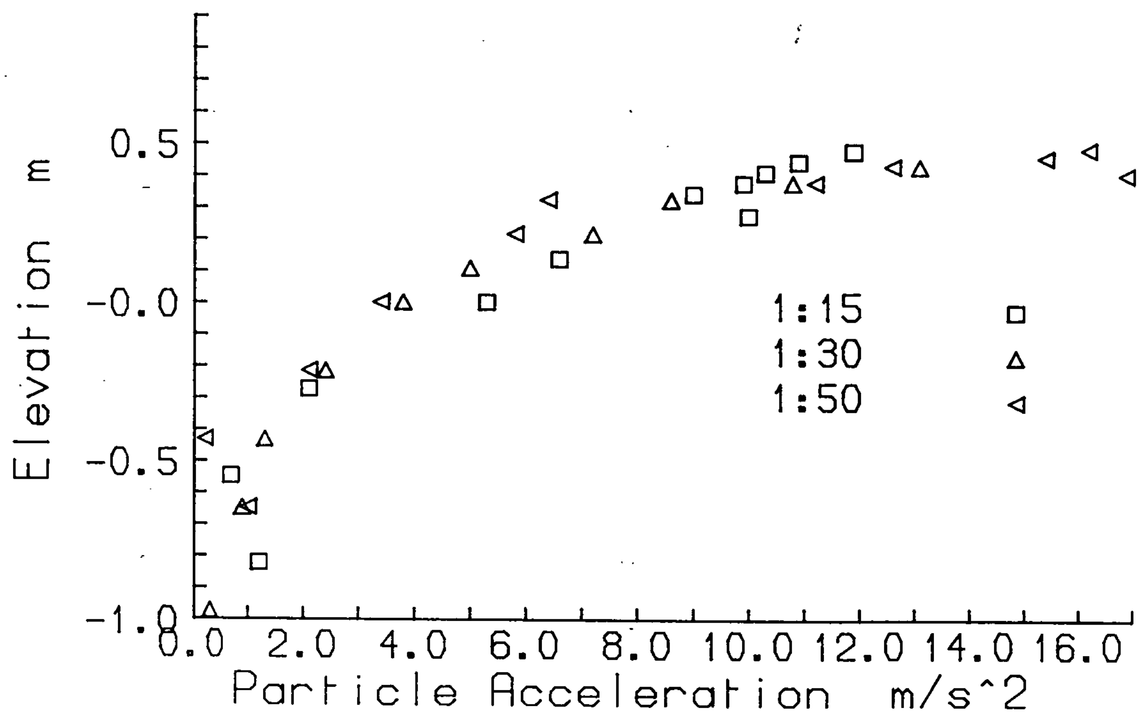

Fig. 5.3.18 Measured vertical particle acceleration, T = 2.7 sec.

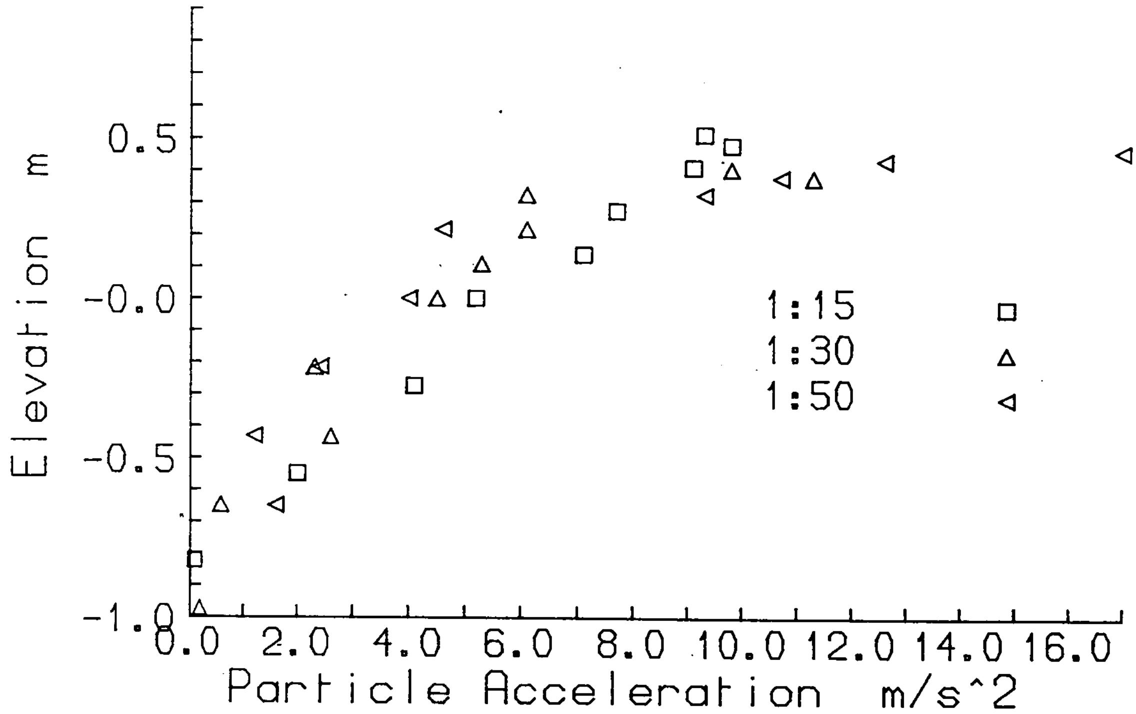

Fig. 5.3.19 Measured vertical particle acceleration, T = 3.1 sec.

5.3.3 Full field results.

Measurements were made over an array of points within four waves. These scaled to waves of about 2.3 sec. period in water of unit depth, and broke on the bed slopes of 1:15 , 1:30 , 1:50 and flat. Thus differences arising from the change in slope are isolated. The flat bed wave is of a slightly longer period than the others, its period being 2.5 sec. The measured values of the internal velocities and accelerations are presented in figures 5.3.20 to 5.3.23 and 5.3.24 to 5.3.27 respectivly.

These flow fields show the localisation of both the extreme velocities and the extreme accelerations in the high crest region.

Comparison of the velocities and accelerations for each wave shows them to be roughly 90 degrees out of phase for most of the wave. However in the front of the wave crest the phase difference can be as little as 60 degrees, and in the back of the crest, as great as 120 degrees.

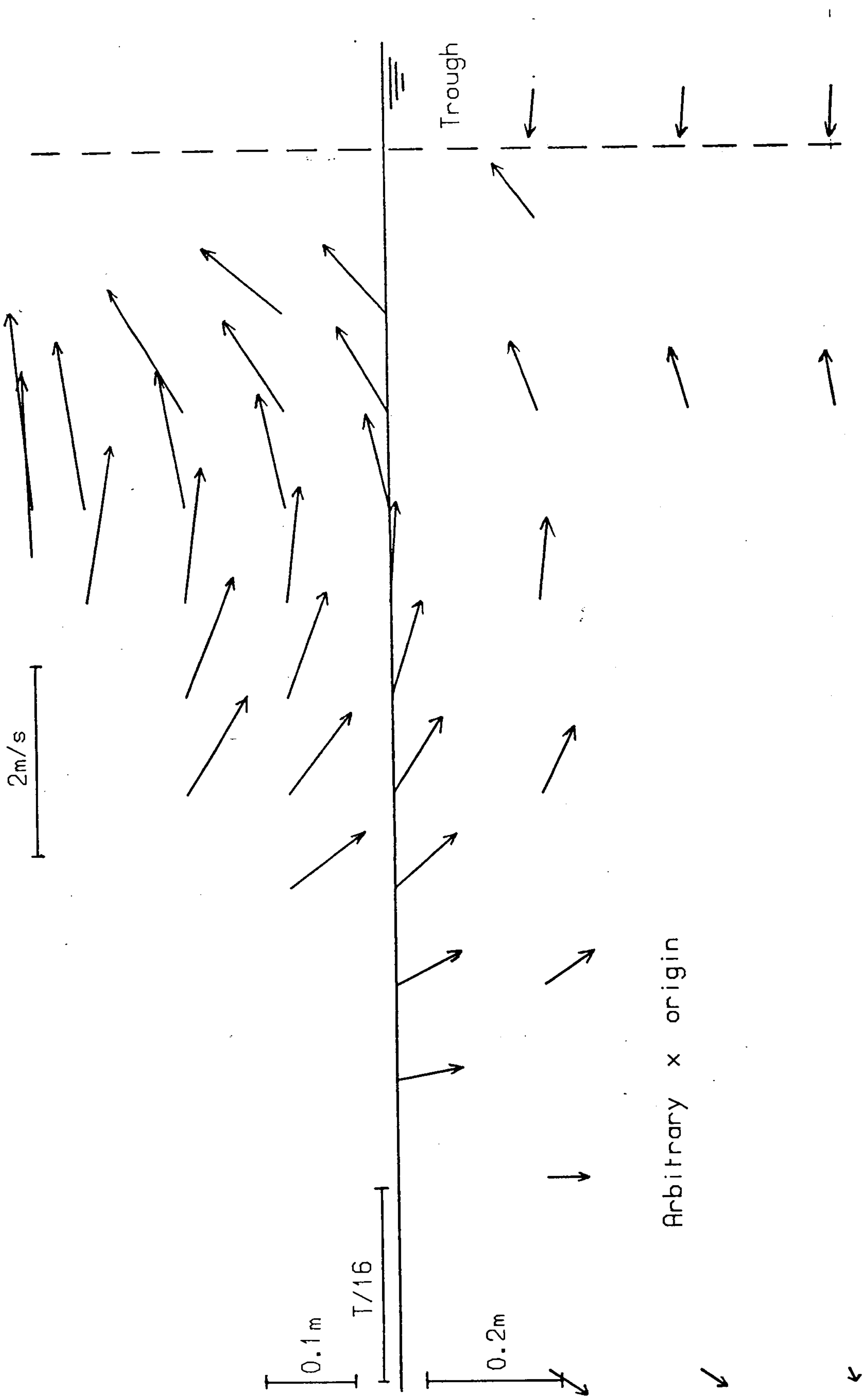

Fig. 5.3.20 Velocity field , flat bed.

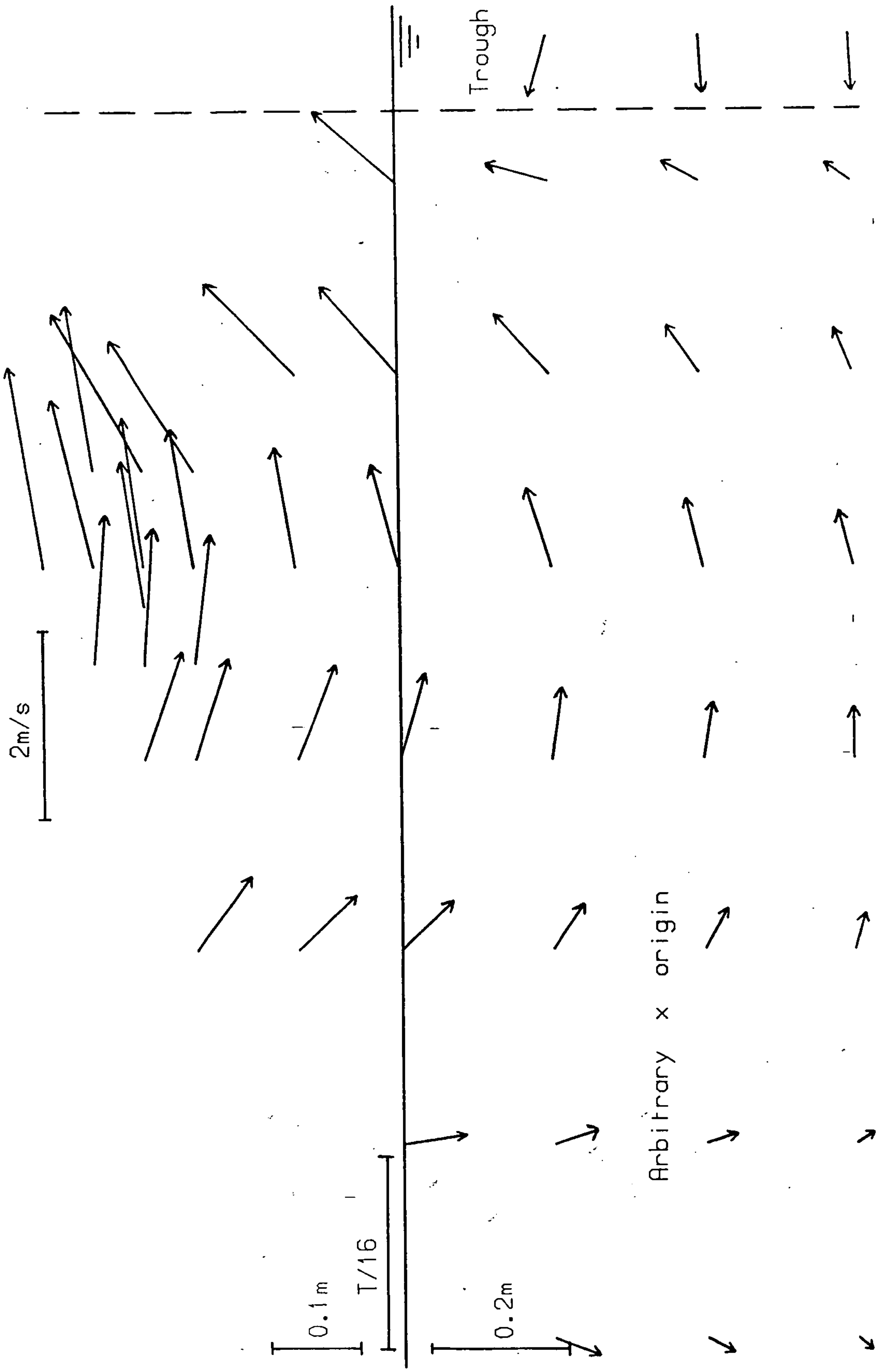

Fig. 5.3.21 Velocity field , 1:50 slope.

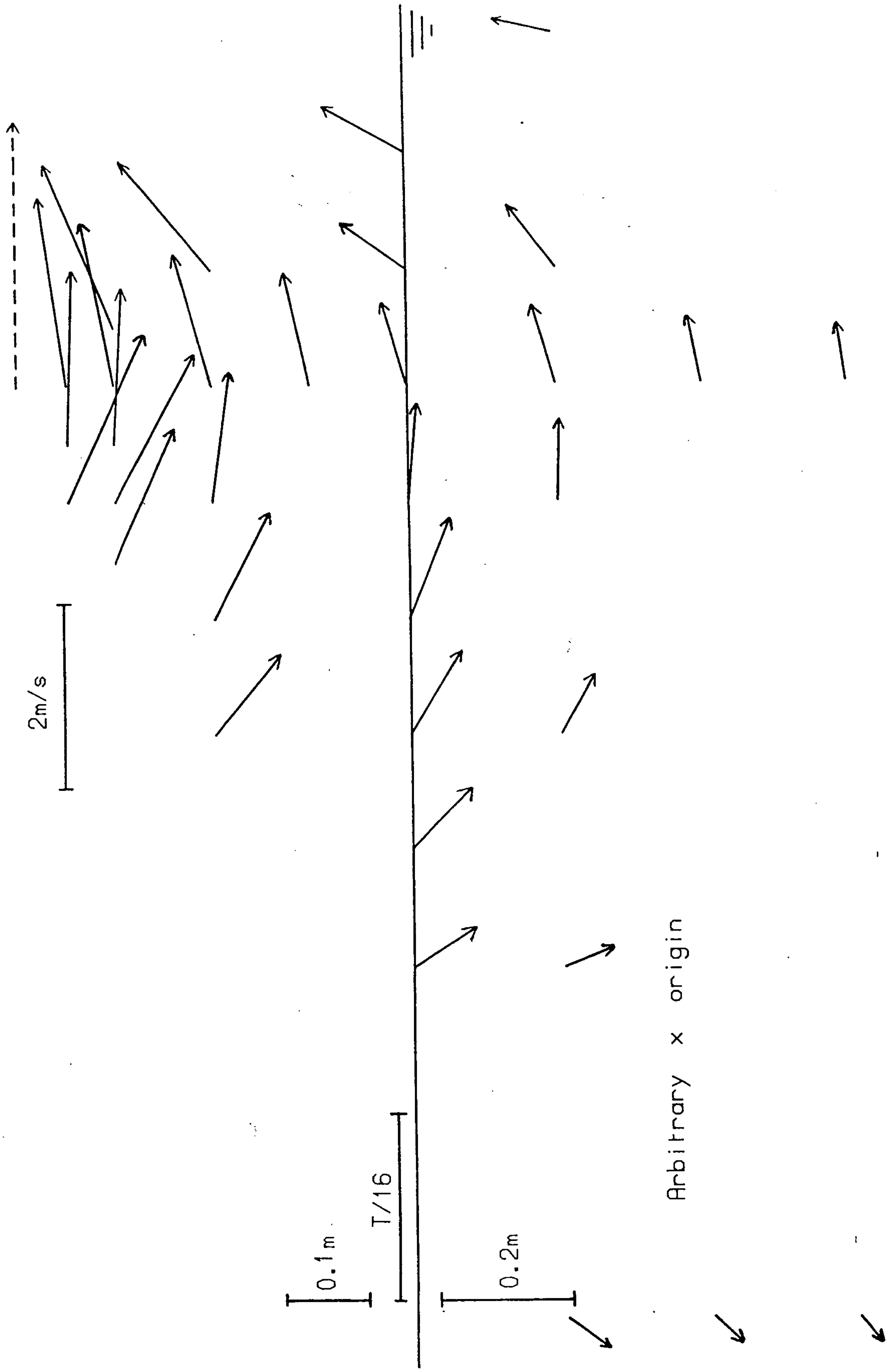

Fig. 5.3.22 Velocity field , 1:30 slope.

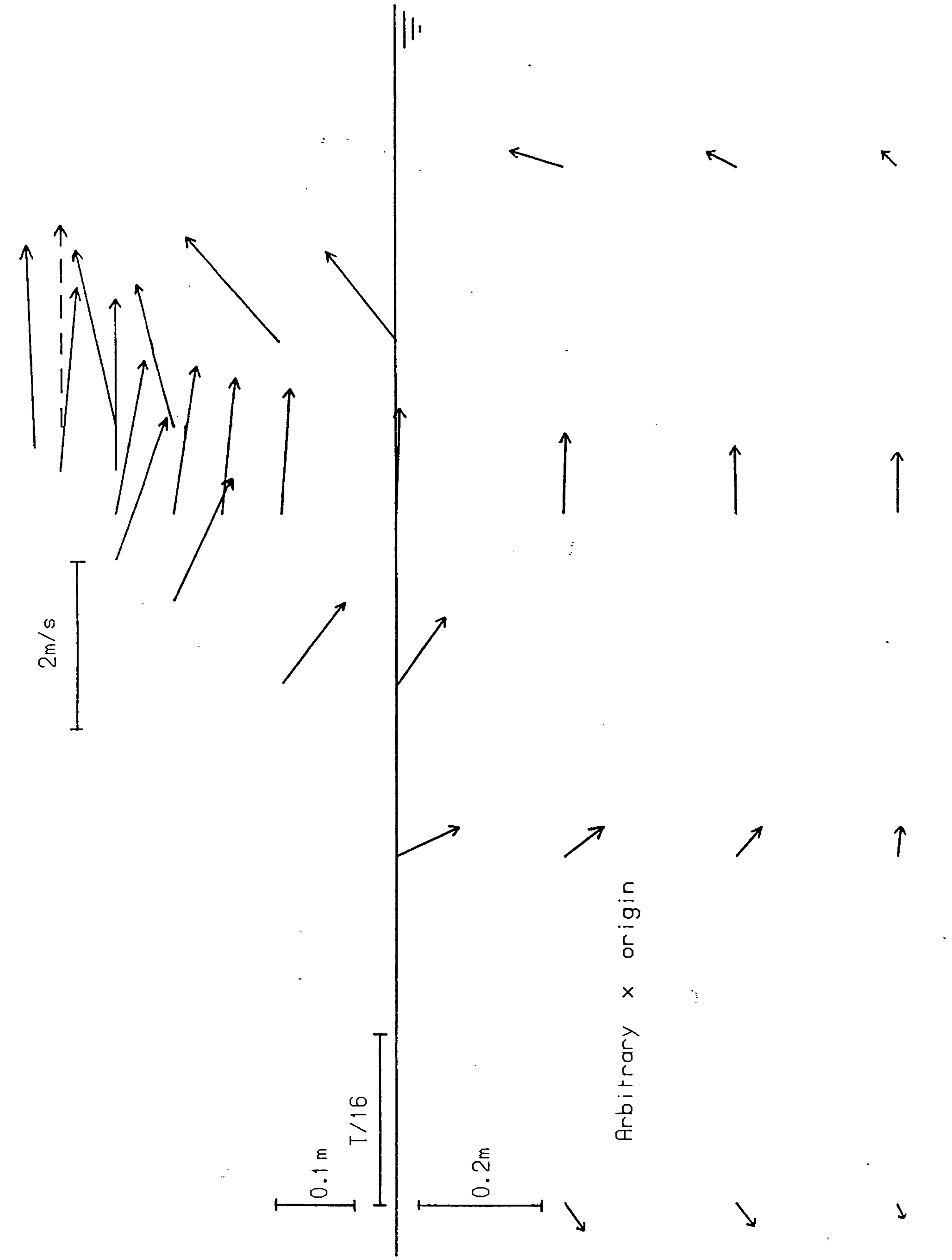

Fig. 5.3.23 Velocity field , 1:15 slope.

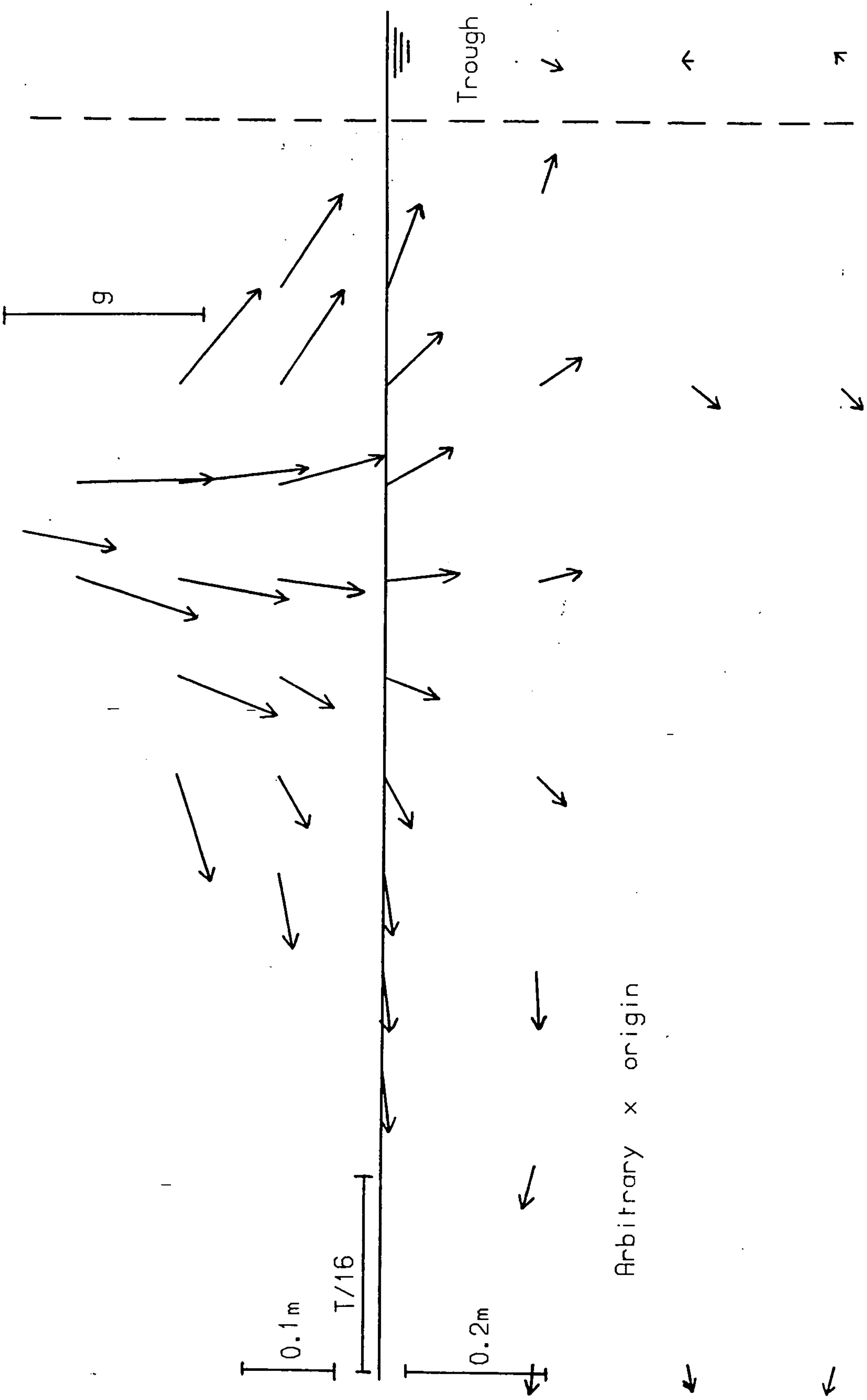

Fig. 5.3.24 Acceleration field , flat bed.

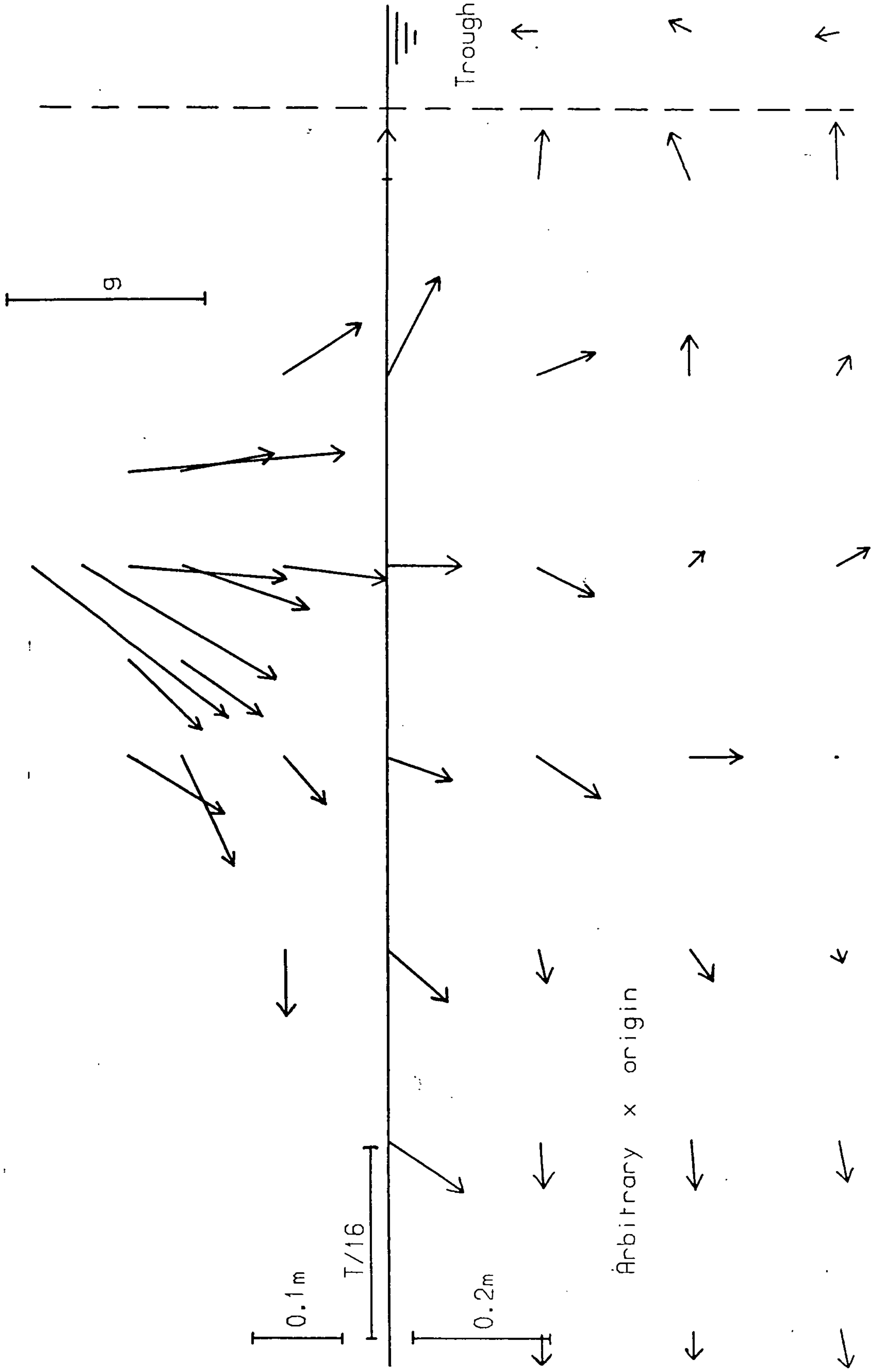

Fig. 5.3.25 Acceleration field , 1:50 slope.

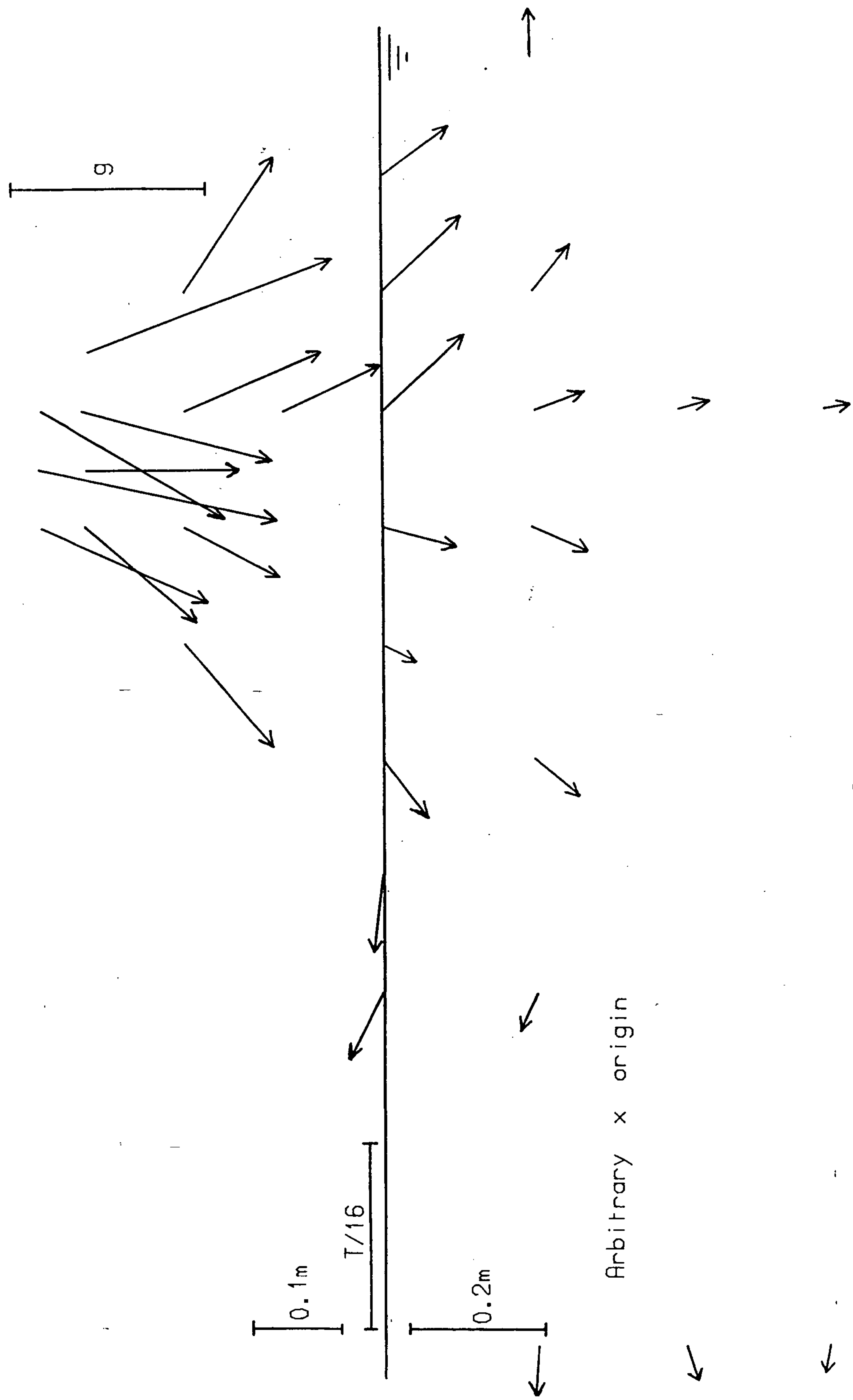

Fig. 5.3.26 Acceleration field , 1:30 slope.

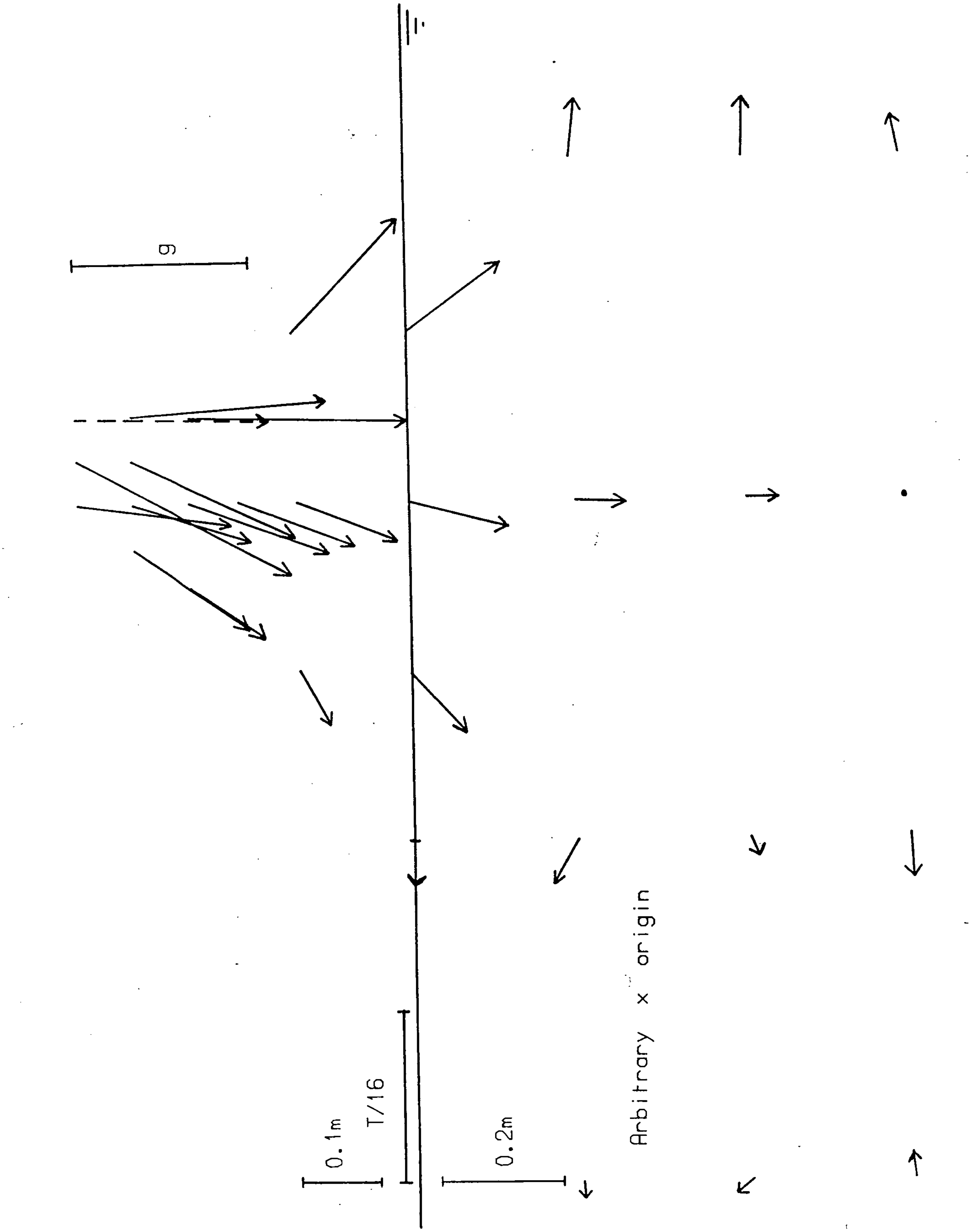

Fig. 5.3.27 Acceleration field , 1:15 slope.

5.4 COMPARISON WITH MATHEMATICAL MODEL RESULTS.

The comparisons made here use the velocities measured within the waves breaking on the 1:30 slope. The models accept the wave as defined by its measured depth, period and amplitude and make the assumptions of the "design wave". Perigrine also modelled the 1:30 slope; how this was attempted is described in chapter 2.

The theories used for comparison are :- linear , Stokes 5th , Dean's 3rd and 9th , Chaplin's high order stream function , Peregrine's time stepping and Cnoidal. The Dean's and Stokes models were not stable in all circumstances and the Cnoidal solutions are only included for the two longest waves.

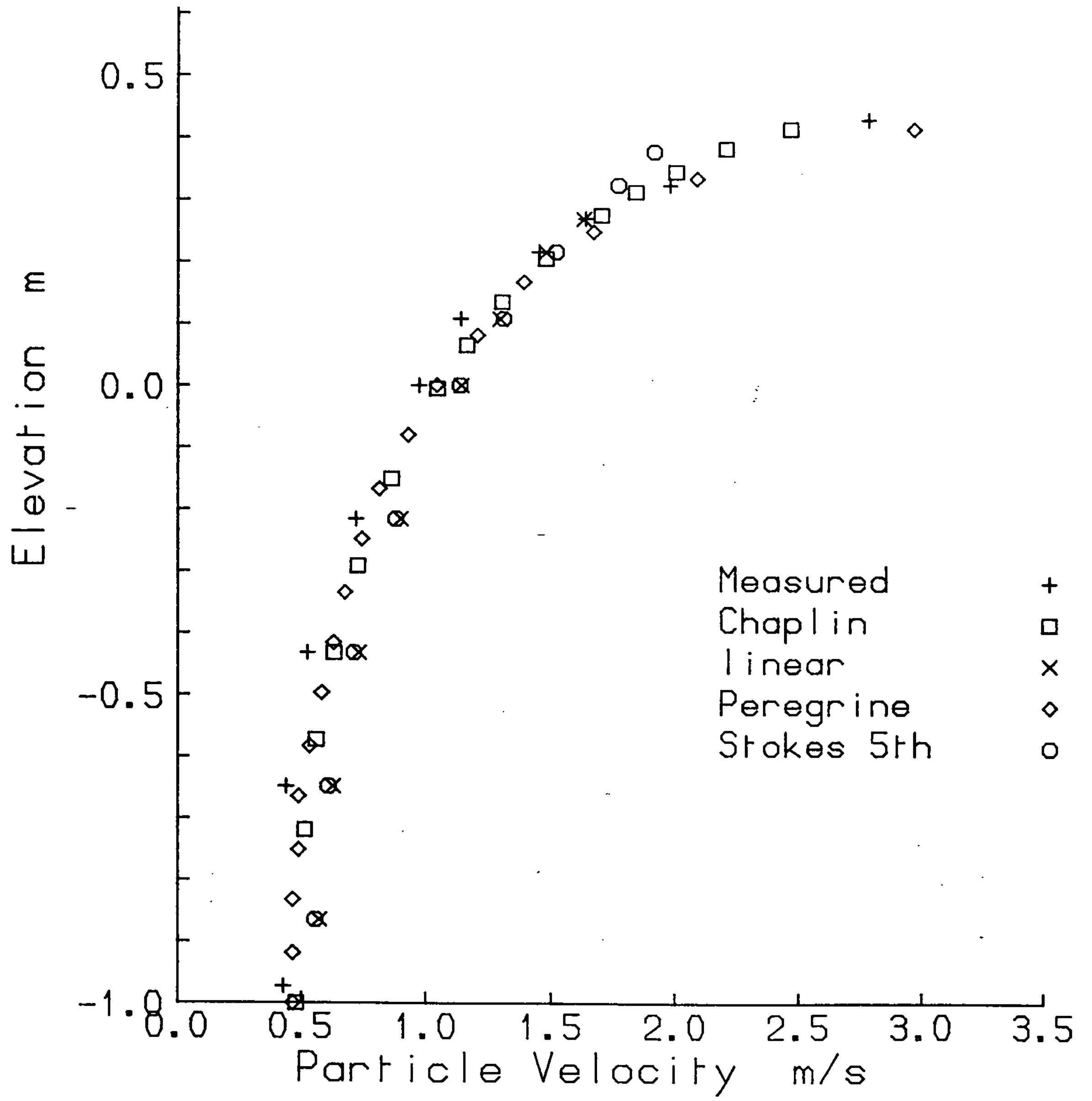

Fig. 5.4.1 Comparison with theory , 1.86 sec wave.

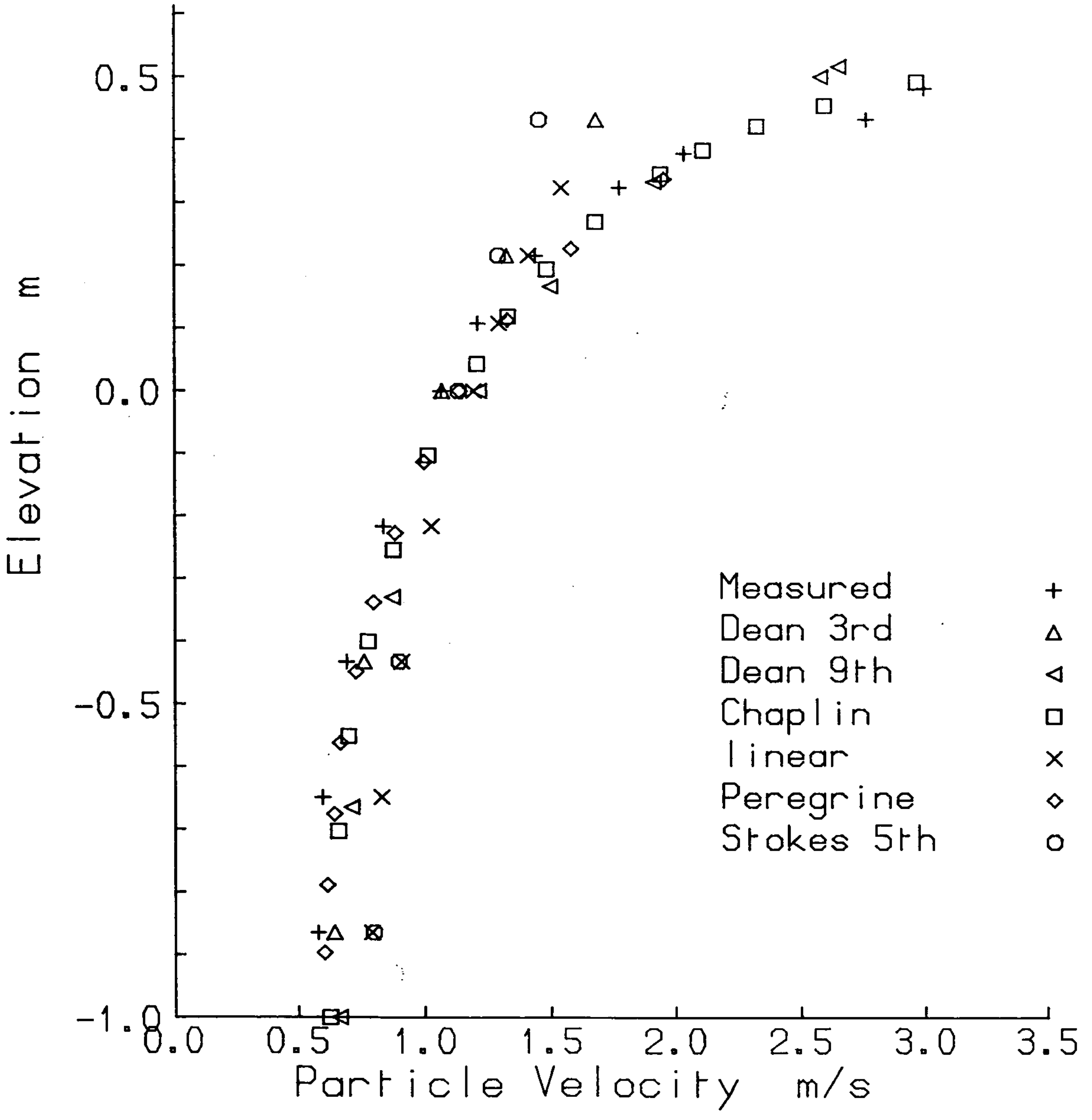

Fig. 5.4.2 Comparison with theory , 2.32 sec. wave.

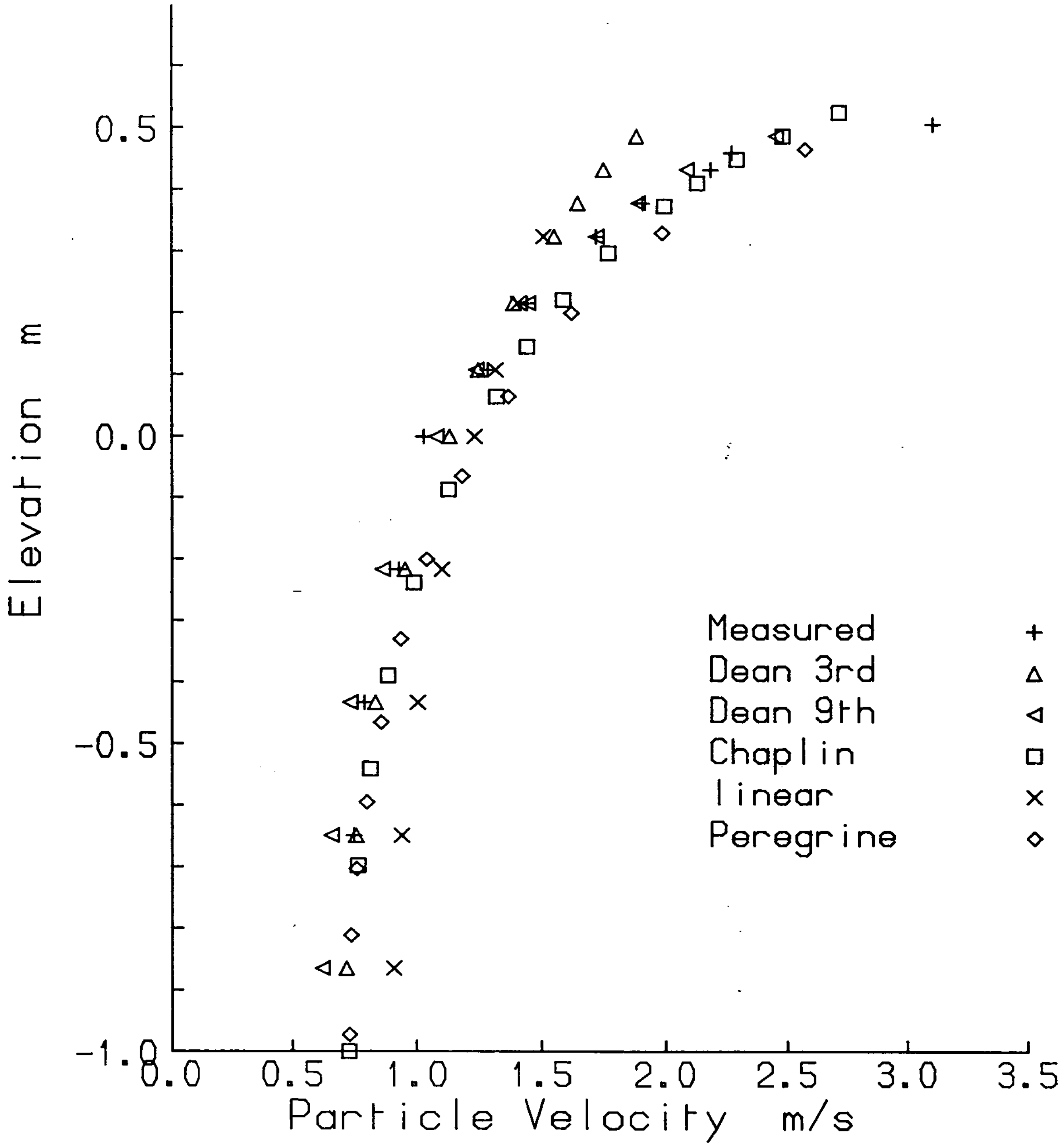

Fig. 5.4.3 Comparison with theory , 2.65 sec. wave.

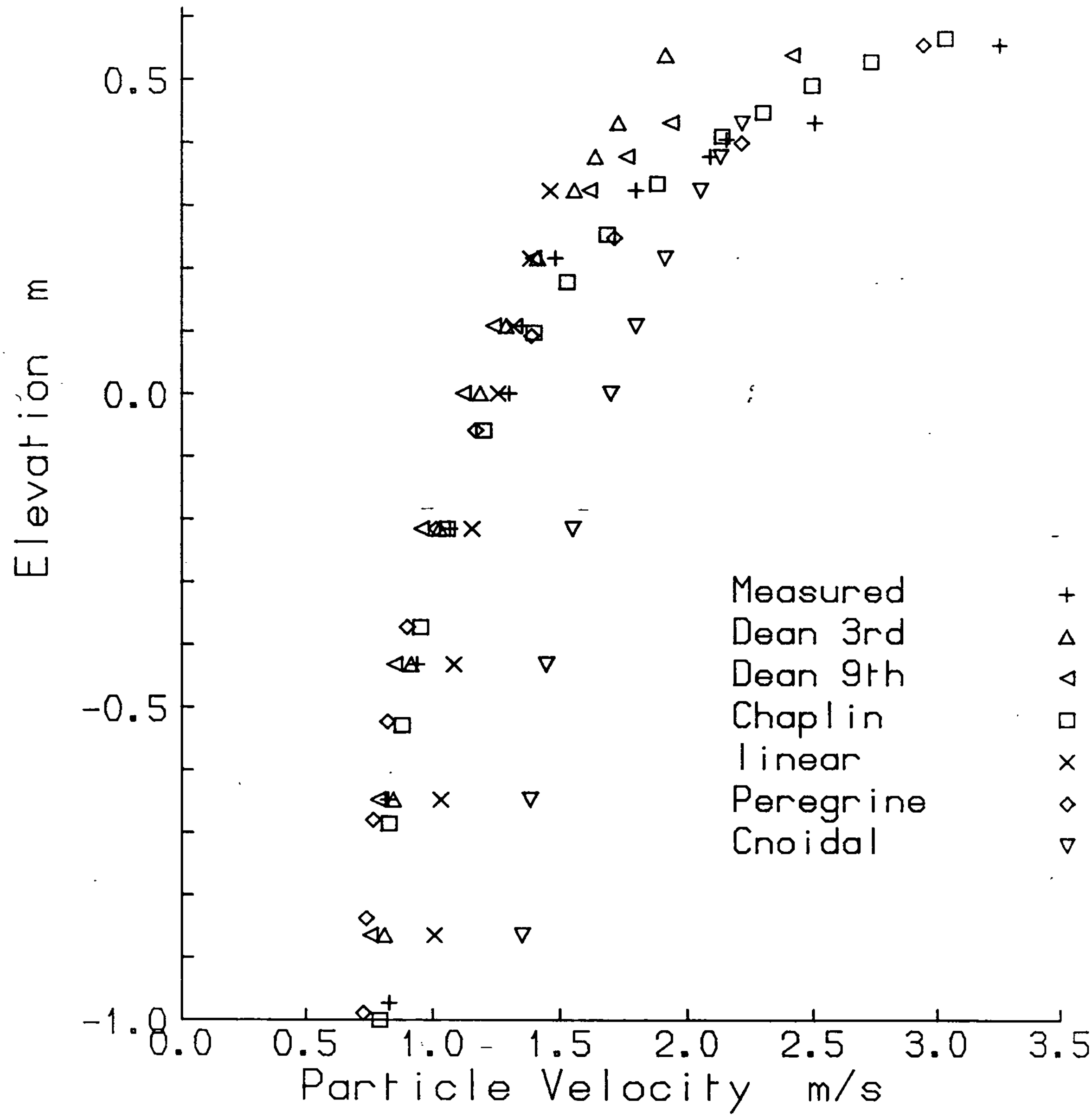

Fig. 5.4.4 Comparison with theory , 3.10 sec. wave.

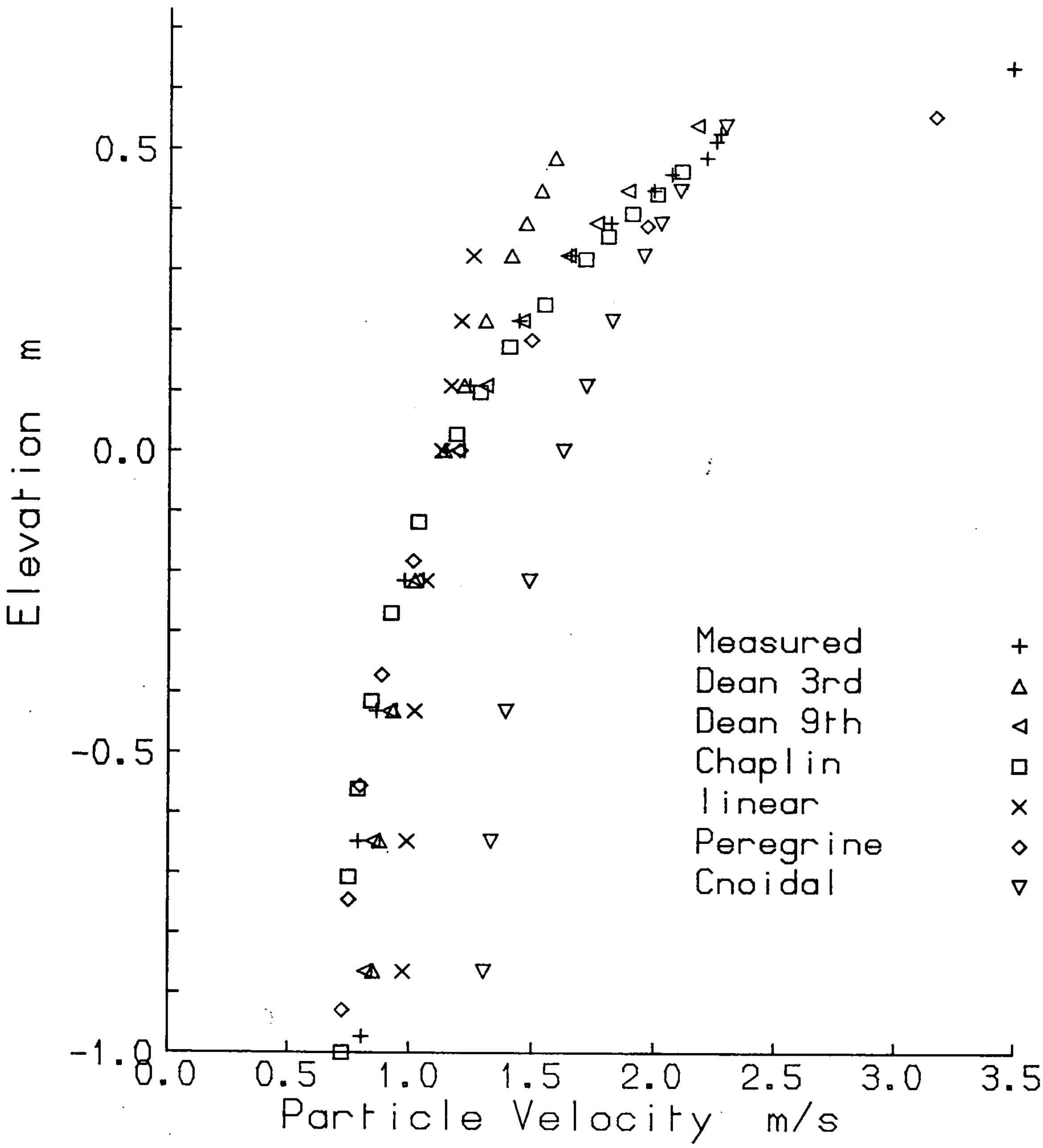

Fig. 5.4.5 Comparison with theory , 3.72 sec. wave.

From the graphs, it can be observed that :

1 Below still water level there is generally good agreement, the exception being the Cnoidal results which grossly over-predict velocities.

2 The agreement improves with the reduction in wave period.

3 The linear theory is good given its simplicity, but is curtailed at an elevation equal to half the wave amplitude. Where it is calculated, it is conservative.

4 The waves are specified by amplitude, and the theories determine the proportion carried in the crest. Most have good agreement with the measured elevation but the linear theory, being sinusoidal in profile, rises to only half the wave amplitude, a significant shortfall.

5 In the high crest region differences in the velocities are pronounced. The low order theories are unable to match the rapid increase in velocity with height; the shortfall increases the lower the order of the theory. This can be as much as a 50% under-prediction (see Dean's 3rd in the 3.72 sec. wave and Stokes 5th in the 2.32 sec. wave).

6 There is generally good agreement from the bed up to a level midway between the still water level and the top of the crest. Previous comparisons, which did not include comparison in the high crest region, drew false conclusions.

7 Chaplin's and Perigrine's models both follow the measurements very closely indeed.

Important. These comparisons are only for the 1:30 slope. It is important to compare these results with the waves from the steeper 1:15 slope. It is shown explicitly in chapter 6 that the theories are grossly in error when compared to the severe plunging breakers. The comparison can easily be made by looking at figs. 5.3.9 to 5.3.15 and assuming that the models follow the results for the spilling 1:30 cases.

5.5 COMPARISON WITH OTHER MEASURED VALUES

Results from many wave studies are available in the literature and comparison is made with the present results in two sections. This section considers those results which are directly comparable ; that is, those for two-dimensional wave breaking. Comparison with waves breaking by more general means is made in section 6.5.

Here the maximum horizontal water particle velocity is used to compare the results of several researchers. This is a single value extrapolated from the measured internal kinematics, it is chosen as it represents the most extreme local drag condition and because it is very sensitive to the flow conditions. Table 5.5.1 lists the ratio of Umax to the wave celerity, the source of the data and the type of breaking wave measured.

Table 5.5.1 Measured Umax.

SOURCE	BREAKER TYPE	SLOPE	H/d	DEPTH d/gT^2	Umax/c	
Divoky et al (1970)	Sp.	flat		0.0063 0.0014	0.5	x
Van Dorn and Pazan (1975)	Sp. Pl.			deep deep	0.85 0.95	
Kjeldsen and Myrhaug (1980)	Pl.			deep	2.8	x
Hedges and Kirkgoz (1981)	Sp. Pl.	1:15 1:4.5			1.0 0.3-0.45	 x
Mizuguchi (1986)	Pl.	1:20		0.0045	1.1	
Skjelbreia (1987)	Sp. Pl.	1:160 1:50	0.84 1.24		0.8 >1.0	
Present results	Sp. Pl.	flat 1:15		0.016 0.0058	1.0 1.0	

These results have a mean of Umax/c = 1.03. If the spurious results, marked in the table by an x, are removed, then the remaining values show good accord, with a mean of 0.96. Note that the results for plunging breakers are higher than those for spilling breakers.

In the light of the present work the fact that the previous results, in particular those for spilling breakers, were less than unity can be explained as follows: Velocity increases rapidly with height in the crest, so if measurements are made in the crest but are restricted to positions of low level, then the rapid increase of velocity will not be observed and extrapolation will yield low maxima. This will be more pronounced in spilling breakers where the rapid increase is confined to the near surface region. Plunging breakers, by contrast, have a more uniform forward motion. This explains the extremely low result of Divoky et al (1970) who measured on average only the lower 65% of the crest from still water level.

Hedges and Kirkgoz (1981) produce their waves on beaches which pierce the water surface. In the case of their plunging waves, their results are significantly affected by the backrush from previous waves. Any interpretation of their plunging wave results should take full account of the strong reverse currents produced in this backrush and its influence on particle velocity and in particular on the local wave celerity.

The extreme nature of the Umax/c = 2.8 result, Kjeldsen and Myrhaug (1980), is probably more due to their method of determining the wave celerity than to the size of Umax. The wave considered was created by the superposition of many waves of various periods, and c was calculated from the local wave period. While the water particle velocities correspond to those of the sum of the constituent waves, the local period, unspecified in the text, may be dominated by the zero crossings of the higher frequency components. This could easily account for the three-fold decrease in celerity and corresponding increase in Umax/c ratio.

Chapter 6 Breaking waves in offshore design.

6.1 DESIGN METHOD.

There are several standards and guidelines used in design. In the UK the Department of Energy "Offshore installations: Guidance on design and construction." sets out the national standards. These are imposed by the need of all offshore installations in waters around the UK to be certified. The different national design standards all recommend similar methods for design.

The design method, as it relates to extreme waves, is described in section 1.6 and the main stages are listed here.

(i) Measurement of environmental data for waves and current.

(ii) Prediction of an extreme event for wave and current.

(iii) Calculation of the water motion within the wave.

(iv) Combination of the water motion from the extreme wave and current.

(v) Calculation of force from the water flow.

(vi) Calculation of the global force and overturning moments, and the extreme elemental member loads.

Fatigue loading is also of fundamental importance in offshore design but is calculated from the integrated effect of less extreme waves and is not considered here in detail. However, breaking is likely to occur in many of the less extreme waves. It is expected that the breaking will be predominantly spilling, but because of the increased drag and the extreme slam forces that are produced by plungers, some estimate of their likelihood should be sought.

There are four areas in this design process that are ill understood and which could be greatly aided by fundamental research. These are :

(a) The prediction of extreme and breaking events. The DOE guidance on design recommends two possible methods for predicting extreme wave events. The first uses the wind speed in a wave forecasting technique (Darbyshire and Draper, 1963). The second is the extrapolation of environmental wave data. This second method is preferable in so far as it reflects the complex phenomena affecting waves at the site of interest; in particular it includes the effects of refraction and three-dimensionality. But, very significantly, this method does not reflect all scale dependent behaviour. The extreme waves being longer than the waves used in their prediction would be depth and breaking dependent in ways different from the smaller waves. Other criticisms of the present method are:

That the records it predicts from are often only two-dimensional.

The records do not contain simultaneous wave and current data.

That the wave gauges often fail to record extreme events.

That different methods of extrapolation produce significantly different predictions for an extreme wave (Department of Energy , 1986).

(b) The effect of wave breaking on force prediction and the validity of using a non-breaking design wave. The extreme waves at sea are frequently observed to be breaking (Holthuijsen and Herbers, 1985) and sometimes by plunging (Kjeldsen and Myrhaug, 1980), yet the design is usually based on a non-breaking wave theory. This is frequently, if not always, defended by a bogus appeal to the breaking height to depth or steepness ratios. As shown earlier in this work, the difference is negligible in cases where the breaking is of the spilling type. However in the rarer cases where the breaking is by plunging, the forces that occur will be substantially higher than predicted. The most extreme case measured here would result in forces 70 % greater than would have been predicted by the present design method using an high order theory. These same waves would also produce very large impact or slam forces. The use of a low order theory would reduce further the values of horizontal velocity in the high crest.

(c) The interaction and combination of wave and current motion. This affects design at two points. First in the prediction of the extreme events, where if the environmental data does not contain information on the current motion then the true period of the measured waves will be unknown. Second, when summing the motions of the extreme waves and currents. Here assumptions about wave/current interaction must be made. The common assumption is that the two can be added vectorially with either no alteration to the wave behaviour or a simple Doppler shift in period. While the latter is true for the superposition of a wave on a slab current, it does not describe the change in behaviour when a shear current is involved. Although little is known about the effects of shear currents on waves, it is known that they are present during storms because they are caused by large amplitude and breaking waves and by wind shear.

(d) The effect of three dimensional and polychromatic seas. The present design process assumes that the extreme wave that is predicted can be adequately or conservatively represented by a two-dimensional and monochromatic wave. This may be true given the generous allowance for error in the design. However, the wave behaviour is fundamentally different; in particular three-dimensional waves achieve heights that are impossibly large for their two-dimensional counterparts, and the breaking of high frequency waves causes premature energy loss from longer waves.

6.2 CONTRIBUTIONS OF THIS THESIS TO THE ESTABLISHED METHOD.

6.2.1 Breaking criteria.

The breaking criteria that are used at present in design are based on two limiting cases of a problem that has many dimensions. This limit has been studied here over a wide range of shoaling conditions from shallow to quasi-deep water. The non-dimensional breaking depth, which is the fundamental parameter describing waves used in design (see section 4.3), ranged from 0.004 to 0.035 and the breaking occurred on slopes ranging from flat to 1:15. This covers all depth and period combinations that are likely to occur in offshore design and it is hoped that the slopes induce breaking as severe as any produced by energy focusing at sea. This is a key area requireing study, see section 6.6.

As is seen in section 6.4, fig 6.4.1, the breaking height to depth limit is not a single value, but is rather a function of both non-dimensional breaking depth and bed slope. The often quoted limit of 0.78 is seen in context as the shallow water limit of the flat bed results. The reduction in the value of this parameter as the non-dimensional depth increases is clearly seen, as is its increase with bed slope.

The present work does not include the deep water steepness limit though the most frequently used value of 0.142 appears from other experiments to be too large, the correct value being between 0.13 and 0.142.

It is strongly suggested that the present flat bed results be used as a standard wave breaking limit. However, the implications of a situation where the design wave exceeds this breaking limit are not obvious. It can be taken to imply that many of the extreme waves encountered would be breaking, but this is to be expected a priori in all cases. The severity of the breaking and the danger that it will pose in design remains uncertain. It seems reasonable to expect that where predicted design wave heights are larger the breaking will be more severe.

6.2.2 Kinematic prediction.

The measured water particle motion at the most critical point in the wave cycle, has been found to vary in its agreement with the predictions of non-breaking wave theories. Considering the results from Chaplin's extension of Deans and Peregrine's time stepping solution (section 5.4), the agreement with the measured results is very good for spilling breakers but is lost on the 1:15 slope where the breaking is more severe. In severe cases the spout formation and plunging are more pronounced and the measured velocities are in excess of the predictions. The differences in velocity are strongly depth dependent, rising from 1% when the non-dimensional depth is above 0.02 to 30% when the non-dimensional depth is below 0.004.

The 30% increase in particle velocity causes a 70% increase in force. This makes it very important to know the likelihood of these plunging waves, and whether plunging caused by energy focusing at sea contains the increased kinematics measured in the shoaling monochromatic waves.

The error is greatly enhanced if a low order theory is used in the prediction of velocities. Again, considering the longest wave studied. The percentage increases in the horizontal water particle velocities between the Dean's 3rd order and the Dean's 9th order solution grow from less than 5% below the still water level to above 35% in the high crest. Thus, the force predicted from the velocities measured here is 70% above that predicted from the Dean's 3rd for regions below the still water level but this rises to beyond 300% for positions in the high crest region.

6.3 PROPOSED "BREAKING LIMITED" DESIGN METHOD.

One expensive and possibly redundant part of the design process is the measurement and extrapolation of field data to predict the design wave height. This process begins with the collection or purchase of wave elevation data recorded at or near the design site. These may contain storm wave data but are in general records of non-extreme events. Using one of several statistical methods these are extrapolated to the 50 year design wave. The validity of these extrapolations is in doubt for several reasons. The various methods of extrapolation yield different predictions for the extreme events (Department of Energy, 1986). Also, statistical distributions which fit the body of the wave data are often found to be a misfit with the largest measured events. This is hardly surprising as the physical processes of depth limited breaking which occur in the extreme events being period dependent are rare or possibly absent in the data used for the extrapolation.

The resulting 50 year waves are subsequently compared with the limiting breaking wave ratios. Thus having gone to considerable expense, the readily available depth limited height is used to validate the results.

It is proposed here that the well defined monochromatic breaking limit could be used to predict the wave height without the rigmarole of measuring and extrapolating high period, low amplitude, wave elevation data. The required input is the water depth and the fetch or time limited extreme wave period. These could simply be read from existing sources or calculated from the wind speed in accordance with the recommendations extant in the Department of Energy guidance notes. The measured properties of these waves are shown on figure 6.4.1.

When a storm is young the spectrum is that associated with deep water. Here even the longest waves are depth independent. As the fetch increases so energy is passed to larger period waves. These longer waves grow until they reach their depth limit. This is the limit studied in this research. The longer the fetch the larger the periods are that are excited and this increase of period is tantamount to a decrease in the non-dimensional breaking depth. The effect of this on the breaking limited waves can be read from figure 6.4.1.

Wave breaking in this environment will consist of two types; the large period waves will be breaking in a depth limited manner, but there will also be deep-water breaking occurring among the higher frequency waves.

The wind speed and fetch produce limits to the extent of the sea state development. If the wind speed or fetch are not sufficiently large, for the given depth, then the sea state will stabilize before it is depth limited. For higher winds there will be a range of spectra associated with the various wind speed to depth ratios. Small values of this ratio will reflect deep water behaviour and as the value increases so the depth limit governing the behaviour of higher period waves will dominate a larger range of the spectrum. In a storm these two limits operate simultaniously. The influence of breaking on spectral shape has been discussed in the literature (Longuet-Higgins, 1969)

One significant validation of this method would be the comparison of design waves predicted by this method with those predicted by extrapolation. If the 50 year design waves do not coincide exactly with the breaking limit, it may be possible to show that the monochromatic limit is equivalent to the design wave with a particular probability of occurrence. It should be expected that some sites would demonstrate full wind speed limited behaviour, and that in other locations, the period would be fetch limited. Such a comparison has not been made as the data required is not freely available.

6.4 SUMMARY OF RESULTS.

All the main results in this thesis combined with relevant data from the literature are presented here in concise form. The graph, figure 6.4.1 summarises all these results in one plot. The results presented are for the celerity cb, crest elevation H1b, the trough depth H2b, the crest front steepness cfs, and the height to depth ratio Hb/db. The last two parameters show the effect of the differing bed slope.

The x ordinate is the design depth divided by the gravitational acceleration and the square of the extreme period, that is the non-dimensional depth. The y axis is common to all the measured parameters. The scaling required to achieve this is shown in the equations defining the parameters on the graph.

The internal kinematics directly below the crest are described by their exceedence of the predictions of Chaplin's high order Dean's solution. The assumption is that the theoretical predictions are accurate for gentle spilling breaking, see section 5.3 but that for more severe breaking there is an almost uniform increase in velocity at all levels. All slopes of 1:30 or shallower have very good agreement between measured and theoretical results. However, the breaking on the 1:15 slope shows an exceedence in the measured results which increases as the breaking moves towards shallow water and the plunging becomes more pronounced. The exceedence of the measured velocities as a percentage of the theoretical velocity rises from zero for deep water to 30% for db' = 0.0058 .

This substantial increase in velocity and extreme increase in force (up to 70 %) should not be dismissed as only occurring on steep slopes as plunging does occur through the processes of energy focusing at sea (Kjeldsen and Myrhaug, 1980).

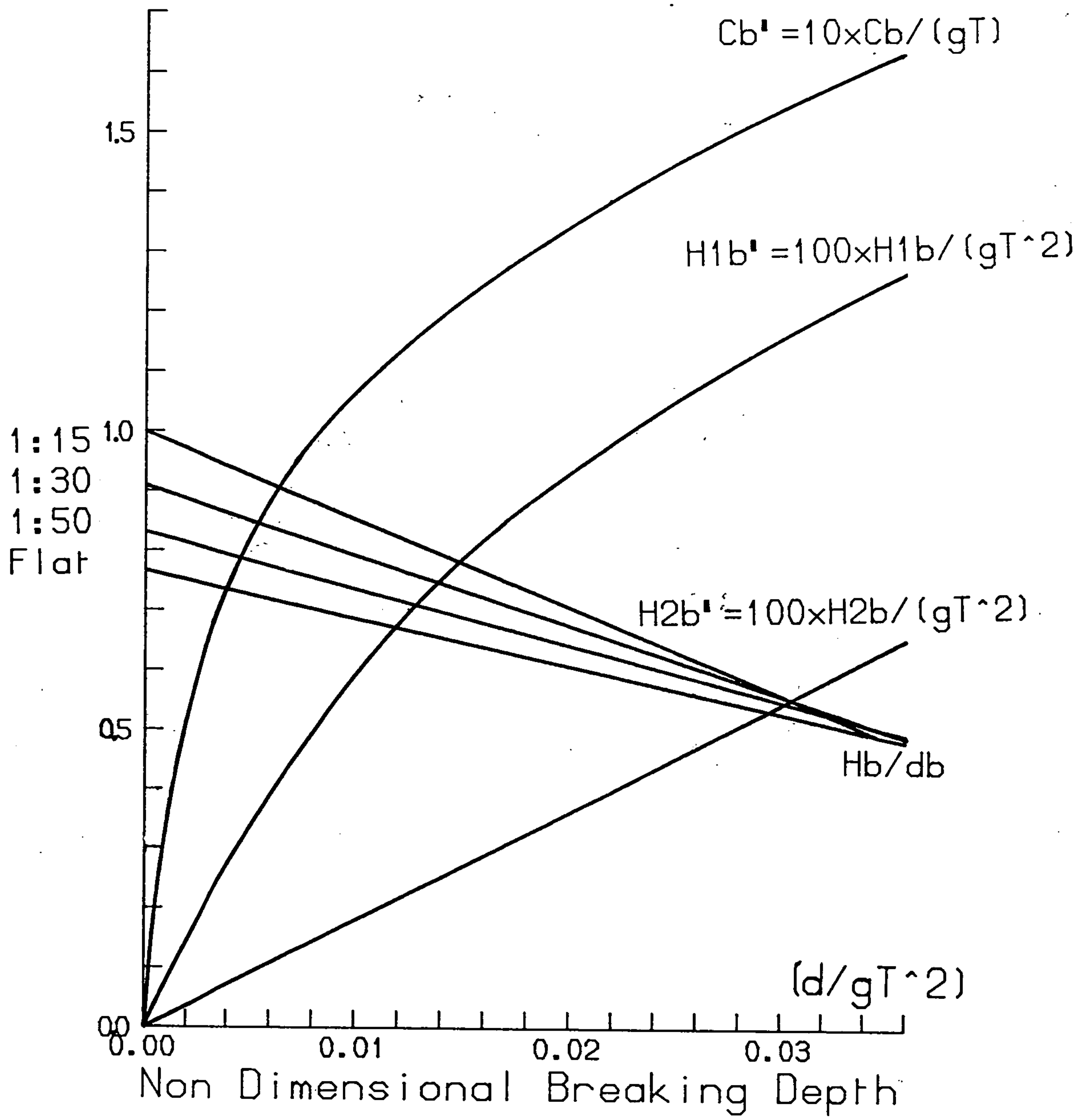

Fig. 6.4.1 Measured properties of depth limited breaking waves.

6.5 RELATION OF MONOCHROMATIC SHOALING TO OTHER TYPES OF BREAKING.

All the analysis in this thesis relates to monochromatic wave shoaling. This is only one cause of breaking and is not the dominant cause in the offshore environment. If the results of this work are to find application wider than the particular problem that has been addressed in the laboratory then some knowledge of the relation between the breaking caused by different mechanisms must be sought. There are two areas where this becomes important ;

(i) It is important to establish the statistical relations between breaking of the present types and that occurring in the design environment. In particular the probability of occurrence of plunging breaking.

(ii) As shown up clearly in this work, plunging breaking causes a particular and very significant danger to offshore structures and shipping. In the extreme case that was studied here the effect was a 30% increase in the internal water particle velocity with a consequent 70% increase in total force. It is very important to establish the relation between the internal kinematics of plungers caused by different physical processes.

There are three main effects which make breaking in the design environment different in character from the monochromatic wave shoaling. These are, the interaction of waves of different periods, and those from different directions and the interaction of waves with currents. Other processes affect the wave breaking to a lesser extent. Dominant amongst these are the effects of bed geometry either by change of slope or by refraction and also the effect of the wind.

(a) Polychromatic seas, are those where there are many waves of different periods present simultaneously. These waves travel at different celerities and cause breaking by the concurrence of wave crests. Breaking by this method has a similar range of type to monochromatic shoaling; a slow localisation of crests causes spilling and a rapid localisation causes plunging. Some studies have been made of the behaviour of two-dimensional random seas. However it is not simple to parameterise the breaking limits. Kimura and Iwagaki (1978) shows the height to depth ratio for extreme waves varying from 1.1 to 0.4 as their non-dimensional breaking depth varied from 0.0064 to 0.029 for random waves shoaling on a 1:10 slope. For a 1:20 slope, H/d varied from 0.6 to 0.3 as non-dimensional depth ranged from 0.012 to 0.064. These results support the view that random waves break earlier and less violently than monochromatic waves. This may be the result of the parasitic breaking of small period waves causing energy loss in the longer period waves, reducing the chance of their ever reaching their monochromatic breaking limits. The 1:20 results show a depth dependence akin to the present results but with all H/d values about 13% smaller. The 1:10 results show a more rapid increase with decreasing depth, resulting in values of H/d in the shallow region 20 % greater than our 1:15 slope results.

(b) Waves in the offshore environment are three-dimensional. This again introduces extra physical effects and makes the description more complex. Short crested breaking waves can obtain heights very much higher than those possible in two-dimensional or long-crested waves (Kjeldsen, 1983a). Little work has been performed on the breaking of three-dimensional seas, one exception, Halliwell and Machen (1981), studies the breaking of two intersecting trains of long crested waves. These waves ran up a slope of 1:27.5 and broke with height to depth ratios ranging between 2 and 1. It is observed there that the breaking was invariably plunging.

(c) Currents have large effects on extreme waves. Slab currents cause a Doppler shift in the wave period. A wave moving from water travelling at one speed to water travelling at another will retain its period in any inertial reference frame but will change its period with respect to the water in which it is propagating. If the wave moves onto water moving in the direction of the wave advance then, with respect to the water, the wave is of a larger period, is longer and has a height less than the breaking limit. If in the other case the wave period is reduced, the wave becomes shorter and more extreme, often exceeding the limit of its stability and possibly causing severe breaking. The effect of shear currents is unknown but it is expected that they will cause or restrain breaking, depending on whether they increase or decrease the velocity of the fluid in the wave crest. In storm conditions the shear currents will act to increase the local particle velocity in the crest and are therefore expected to reduce the heights that waves attain before breaking and to encourage spilling and discourage plunging.

6.6 SUGGESTED FURTHER RESEARCH.

In the course of the present work many neighbouring areas of research have been studied and regions of potential research observed. The latter are described here, split between three sections. The first section includes all areas of direct interest to design. This set also includes suggestions that are of longer term interest than are included in the other sections. The second section contains descriptions of experiments that have been more thoroughly thought out and which are designed to match the skills and equipment that are available at Edinburgh. The third, the miscellaneous section, mops up suggestions that are entertaining but essentially esoteric.

6.6.1 Design related research.

What appears as the main problem from a design perspective is the bridging of the gap between the laboratory results presented here for the restricted case of monochromatic wave shoaling and the general and chaotic breaking that occurs in the real sea. There are several contributions that can be made to this.

(i) The comparison of design waves predicted by the extrapolation of measured field data with the breaking limit presented here. This data exists but unfortunately is not freely available.

(ii) The establishment of the return period associated with the breaking limit presented here. This would be based on long term records of sea elevation.

(iii) The establishment of the probability of occurrence of breaking by plunging in (a) extreme wave environments and (b) in less extreme conditions important in fatigue analysis. This should be linked to the ongoing research on impact loads.

(iv) The establishment of the probability of breaking of waves in a storm of periods other than the peak of the spectrum. In particular that of the longer more depth dependent and faster moving low frequency components.

(v) The study of the low frequency waves in storms, where even away from breaking, their large velocities may contribute to severe loads.

(vi) The extension of the use of maximum crest front steepness as a signature of severe, plunging, breaking.

(vii) The development of the energy balance equations and the description of sea states by spectral form with understanding of the breaking associated with the different regions. In particular the distinction of the deep water high frequency breaking from the low frequency depth limited breaking and the scrutiny of severe storm spectra for the depth induced breaking limit.

6.6.2 Proposed experiments.

There are three areas of wave breaking research that require special attention. These are the analysis of the breaking that occurs due to the superposition of waves in a two-dimensional environment, the analysis of three-dimensional breaking and the interaction of waves with shear currents. There are two results that are desired from all these studies; firstly the effect of the process on the statistics of the sea state, in particular those of wave breaking, and secondly, the effect that the process has on the internal kinematics of the extreme events.

(i) Two-dimensional polychromatic breaking. There are two approaches that might be taken to this problem: Firstly the superposition of a very small number of component waves and the subsequent analysis of the effect that they have on each other. Secondly, the analysis of a sea state containing a very large number of component waves. In the first case the range of conditions examined would be small but the amount of information about each case large. Conversely, using the second approach, the number of examples would be very large but the measurements would be restricted in scope.

Results from experiments of the first type may find favour with researchers who are trying to understand the non-linear processes that occur between finite amplitude waves. However the analysis of random wave behaviour is important for engineering design, and the second approach is likely to lead more immediately to results of use to the engineer.

The recent development of particle image velocimetry (PIV) at Edinburgh University has made it possible to measure the internal kinematics of waves which have repeat times so large that they could not be measured using earlier techniques. In particular this is useful in the analysis of random seas, where better representation of sea spectra can only be achieved by smaller separations between component frequencies and consequent longer repeat times.

It is proposed that an experiment be set up with finely modelled sea states of various spectral forms shoaling on a bed of gentle gradient. The statistics of extreme events could be found by setting wires running above the flume at various fixed height to depth ratios. Each wire could be an electrode with the water being used to complete the circuit. These would be connected to incidence counters and the sea state left to run for its complete repeat time. The repeat time could be in the order of hours or days as the experiment would run unmanned.

Two additions should be made to this scheme. First because the input spectrum is fixed, a time and length scale is defined, and the change in depth introduces changes in behaviour. In particular the height to depth ratio is expected to be depth dependent. This could be measured by discretising the wires along their length. Second, the PIV system could be set to trigger automatically from the closure of the circuits. Thus in one run the internal kinematics of the extreme events as well as their probabilities could be measured.

(ii) Three-dimensional breaking.

(a) Full three-dimensional breaking. The above experiment could be extended to three-dimensions and mounted in the wave basin at Edinburgh University. Unfortunately the measurement of the internal kinematics would pose difficulties. The PIV system can in principle be modified to work under water but this would require substantial development. The production of a sheet of light in water would be more difficult and more dangerous than its production in air and the water-proofing and mounting of a camera and trigger system would not be easy and would probably result in a loss in quality in the photographs. The measurements of extreme wave statistics would be essentially the same as in two-dimensions and the results would be extremely valuable. Photographs of the crest from above would show breaking type and could be used for measuring the wave celerity.

(b) Symmetrical conditions.

The effect on internal kinematics caused by the three-dimensionality of the breaking could be studied in a restricted manner by causing waves to break along the glass side wall of the three-dimensional tank and using a slightly modified version of the existing PIV system. This study would be restricted to symmetrical wave patterns but these could include both circular crests and crossing waves. The circular wave fronts would have a limit of being two-dimensional for large radii of curvature and would be much more highly focused where the breaking occurred nearer the centre of the pattern. The radius of curvature at breaking is an obvious parameter and could be varied by altering the initial wave steepness. Similar waves have been studied using a flume of narrowing cross section (see Van Dorn and Pazan 1975). Some work has also been done on the breaking of crossed waves, (Halliwell and Machen, 1981), but the systematic study of three-dimensional breaking has so far been inadequate.

(iii) Current/wave effects.

Wave current interaction can be split into two areas. Firstly where the water has no initial current and the interest is in the creation of a current by the waves. Further work on this could include the building of a re-circulating or even a circular wave tank where the cumulative effect could be studied. Knowledge of the induced current is important in the interpretation of currents measured in the presence of waves when models assuming certain current conditions are to be used. Secondly the effect of currents on wave behaviour is also important, not least where it affects breaking. The study of the effect of various shear currents on breaking wave behaviour is part of the ongoing wave research at Edinburgh University.

6.6.4 Miscellaneous.

(i) Waves break in different forms, the two types studied here are the spilling and the plunging type. It is suggested that there is an identifiable distinction within plunging breakers. That is that severe plungers form an overturning crest that drops and penetrates the water preceding the crest. However less severe plungers form spouts that hit the preceding water at a more acute angle and appear to fail to penetrate the bulk of the water, but rather the spout is reflected and shoots out along the surface. These could be referred to as shooting breakers. The distinction could be tested by dyeing water in the spout and photographing the wave late in its breaking to see when the dye becomes mixed with the clear water.

(ii) Measurements of internal kinematics could be used to test whether the 0.5g limiting acceleration is a valid breaking threshold. Ref Snyder et al. (1983).

(iii) The interaction of waves with additional energy supplied or removed from its harmonics. In particular, if a wave has one of its harmonics created in anti-phase to what would naturally occur, does this wave travel at the speed of the fundamental or at its own speed and does the energy become locked to the wave when the correct phase is reached?

(iv) Waves of finite amplitude show the growth of harmonics, with properties , particularly the celerity, dependent on the fundamental. It may be possible to find orthogonal functions that describe finite amplitude waves more naturally than the presently used circular or cnoidal functions.

CHAPTER 7 CONCLUSIONS.

CONCLUSIONS FROM SURFACE MEASUREMENTS.

In this section breaking is taken to mean monochromatic wave breaking on straight rigid impermeable beaches.

Two parameters are necessary and sufficient to describe breaking. With the corollary that ; no single shoaling parameter exists that completely describes breaking.

Both (slope and deep water steepness) and (slope and non-dimensional breaking depth) form pairs of non-collapsed orthogonal parameters. Both pairs adequately parameterise breaking.

Empirical values for the surface parameters of celerity, crest elevation, trough depth and height to depth ratio, at breaking are accurately known for combinations of non-dimensional breaking depth from 0.001 to 0.035, and slopes from flat to 1:15.

Both the "crest front steepness" and the "maximum crest front steepness" are sensitive to breaker type.

The H/d ratio is a function of both slope and non-dimensional breaking depth. The results measured here show values of 0.5 in deep water to 1.0 in shallower water on the 1:15 slope.

CONCLUSIONS FROM MEASURED INTERNAL KINEMATICS.

The most extreme loading (ignoring the effects of slam), on a drag dominated vertical cylinder will occur when a wave first becomes vertically fronted. This loading occurs at the crest phase of the wave.

For this condition:

Internal velocities approach the wave celerity at the crest elevation.

The increase in velocity to the wave celerity is localised to the high crest region in spilling breakers.

Horizontal velocities are greater in plunging breakers than in spilling breakers.

Plunging enhances the forward motion at all levels. The rate of increase to the wave celerity that occurs in the crest is more gradual.

The plunging severity, and the horizontal component of particle velocity, increase as the beach slope increases and as the non-dimensional breaking depth decreases.

The largest measured increase in forwards velocity occurred between waves of non-dimensional breaking depth of 0.0075. For this case, the plunging breaker on a 1:15 slope had horizontal velocities consistently 30% greater than an equivalent wave spilling on a flat beach.

Large accelerations occur at breaking. Values in excess of 16m/s were measured. The accelerations grow rapidly with elevation, appearing to increase asymptotically at the crest elevation.

The phase angle between velocity and acceleration is not always 90 degrees. Phases of 120 degrees were measured in the back of the crest and phases of 60 degrees were measured in the front of the crest.

CONCLUSIONS DRAWN FROM THE COMPARISON WITH WAVE MODELS.

The internal kinematics of spilling breakers are well described by high order solutions.

Mid order solutions such as Dean's solution at 9th order, do not reflect fully the rapid increase in velocity in the very high crest region.

Low order solutions, Stokes 5th and Deans 3rd are inadequate for elevations above the still water level. The theories under-predict horizontal velocities; the errors vary. The largest errors, occuring for small values of non-dimensional breaking depth, amount to a 50% under-prediction of velocity.

Linear theory gives reasonable results below the still water level.

The use of a sinusoidal surface with the linear theory leads to a lack of predicted results for elevations above half the wave amplitude. This is consequently a very poor description of the wave.

CONCLUSIONS RELATING TO DESIGN.

The confidence with which a random and three-dimensional sea state may be represented by a two-dimensional monochromatic wave remains uncertain.

The ability of high order wave models to represent two-dimensional monochromatic spilling breakers is proven.

Lower order theories, Dean's 9th and below, become inadequate in the high crest. Errors at the level of the crest can be as large as 50% of velocity, corresponding to a factor of 4 in the drag.

The increase in internal velocities and hence loading that is associated with two-dimensional monochromatic plunging breaking is measured. The worst case reported shows a 30% increase in velocity over the equivalent spilling breaker. (Equal non-dimensional breaking depth.) This corresponds to a 70% increase in drag force.

Whether these high velocities occur in plunging waves caused by wave/current or wave/wave interaction is uncertain.

There is a lack of knowledge about the likelihood of occurrence of the breaking of various types.

The design ratio, $H/d = 0.78$, often used to determine whether a design wave is breaking is shown in context as one limiting value of a ratio that is both non-dimensional breaking depth and slope dependent. Results measured here show it to take values ranging from 0.5 to 1.0.

The use to which the H/d ratio has been put in the past - determining whether wave breaking should be considered in design at specific sites - is unjustified. Extreme waves at all sites should be expected to be breaking.

The value of the H/d ratio measured at a specific site may correlate to the severity of breaking ~~occurring at various sites~~, but this is at present speculative and un-quantified.

The crest front steepness of breaking waves is a useful indicator of breaking severity in monochromatic waves.

The usefulness of crest front steepness in random seas is gravely doubted. This is because wave/wave interaction makes the mean water level associated with a single breaking crest somewhat arbitrary.

The maximum crest front steepness is independent of still water level and is shown to be a useful indicator of breaking severity in monochromatic wave breaking.

Maximum crest front steepness should be used in analysing extreme events in random seas.

CONCLUSIONS RELATING TO FURTHER RESEARCH.

The kinematics of plunging breakers created by wave/current and wave/wave interaction should be measured.

For fixed structures, the effect of plunging on drag, inertial and slam forces should be studied.

The effect of plunging breaking on ships should be studied further, with respect to the qualitative changes in wave motion.

The probability of occurrence of plungers of all severities and produced by all methods should be measured.

The H/d ratio in random and three-dimensional seas should be measured.

The maximum crest front steepness should be tested as a measure of breaking severity.

RECOMMENDATION.

It is recommended that a design wave should have a period calculated from the climatic wind conditions and an height predicted from the breaking limit for this period at the local water depth.

REFERENCES.

Airy G.B. 1845
Tides and waves.
Encyclopedia Metropolitan, London, section V. pp 241 - 396

Banner M.L. and Phillips O.M. 1974
On the incipient breaking of small scale waves.
JFM Vol. 65, part 4, pp 647 - 656

Basco D.R. 1985
A qualitative description of wave breaking.
JWPC&O Eng. Div. ASCE III

Battjes J.A. and Stive M.J.F. 1985
Calibration and verification of a dissipation model for random breaking waves.
JGR Vol. 90 No. C5 pp 9159 - 9167

Benjamin T.B. 1962
The solitary wave on a stream with arbitrary distribution of vorticity.
JFM 27 , 3 , pp 97 - 116

Bishop J.R., Tickell R.G. and Gallagher K.A. 1980
The UK Christchurch bay project ; a review of results.
NMI R87

Bonmarin P. and Ramamonjiarisoa A. 1985
Deformation to breaking of deep water gravity waves.
Exp. in Fluids, 3 , pp 11 - 16

Boussinesq, J. 1871
Theorie de l'intumescence liquid appelee onde solitaire ou de translation se propageant dans un canal rectangulaire.
Institut de France, Academie des sciences, Comptes rendus p 755

Bruce T. 1987
Power spectra of water waves.
Honours project. Edinburgh University, dept. of Physics

Bryden I.G. and Greated C.A. 1984
Generation of three-dimensional random waves.
J.Phys. D: Appl. Phys., 17 2351 - 2366

Buhr Hansen J. and Svendsen Ib A. 1979
Regular waves in shoaling water experimental data.
Inst. Hydrodyn. and Hydraulic Engineering. Tech. Uni. Denmark Series paper 21

Chakrabarti S.K. 1971
Discussion on 'Dynamics of single point mooring in deep water'.
JWPC&O Eng. Div. ASCE 97 (WW3) pp 588 - 590

Chaplin J.R. 1980
Developments of stream-function wave theory.
Coastal Engineering 3, pp 179 - 205

Chappelear J.E. 1962
Shallow water waves.
JGR Res., 67 , 12 , pp 4693 - 4704

Cokelet E.D. 1977
Steep gravity waves in water of arbitrary uniform depth.
Phil. Trans. Roy. Soc. A. 286 , pp 183 - 230

Dalrymple R.A. 1974
A finite amplitude wave on a linear shear current.
JGR Vol. 79 , No. 30 , pp 4498 - 4504

Dean R.G. 1965
Stream function representation of nonlinear ocean waves.
JGR 70, pp 4561 - 4572

Dean R.G. 1968
Relative validities of water wave theories.
Proc. Conf. on Civ. Eng. in the Oceans, San Francisco , Sept 1967 pp 1 - 30

Department of Energy 1986
Carter D.J.T., Challenor P.G., Ewing J.A., Pitt E.G., Srokosz M.J. and
Tucker M.J. 1986
Estimating wave climate parameters for engineering applications.
HMSO OTH 86 228

Department of Energy 1984 (1974)
Offshore installations: Guidance on design and construction.
HMSO Dd 736730 c15 10/84

Divoky D., Le Mehaute B. and Lin A. 1970
Breaking waves on gentle slopes.
JGR Vol. 75 , No. 9 pp 1681 - 1692

Drabble M. J. 1989
Turbulent wind action on tension leg platforms.
PhD. Thesis Heriot-Watt University, Edinburgh

Duncan J.H. 1983
The breaking and nonbreaking wave resistance of a two dimensional hydrofoil.
JFM 126 , pp 507 - 520

Durrani T.S. and Greated C.A. 1977
Laser systems in flow measurement.
Plenum New York.

Douglass S.L. and Weggel J.R. 1980
Laboratory experiment on the influence of wind on nearshore wave breaking.
CEC Malaga Chapter 46 pp 632 - 643

Easson W.J. and Greated C.A. 1984
Breaking wave forces and velocity fields.
Coastal Engineering, 8 , pp 233 - 241

Easson W.J. and Greated C.A. 1985
Acceleration measurement using laser doppler anemometry.
SPIE Vol. 599 Optics in engineering measurement. pp 380 - 386

Easson W.J., Griffiths M., Sharpe J. and Greated C.A. 1986
Measurement of fluid velocity and acceleration using pulsed correlation techniques.
Presented at Electro-Optics UK Brighton 1986

Eastwood J.W., Townend I.H. and Watson C.J.H. 1987
The modelling of wave-current velocity profiles in the offshore design process.
Advances in underwater technology, Volume 12: Modelling the offshore environment. Soc. for underwater technology (Graham and Trotman.)

Edinburgh wave power project 1978
Forth year report, Volume 3 of 3, July.
Edinburgh University.

Fenton J.D. 1979
A high order cnoidal wave theory.
JFM 94(1), pp 129 - 161

Flick, R.E. and Guza R.T. 1980
Paddle generated waves in laboratory channels.
J. Waterway, Port and Coastal Eng. Div. ASCE 106 (WW1) pp. 79 - 97

Galvin C.J. 1968
Breaker type classification on three laboratory benches.
JGR Vol. 73 No. 12

Galvin C.J. 1969
Breaker travel and choice of design wave height.
J. Waterways and harbors Div. ASCE WW2 pp 175 - 200

Gray C. and Greated C.A. 1988
The application of Particle Image Velocimetry to the study of water waves.
Optics and Lasers in Engineering ,9 , pp 1 - 12

Griffiths M. 1985
Computer simulation.
Uni. of Edinburgh fourth year report.

Guza R.T. and Thornton E.B. 1985
Observations of surf beat.
JGR Vol. 90, No. C2 pp 3161 - 3172

Halliwell A.R. and Machen P.C. 1981
Short-crested breaking waves in water of limited depth.
Proc. Inst. Civ. Eng. Part 2, pp 663 - 674

Hasselmann, K. et al. 1973
Erganzungsheft zur Deutschen Hydrographischen Zeitschrift.
Deut. Hydrogr. Inst., Hamberg.

Hasselmann, K. et al. 1973
Measurement of wind-wave growth and swell decay during the Joint North Sea Wave Project (JONSWAP)
Dt. Hydrogr. Z Reihe A (8'), Nr. 12 95 pp

Hedges T.S. and Kirkgoz M.S. 1981
An experimental study of the transformation zone of plunging breakers.
Coastal Engineering 4, pp 319 - 333

Holthuijsen L.H. and Herbers T.H.C. 1986
Statistics of breaking waves observed as whitecaps in the open sea.
JPO Vol. 16 pp 290 - 297

Houmb O.G. and Overvik T. 1976
Parameterization of wave spectra and long term joint distribution of wave height and period.
BOSS pp 144 - 169

Iribaren C.R. and Nogales C. 1949
Protection des portes Section II Comm. 4
XVII Int. Nav. Congress, Lisbon.

Iwagaki A.T. 1968
Hyperbolic waves and their shoaling.
CEC London chapter 9 , pp 124 - 144

Jansen P.C.M. 1986
Laboratory observations of the kinematics in the aerated region of breaking waves.
Coastal Engineering, 9, pp 453 - 478

Kimura A. and Iwagaki Y. 1978
Wave length, wave velocity and shoaling characteristics of random waves.
Coastal engineering Chapter 17 , pp 320 - 339

Kirkgoz M.S. 1986
Particle velocity prediction at the transformation point of plunging breakers.
Coastal Engineering, 10, pp 139 - 147

Kjeldsen S.P. 1981
Design Waves.
NHL Trondheim, Norway. Report No. 1 81008

Kjeldsen S.P. 1983a
2- and 3-dimensional deterministic freak waves.
NHL Trondheim Norway, Publication R-149.83

Kjeldsen S.P. 1983b
Determination of severe wave conditions for ocean systems in a 3-dimensional irregular seaway.
Contribution to the VIII congress of the pan-american institute of naval engineering.

Kjeldsen S.P. and Myrhaug D. 1978
Kinematics and dynamics of breaking waves.
Rept. No STF60 A78100 Ships in rough seas Part 4 NHL Trondheim Norway.

Kjeldsen S.P. and Myrhaug D. 1980
Wave-wave interactions, current-wave interactions and resulting extreme waves and breaking waves.
Coastal engineering chapter 137 pp 2277 - 2303

Kjeldsen S.P., Vinge T., Myrhaug D. and Brevig P. 1980
Kinematics of deep water breaking waves.
OTC pp 317 - 325

Koh, R.C.Y. and Le Mehaute B. 1966
Wave shoaling.
JGR 71 , pp 2005 - 2012

Korteweg, D.J. and De Vries, G. 1895
On the change of form of long waves advancing in a rectangular canal on a new type of long stationary waves.
London, Dublin and Edinburgh, Philosophical Magazine, Ser. S. 39

Kuo C.T. and Kuo S.J. 1974
Effect of wave breaking on statistical distribution of wave heights.
Civil Eng. in the Oceans 3 pp 1211 - 1231

Kuo Y.Y and Wang H.M. 1986
Nonlinear theory on particle velocity and pressure of random waves.
CEC

Laing A.K. 1986
Nonlinear properties of random gravity waves in water of finite depth.
JPO Vol. 16 pp 2013 - 2030

Laitone E.V. 1960
The second approximation to cnoidal and solitary waves.
JFM 9, pp 430 - 444

Lamb H. 1932 (1945)
Hydrodynamics.
Cambridge University Press, 1932 and Dover publications, 1945

Le Mehaute B., Divoky D. and Lin A. 1968
Shallow water waves: a comparason of theories and experiments.
CEC London pp 86 - 107

Lighthill J. 1986
Fundamentals concerning wave loading on offshore structures.
JFM Vol. 173 pp 667 - 681

Longuet-Higgins M.S. 1969
On wave breaking and the equilibrium spectrum of wind-generated waves.
Proc. Roy. Soc. A. 310, pp 151 - 159

Longuet-Higgins M.S. 1980
The unsolved problem of breaking waves.
Coastal Engineering Conference, Keynote address, Sydney. pp 1 - 28

Longuet-Higgins M.S. 1983
Wave set-up, percolation and undertow in the surf zone.
Proc. Roy. Soc. London. A 390, pp 283 - 291

Longuet-Higgins M.S. 1985
Accelerations in steep gravity waves.
JPO Vol. 15 pp 1570 - 1579

Longuet-Higgins M.S. 1986
Accelerations in steep gravity waves. II: Subsurface accelerations.
JPO Vol. 16 pp 1332 - 1337

Longuet-Higgins M.S. and Cokelet E.D. 1976
The deformation of steep gravity waves on water:
I A numerical method of computation.
Proc. Roy. Soc. Lon. A. 350 pp 1 - 26
II Growth of normal mode instabilities.
Proc. Roy. Soc. Lon. A. 364 pp 1 - 28

Longuet-Higgins M.S. and Fox M.J.H. 1977
Theory of the almost highest wave: The inner solution.
JFM , 80 , pp 721 - 741

Longuet-Higgins M.S. and Smith N.D. 1983
Measurement of breaking waves by a surface jump meter.
JGR Vol 88 C 14 pp 9823 - 9831

Melville W.K. 1982
The instability and breaking of deep-water waves.
JFM 115, pp 165 - 185

Michell J.H. 1893
On the highest waves in water.
Philosophical Magazine Vol. 36, 5th series, pp 430 - 437

Miller R.L. 1972
The role of surface tension in breaking waves.
Coastal Engineering 6 , pp 433 - 449

Mizuguchi M. 1986
Experimental study on kinematics and dynamics of wave breaking.
Coastal Engineering Chapter 45 pp 589 - 603

Mo O. and Moan T. 1984
Environmental load effect analysis of guyed towers.
Offshore mech. and arctic eng. symp. New Orleans.

Morison J.R., O'Brien M.P., Johnson J.W. and Schaaf S.A. 1950
The force exerted by surface waves on piles.
Petrolium Transactions AIME Vol. 189

Munk W.H. 1949
The solitary wave theory and its application to surf problems.
Annals of the N-Y Academy of science, Vol. 51 pp 376 - 462.

Myrhaug D. and Kjeldsen S.P. 1984
Parametric modelling of joint probability density distributions for steepness and asymmetry in deep water waves.
Applied Ocean Research, Vol. 6, No. 4 pp 207 - 220

Myrhaug D. and Kjeldsen S.P. 1987
Estimation of occurrences of steep and high waves in deep water.
JWPC&OEng. Vol. 113 , No. 2 , pp 122 - 138

Nath J.H. and Ramsey F.L. 1976
Probability distributions of breaking wave heights emphasizing the utilation of the JONSWAP spectrum.
JPO Vol. 6 pp 316 - 323

New, A.L. McIver P. and Peregrine D.H. 1985
Computations of overturning waves.
JFM Vol. 150, pp 233 - 251

Ochi M.K. and Tsai C-H. 1983
Prediction of occurrences of breaking waves in deep water.
JPO 13 , pp 2008 - 2019

Ochi M.K. and Tsai C.H. 1983
Prediction of occurrence of breaking waves in deep water.
JPO Vol. 13 pp 2008 - 2019

Peregrime D.H. 1983
Breaking waves on beaches.
Ann. Rev. Fluid Mech. 15 , pp 149 - 178

Phillips O.M. 1985
Spectral characteristics of breaking waves.
The ocean surface. (Toba Y. and Mitsuyasu H. eds.) D.Reidel pp 111 - 123

Phillips O.M. 1958
The equilibrium range in the spectrum of wind generated waves.
JFM 4, pp 426 - 434

Phillips O.M. and Banner M.L. 1974
Wave breaking in the presence of wind drift and swell.
JFM Vol. 66, part 4, pp 625 - 640

Pierson W.J. and Moskowitz L. 1964
A proposed spectral form for fully developed wind seas based on the similarity theory of S.A. Kitaigorodskii.
JGR Vol. 69, No. 24 pp 5181 - 5190

Powell K.A. 1988
The dynamic responce of shingle beaches to random waves.
Coastal Engineering Conference. Vol. 2 pp 1763 - 1773

Ramberg S.E. and Griffin O.M. 1987
Laboratory study of steep and breaking deep water waves.
JWPC&O Eng. Div. ASCE Vol. 113, No. 5 pp 493 - 506

Ramberg S.E. and Griffin O.M. 1987
Laboratory study of steep and breaking deep water waves.
JWPC&OEng. Vol 113 , No. 5 , ASCE pp 493 - 506

Rayleigh, Lord 1876
On waves.
London, Dublin and Edinburgh, Philosophical Magazine, Ser. 5
Vol. 1.

Rayleigh, Lord 1914
On the theory of long waves and bores.
Proceedings of the royal society of London. Ser. A Vol. 90,

Russell, S. 1844
Report on waves.
British association reports.

Sakai S., Hiyamizu K. and Saeki H. 1986
Wave height decay model within a surf zone.
CEC pp 686 - 696

Sakai T. and Iwagaki Y. 1978
Estimation of water particle velocity of breaking wave.
Coastal engineering chapter 31

Sakai T., Mizutani T., Tanaka H. and Tada Y. 1986
Vortex formation in plunging breaker.
CEC pp 711 - 723

Sarpkaya T. and Isaacson M. 1981
Mechanics of wave forces on offshore structures.
San Francisco, Van Nostrand Reinhold Company.

Sawaragi T. and Iwata K. 1976
Wave spectrum of breaking wave.
CEC pp 581 - 594

Schwartz L.W. 1974
Computer extension and analytic continuation of Stokes' expansion for gravity waves.
JFM 62, pp 553 - 578

Simmen J.A. and Staffman P.G. 1985
Steady deep water waves on a linear shear current.
Studies in applied maths. 73 , pp 35 - 57

Skjelbreia J.E. 1987
Observations of breaking waves on sloping bottoms by use of laser Doppler velocimetry.
PhD. Thesis California Inst. of Technology. Pasadena.

Skjelbreia L. and Hendrickson J. 1961
Fifth order gravity wave theory.
CEC pp 184 - 194

Snyder R.L., Smith L. and Kennedy R.M. 1983
On the formation of whitecaps by a threshold mechanism.
Part III : Field experiment and comparison with theory.
JPO Vol. 13 pp 1505 - 1517

Sobey R.J. 1986
Wind-wave prediction.
Annual review of fluid mechanics. pp 149 - 172

Srokosz M.A. 1986
On the probability of wave breaking in deep water.
JPO Vol. 16 pp 382 - 385

Srokosz M.A. 1987
Models of wave-current interaction.
Advances in Underwater Technology. Volume 12: Modelling the offshore environment. Soc. for underwater technology (Graham and Trotman.)

Stive M.J.F. 1984
Energy dissipation in waves breaking on gentle slopes.
Delft Hydraulics Laboratory, Publication no. 321

Stive M.J.F. 1985
A scale comparison of waves breaking on a beach.
Coastal engineering 9, pp 151 - 158

Stoker J.J. 1957
Water waves. The mathematical theory with applications.
Interscience publishers, New York and London.

Stokes G.G. 1847
On the theory of oscillatory waves.
Trans. Camb. Phil. Soc. 8, pp 441 - 455
also Math. Phys. Papers Vol 1 , CUP 1880

Stokes G.G. 1880
On the theory of oscillatory waves. B. Considerations relative to the greatest height of oscillatory irrotational waves which can be propagated without change of form.
Mathematical and Physical papers. Vol.1 CUP.

Su M-Y. Bergin M. Marler P. and Myrick R. 1982
Experiments on non-linear instabilities and evolution of steep gravity-wave trains.
JFM 124, pp 45 - 71

Svendsen I.A. and Jonsson I.G 1980
Hydrodynamics of coastal regions.
Technical university of Denmark, Lyngby

Svendsen I.A. and Lorenz R.S. 1988
Three dimensional flow profiles on littoral beaches.
CEC Vol.1 pp 705 - 717

Svendsen Ib A. and Buhr Hansen J. 1976
Wave set-down near breaking.
Prog. Rept. 41 pp 31 - 36 IHHE Tech. Uni. Denmark

Tayfun M.A. 1981
Breaking-limited wave heights.
JWPC&O Eng. Div. ASCE Vol. 107, No. WW2 pp 59 - 69

Technical advisory committee on protection against inundation 1972
Golfoploop en Golfoverslag.
Government publishing office - The Hague.

Technical advisory committee on protection against inundation 1974
Wave run up and overtopping.
Government publishing office - The Hague.

Tsao S. 1959
Behavior of surface waves on a linearly varying current.
Tr. Mosk. Fiz.-Tech. Inst. Issled. Mekh.

Van Dorn W.G. 1976
Set-up and run-up in shoaling breakers.
CEC Vol. 1 pp 738 - 751

Van Dorn W.G. 1978
Breaking invarients in shoaling waves.
JGR Vol. 83 , No C6 pp 2981 - 2988

Van Dorn W.G. and Pazan S.E. 1975
Laboratory investigation of wave breaking.

Part II Deep water waves.

Part I never produced.

AOEL Scripps Inst. of Oceanography, UC San Diego, Rept. 71

Vyas Y.K., Lohrmann A., Heideman J.C., Dahl F.E. and Vermersch J.A. 1988
Storm driven current profiles for design of offshore platforms.
BOSS pp 519 - 534

Weissman M.A., Atakturk S.S. and Katsaros K.B. 1884
Detection of breaking events in a wind-generated wave field.
JPO Vol. 14, pp 1608 - 1619

Wheeler J.D. 1970
Method for calculating forces produced by irregular waves.
J. of Petrolium Technology pp 359 - 367

appendix

Measurement of Fluid Velocity and acceleration using

Pulsed Correlation Techniques.

Easson, W.J., Griffiths, M., Sharpe, J., and Greated, C.A.

Abstract

Laser anemometry provides a sensitive tool for measuring fluid flows. However, continuous analysis of the Doppler signal does not always prove the optimum method of processing. Gating the signal with one, two or a regular series of pulses can provide detailed information on particular aspects of time-dependent flows. Some theoretical aspects of pulsed correlation are presented with particular application to the measurement of acceleration in water waves and periodic acoustic flows.

Introduction

Laser anemometry provides an excellent tool for the measurement of velocities in various types of fluid. The use of this technique is well documented in the literature (Durrani and Greated 1977). Several methods of signal collection and analysis are available. For well seeded flows a continuous current may be produced by a photodiode; for signal collection in other flows (e.g. air) a photomultiplier is normally used. In either case the resulting doppler signal may be tracked, correlated or the direct spectrum may be obtained from a spectrum analyser. The spectrum analyser and tracker have inadequate response time for the measurement of many flows where large fluctuations are present. Therefore, if a more detailed picture of the flow than a time average is required a correlator must be used.

To localise the correlogram around the time of interest a gate is applied to the incoming doppler signal. This gate usually takes the form of a square pulse. However, the application of these distorts the final correlogram and any spectra obtained. Hence it is necessary before using this technique, to fully investigate the consequences to the correlogram of applying a gate to the signal. This will be studied in section 2 for the single pulse, double pulse and regular pulse, with illustrations using a single sine wave as the signal. Then in sections 3 and 4 these will be applied to the problems of measuring fluid acceleration and harmonic flow.

2. Signal Gating.

2.1 Gating a mean-zero doppler signal.

Figure 2.1 shows a typical gated doppler signal. To find the auto-correlation we first form the product

$$I(t) = c(t)\emptyset(t), \qquad 2.1$$

where $I(t)$ is the gated detector current, $c(t)$ is the continuous doppler signal and $\emptyset(t)$ is a pulse which takes the value 1 between t_1, t_2 and 0 elsewhere. For $c(t)$ a stationary process (Papoulis, 1965) the autocorrelation of $I(t)$ is

$$R_I(\tau) = R_c(\tau)R_{\emptyset}(\tau) \qquad 2.2$$

since $c(t)$ and $\emptyset(t)$ are independent.

The autocorrelation of a square pulse is a triangular pulse, therefore $R_I(\tau)$ is a linearly damped correlogram where the damping becomes total at $\tau = t_2 - t_1$, the pulse width. Figure 2.2 shows the autocorrelation of a gated sinusoid for various pulse widths.

2.2 Gating a pedestal signal.

In some applications the gated signal rides on a pedestal current (fig. 2.3). In this case the detection current may be written as

$$I(t) = (c(t) + p)\,\emptyset(t) \qquad 2.3$$

where p is the constant pedestal current. The autocorrelation of this has four product terms, the cross-products being indentical:

$$R_I(\tau) = R_c(\tau)R_{\emptyset}(\tau) + p^2R_{\emptyset}(\tau)$$

$$+ 2p\,\overline{c(t)} \qquad 2.4$$

where $\overline{c(t)}$ is the mean doppler signal, which is zero by definition. The second term in equ. 2.4 adds a sloping baseline to the autocorrelation. This is demonstrated in fig. 2.4.

2.3 Gating twice.

The autocorrelation of two pulses is shown in fig. 2.5 where Δ is the pulse length and θ is the time between pulses. The first triangle is the sum of the autocorrelations of each pulse; the second is the cross correlation of the two pulses.

If a doppler signal is gated by these pulses then the section $\tau = 0 \rightarrow \Delta$ of the autocorrelation will contain the sum of the autocorrelations both signals. This may be seen clearly if the signals are two sine waves, as in fig. 2.6. It is therefore to no advantage to use a correlogram length of greater than the pulse width Δ.

If $\theta < 2\Delta$ then the triangles in 2.5 will overlap and interfere so it is advisable to avoid this situation (Grant & Greated, 1980).

2.4 Multiple gating.

In analysis of a harmonic phenomenon it may be advantageous to gate the doppler singal in phase with some known cycle of the experiment. The autocorrelation of a continuous square wave is an infinite series of triangular pulses as in fig. 2.5 but each pulse is of the same height. Again the first triangle contains the sum of the autocorrelations of all the pulses observed and represents an average doppler signal for that phase in the cycle.

2.5 Spectrum of the autocorrelation.

Using the identities,

$$S_z(\omega) = S_z(\omega)*S_y(\omega) \text{ if } R_z(\tau) = R_x(\tau)R_y(\tau) \qquad 2.5$$

and

$$S_z(\omega) = S_x(\omega) + S_y(\omega) \text{ if } R_z(\tau) = R_x(\tau)+R_y(\tau) \qquad 2.6$$

the power spectrum of the gated doppler signal is, for a single pulse,

$$S_I(\omega) = S_c(\omega)*S_\emptyset(\omega). \qquad 2.7$$

and, for a series of pulses,

$$S_I(\omega) = \sum_{i=1}^{n} S_i(\omega)*S_\emptyset(\omega) \qquad 2.8$$

where $S_i(\omega)$ is the spectrum of the doppler signal in each pulse and n is the total number of pulses observed.

Therefore, the spectrum of a signal with many gates is simply the sum of the spectra of each gated element $S_i(\omega)$. This property will be used in section 3 to find the difference in doppler signal at two times and in section 4 to find the average doppler signal at one phase of a harmonic wave.

3. Measuring acceleration with a Double Pulse.

3.1 Linear decay correction.

It is possible to correct for the linear decay (equ.2.2) due to the finite length of signal equal to the length of the correlogram required (see fig. 3.1). This effectively increases the gate width on the correlogram to $\Delta + \tau_{MAX}$, but has the advantage of making the correlogram simpler to analyse. This facility is available on the HP 3721A correlator used in the following experiment.

3.2 Method

The local acceleration in the frame of reference of the laboratory is simply given by

$$\frac{\partial v}{\partial t} \approx \frac{v(t_2) - v(t_1)}{t_2 - t_1} \qquad 3.1$$

In non-turbulent flow the spectrum of the doppler signal over a small interval is a delta function at the doppler frequency. Therefore, applying equation 2.5 we only need provide two pulses in the gating signal at known separation to find the change in doppler frequency from the peaks in the spectrum. Figure 3.2 shows two peaks from the spectrum of a double pulsed doppler signal under a breaking wave.

Waves are produced in a narrow flume by an absorbing paddle with micro-computer control. The breaking is initiated by causing a local increase in wave energy at a particular crest. The velocity over some part of the crest will then be larger than the phase velocity of the wave. The crest forms a spout and plunges forward.

Such waves are of major importance to shipping and offshore drilling as the internal velocities and accelerations are larger than those found in waves of a regular form. Laser anemometry provides the only accurate tool for measuring in this type of crest. Figure 3.3. shows the acceleration field obtained with the methods described in this paper. These demonstrate that large accelerations, in excess of g, are found at the leading edge of the crest and under the peak of the wave. The forces on members of offshore structures due to the high velocities and accelerations present in breaking waves may be several times larger than predicted by traditional methods (Easson & Greated, 1984).

4. Using pulsed correlation techniques to determine the velocity at various phase posisitons of a harmonic wave.

In this section the gating technique is applied to measuring the velocities at various phase positions of a harmonic wave. The method essentially relies on the gating of the signal from a laser doppler anemometer, supplying point velocity information in any specified direction as well as phase information.

4.1 Experimental Setup.

The experimental setup is shown schematically in Figure 4.1.

The optics consist of an 8 mW He-Ne laser and beam splitter which produces 2 parallel beams separated by 2 cm. These pass through a phase shift and are focussed down to a point on the axis of the tube using a 20 cm focal length lens. The sound field in a 47 cm long tube is generated using a miniture loudspeaker positioned about 1.5 cm from the open end and a probe microphone is inserted through the closed end allowing the sound intensity at the focus of the laser beams to be monitored. The signal from the probe microphone could be sent to the microcomputer to trigger the gating pulses and these pulses used to gate the photomultiplier. Using these gating pulses means that the photomultiplier only produces a signal for the duration of the pulses. The photmultiplier was set at the rather large angle of 35° to the straight through position in order to minimise the effect of light scattered from the tube walls.

4.2 Gating

The microcomputer is programmed to provide gating pulses of various duration and at various delays from the zero upcrossing of the signal from the probe microphone. Both the signal and the pulses were monitored throughout the experiment and a typical setting is shown in Figure 4.2.

4.3 Measurements and results

The air in the tube was excited to its 2nd harmonic (526 Hz) and the observation volume of the laser probe sited near one of the antinodes in order to observe large velocity fluctuations. The sound intensity was measured at this position and found to be 119 dB.

Using a phase shift of 83.3 kHz and a sample time of 1.5 μs and with no gating employed the photon correlogram took the form of a heavily modulated cosine curve (Durrani & Greated, 1977, Greated, 1986) (Figure 4.3).

With gating applied however the correlogram showed the form deduced in Section 2, being damped and riding on a sloping lose line. (Figure 4.4). The damping is almost entirely linear, due to the pulse gating, therefore the flow in the sound field is essentially non-turbulent. By varying the delay time it was possible to obtain a plot of the velocities throughout the full period of the signal (Figure 4.5). The velocity is approximately sinusoidal over each cycle, with a mean of zero and amplitude of 12 cms^{-1}

5. <u>Conclusions</u>

The use of a pulsed correlation provides detailed information for complex flow fields. However, care is required in the interpretation of the correlograms to extract the original signal data. The method is ideal for examining high frequency harmonic flows and measuring fluid acceleration.

6. <u>Acknowledgements</u>.

The breaking waves project is funded by the Marine Technology Direcorate of the S.E.R.C. Mr. Griffiths is in receipt of a CASE studentship with B.P. Mr. Sharpe is funded by the Department of Education, Northern Ireland.

7. References.

Durrani, T.S. and Greated, C.A., 1977, "Laser Systems in Flow Measurement". New York, Plenum.

Easson, W.J. and Greated, C.A. 1984, "Breaking wave forces and velocity fields". Coastal Engineering, Elsevier, Amsterdam.

Grant, I.G. and Greated, C.A., 1980, "Periodic sampling in laser anemometry", J. Phys. E.: Sci. Instrum., Vol. 13.

Greated, C.A., 1986, "Measurement of acoustic velocity fields", Strain.

Papoulis, A., 1965, "Probability, Random Variables and Stochastic Processes, McGraw-Hill.

Fig. 2.1 Gated signal with pulse of length $\Delta = t_2 - t_1$ applied.

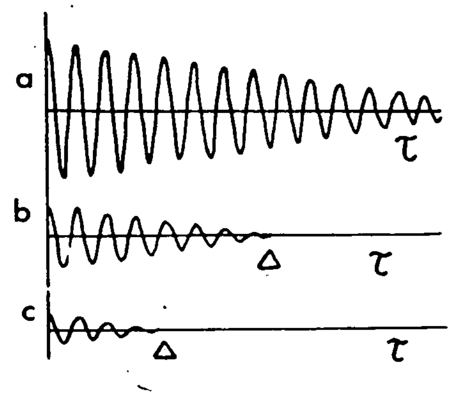

Fig. 2.2 Correlograms of gated sinsoid. The pulse length in each diagram is half the previous pulse length.

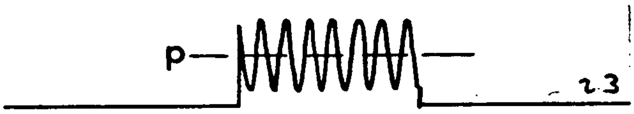

Fig. 2.3 A gated signal where the pulse also adds a pedestal current.

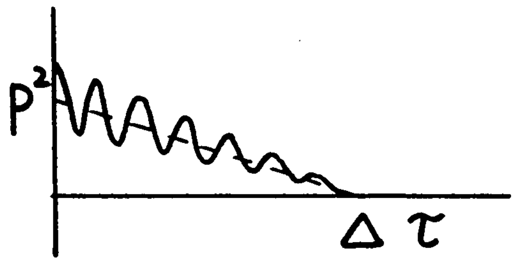

Fig. 2.4 Correlogram of a gated pedestal sinusoid. The base slope and damping are both linear reaching zero at $\tau = \Delta$.

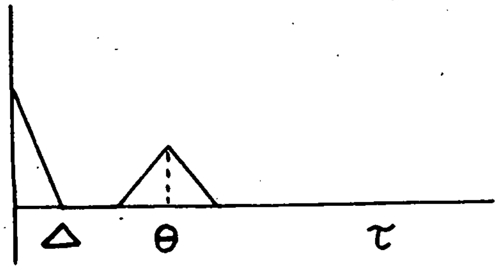

Fig. 2.5 Correlogram of two identical square pulses of width Δ, separation θ.

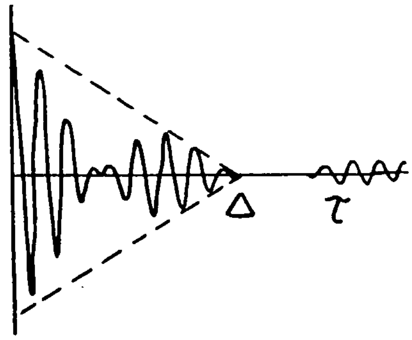

Fig. 2.6 Correlogram of a double pulse applied to a varying signal. The interval to $\tau=\Delta$ contains the sum of the correlograms of the signal carried by each pulse. The beginning of the cross correlation of the two gated signals may be seen.

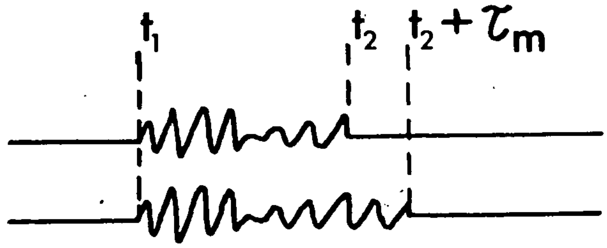

Fig. 3.1 The linear decay in the correlogram may be avoided by providing an extra record length equal to the length of correlogram required (τ_m).

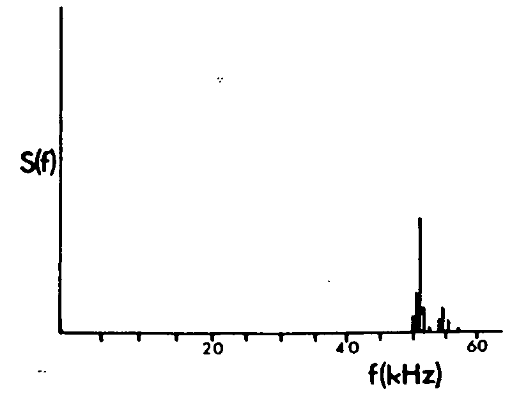

Fig. 3.2 Spectrum from a double pulsed doppler correlogram. The two peaks are easily resolved to provide the acceleration information.

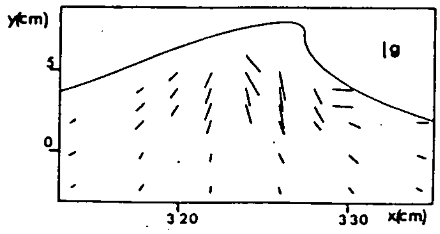

Fig. 3.3 Acceleration field under a breaking wave crest. Vectors are normalised with respect to g as indicated.

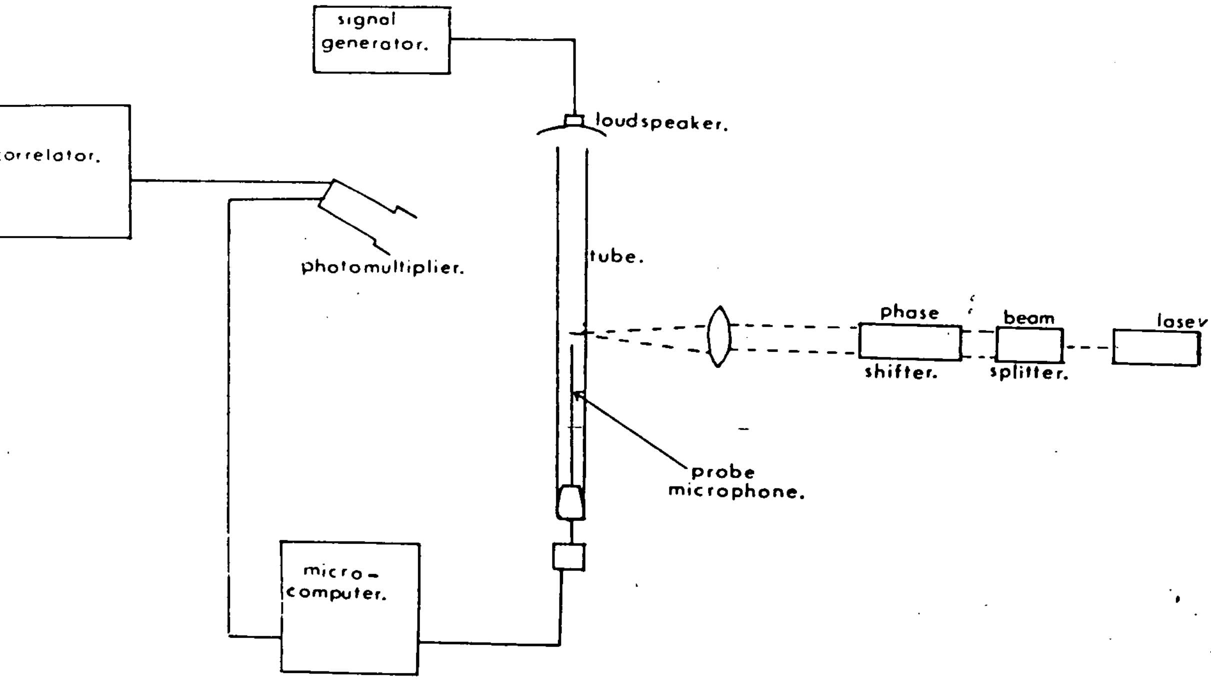

ig. 4.1 Schematic diagram of acoustic experiment.

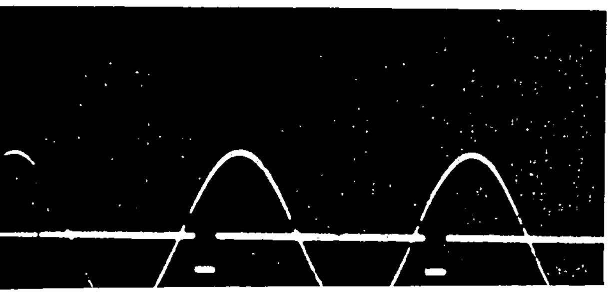

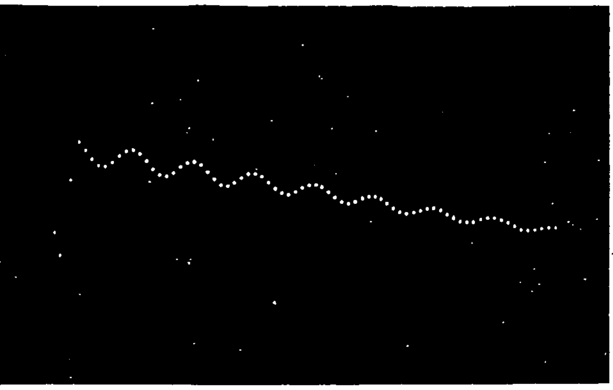

Fig. 4.4 Photon correlogram of same field with gating applied.

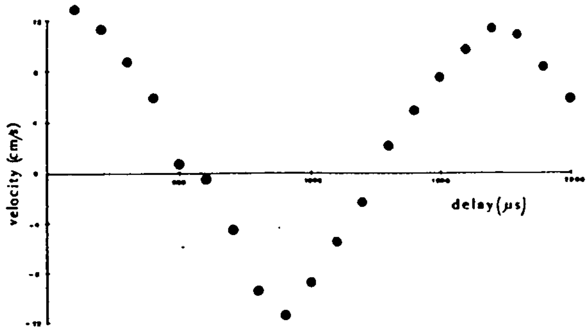

Fig. 4.5 Velocity variation over one cycle of the microphone signal.

Papers presented at the Third International Symposium on Integrity of Offshore Structures, 28–29 September 1987, held at the Kelvin Conference Centre, University of Glasgow, Scotland, organised by the University of Glasgow, Departments of Naval Architecture and Ocean Engineering and Mechanical Engineering.

INTEGRITY OF OFFSHORE STRUCTURES—3

Edited by

D. FAULKNER†

M. J. COWLING*

and

A. INCECIK†

* *Department of Mechanical Engineering,*
† *Department of Naval Architecture and Ocean Engineering,*
The University, Glasgow, Scotland

ELSEVIER APPLIED SCIENCE
LONDON and NEW YORK

4

LARGE WAVE LOADING ON STRUCTURES - A REAPPRAISAL

M. GRIFFITHS, W.J. EASSON and C.A. GREATED

Department of Physics, University of Edinburgh,
Edinburgh, U.K.

ABSTRACT

Results are presented on breaking characteristics of laboratory generated water waves, and used in a criticism of present design practice. Two areas are discussed in detail, (i) the choice of design wave and the use of the breaking height ratios, (ii) the use of computer models to predict the internal kinematics.

It is suggested that present design is (i) overly conservative in choice of breaking limit for intermediate to deep water and (ii) generally conservative in its prediction of kinematics except for the high crest region, where local high velocities are observed to occur, in excess of those calculated by Stokes' or Dean's methods.

1. INTRODUCTION

The present design method, for calculating the extreme loading on offshore structures uses what is termed the 'design wave'. This is an extreme wave and is usually chosen as the highest wave likely to occur within a given period, typically fifty or one hundred years. Two criticisms are raised here both arising from observations made during experimental research on wave breaking. The first is that the observed height at which breaking occurs is often substantially below that suggested in design codes and hence offshore structures may be being designed to withstand waves that can never physically exist. The second criticism is that the models used to predict kinematics for the design waves are inadequate in their descriptions of velocities in the high crest region, which could lead to serious local underdesign.

Choice of design wave is based on extrapolation from wave height data gathered in the locality of the proposed site. Details of methods used are given in, for example, Carter D J T and Challenor P G[1]. This method avoids explicit knowledge of the physical processes occurring at sea, such as wind and current interaction with the waves and the effects of bed topology. The contributions of all of these are included implicitly in the environmental wave elevation data and hence accounted for in the estimation of the extreme waveheight and period. Some influence of wave breaking will also be included, but as this is height dependent, it will show up less in normal conditions but will almost certainly be the major influence in the extreme condition represented by the design wave.

Recent analysis of the estimation of wave climate parameters, Carter et al,[(2)] draws attention to the large difference in results for extreme wave heights that occurs when the tail of the probability distributions used for extrapolation is started at various points.

The effect of wave breaking is curently introduced explicitly into the design procedure in an ad hoc manner. Given a design wave of specified height, period and water depth, rules are applied to see if the wave is breaking, and if it is, then the design height is reduced to the highest non-breaking wave. The rules applied are, checking the ratio of H/d for shallow water or H/gT^2 (or H/L) for deep water and also checking the stability of the various simulations available. For most offshore situations, the commonly used limits for H/d and H/gT^2 are excessively conservative. These are discussed at more length in ¶5. The use of the stability of computational methods as justification of a reduction in design wave height should be regarded as unacceptable until such time as it is demonstrated that this reflects a physical limit rather than a modelling inability.

For a given design wave, the structural analysis is performed by simulating the wave using a Deans or Stokes type model. The resulting internal velocity and acceleration fields are used with a Morison type expression to calculate the forces experienced by the structure as the wave passes. The models used in these simulations can not describe wave breaking and must be seen as approximations. In section ¶6 we present results of measured velocities and accelerations below a breaking wave. These are used to demonstrate the general agreement with a Deans model and the important local under prediction in the high crest region.

All the work reported here was performed on a 1 : 30 slope in a 2-dimensional wave flume. This is part of a more general study of extreme and breaking waves presently in progress at Edinburgh.

2. ANALYSIS OF PREVIOUS RESULTS

(a) Breaking Height

A large amount of work has been done on estimating environmental wave parameters, from both theoretical and experimental approaches. But as yet no comprehensive analysis has been forthcoming. There are several aspects of the problem that make analysis difficult. For extreme waves, mathematical models are at the limit of their validity; in the laboratory the waves are at the limit of their stability; and at sea they occur in very hostile conditions. Also, the random nature of waves at sea has channelled interest towards an entirely non-deterministic approach, which although essential to present design practice has diverted attention from studies of the physics involved.

As a first step towards a more deterministic approach, the physical limit set by wave breaking can be and to some extent already is used in the choice of design wave. In engineering practice, there are two commonly used expressions for H_b, the height at which a wave begins to break.

For shallow and intermediate water depth the limit of

$$\frac{H_b}{d_b}$$

is usually used, very often taken as 0.78 following "Solitary wave theory" Munk W H 1949[(3)]. More recently as a result of experimental work and derivations from solitary theory a range of

$$0.6 < \frac{H_b}{d_b} < 0.83$$

has been suggested by Carter et al.[(2)]. And an expression of H_b/d_b as a function of bottom slope m and H_b/T^2 was found empirically by Weggel[(4)].

These expressions along with results for a 1 : 30 slope from Iwagaki et al. '74[(5)] and Sakai and Iwagaki '78[(6)], show a very considerable range of values, from 0.6 to 0.98, and are plotted with the results obtained here, in ¶5.

In the deep water limit, H/d is meaningless and other criteria have been suggested. The most common of which is that of

$$\frac{H_b}{L_b} = \frac{1}{7}$$

found theoretically by Michell 1893[7].

Latterly the limit for H has been non-dimensionalised by gT^2 rather than by L_b. For comparison, the deep water finite amplitude expression

$$L_b = 1.2 \frac{gT^2}{2\pi}$$

can be used to derive the above limit as

$$\frac{H_b}{gT^2} = 0.027.$$

Ochi and Tsai[8] found limits for both regular and random waves of 0.027 and 0.020 respectively.

The other expression for a breaking limit is in terms of the downwards acceleration at the crest $\ddot{\xi}$. A value of 0.5g is suggested by Snyder and Kennedy[9]. This was shown, Carter et al.[2] to correspond to limits in terms of H/gT^2 of 0.025 and 0.022 depending on how they applied linear theory in the conversion.

Although the results presented here are for shallow and intermediate water depths, the results for the deep water are seen as the limiting case of H/gT^2 as deep water steepness attains its largest value. It is hoped to extend the research to cover deep water breaking.

(b) Particle Kinematics

Studies have been made on the kinematics of large and breaking waves but, as has been noted with concern within the offshore industry, without consensus. As a method of comparison, the maximum values of velocities and accelerations both measured and predicted are presented in Table 1.

Table 1 : Maximum velocities and acceleration

Source	Velocity		Acceleration	
	Measured	Predicted	Measured	Predicted
Stokes,[10]		1.0c		(∞)
Divoky et al 1970[11]	0.5c			
Kjeldsen & Myrhaug 1978[12]	1.27c	1.6c		1.6g
Kjeldsen et al 1980[13]	2.8c	1.7c		3.0g
Easson & Greated 1985[14]	1.0c		1.8g	

Not only are there large differences in the velocities quoted here, but when used to predict the drag force, the values are squared and these differences therefore exaggerated. For the velocities of 0.5c × 2.8c, there is factor of 30 between their squared values. Account must also be taken of these uncertainties when designing for slap and slam forces. However, this discrepancy is mostly localised in the high crest region, where with informed design its effects can be minimised.

3. THE EXPERIMENTAL SYSTEM

As there is considerable error within both experimental results and the theoretical ones, it is very important that further research is accurate and reliable. There are many difficulties intrinsic within the study of breaking waves. Being at the limit of their stability, it is important that the cause of breaking is the mechanism being studied rather than any spurious interference from other physical processes or instabilities.

Many advances have been made in both wave generation and in measurement techniques.

These experiments were performed in a wave flume 9 m long 0.33 m wide with the waves breaking on a 1 : 30 beach. The waves used were regular waves whose period and amplitudes could be chosen and a range of such values was used for the results ¶4 and 5. These waves were generated by a hinged absorbing wave paddle. The absorbing nature of the paddle greatly reduces the reflection of waves at the paddle and expanded aluminium mesh was used to reduce reflection at the beach end of the tank. The waves were generated in a deep water section of the tank before being channeled into the shallower working section by a steep slope, see Fig. 1. This technique of deep water generation has been observed, Flick and Guza[15], to virtually eradicate the free harmonics which often interfered with earlier work. (For a detailed discussion of the difficulties and sources of error associated with this type of work, see, Design Waves 1981 NHL.)

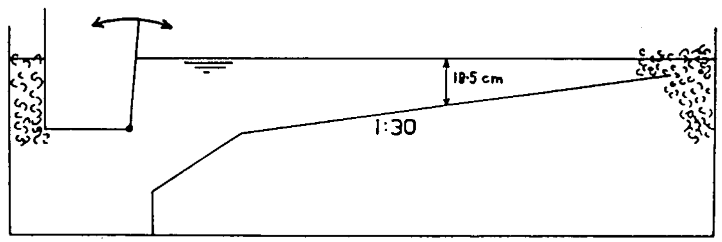

Fig. 1:

The measurement of the fluid kinematics also has inherent problems. In unstable regimes like breaking waves there is a danger that an intrusive measuring device may influence the flow. The LDA system whilst having the benefit of being non-intrusive, has in other wave research (Stive 1980[16]) been hampered by the discontinuous nature of the signal at levels above that of the wave trough. The system, reported here for the first time, makes use of a digital transient recorder which captures a length of doppler signal at a determined time. This signal is then passed to a BBC microprocessor where it is analysed. The system as set up in Edinburgh offers a selection of options for the processing. Based on use of an FFT chip, they allow the operator a choice of transforming all the 2048 points or preferred sections of the record; or for acceleration measurements, the separate transformation of the first and last quarters of the

record. The acceleration is then calculated as the difference of these velocities divided by the time between them.

This system, because it has no dependence on the signal quality prior to the length of record it is analysing, has very quick response. The length of signal required for measuring flows of around $1\ m\ s^{-1}$ is 2 ms for velocity measurements. Accelerations measured as the change of velocity over a known time interval depend on having two sections of 2 ms length with good signal separated by a period of the order of 10 ms. Normally a section of good signal of length 10 ms is used, with the central 6 ms section discarded.

4. MEASURED SURFACE PARAMETERS

As shown in ¶2 previous results of both internal kinematics and breaking height characteristics are not in good agreement. Therefore as a preliminary to measurements of these quantities, care must be taken to establish the credibility of our results.

Fundamental to the study of waves and to the design procedure is the assumption of Froude scaling, with its corollory that the characteristics of wave motion up to breaking should be uniquely determined by their geometry, and independent of scale. Thus any parameters measured at breaking can be determined from a full description of the initial geometry. As our bed slope was fixed at 1 : 30, we had only to describe the deep water geometry, this we chose to do in terms of the single deep water steepness parameter ($S = H_0/L_0$).

Any deviation from a functional relation to S in any of the breaking parameters would be a demonstration of either a shortcoming in the Froude scaling assumption or most likely, the influence of tank idiosyncrasies and experimental error.

We took as the point of breaking the first point where any part on the front of the wave becomes vertical. This is obvious for plunging breakers but still applies to spillers which are initiated by the formation of small spouts in the high crest region. At breaking, the following surface parameters were measured, the crest height (H_{1b}) and the trough depth from still water level (H_{2b}), the celerity and the wavelength measured independently and the depth from SWL.

For analysis, the wavelength results were converted to celerities and averaged with the measured celerity values, and all the parameters then non-dimensionalised by the appropriate combination of g and T, the gravitational acceleration and the wave period (which was very accurately known). Figures 2 and 3 show non-dimensional breaking depth and celerity as functions of S. On both of these a clear functional relation is apparent with errors in both cases below 5%.

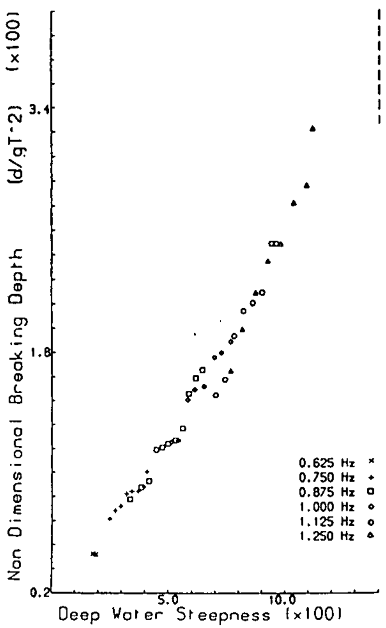

Fig. 2

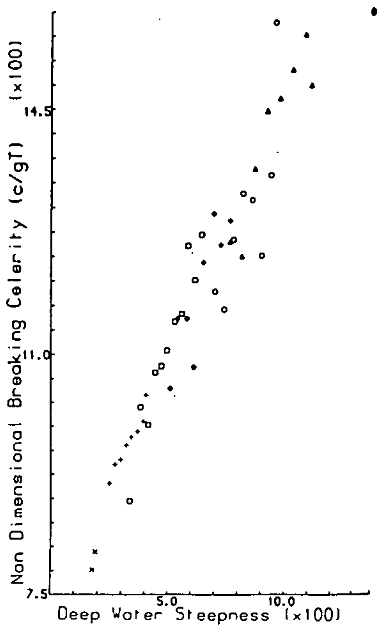

Fig. 3

The good behaviour of these results and those for the crest and trough elevations presented in ¶5 provide a demonstration of Froude scaling over the range of our experiment; it is seen that waves of

different size but the same steepness break in an essentially identical manner.

The validity of Froude scaling has been demonstrated Stive(17), over the range from the present scale 10 m to the much larger scale of 1.5 m.

The low degree of scatter in the results is also evidence that the breaking we are observing is indeed the result of shoaling on the 1 : 30 bed, rather than any tank idiosyncrasies.

5. DESIGN RATIOS RE-ASSESSED

There are two criteria commonly used to judge whether a design wave is breaking or not. For deep water the limiting height is expressed as proportional to gT^2, the constant of proportionality being variously estimated, typically in the range 0.022 to 0.027. The frequently cited limit of deep water steepness, $\frac{H_b}{L_b}$ of $\frac{1}{7}$ can be expressed by using the finite amplitude deep water relation of

$L_b = 1.2 \ \frac{gT^2}{2\pi}$ to give a value of $\frac{H_b}{gT^2}$ of 0.027.

For intermediate and shallow water the height to depth ratio is used with its value very often taken as 0.78 although other values have been proposed over the range 0.6 to 0.98.

The results of experiments described in ¶3 and ¶4 are given here in terms of these two design ratios. Following the analysis used in ¶4 our results are presented as functions of the deep water steepness. The work described here has not yet been extended to deep water so estimation for the limiting value of H/gT^2 must be based on an extrapolation from intermediate depth.

Fig. 4 shows H/gT^2 as a function of deep water steepness and the graph demonstrates a clear linear relationship for values of S from 0.02 to over 0.11. Extrapolation to 0.14 yields an estimate of $H/gT^2|_0$ of just below 0.022, in agreement with the lowest of the previous results, but it must be stressed that until measurements are extended to deeper water, this value must be regarded with caution. Included on the graph is the value of $H/gT^2|_0$ of 0.02 which is Ochi and Tsai's experimental result for breaking of deep water random waves(11).

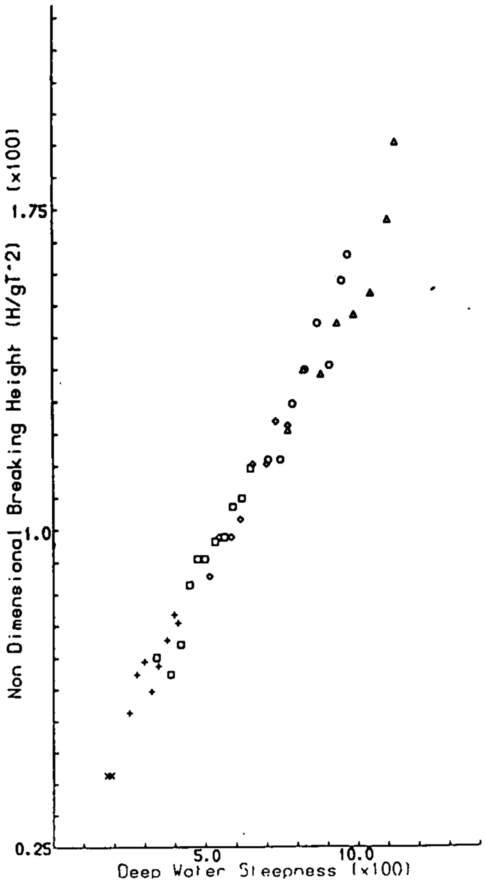

Fig. 4

Fig.5 shows the results for H_b/d_b. Our results, plotted with the larger symbols, again show a simple linear relationship with deep water steepness. The deep water limit of H/d → 0 as S → 0.14 is included and it is immediately obvious that extrapolation of our results to deep water would yield an incorrect result, again suggesting that caution should be used with the previous extrapolation of H/gT^2.

Also drawn on the graph are results from Iwagaki et al[5] and Sakai and Iwagaki[6], the commonly used value of 0.78 and the empirical line derived by Weggel[4].

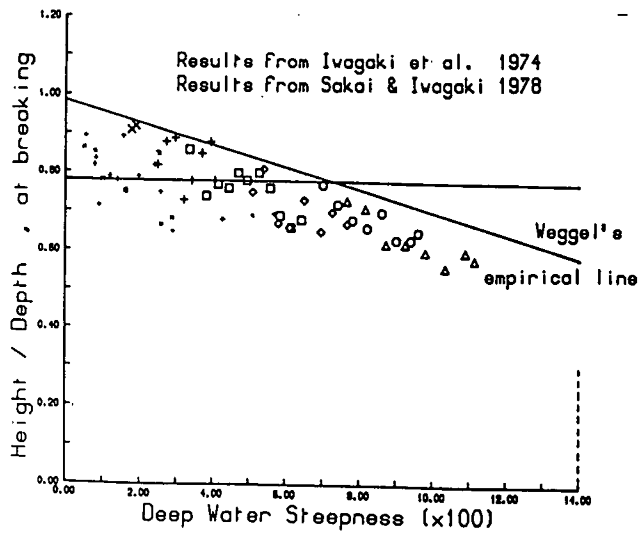

Fig. 5

Our results, while agreeing well with the steepness dependence of Weggel's results, show a consistent under-prediction of about 0.1 in the H/d ratio.

The value of 0.78 offers a good mean value for the shallower water region but it considerably overestimates H/d for deeper water $0.07 < S < 0.14$. This is not unexpected as the value of 0.78 is based on solitary wave theory, corresponding to the limit of S → 0.

Also included in this section on design ratios is Fig. 6. where the ratio of elevation of height at breaking is plotted as a function of S. This quantifies the observation that as waves become longer, the crests become peakier and higher and the troughs flatter and lower. Design, particularly of clearance, must account for this assymetry.

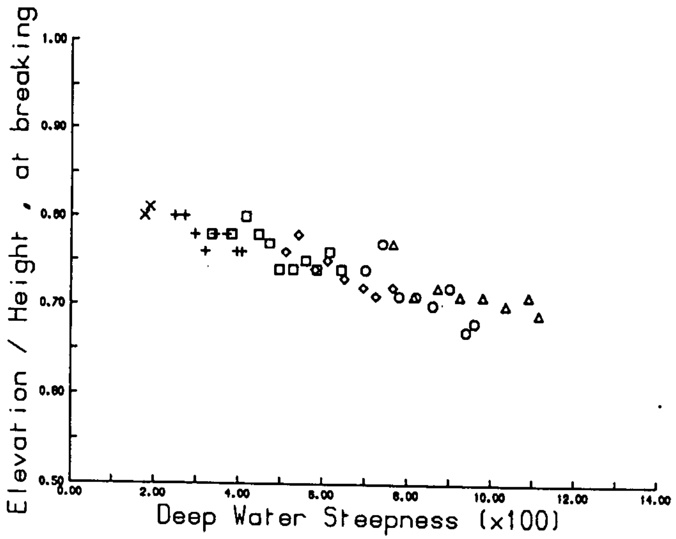

Fig. 6

6. WATER PARTICLE KINEMATICS WITHIN A BREAKING WAVE

Besides the limit to growth of a wave, breaking waves are highly relevant to design as the phenomenological changes that occur at breaking lead to loads far in excess of those due to non-breaking waves. Most notable are those due to slap and slam with their almost impulsive loads and, less dramatically, increased velocities and accelerations lead to larger drag and inertia forces.

To study the kinematics of breaking waves, we have developed at Edinburgh a dedicated LDA system, here we present the velocity and acceleration measurements within a 1 Hz wave. The wave was generated in deep water and made to break on a 1 : 30 slope at a depth of 18.5 cm. This wave had a crest elevation of 8.7 cm, a trough depth of 4.0 cm and a wavelength of 131 cm as measured at breaking.

The resulting flow is presented here along with the Dean's 3rd, the Stokes 5th and the linear solutions for the velocities, Fig. 7. It can be seen that there is good general agreement of the velocities but there is however some significant difference in the high crest region. The simulated flow at the crest phase underestimates the true

velocities over the region of the top third at the crest above SWL. This is not a quirk of this particular wave, in previous work done by the present authors, this has been a recurring phenomenon in breaking waves and is not described by Deans' higher order solutions (up to 9th) where these are stable.

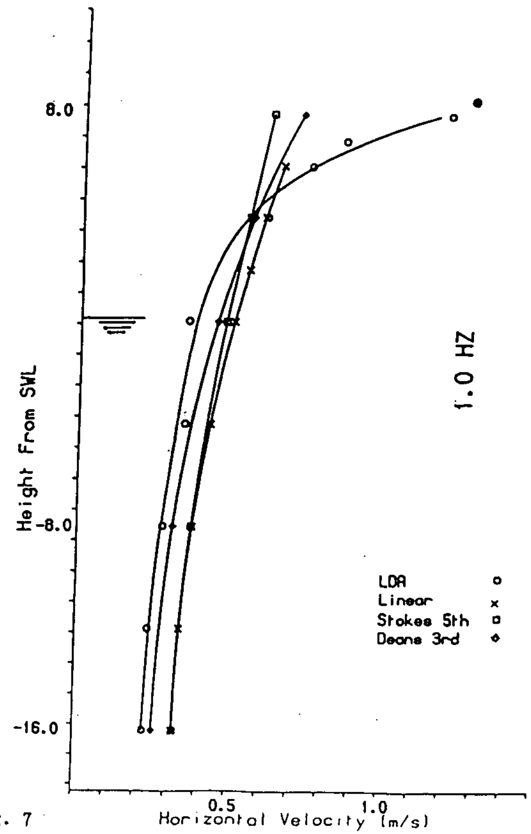

Fig. 7

The size of this under-prediction is not trivial, the highest measured horizontal velocity was 1.25 m s^{-1}. By comparison, the extreme horizontal velocity calculated by the Dean's method was 0.77 m s^{-1}. And in design terms there is more than a 2.5 fold increase in v^2 and hence force. The crest elevation of the wave is marked by a heavy dot at the velocity corresponding to the wave celerity. The increase in velocity with height is seen to be very large in this high crest region, giving an extrapolated value of crest velocity, of considerably over c, though the height and therefore the volume of the wave where this occurs are very small.

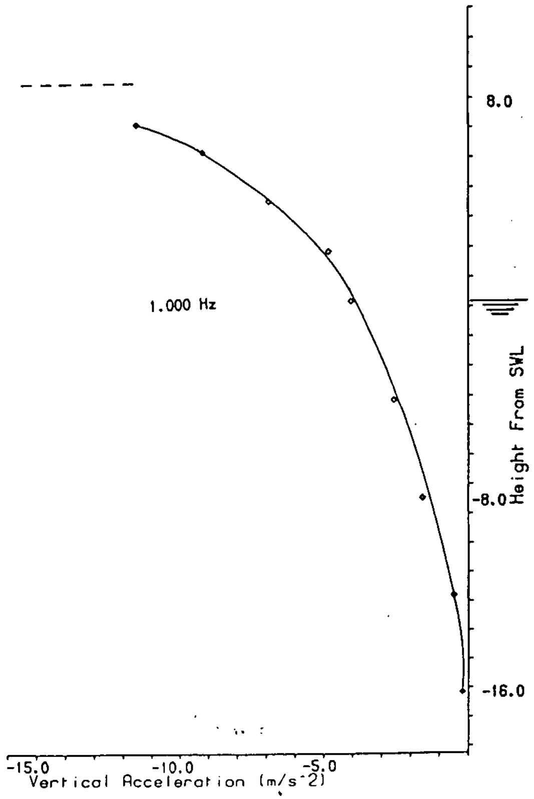

Fig. 8

The accelerations presented here are Eulerian accelerations, i.e. the rate of change of water particle velocity measured at a fixed point. This is therefore directly applicable to a Morison type analysis. As mentioned in 13, measuring difficulties and therefore

inaccuracies for acceleration measurements, increase in the less well behaved region of the crest, but plot Figure 8 can be extrapolated yielding a maximum acceleration in the crest much in excess of g.

7. CONCLUSIONS AND DESIGN IMPLICATIONS

Within a design procedure which chooses as its extreme loading, a high or extreme regular wave, it is necessary to know the kinematics of such waves. The accepted approach is to use a computer simulation typically a Stokes or Dean type of low or medium order (3rd to 9th). The accuracy of these simulations has for some time been in question, not least as they describe horizontally symmetric waves and besides becoming mathematically unstable have no way of describing wave breaking.

The breaking of extreme waves is included in the design in two ways. Empirical data is used in the choice of design waves, and being based on real sea data, implicitly includes the upper bound on waveheight caused by wave breaking. Secondly, use is made of the height to depth ratio at breaking often taken simply as a constant 0.78 or for deep water the limiting steepness of $H/L = 1/7$ (or corresponding H/gT^2 limit of 0.027) to check that the design height is below the breaking limit.

It must be noted that this procedure is constructed in such a way that it seldom, if ever, predicts wave breaking. The value 0.78 is a good mean for H_b/d_b but there is a marked trend for decreasing H_b/d_b with D.W. steepness. And the deep water steepness parameter in one sense describes depth of breaking from shallow water (low S) to deepwater (high S).

For our results on a bed slope of 1 : 30, H_b/d_b falls to as little as 0.56, this in the region of large S, that is the deeper water area, of particular interest in design.

The previous inability to measure accurately the particle kinematics in the high crest region led to a belief, included in design guidance, that "non-linear regular wave theories over-predict particle velocities at all levels. Crest velocities are particularly over-predicted". (Guidance notes on the design and construction of offshore structures.(18))

From our observations it is seen that this is generally true, except for the high crest region where the theories significantly under-predict. Also the measured velocities are increasing with height far more rapidly than the theoretical velocities. Though the extrapolation is unproven, a maximum particle velocity at the top of the crest just over the wave celerity could be used as a guide.

It is strongly urged that this is used rather than the maxima predicted by the various models for any design in the high splash zone. And account must be taken of it in terms of fully immersed flow via a Morison type expression and also when considering surface penetration problems of slam and slap. In this regard it is noted that at the front of the crest particle velocities are consistently normal to the surface.

Measurement also yielded extreme values of Eulerian acceleration in the crest greater than 1.3 g, showing a quick decrease away from the top of the crest.

Here again designers must regard the simulation techniques in this high crest region with some scepticism until good correlation with experiment is achieved. The Stokes limiting wave has a mathematical singularity in surface acceleration at this point giving an infinite acceleration, empirical results could be used to restrict such models to finite, justifiable values around this singularity.

The implications for design drawn from the breaking height measurements must only be regarded as introductory. It is seen in ¶5 that previous estimates of breaking heights for quite deep water are considerably above those presented here. And if substantiated by broader based research on the mechanisms leading to breaking, these lower values could be incorporated into the design method as maximum limits for the height of design waves. The experimental work presented has considered breaking induced solely by shoaling. It is very important, if breaking height is developed as a design limit, that all the factors that effect the breaking are considered. It is believed by the present authors that factors can be reduced to (1) the rate at which energy is localised in a wave, by such methods as wind-wave interaction, gradual convergence of waves by refraction, decreasing water depth and via the effect on wave type by current; (2) fully three-dimensional effects of intersecting wave trains; (3) effects of randomness in a two-dimensional sea and (4) effects of vorticity and

current profile. Of these, the three-dimensional effects could lead to a significant increase in maximum height, and it has been observed, Ochi and Tsai[8] that randomness leads to a considerable reduction in breaking height.

With increasing understanding of extreme wave behaviour and breaking, it is hoped that a simplification of design procedure may be possible, based on a more deterministic choice of design wave and that physical limits will guide the choice rather than extrapolation from biased data.

ACKNOWLEDGEMENTS

This work is funded by the Marine Technology Directorate Fluid Loading Programme. Mr. Griffiths is in receipt of a CASE (BP) studentship.

REFERENCES

1. CARTER, D.J.T. and CHALLENOR, P.G.: 'Estimating return values of wave height', IOS Report No. 116, 1981

2. CARTER, D.J.T., CHALLENOR, P.G., EWING, J.A., PITT, E.G., SROKOSZ, M.A. and TUCKER, M.J.: 'Estimating wave climate parameters for engineering applications', Dept. of Energy Offshore Technology Report OTH86 228, HMSO, 1986

3. MUNK, W.H.: 'The solitary wave theory and its application to surf problems,' Annals of the New York Academy of Science, Vol. 51, pp376-462, 1949

4. WEGGEL, J.R.: 'Maximum breaker height for design', Coastal Engineering, pp419-432, 1982

5. IWAGAKI, Y., SAKAI, T., TSUKIOKA, K. and SAWAI, N.: 'Relationship between vertical distribution of water particle velocity and type of breakers on beaches', Coastal Engineering in Japan, Vol 17, pp51-58, 1974

6. SAKAI, T. and IWAGAKI, Y. 'Estimation of water particle velocity of breaking wave', Coastal Engineering, pp551-568, 1978

7. MICHELL, J.H.: 'On the highest waves in water', Philosophical Magazine, Vol. 36, 5th Series, pp.430-437, 1893

8. OCHI, M.K. and TSAI, C.H.: 'Prediction of occurrence of breaking waves in deep water', J. Physical Oceanography 13, pp2008-2019, 1983

9. SNYDER, R.L. and KENNEDY, K.M.: 'On the formation of whitecaps

by a threshold mechanism, part 1, basic formalism', J. Physical Oceanography 13, pp1482-1492, 1983

10. STOKES, G.G.: 'On the theory of oscillatory waves', Trans. Camb. Phil. Soc., 8, pp441-455, 1847

11. DIVOKY, D., Le MEHAUTE, B. and LIN, A.: 'Breaking waves on gentle slopes', J.G.R., Vol. 75, pp1681-1692, 1970

12. KJELDSEN, S.P. and MYRHAUG, D.: 'Kinematics and dynamics of breaking waves', Rep. STF 60A 78100, River and Harbour Lab., Trondheim, Norway, 1978

13. KJELDSEN, S.P., VINGE, T., MYRHAUG, D. and BREVIG, P.: 'Kinematics of deep water breaking waves', Proc. 12th Offshore Technology Conf., pp317-325, 1980

14. EASSON, W.J. and GREATED, C.A.: 'Acceleration measurements using Laser Doppler Anemometry', Optics in Engineering Measurement, SPIE, Vol. 599, pp380-386, 1985

15. FLICK, R.E. and GUZA, R.T. 'Paddle generated waves in laboratory channels', J. Waterway Port, Coastal Eng. Division ASCE 106 (WW1) pp.79-97, 1980

16. STIVE, M.J.F.: 'Velocity and pressure field of spilling breakers', Coastal Enginering, 1980

17. STIVE, M.J.F.: 'A scale comparison of waves breaking on a beach', Coastal Engineering, 9, pp.151-158, 1985

18. DEPARTMENT OF ENERGY: 'Guidance notes on design and construction of offshore structures, 1985

Twenty-first Coastal Engineering Conference

Proceedings of the International Conference

VOLUME 1

June 20-25, 1988
Costa del Sol-Malaga, Spain

Conference held under the auspices of the
Coastal Engineering Research Council of the
American Society of Civil Engineers

Organized by the Colegio de Ingenieros de
Caminos, Canales y Puertos de Espana

and cosponsored by the
Directorate General for Ports and Coasts of the
Spanish Ministry of Public Works
Polytechnical Universities of
Madrid, Barcelona, Santander,
and Valencia

Edited by Billy L. Edge

Published by the
American Society of Civil Engineers
345 East 47th Street
New York, New York 10017-2398

CHAPTER 65

Kinematics of Breaking Waves in Coastal Regions

William J. Easson[1], Matthew W.P. Griffiths[2] and Clive A. Greated[3]

Waves breaking on various slopes in a wave flume are examined. Plunging and spilling breakers are considered. The parametric results show the consistency of the measurement and the independence of scale. A method is given for predicting the maximum breaking height for a wave of known period in a known depth. The velocity is measured to the crest of the wave and comparisions with numerical and analytical solutions demonstrate the shortcomings of many of the established methods of predicting wave kinematics.

Introduction

Breaking waves are of significant importance in the design and understanding of many aspects of Coastal Engineering such as breakwaters, bed movement and inshore construction. Yet the kinematics of these waves are not fully understood despite considerable advanced theoretical and numerical work (e.g. New et. al., 1985). Mathematical models are limited in several ways at present. For example, although deep and shallow waves may be modelled it has not been possible to include changes in bed topography such as linear slopes. Also, the flow field becomes complex when the plunging jet of a breaker hits the forward face making the spilling or surging breakers difficult to model.

Experimentally, the measurement of kinematics is complicated by the two-phase situation which exists above the still water level precluding the use of many standard velocity probes. For this reason mathematical models have usually been inadequately compared with surface profiles.

Due to the difficulty of obtaining breaking wave kinematics, designers have tended to rely on the tried and tested industry standards such as Stokes and Cnoidal theory or Dean's stream function. Recently, higher-order versions of Dean have been available, applicable to larger waves (Chaplin, 1980). All of these assume two dimensional, regular non-breaking waves and necessarily provide limited

---

1. Lecturer, Department of Mechanical Engineering, University of Edinburgh, The King's Buildings, Mayfield Road, Edinburgh EH9 3JL, UK

2. Postgraduate student, Fluid Dynamics Unit, Department of Physics, University of Edinburgh.

3. Director, Fluid Dynamics Unit, Department of Physics, University of Edinburgh.

descriptions.
Furthermore none of the above methods can give a reliable limiting wave height and the question of whether the 'design wave' might be breaking is dependent on data gathered from elsewhere on height over depth ratios (Griffiths et al, 1987). For this reason several companies have commissioned site-specific studies at the Edinburgh

Fluid Dynamics Unit to discover if the design wave was a breaker and if so what its kinematics were (Birkinshaw et. al., 1988).

This paper will look at spilling and plunging breakers on beds of various slopes in terms of their parameterisation and internal kinematics. A method of using these results will then be proposed.

Experimental method

Regular waves are generated in a narrow tank by a computer-controlled absorbing wavemaker. The wavemaker is in 'deep' water (0.9 m) and the waves are run up a slope of variable degree. For gentle slopes and flat beds an initial steep slope is used (fig. 1).

The velocity measuring technique is Laser Doppler Anemometry. The non-intrusive system records the frequency of variation of light scattering intensity as minute seeding particles pass through the crossing volume of two laser beams. The application of this technique to breakers may be found in Easson & Greated (1984). The method of signal analysis allows measurements up to the crest of the breaking wave which is not common in most systems but will be shown to be of great importance.

Wavelength, height, and velocity were measured using still photography and a video-camera. (figs. 2, 3).

Results

(a) Parametric

The wave parameters measured were deep water height (H_o), breaking height (H_b), breaking depth (d_b), maximum crest elevation (H_{1b}) and trough depression (H_{2b}) wavelength at breaking (L_b) and velocity at breaking (C_b) (see fig. 4). The breaking point is when the crest first becomes vertical. For ease of presentation and application of the results the deep water steepness ($S_o = H_o/l_o$) has been used as the reference axis. This has been shown to be useful and valid over the range $0.015 < So < 0.115$ in a previous publication (Griffiths et al, 1987), as would be expected since Froude scaling applies here. Furthermore no correction factors are required in applying these results to full scale waves.

The range of slopes considered is 1:15, 1:30, 1:50 and flat bed. Most of the waves produced spilling breakers but the longest waves on the 1:30 slope (small S_o) and most of the waves on the 1:15 slope became plunging breakers.

The first plot (fig. 5) shows the depth at which the waves broke. All length scales have been non-dimensionalised by the deep water wavelength so $d_b' = d_b/gT^2$. This shows that the depth of breaking is independent of slope or period and is purely a function of deep water steepness.

The limits are as expected with the graph passing through zero (no height, no breaking) and tending towards the deep water breaking limit ($S_o \approx 0.14$) as the breaking depth increases. Figure 6 shows the breaking wave height which is also independent of slope or period and tend towards a deepwater limit of 0.022 at $S_o = 0.142$. This has been compared with the regular criteria of $H_b' = 0.027$ and the irregular limit of $H_o' = 0.020$. (Ochi and Tsai, 1983).

It is possible, using figs 5 and 6, to read off the breaking wave height given the design parameters of depth and period. For example, a 12.5s wave in a depth of 25 m (typical North Sea) gives $d' = d/gT^2 = 0.016$. From fig. 5, $S_o = 6.0$ which from fig. 6 gives $H' = 0.011$. Therefore the breaking wave limit height is $H_b = gT^2 \times H' = 16.8$ m. If hindcasting has predicted a height greater than this then the wave will be breaking.

Designers have often used the criterion $H_b/d_b > 0.78$ to determine whether a wave is breaking. This is derived from shallow water solitary wave theory (Munk, 1949) and should not be used for intermediate depths. Figure 7 shows H_b/d_b against S_o for our results. Previously (Griffiths et al, 1987) the 1:30 results were shown to match the results of other investigators on this slope; they also extended the range to deeper water. Weggel (1982) proposed an empirical upper limit based on the 1:30 slope results. Several significant points may be drawn from this figure. Firstly, the flat bed results tend to the solitary wave limit at small S_o and the Weggel line is overly conservative. Secondly, the $H/_d$ ratio is slope dependent - a fact which is not apparent from figures 5 and 6. Finally, the Weggel line cannot be applied to slopes greater than 1:30 as the plunging breakers here exceed the H_b/d_b ratio predicted.

Svendsen and Buhr Hansen (1976) plot wavelength over depth at breaking as a function of deep water steepness. The results here (fig. 8) confirm the slope of Svendsen's empirical mean value line and extend the range of results towards the deep water limit.

(b) Kinematic results

Velocities were measured under the crest of the wave at a range of elevations from the bed to the crest peak at the instant of breaking. Figure 9 shows the velocity variation from bed to crest of five wave frequencies breaking at a particular depth (185 mm) on a 1:50 slope. The most important general characteristic is the large increase in velocity in the crest where the graph steepens considerably. Thus although the near bed velocities are as expected the crest velocities differ considerably from non-breaking waves. The curvature of the graph is greatest for the short waves which have lower velocities below SWL. The group of points to the right of the graph are the five celerities associated with the frequencies studied, plotted at the maximum elevation of the crest. In each case the velocity curve tends towards the celerity at crest indicating that this is the maximum velocity (although it may only pertain to a very small fraction of the crest volume) and that the condition v = c does indeed represent a useful criterion for wave breaking.

Figure 10 shows the velocity under the crest of a 1 Hz wave breaking at 185 mm depth for different slopes. There is no significant difference between the 1:50 and 1:30 results but higher velocities were measurable for the 1:15 slope due to the larger volume of water travelling at velocities around c in the plunging jet. (c.f. figures 2 & 3). The plunging breaker was also slightly higher than the others.

Finally, the quality of these results has enabled a direct comparision with some of the established theories. This is only possible when crest values can be obtained. The lack of crest values invalidates the comparisons made by previous investigators as this is where the major differences between breakers and non-breakers arise. Figure 11 shows the velocity variation with elevation for one particular wave but the trends are typical over the full range of conditions investigated. The comparisons are with Linear, Stokes V and Deans V and IX. (We are grateful to Professor J. Chaplin for the comparison with Deans IX (Chaplin, 1980)). The measured velocities tend towards the indicated celerity/height point and the best fit curve has been drawn. The Stokes V has also been indicated by a full curve. Interestingly, the linear theory gives a better fit than Stokes in the crest. The two Deans solutions are better approximations with the ninth giving a significant improvement in the crest. However, even this falls 20% short of the maximum expected velocity. Note that all the theories tend to over-predict the velocity below SWL.

Conclusions

By testing a range of frequencies, Froude scaling has been shown to apply to breaking waves. The parametric results have shown good agreement with those of other experimenters and have usefully extended the range of measurements. A method has been presented for the evaluation of limiting wave heights in the design of offshore structures using graphical procedures. The H/d ratio for breaking is slope dependent but is only significantly so for shallow/plunging breakers. Throughout the range measured the velocity in the crest tends to a maximum equal to the celerity at the highest point of the wave. The established theories tend to underestimate the crest velocity and overestimate the velocites below SWL.

It is important to remember, in the application of these results, that the two-dimensional, regular wave assumption has been made, as is the present industry practice. A project is currently under way, at Edinburgh University, using the instantaneous full-field anemometry technique known as Particle Image Velocimetry (PIV) (Gray & Greated, 1988) to measure the velocities under irregular breaking waves.

Acknowledgements

Mr. Griffiths is a postgraduate student in receipt of a CASE studentship with B.P International. The authors would particularly like to acknowledge the help and access to industrial procedures afforded by B.P. This project is part of the managed Fluid Loading Programme of MTD Ltd. We are also grateful for the encouragement and interest shown by various members of that organisation.

REFERENCES

1. Birkinshaw, M., W.J. Easson, C.A. Greated, and R.M. Webb, "Breaking wave design - a case histroy," Proc. Inst. Civil Engineers, part 2, vol. 85, pp. 415-433 1988.

2. Chaplin, J.R., "Developments in stream function wave theory," Coastal Engineering, vol. 3, pp. 179-205, 1980.

3. Easson, W.J. and C.A. Greated, "Breaking wave forces and velocity fields," Coastal Engineering vol. 8, pp. 273-241, Elsevier, Amsterdam, 1984.

4. Gray, C. and C.A. Greated, "The application of particle image velocimetry to the study of water waves," Lasers and Optics in Engineering, Elsevier Applied Science. In Press

5. Griffiths, M.W.P., W.J. Easson, and C.A. Greated, "Large wave loading on structures - a reappraisal," Integrity of Offshore Structures - 3, pp. 77-94, Elsevier, London, 1987.

6. Munk, W.H., "The solitary wave theory and its application to surf problems," Annals of the New York Academy of Science, vol. 51, pp. 376-462, 1949.

7. New, A.L., P. McIver, and B.H. Peregrine, "Computations of overturning waves," J.F.M., vol. 150, pp. 233-251, 1985.

8. Ochi, M.K., and C.H. Tsai, "Prediction of occurrence of breaking waves in deep water," J. Physical Oceanography, Vol. 13, pp. 2008-2019, 1983.

9. Svendsen, I.A. and J. Buhr Hansen, "Deformation up to breaking of periodic waves on a beach," Proc. Coastal Engineering, pp. 477-496, 1976.

10. Weggel, J.R., "Maximum breaker height for design," Coastal Engineering, vol. 6, pp. 551-568,

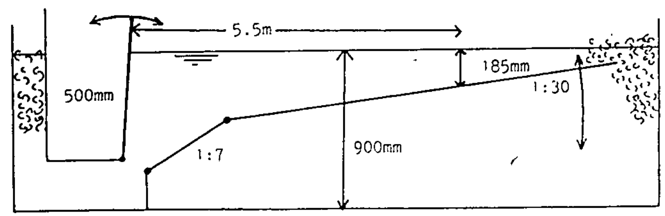

Fig. 1 - Typical beach dimensions

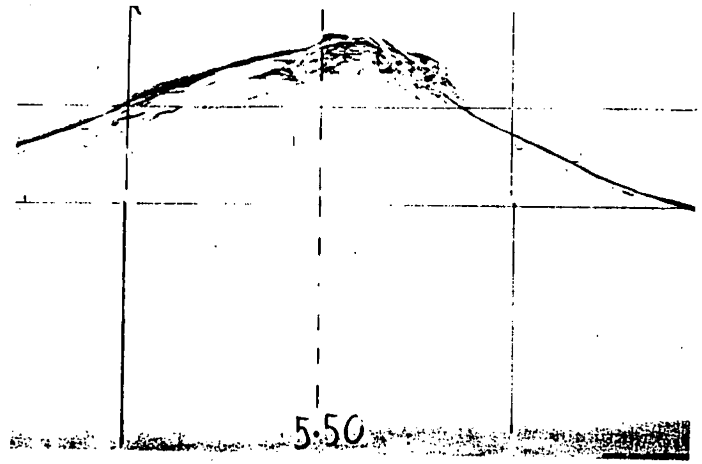

Fig. 2 - Depth induced spilling

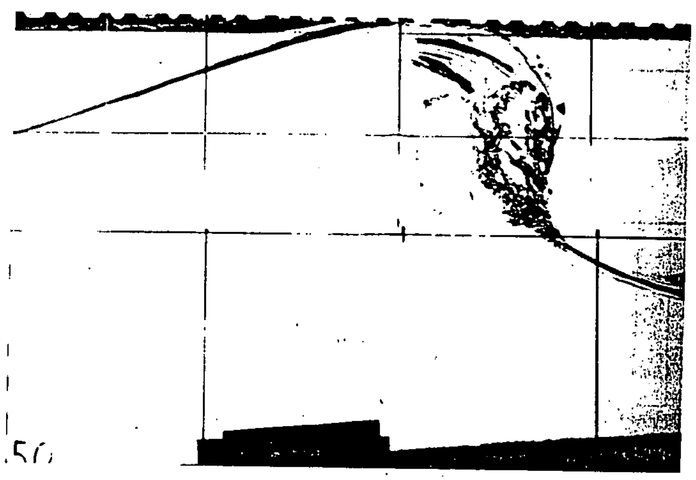

Fig. 3 - Depth induced plunging

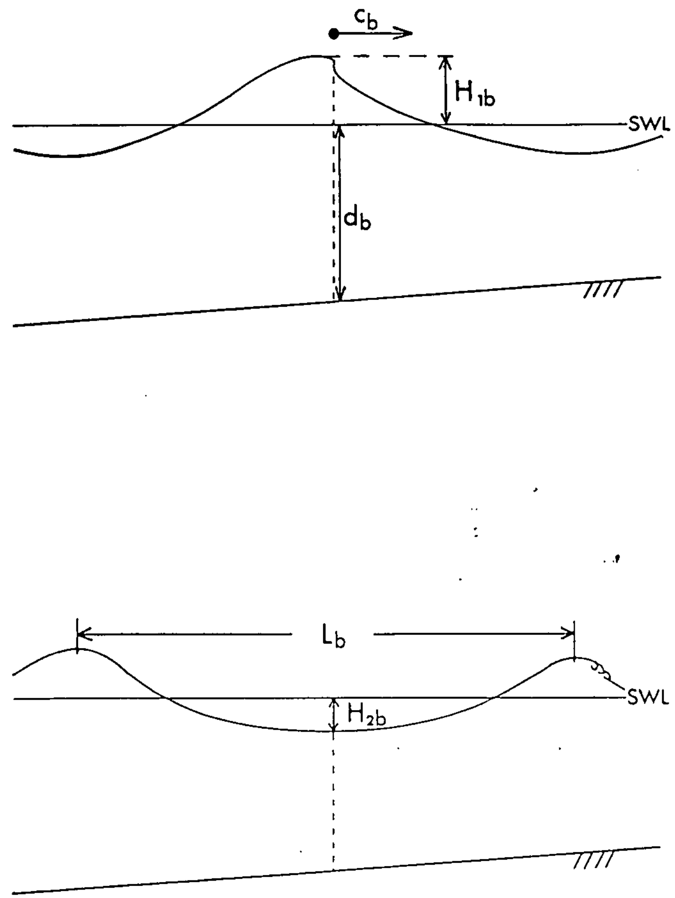

$$H_b = H_{1b} + H_{2b}$$

Fig. 4 - Definition of parameters at measuring point

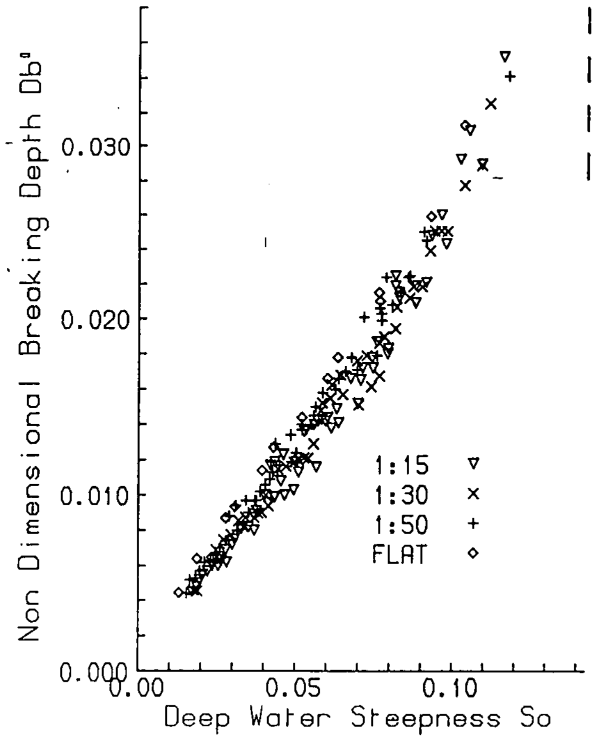

Non Dimensional Breaking Depth Db'
0.000
0.010
0.020
0.030
0.00
0.05
0.10
Deep Water Steepness So
1:15
1:30
1:50
FLAT

Fig. 5 -

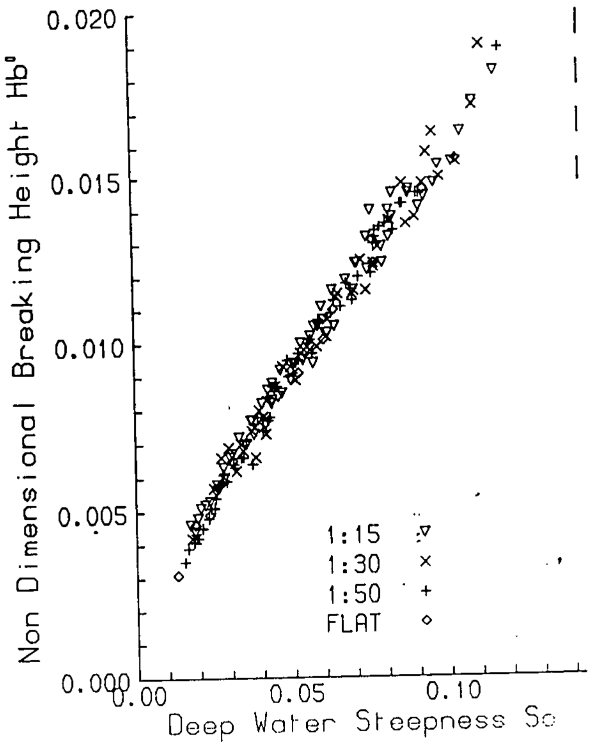

Non Dimensional Breaking Height Hb'
0.000
0.005
0.010
0.015
0.020
0.00
0.05
0.10
Deep Water Steepness So
1:15
1:30
1:50
FLAT

Fig. 6 -

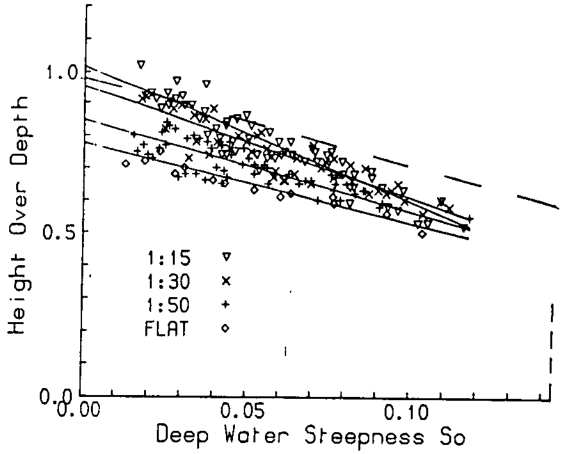

Fig. 7 - H/d at breaking. The four solid lines are best fits to the results from each slope (steepness increases with greater H/d. The dashed line is Weggel's empirical line).

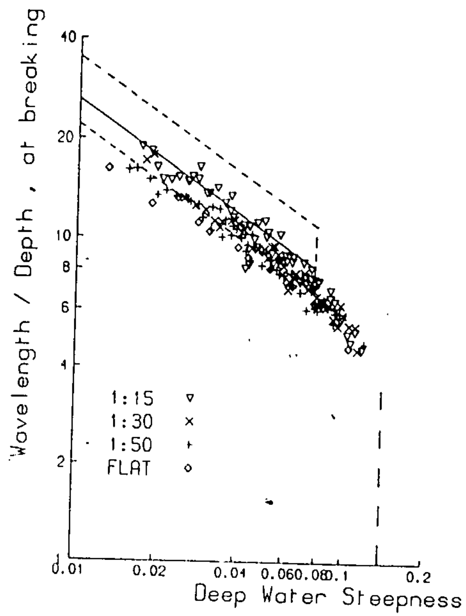

Fig. 8 - Comparison with Svendsen (boxed area indicates extent of Svendsen's scatter)

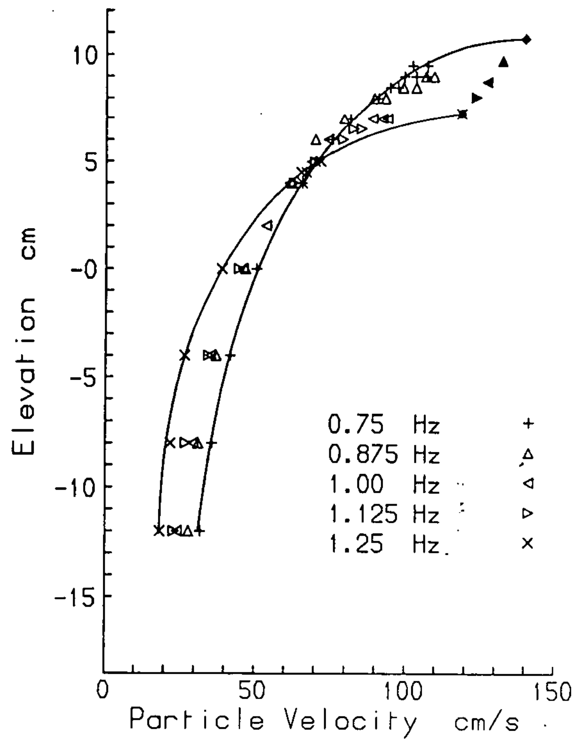

Fig. 9 - Particle velocity v. elevation. Dependence on frequency (1.50 slope)

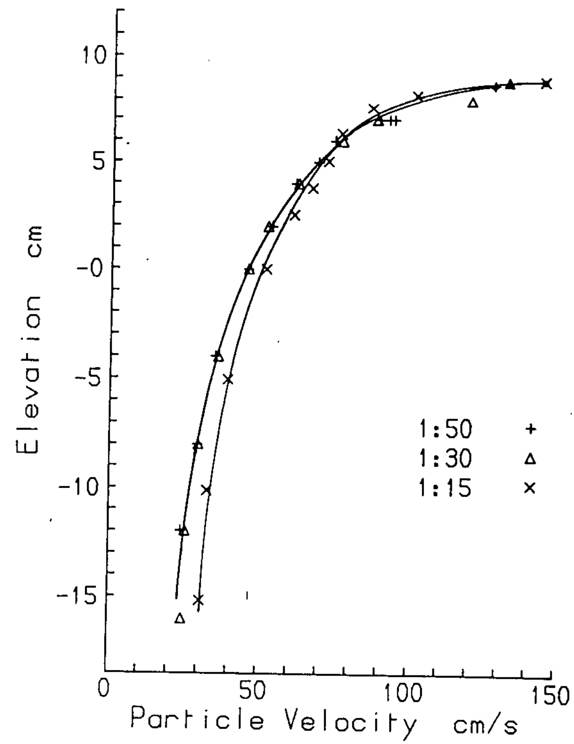

Fig. 10 - Particle velocity v. elevation. Dependence on slope. (1 Hz wave.)

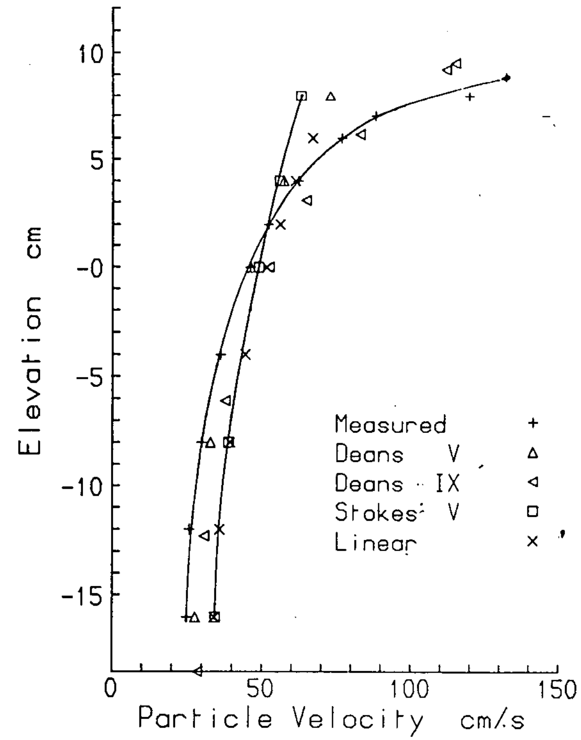

Fig. 11 - Particle velocity v. elevation. Comparison with theory (1 Hz, 1.30 slope.)